CHIRAL BICYCLIC GUANIDINE CATALYZED DIELS–ALDER REACTIONS OF ANTHRONES

SHEN JUAN

NATIONAL UNIVERSITY OF SINGAPORE

2008

CHIRAL BICYCLIC GUANIDINE CATALYZED DIELS–ALDER REACTIONS OF ANTHRONES

SHEN JUAN **2008**

CHIRAL BICYCLIC GUANIDINE CATALYZED DIELS–ALDER REACTIONS OF ANTHRONES

SHEN JUAN

(BSc., Suzhou University)

A THESIS SUBMITTED

FOR THE DEGREE OF DOCTOR OF PHILOSOPHY

DEPARTMENT OF CHEMISTRY

NATIONAL UNIVERSITY OF SINGAPORE

To my parents, brother, and Dongsheng,

for their love, support, and encouragement

Acknowledgements

First and foremost, I would like to take this opportunity to thank my supervisor, Assistant Professor Tan Choon-Hong, for his guidance and encouragement throughout my PhD research and study.

I appreciate Mr. Santhosh's help in proofreading this manuscript. Miss Loh Wei Tian, Miss Lin Shishi and Mr. Lee Zhong Han's suggestions and comments also helped improve this thesis.

I would also like to thank all my labmates for creating such a harmonious, encouraging, and helpful working environment. My special thanks go to Ms. Thanh Truc Nguyen, Mr. Yong-Peng Goh, and Ms. Junye Xu, for their participation in different stages of this project.

I thank Mdm Han Yanhui, Miss Ler Peggy and Mr. Wong Chee Ping for their assistance in NMR analysis, and Mdm Wong Lai Kwai and Mdm Lai Hui Ngee for their assistance in Mass analysis as well. I also owe my thanks to many other people in NUS chemistry department, for their help and assistance from time to time.

Last but not least, I thank all my friends in Singapore who helped me settle down at the beginning. Singapore is a great place and I enjoy the life here.

Table of Contents

Summary

The aim of this study is to develop highly enantioselective Diels–Alder reactions of anthrones catalyzed by a chiral bicyclic guanidine.

We try to find an efficient type of catalyst, and three categories of catalysts were screened for the Diels–Alder reaction between anthrone and *N*-phenylmaleimide, including bis(oxazoline) (BOX), imidazoles, guanidines. 2,3,5,6-Tetrahydro-2,6-dibenzyl-1*H*-imidazo[1,2-*a*]imidazole, a bicyclic guanidine base, was found to be the most efficient organocatalyst. A wide variety of Diels–Alder dienes and dienophiles can participate in these reactions using 10 mol% of the chiral bicyclic guanidine. The conjugate addition between 1,8-dihydroxy-9(10*H*)-anthracenone (dithranol) and different dienophiles also works very well with the chiral bicyclic guanidine. These reactions are mild, fast, easy to perform, and proceed with high yields. The enantioselectivities generally range from 85-99%, with yields between 80-96%.

The mechanism of both triethylamine (Et_3N) and 2,3,5,6-tetrahydro-2,6-dibenzyl-1*H*-imidazo[1,2-*a*]imidazole catalyzed reactions of anthrones has been investigated though VT-NMR. When using Et_3N as the catalyst, it fouctions as a normal base to abstract a proton from anthrone. The anthrone works a reactive diene in Diels-Alder reaction. When chiral bicyclic guanidine was used as the catalyst, it works as a bifunctional catalyst; it activates both the diene and dienophile at defined positions simultaneously.

An enantioselective synthesis of anthrone-derived *N*-hydroxyphthalimide (NHPI) analogues has been developed. One of these analogues, in combination with Co salts, was employed to catalyse the aerobic oxidation of benzylic compounds and diols. Exploratory studies using a racemic version of the catalyst were also conducted. Radical addition of dioxolanes or alcohols to activated alkenes with molecular oxygen as the terminal oxidant was also shown to be catalysed with NHPI-analogues.

List of Schemes

List of Tables

List of Figures

List of Abbreviations

AcOH	acetic acid
Ac	acetyl
[α]	optical rotation
aq.	aqueous
Bn	benzyl
*i*Bu	*iso*-butyl
*t*Bu	*tert*-butyl
Ph	phenyl
c	concentration
^{o}C	degrees (Celcius)
T	Kelvin
δ	chemical shift in parts per million
DMAP	4-dimethylaminopyridine
DMSO	dimethyl sulfoxide
dd	doublet of doublet
dr	diastereomeric ratio
ee	enantiomeric excess
EI	electron impact ionization
ESI	electro spray ionization
Et	ethyl
FAB	fast atom bombardment ionization

FTIR	fourier transformed infrared spectroscopy
g	grams
h	hour(s)
HPLC	high pressure liquid chromatography
HRMS	high resolution mass spectroscopy
Hz	hertz
i.d.	internal diameter
IR	infrared
J	coupling constant
LRMS	low resolution mass spectroscopy
Me	methyl
MeCN	acetonitrile
MeOH	methanol
mg	milligram
MHz	megahertz
min.	minute(s)
ml	milliliter
µl	microliter
mmol	millimole
MS	mass spectroscopy
NMR	nulcear magnetic resonance
ppm	parts per million
*i*Pr	isopropyl

rt	room temperature
TBD	1,5,7-triazabicyclo[4.4.0]dec-5-ene
THF	tetrahydrofuran
TLC	thin layer chromatography
TS	transition state
TsCl	*para*-toluenesulfonyl chloride
TsOH	*para*-toluenesulfonic acid
Boc	*tert*-butyloxycarbonyl
Ns	2-nitrophenylsulfonyl
M	$mol \cdot l^{-1}$
mM	$mmol \cdot l^{-1}$

Chapter 1

Chiral Guanidine and Guanidinium Derivatives as Asymmetric Catalysts

Arginine **1** is found in the active site of many enzymes and its guanidine side chain typically exists in the protonated form as a guanidinium ion, which is known to interact with phosphates, nucleotide bases, and carboxylate containing biomolecules through double hydrogen bonding.[1] Guanidine is one of the most basic forms of neutral nitrogen compounds and guanidine derivatives are widely used as strong bases in synthetic organic chemistry.[2]

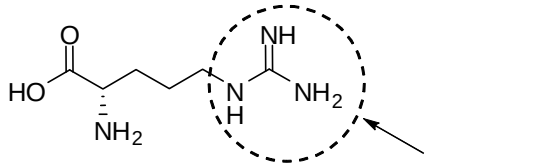

1 Arginine guanidine group

It is anticipated that chiral guanidine derivatives can function as asymmetric catalysts by utilizing the great basicity of the guanidine group and the special hydrogen bonding pattern of the guanidinium ion. This research topic has increasingly attracted great interest and the asymmetric catalytic ability of chiral guanidine or guanidinium has been demonstrated in several reactions. Guanidine catalysts are generally classified into four categories: acyclic guanidine with chiral side chains, mono-to-polycyclic guanidines, phase transfer guanidium salts, and guanidine-thiourea bifunctional catalysts.

1.1 Acyclic guanidines with chiral side chains

Since the isolation of complex **4** (Scheme 1.1), formed between the guanidine 1,5,7-triazabicyclo[4.4.0]dec-5-ene (TBD) **2** and phenylnitromethane **3**, it was anticipated that this type of intermediate could be a good model for an enantioselective guanidine-catalyzed Henry (nitroaldol) reaction.[3]

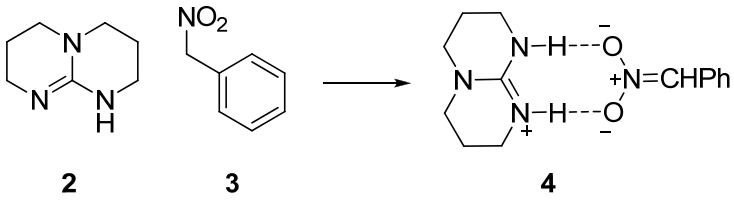

Scheme 1.1. Isolated complex between TBD and phenylnitromethane.

In 1994, the Nájera group tested the Henry reaction between aldehyde **5** and nitromethane **6** using a series of homochiral guanidines as the catalyst.[4] The best enantioselectivity was achieved with C_2-symmetrical guanidine **7**, affording **8a** in 54% ee and **8b** in 33% ee (Scheme 1.2). However, yields were compromised due to the low reaction temperature required for satisfactory enantioselectivity.

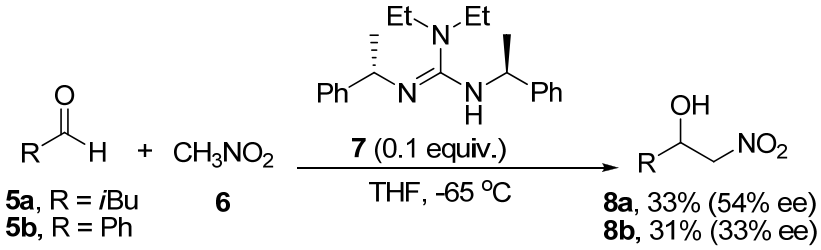

Scheme 1.2. Henry reaction catalyzed by homochiral guanidine.

Ma studied the diastereoselective Henry reactions of α-dibenzylamino aldehydes **9** with nitromethane **6** catalyzed by guanidines (Scheme 1.3).[5] Various chiral guanidines were tested, including acyclic, monocyclic, and bicyclic ones. It was found that acyclic guanidine **10** afforded the product **11**-*anti* with the best diastereoselectivity. Although the reaction was generally high yielding, the diastereoselectivity was highly dependent on the substrates. Products **11a** and **11b** were obtained in good diastereoselectivities (96% and 91% respectively), but other products were achieved in only moderate or poor diastereoselectivities (e.g. **11c**, **11d**).

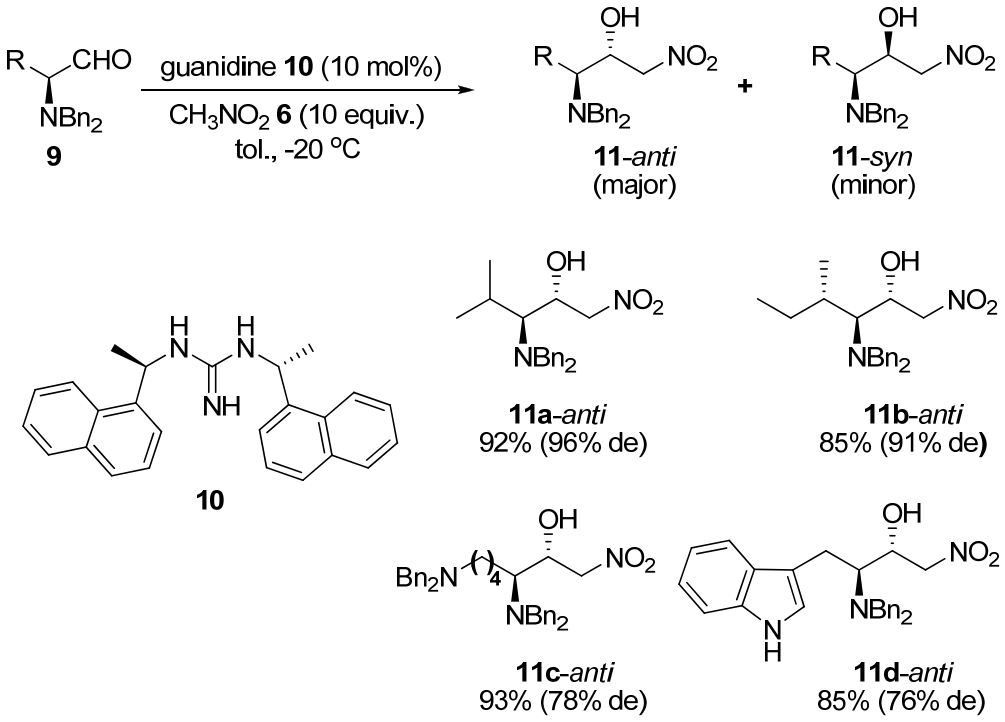

Scheme 1.3. Diastereoselective Henry reaction catalyzed by chiral guanidines.

In 1996, the Lipton group reported the first catalytic asymmetric Strecker reaction using the cyclic dipeptide **13** as the catalyst (Scheme 1.4).[6] The guanidine side-chain of **13** was found to be a prerequisite for asymmetric induction as replacing the guanidino group with an imidazolyl group resulted in a non-enantioselective reaction. It was proposed that the more basic guanidino group enabled the catalyst to accelerate proton transfer in the Strecker reaction. Using only 2 mol% catalyst **13**, good to excellent enantioselectivities (80->99% ee) were usually obtained with the reaction of imines derived from benzaldehyde or electron-deficient aldehydes (e.g. (*S*)-**14a-c**), except (*S*)-**14d**. However, unsatisfactory enantioselectivities were obtained with the heteroaromatic (e.g. (*S*)-**14e**) or aliphatic ((*S*)-**14f**) Strecker products.

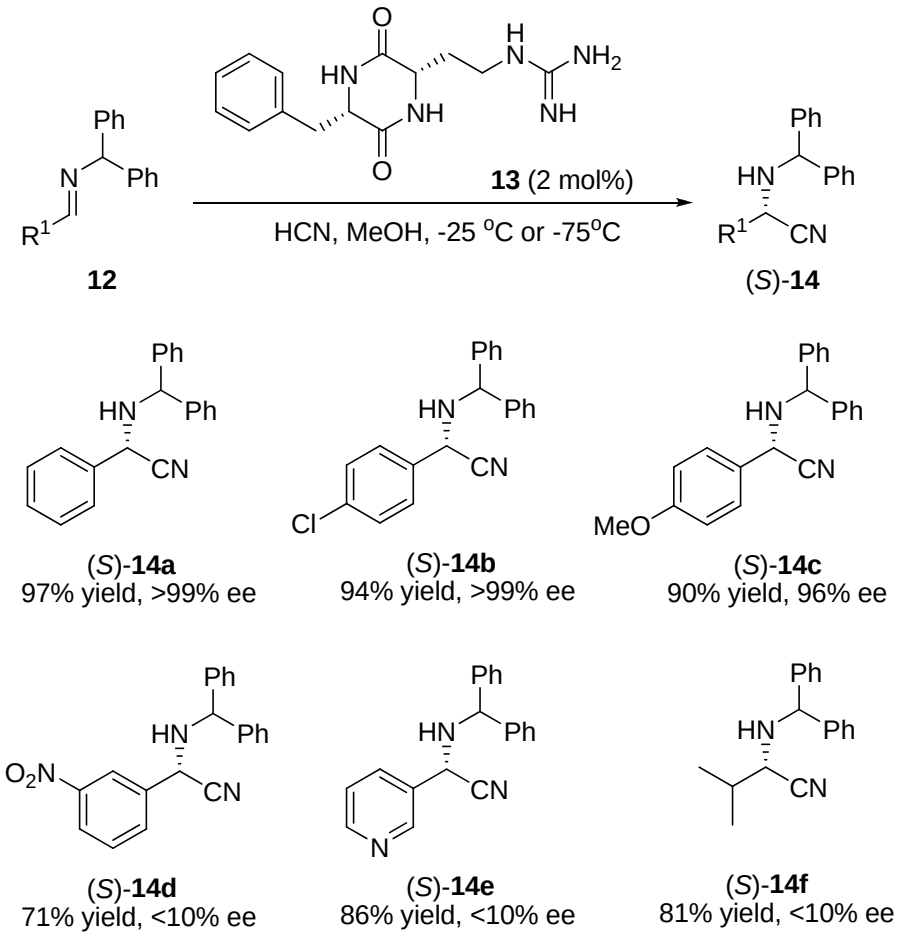

Scheme 1.4. Lipton's cyclic dipeptide catalyzed Strecker reaction.

In 1999, Ma reported that chiral guanidines **17a-d** catalyzed the Michael reaction between glycinate **15** and ethyl acrylate **16** (Scheme 1.5).[7] Although the yield was high, the ee obtained from the four different catalysts only ranged within 6-29%.

Ma also reported that chiral guanidine **17a** catalyzed the Michael reaction and Diels-Alder reaction between anthrone **19a** and *N*-methylmaleimide **20a** (Scheme 1.6).[8] Up to 70% ee and 67% yield were obtained for the Michael addition product **22**, while the Diels-Alder product **21a** was obtained in minimal yield (<3%) with no ee determined.

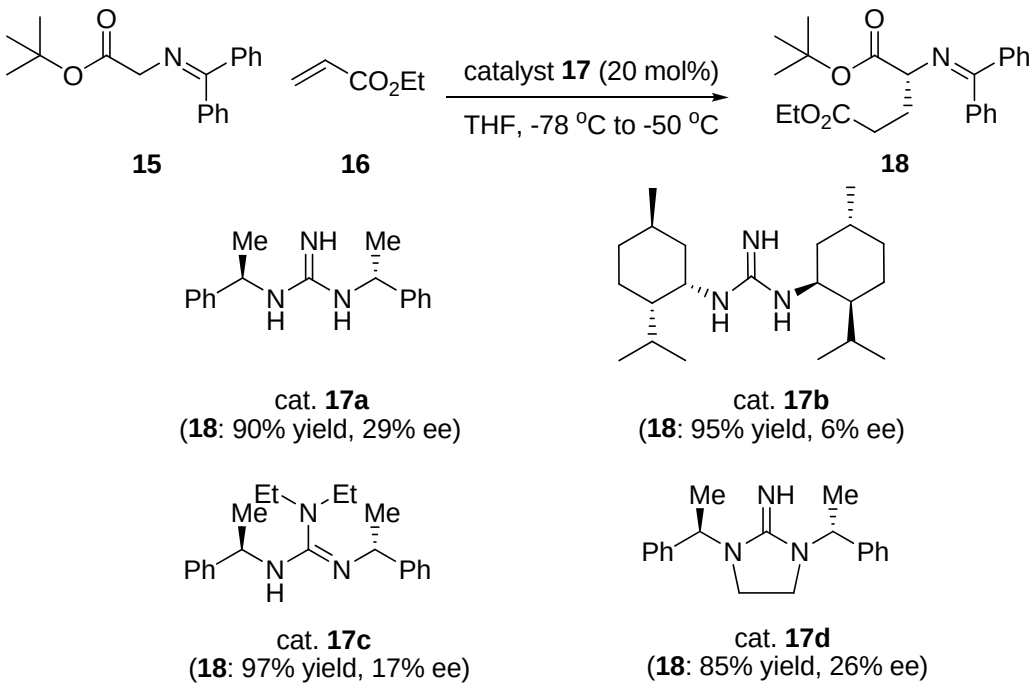

Scheme 1.5. Ma and Cheng's chiral guanidine catalyzed Michael reaction of glycinate.

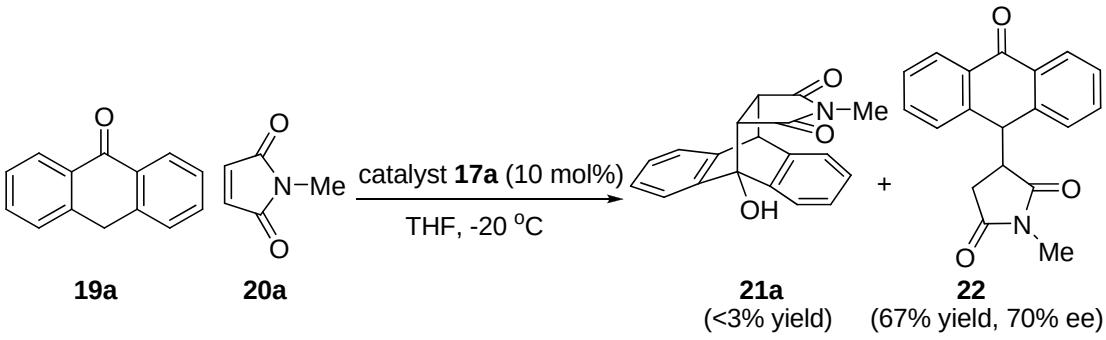

Scheme 1.6. Ma's chiral guanidine catalyzed Michael reaction and Diels-Alder reaction between anthrone and maleimide.

1.2 Mono-to-polycyclic guanidines

In 2001, Ishikawa reported that the guanidine **24** catalyzed the Michael reaction between glycinate **15** and olefins under solvent free condition (Scheme 1.7).[9a] Good yield (85%) and high ee (97%) were obtained for the reaction between glycinate **15** and ethyl acrylate **16**. But it seems that this reaction only works well for acrylates. The reaction between glycinate **15** and acrylonitrile **23** only gave the product **25** in

79% yield and 55% ee. In addition, the typical reaction time was 3-5 days.

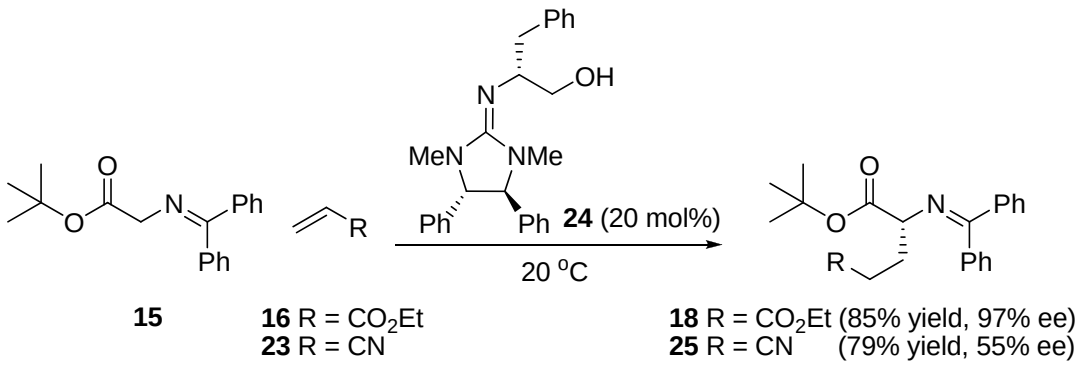

Scheme 1.7. Ishikawa's chiral guanidine catalyzed Michael reaction of glycinate.

This epoxidation of chalcones **26a** was also catalyzed by Ishikawa's monocyclic guanidine **27** (Scheme 1.8).[9b] Using 20 mol% of the guanidine **27**, epoxide **28a** was obtained in 49% and 64% ee for two different hydroperoxides.

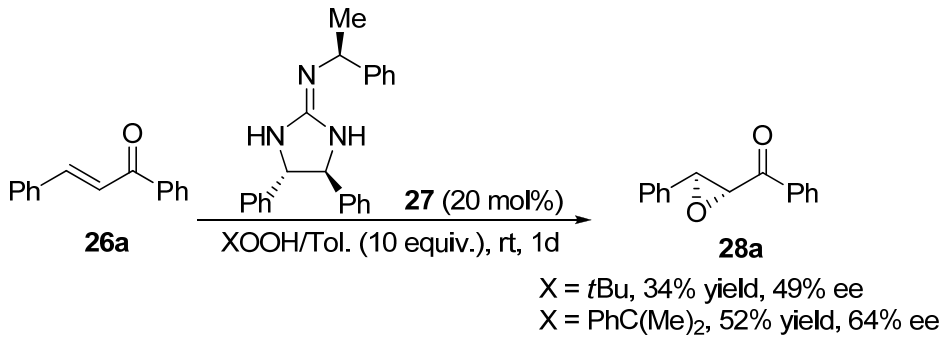

Scheme 1.8. Guanidine promoted epoxidation of chalcone.

Chiral monocyclic guanidines **30a-g** were also found to promote enantioselective epoxidation of enone **29**.[10] A stoichiometric amount of **30** was required to obtain moderate yields. With various chiral *N*-substituents on the guanidine **30**, epoxide **31** was obtained in moderate enantioselectivities ranging from 26-60% (Scheme 1.9).

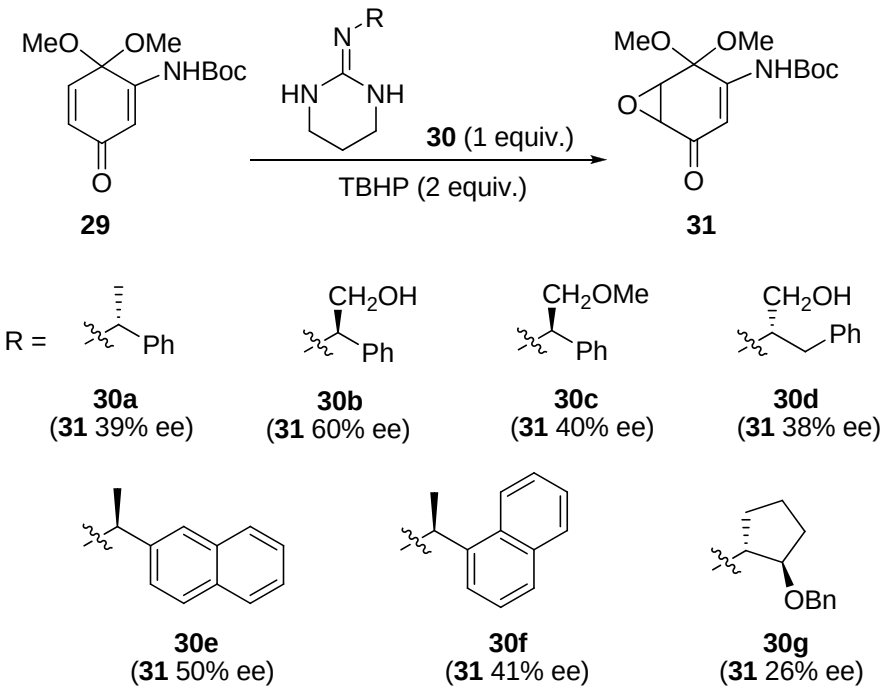

Scheme 1.9. Guanidine promoted epoxidation.

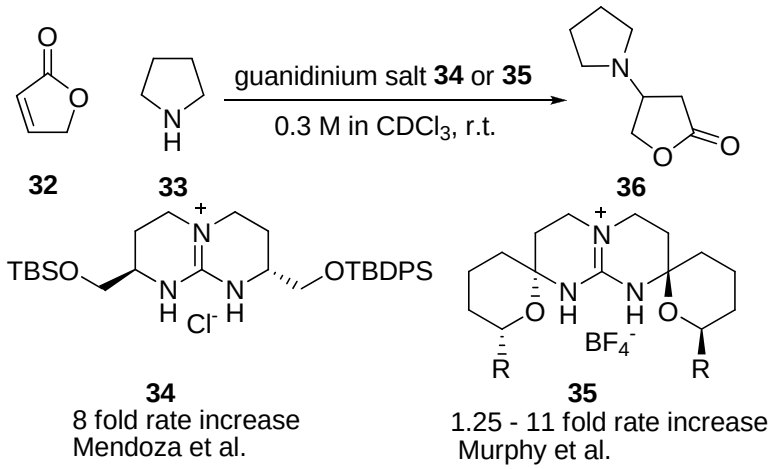

Scheme 1.10. Chiral bicyclic guanidinium salt catalyzed aza-Michael reaction.

Knowing that guanidinium ions interact well with carboxylate ions, both Mendoza[11] and Murphy[12] studied the Michael reaction between unsaturated lactone **32** and pyrrolidine **33**, hoping that the guanidinium ion would interact with the lactone in a similar manner as with the carboxylate ion (Scheme 1.10). Mendoza used bicyclic guanidinium **34** as catalyst and Murphy used tetracyclic guanidinium **35** instead. In both cases, although the reaction rates were increased, no enantioselectivity was

observed.

In 1995, Davis reported that chiral bicyclic guanidine **39** catalyzed the nitro Michael reaction between **37a-c** and **38**, giving products **40a-c** in 9-12% ee (Eq. (1), Scheme 1.11).[13] Similar reaction between 2-nitropropane **41** and chalcone **26a** was catalyzed by Murphy's tetraguanidinium salt **42** in moderate yield (70%) and unsatisfactory ee (23%) (Eq. (2), Scheme 1.11).[12]

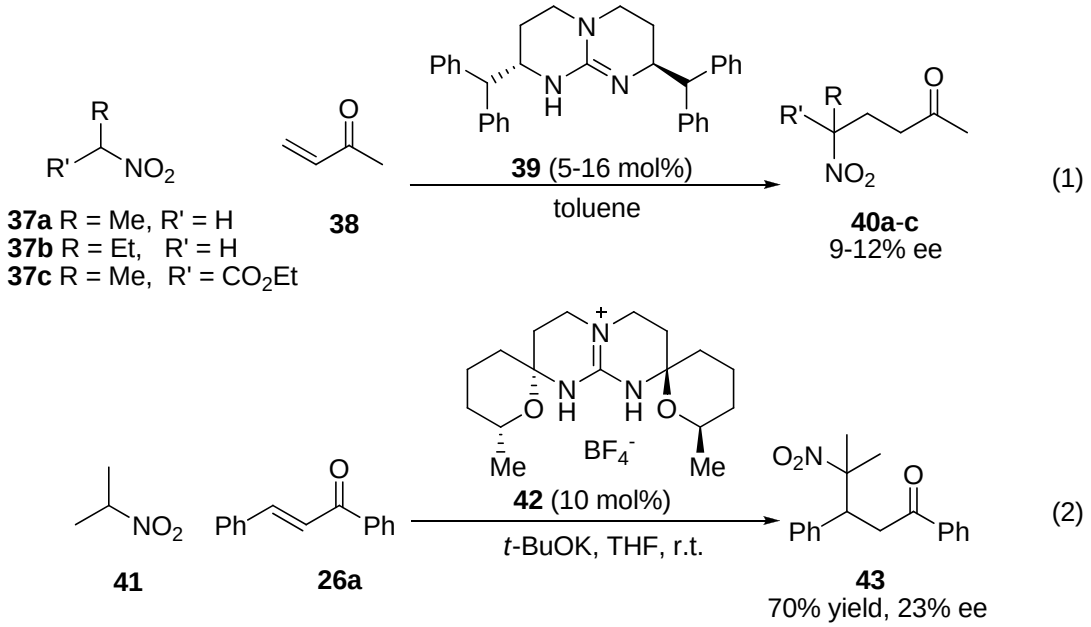

Scheme 1.11. Chiral guanidine or guanidinium catalyzed nitro Michael reaction.

Ishikawa's modified guanidines **45** and **46** were used as the asymmetric reagent for the kinetic silylation of secondary alcohols.[9c] **47a** was obtained in 59% ee and 36% yield with guanidine **45** (Scheme 1.12). When guanidine **46** was employed, **47a** and **47b** were obtained in 58% and 70% ee, respectively. In both cases, one equivalent of the guanidine was required.

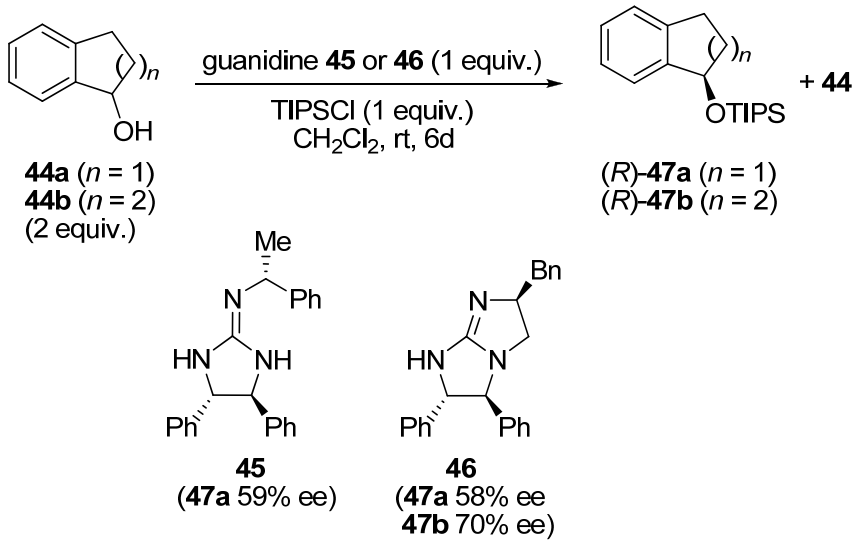

Scheme 1.12. Chiral guanidine catalyzed asymmetric silylation of secondary alcohol.

Ishikawa[9b] also reported that the C_2-symmetrical bicyclic guanidine **48a** catalyzed the TMS cyanation of aliphatic aldehydes **5**, affording the products **49** in quantitative yield and moderate enantiomeric excess (Scheme 1.13). However, low yield and ee were obtained when ketones were utilized in place of aldehydes.

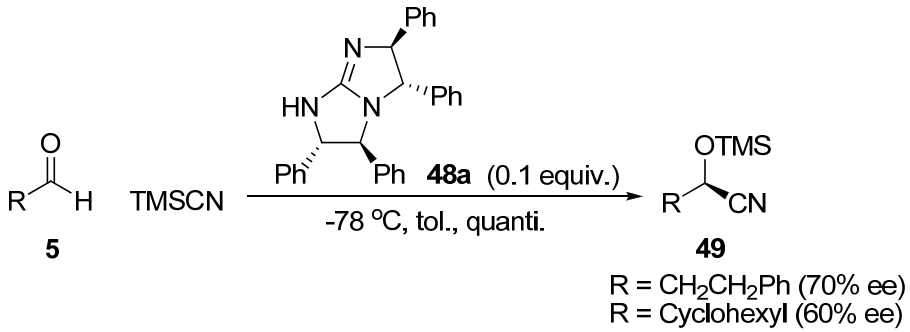

Scheme 1.13. Chiral guanidine catalyzed TMS cyanation of aliphatic aldehydes **5**.

Chiral bicyclic guanidines **48a-b** were also found to promote the kinetic azidation of (±)-1-indanol **44a** (Scheme 1.14).[9b] Stoichiometric amount of the guanidine was used and the product **50** was obtained in 26-30% ee.

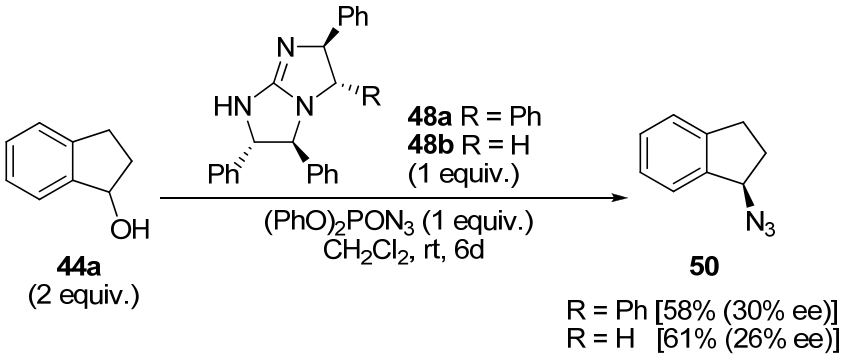

Scheme 1.14. Chiral guanidine mediated azidation of (±)-1-indanol **44a**.

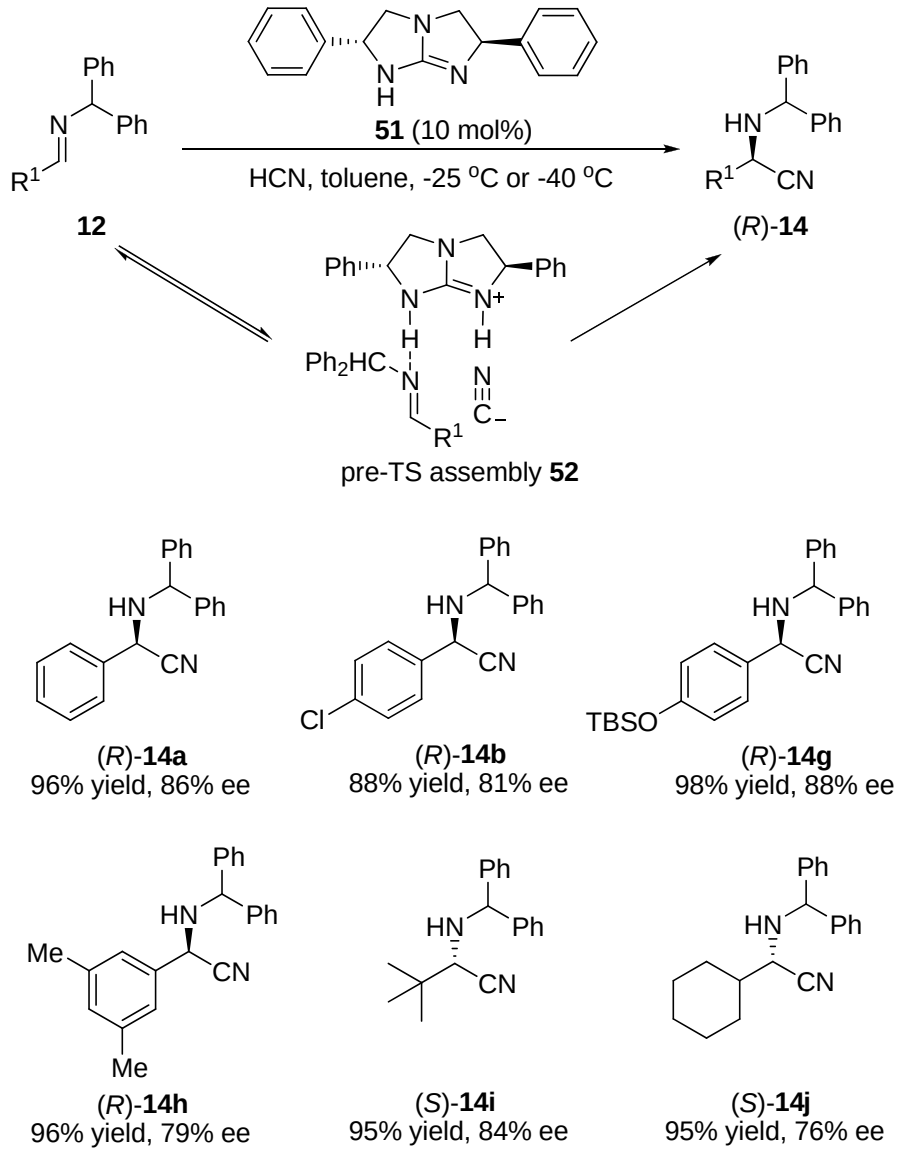

Scheme 1.15. Corey's bicyclic guanidine catalyzed Strecker reaction.

In 1999, Corey and Grogan developed an efficient asymmetric Strecker reaction using the C_2-symmetric bicyclic guanidine **51** as the catalyst (Scheme 1.15).[14] The

N-benzhydryl substituent of the imine substrate **12** was found to be critical to obtain good enantioselectivity (up to 88%), as *N*-benzyl or *N*-(9'-fluorenyl)-substituted imines gave poor ee (0-25%). In contrast with Lipton's diketopiperazine-catalyzed Strecker reaction, the reactions of aliphatic imines gave high yields (ca. 95%) and good enantioselectivities (63-84%).

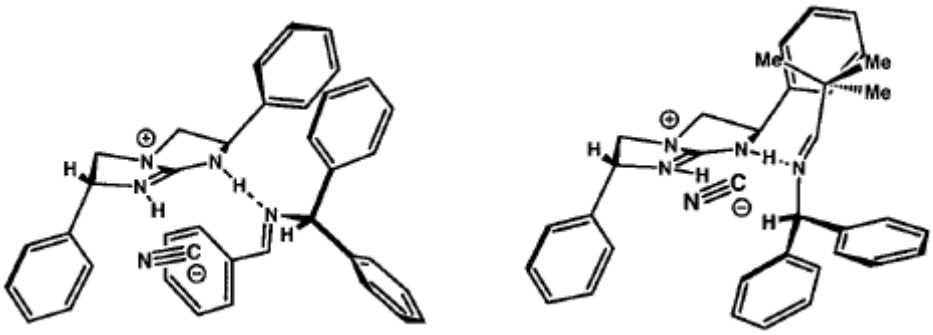

Figure 1.1. Pre-transition-state **52** for the Strecker reactions of *N*-benzhydryl benzaldimine **12a** and *N*-benzhydryl pivalaldimine **12i**.

In the reaction mechanism proposed by the Corey group, the complex **52** was formed, in which both imine and cyanide attach to the guanidinium ion through hydrogen bonds. The pre-transition state assembly modeling also explained the opposite configuration obtained for aromatic (e.g. (*R*)-**14a-h**) and aliphatic (e.g. (*S*)-**14i-j**) Strecker products (Figure 1.1).

Our group developed an efficient asymmetric Michael reaction using the C_2-symmetric bicyclic guanidine **55** as the catalyst (Scheme 1.16).[15] The initial investigation revealed that 1,3-diketones **54a** and β-keto ester **54b** added to maleimides in high enantioselectivity. The Michael adducts **56a-b** were obtained in high yields and high ees. However, it was necessary to use 20 mol% of catalyst, and these reactions were slow. To improve the reaction rate, the more reactive β-keto

thioesters **54c-d** and dithiomalonate **54e-f** were tested. As expected, the reaction rate was considerably enhanced. Using guanidine **55** as the catalyst**,** adducts **56c-f** were obtained in high yields and excellent ees with diastereomeric ratios of approximately 1:1 (**56c-d**). The catalyst loading of **55** can be decreased to 1 mol% for substrate **54d**.

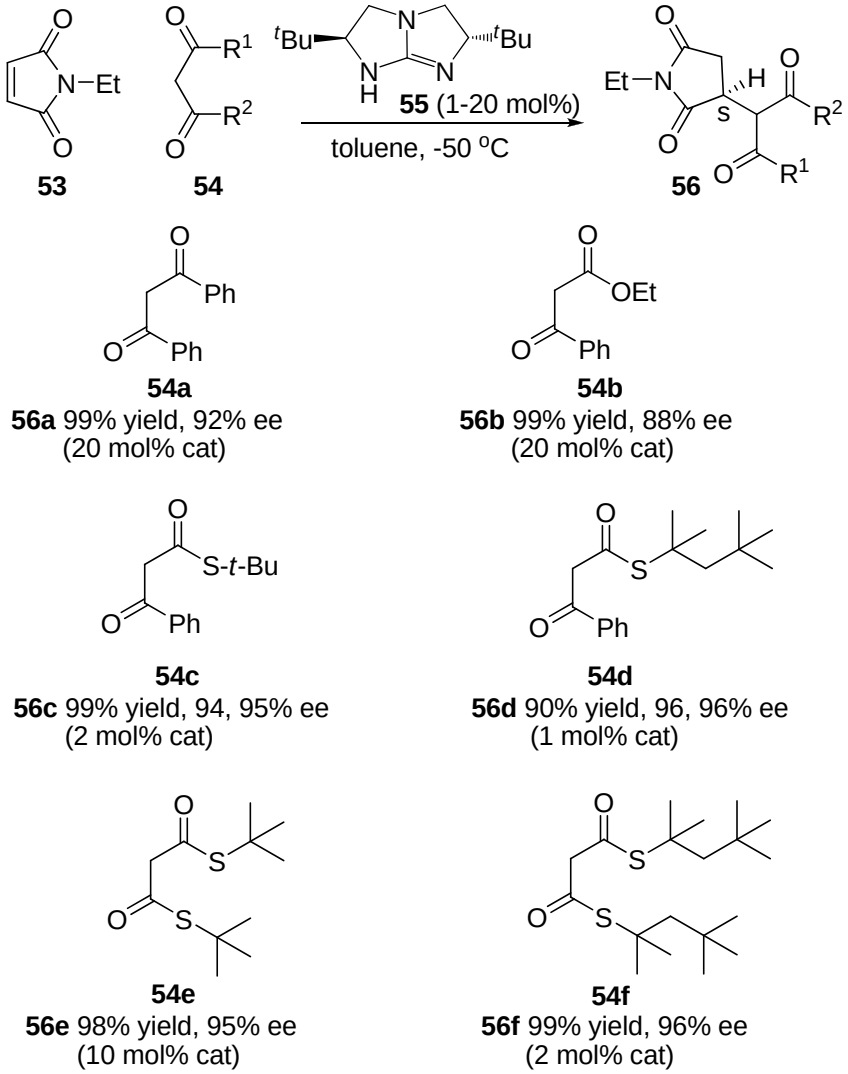

Scheme 1.16. Chiral bicyclic guanidine catalyzed Michael reactions of ethyl maleimide and 1, 3-diketones, β-keto esters, dithiomalonates.

Other cyclic substrates, such as cyclic enones and furanone were also explored as substrates for this reaction (Scheme 1.17).[15] In general, these reactions were slow. The reactions with various thioesters gave adducts **58a-d** in excellent enantioselectivities

and high yields.

To extend the scope of this reaction, it was found that ethyl *trans*-4-oxo-4-phenylbut-2-enoate **59** was a useful acyclic Michael acceptor (Scheme 1.18).[15] Using 5 mol% of guanidine **55**, dialkyl dithiomalonate **54f** reacted with **59** smoothly to give adduct **60** in high yields and high ees.

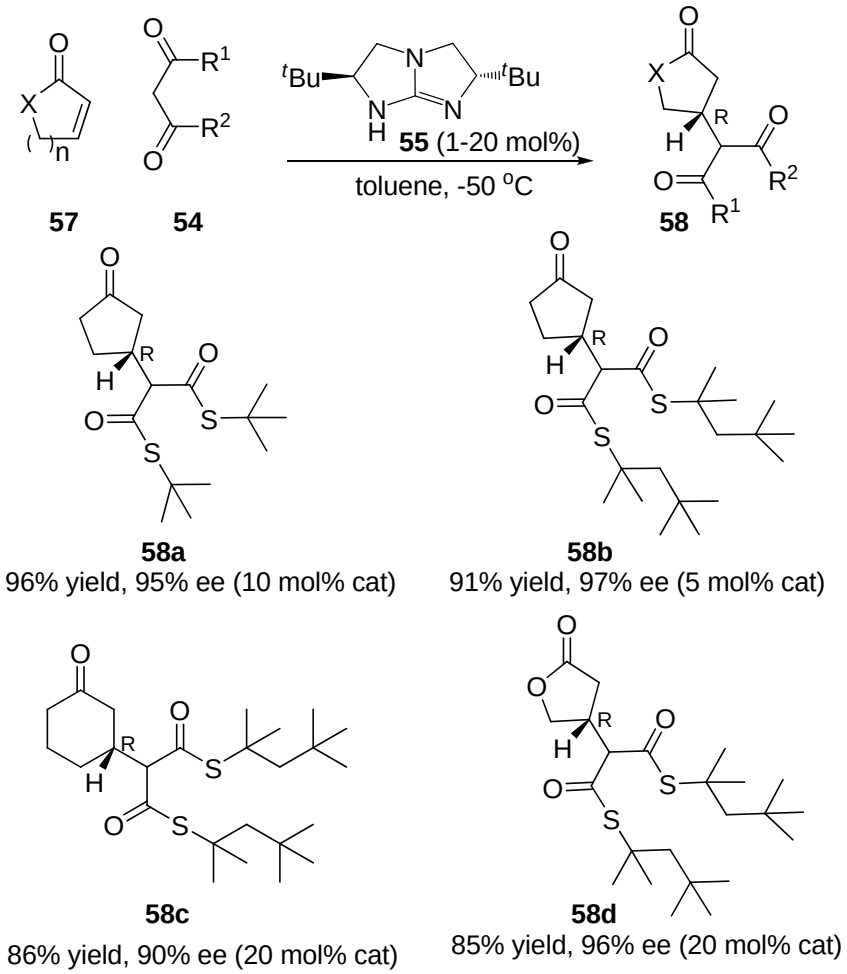

Scheme 1.17. Chiral bicyclic guanidine catalyzed Michael reactions of cyclic enones and furanone.

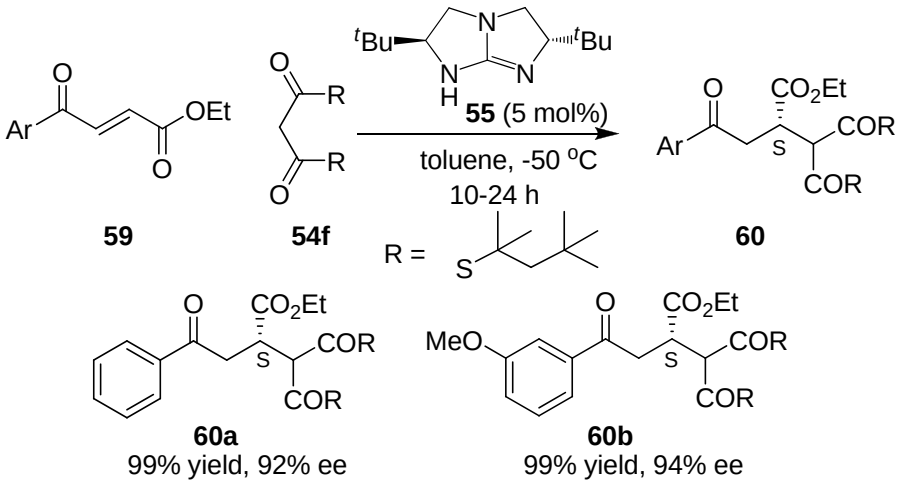

Scheme 1.18. Chiral bicyclic guanidine catalyzed Michael reactions of alkyl *trans*-4-oxo-4-arylbutenoates.

Our group also reported an efficient asymmetric phospha-Michael reaction using the C_2-symmetric bicyclic guanidine **55** as the catalyst. A series of diarylphosphine oxides **61** with β-nitrostyrene **62** were screened, giving the adducts **63a-d** in high yields and decent ees (Scheme 1.19).[16] The best result was achieved with **61d**, generating **63d** in 95% yield and 82% ee. At -40 °C, the addition of **61d** to various aryl(nitro)alkenes were investigated (Scheme 1.20).[16] Adducts **65a-d** were achieved with different substituted aryl(nitro)alkenes in excellent ees and high yields. The substitution pattern on the aryl ring would not affect the enantioselectivity. The optical purity of most adducts **65a-d** can be further enhanced with a single crystallization.

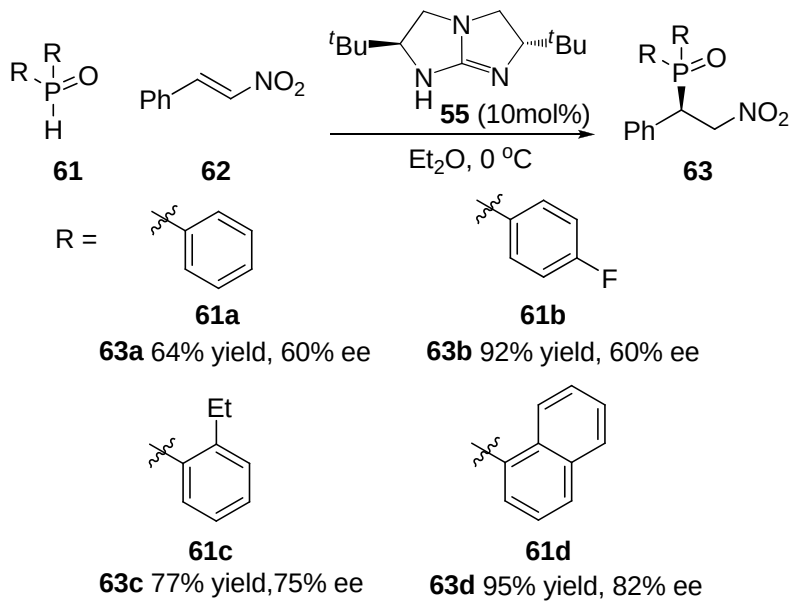

Scheme 1.19. Chiral bicyclic guanidine catalyzed phospha-Michael reactions with various diaryl phosphine oxides.

The diastereoselectivity of this reaction was investigated using two tri-substituted nitroalkenes, (*E*)-β-methyl-β-nitrostyrene **66a** and (*E*)-β-ethyl-β-nitrostyrene **66b**.[16] Using di(1-naphthyl)phosphine oxide **61d** as the donor, good diastereomeric ratios (dr) of 95:5 were observed (Scheme 1.21). Good enantioselectivities of 90 and 93% ee were attained for adducts **67a** and **67b** respectively.

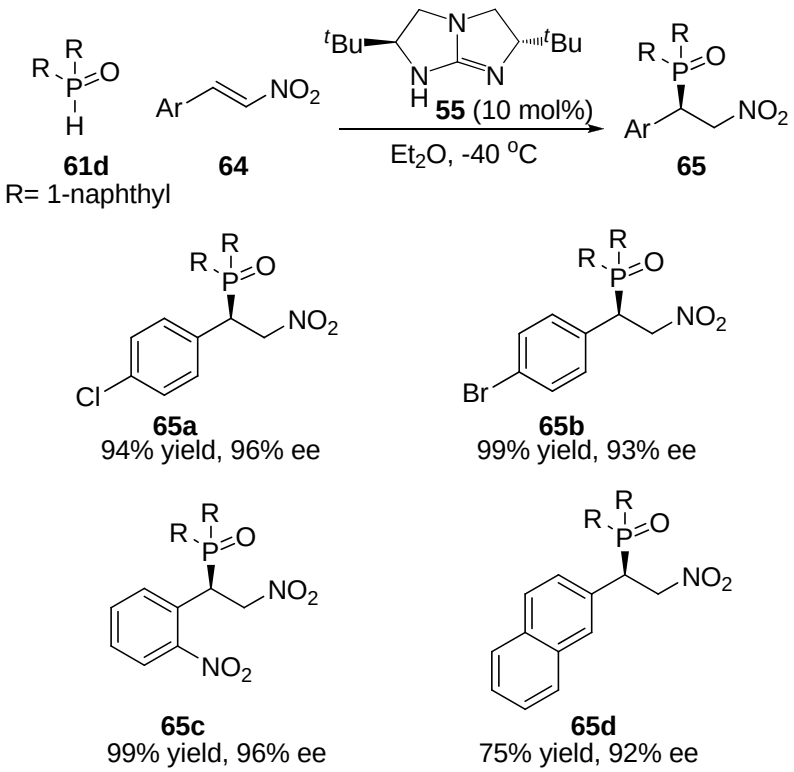

Scheme 1.20. Chiral bicyclic guanidine catalyzed phospha-Michael reactions of aryl nitroalkenes.

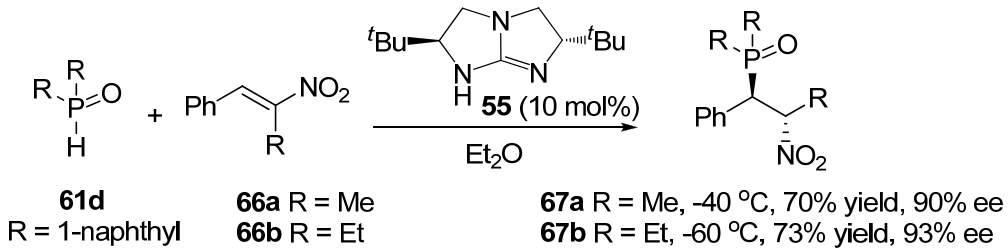

Scheme 1.21. Phospha-Michael reaction between phosphine oxide and trisubstituted nitroalkenes.

The chiral guanidine catalysts discussed above are either acyclic guanidine (e.g. **7, 10, 13, 17a-c**) with chiral side chains or mono-to-polycyclic systems (e.g. **17d**, **24**, **27**, **30a-g**, **34**, **35**, **39**, **42**, **45**, **46**, **48a-b**, **51** and **55**) with central chiralities. Recently, Terada[17a] et al. developed an important type of chiral guanidine catalysts, such as (*R*)-**70**, which introduced an axially chiral binaphthyl backbone with a nine-membered-ring structure. This axially chiral guanidine was found to be a highly efficient catalyst for the Michael reaction between a variety of conjugated

nitroalkenes **68** and several 1,3-dicarbonyl compounds **69**, featuring both high yielding and excellent enantioselectivity (up to 98% ee), with catalyst loading as low as 0.4-2 mol% (Scheme 1.22).

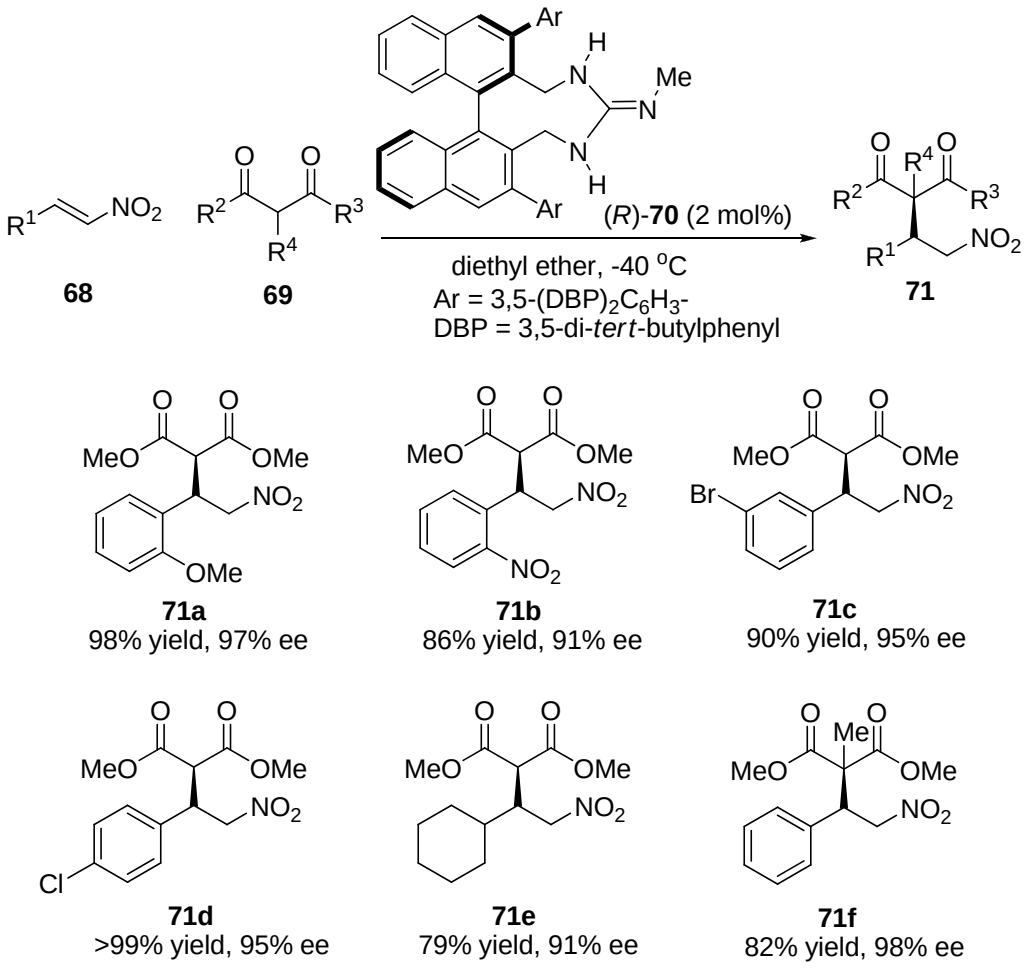

Scheme 1.22. Terada's axially chiral guanidine catalyzed Michael reaction of nitroalkene.

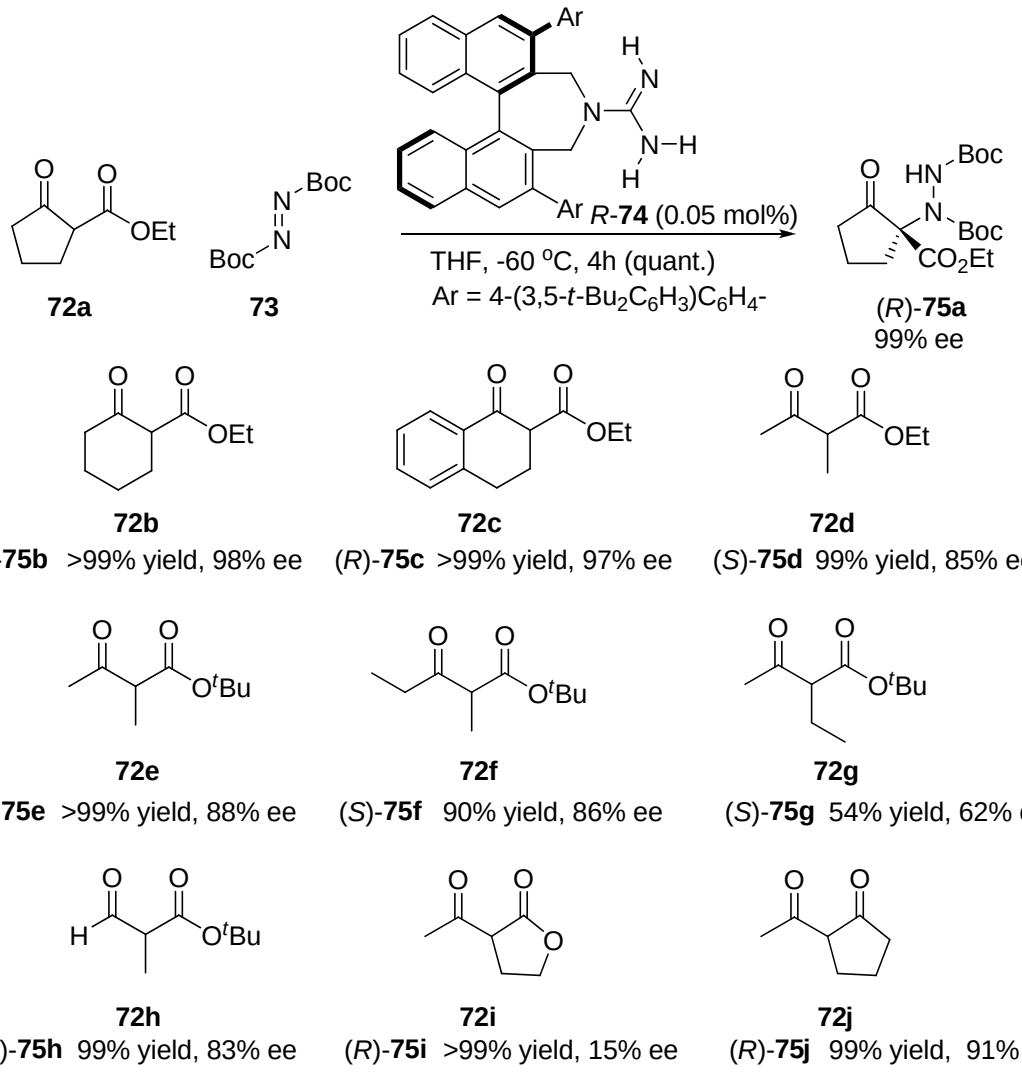

72a **73** (*R*)-**75a** 99% ee

72b (*R*)-**75b** >99% yield, 98% ee

72c (*R*)-**75c** >99% yield, 97% ee

72d (*S*)-**75d** 99% yield, 85% ee

72e (*S*)-**75e** >99% yield, 88% ee

72f (*S*)-**75f** 90% yield, 86% ee

72g (*S*)-**75g** 54% yield, 62% ee

72h (*S*)-**75h** 99% yield, 83% ee

72i (*R*)-**75i** >99% yield, 15% ee

72j (*R*)-**75j** 99% yield, 91% ee

Scheme 1.23. Terada's axially chiral guanidine catalyzed electrophilic aminations reactions.

Later, Terada designed another type of chiral guanidine catalysts, such as (*R*)-**74**, which introduced an axially chiral binaphthyl backbone with a seven-membered-ring structure.[17b] This axially chiral guanidine was found to be a highly efficient catalyst for the electrophilic amination reactions between α-monosubstituted 1,3-dicarbonyl compounds **72** and azodicarboxylate **73** with catalyst loading as low as 0.05 mol% (Scheme 1.23). Cyclic β-keto esters (**72a-c)** with a five or six-membered ring displayed excellent enantioselectivity. Acyclic systems (**72d-f)** with a methyl substituent at the α-position were effective in the present enantioselective catalysis.

The corresponding products (**75d-f**) were obtained in good enantiomeric excess. While the ethyl substituent was employed at the α-position (**72g**), it resulted in a considerable loss of enantioselectivity. 2-Formyl ester (**72h**) was also a useful substrate for this reaction giving the desired product (**75h**) in nearly quantitative yield with 83% ee. Unfortunately, (*R*)-**74** was not effective for β-keto lactone (**72i**) and the enantioselectivity was seriously diminished. In the reaction of 1,3-diketone (**72j**), both excellent yield and high enantioselectivity were obtained. The absolute stereochemistry of cyclic derivative (**75a**) was opposite to that of the acyclic one (**75d**).

Terada also reported 1,4-addition reactions of diphenyl phosphite to nitroalkenes catalyzed by an axially chiral guanidine. It is noteworthy that R and Ar substituents exhibited a strong impact not only on the enantioselectivity but also on the catalytic efficiency (Scheme 1.24).[17c] The enantioselectivity was improved gradually as the alkyl moiety R (**77a-c**) became bulkier. The introduction of 3,5-substituents on the phenyl ring of the Ar substituents was found to be most effective in enhancing both the enantioselectivity and catalytic efficiency (**77d-e**). Further investigation of the temperature and solvent effect, it was revealed that lowering the temperature to -40 ^{o}C resulted in an enhanced enantioselectivity; *tert*-butyl methyl ether was the best solvent among those examined. The catalytic activity of **77e** was prominent; the catalyst loading can be reduced from 5 to 1 mol% without any loss in enantioselectivity (92% ee).

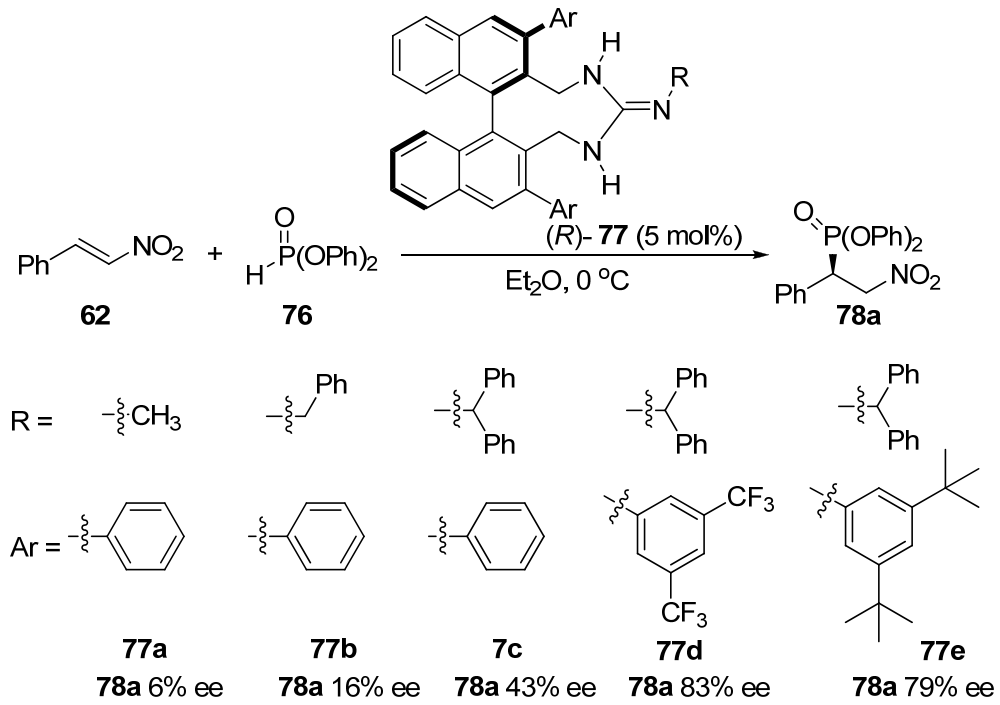

Scheme 1.24. Enantioselective 1, 4-addition reaction of β-nitrostyrene with diphenyl phosphite catalyzed by various axially chiral guanidines.

Under the optimized reaction conditions, the scope of the enantioselective 1,4-addition reaction was investigated using (*R*)-**77e** as a promising catalyst (Scheme 1.25).[17c] A series of nitroalkenes bearing aromatic substituents with various electronic properties proved to be excellent substrates with respect to enantioselectivity and chemical yield. The reaction proceeded smoothly in the presence of 1 mol% catalyst, giving the corresponding product **78b-g** in nearly quantitative yield and high enantioselectivity. In contrast, heteroaromatic-substituted nitroalkenes gave the products (**78h** and **78i**) in modest yield. This problem could be solved by lowering the reaction temperature to -60 ^{o}C and increasing the catalyst loading to 5 mol%. Aliphatic-substituted nitroalkenes exhibited slightly lower enantioselectivities than those of their aromatic counterparts (**78j-l**).

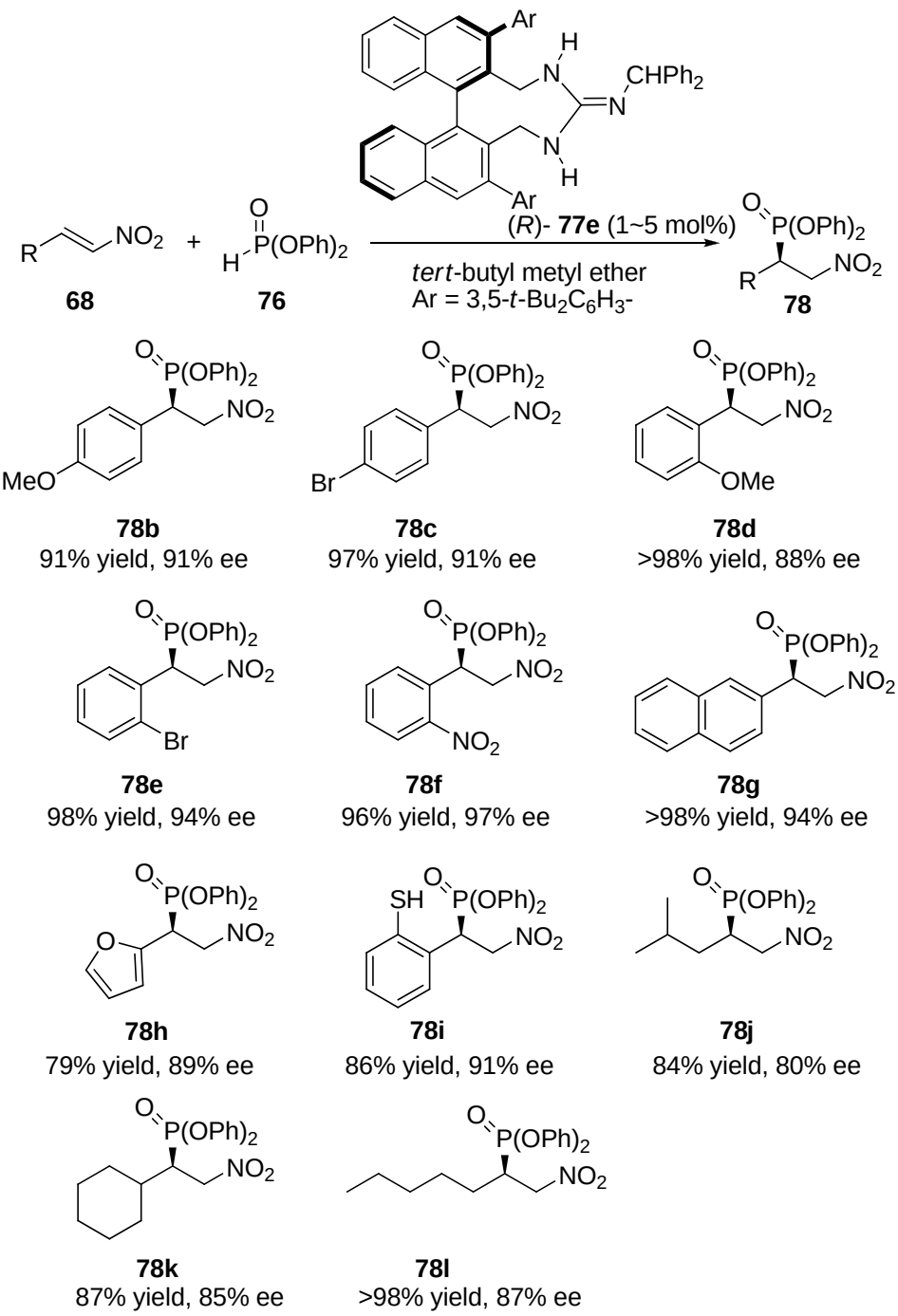

Scheme 1.25. Terada's axially chiral guanidine catalyzed 1, 4-addition reactions of diphenyl phosphite to various nitroalkenes.

1.3 Phase-transfer guanidine

In 2003, Murphy[12] reported that tetracyclic guanidinium salt **42** catalyzed the phase transfer epoxidation of chalcones **26a** and **26b**. High enantioselectivities were

obtained for the products **28a** (93% ee) and **28b** (91% ee) as shown in Scheme 1.26.

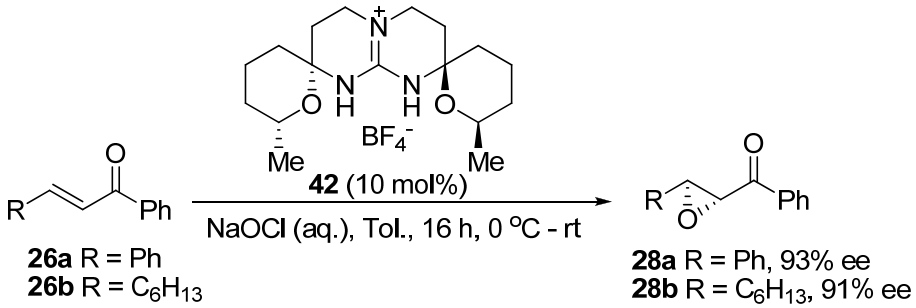

Scheme 1.26. Guanidinium salt catalyzed phase transfer epoxidation.

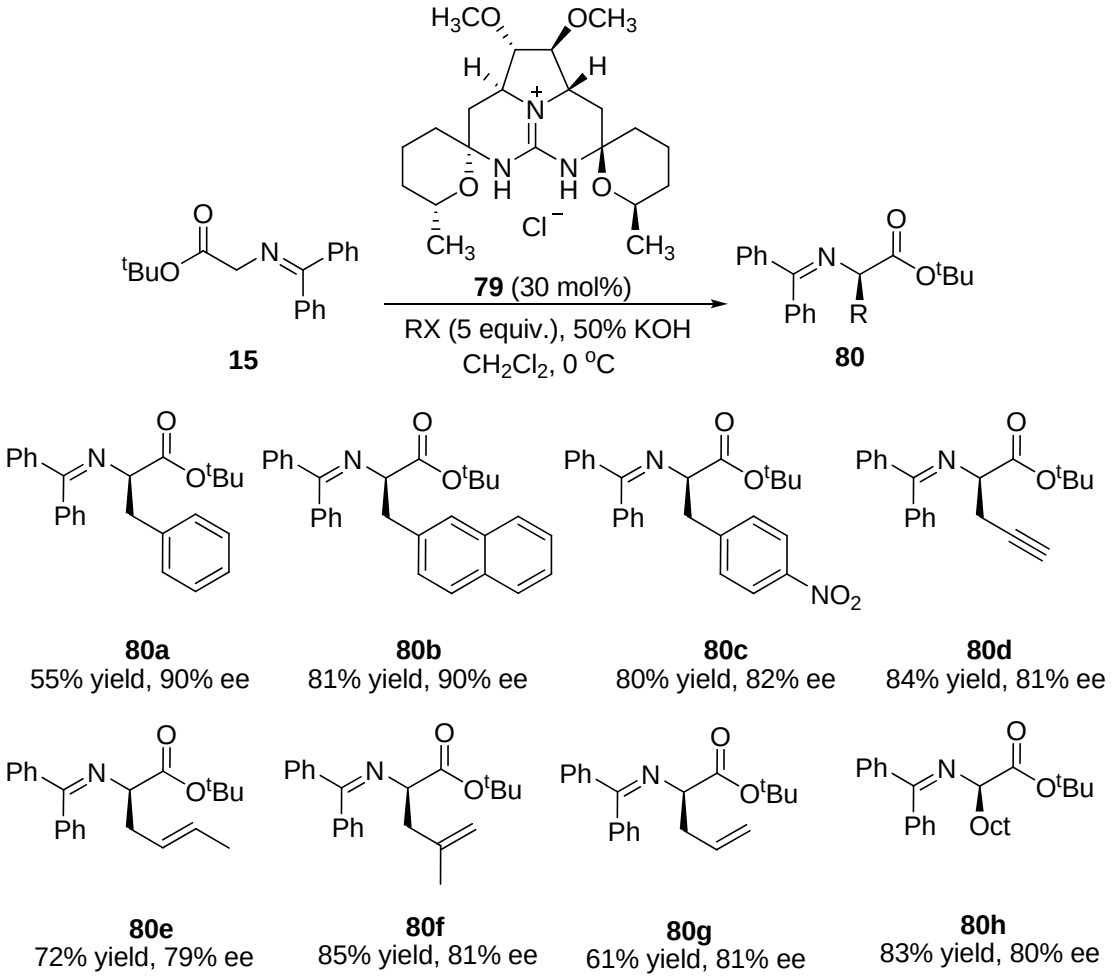

Scheme 1.27. Chiral pentacyclic guanidinium salt catalyzed phase transfer alkylation.

Based on the marine natural product ptilomycalin A and related products, Nagasawa designed a series of C_2-symmetrical pentacyclic guanidiniums.[18] In the presence of 30 mol% of **79** and under phase transfer conditions, glycinate **15**

underwent alkylation reaction with various alkyl halides (Scheme 1.27). (*R*)-**80** was generated as the major product in 80 - 90% ee. The yields were generally moderate to good (55 – 85%), although the reaction usually completed in 95 - 140 hours. It was observed that the stereochemical outcome was controlled by the configuration of the spiro-ether rings of the guanidinium catalyst. The substituent (methyl group) on the spiro ether rings of **79** was found to play a key role in effective asymmetric induction.

Murphy[12] also reported that tetracyclic guanidinium **42**, which is a subunit of **79**, catalyzed the phase transfer alkylation between glycinate **15** and benzyl bromide to afford (*R*)-**80a** in 86% ee (Scheme 1.28). The catalyst was found to be robust and recyclable.

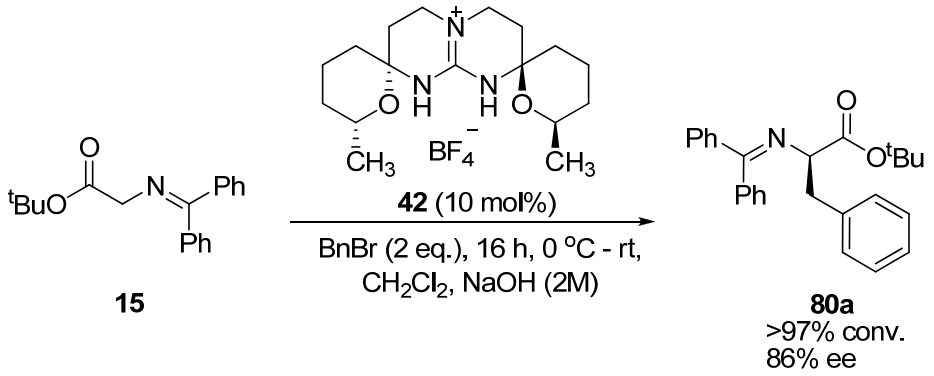

Scheme 1.28. Chiral tetracyclic guanidinium salt catalyzed phase transfer alkylation.

1.4 Guanidine-Thiourea Bifunctional catalyst

Nagasawa[19a] recently developed a highly diastereoselective Henry reaction. Under phase transfer conditions, (*R*, *R*)-**82**, a guanidinium salt with two thiourea groups, effectively catalyzed the Henry reaction between various α-substituted aldehydes and nitromethane **6** (Scheme 1.29). In the reactions of *N*, *N*-dibenzyl α-amino aldehydes, the *anti*-nitro alcohols (e.g. **11e-g**) were obtained in high

diastereoselectivities and high yields. However, low yield was obtained with the bulky β-branched aldehyde **11a** (R = *i*Pr). Reactions between **81** and nitromethane **6** proceeded to give the products with good diastereoselectivities and high yields (e.g. **83a**, **b**).

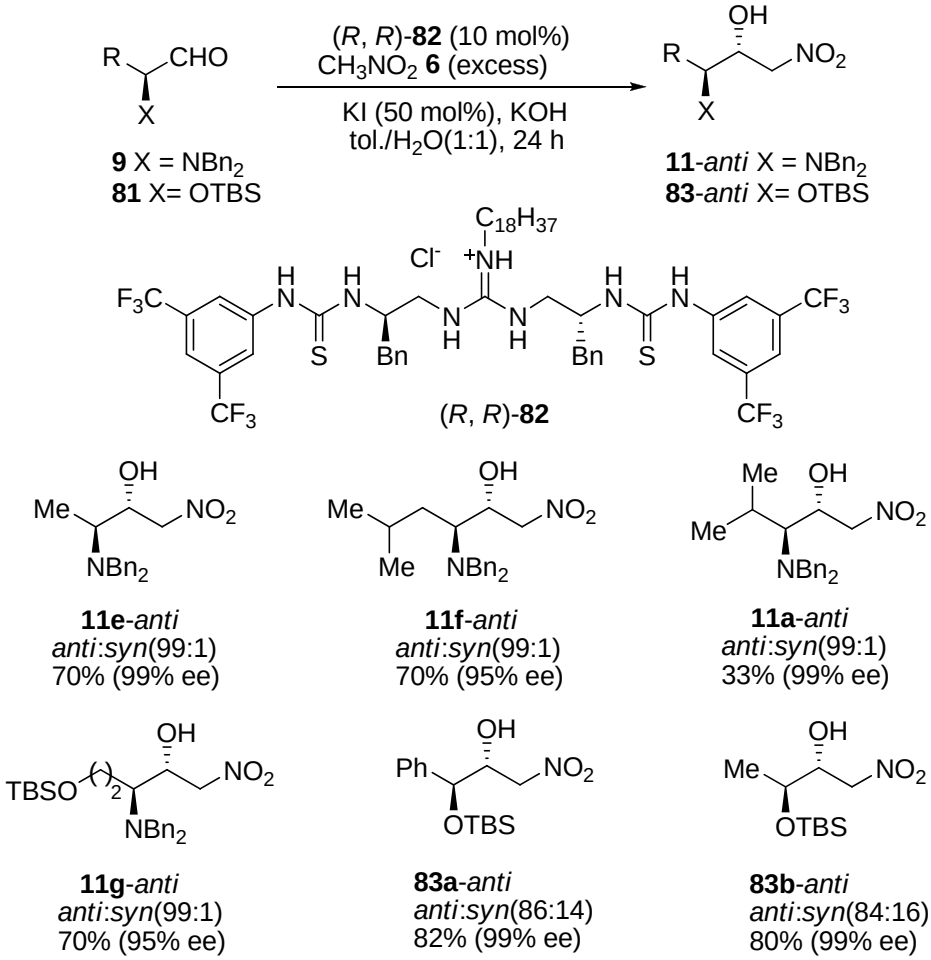

Scheme 1.29. Diastereoselective Henry reaction catalyzed by a guanidine-thiourea catalyst.

In 2005, Nagasawa reported a guanidine-thiourea bifunctional organocatalyst for the asymmetric Henry (nitroaldol) reaction (Scheme 1.30).[19b] The reaction works well with aliphatic cyclic and α-branched-chain aldehydes in high yield and high ee of 82-88%. However, the unbranched aliphatic aldehyde gave the adduct **8h** in moderate

enantiomeric excess of 55%. The reaction rate can be controlled by changing the amount of KOH. In case of reactive aldehyde, a lower amount of KOH (5-10 mol%) probably contributed to high asymmetric inductions by reducing the reaction rate.

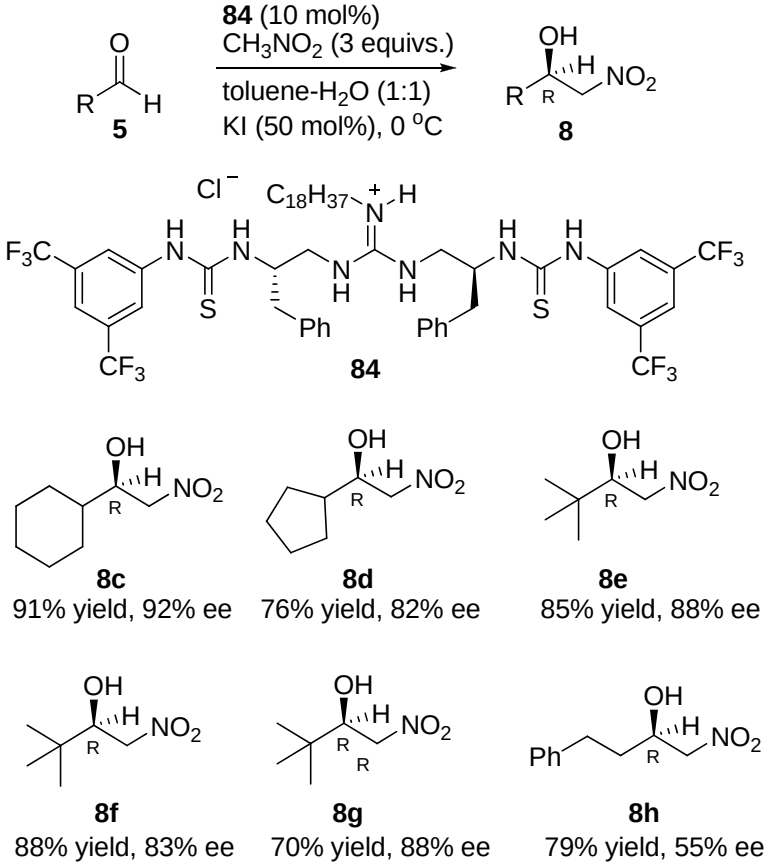

Scheme 1.30. Asymmetric Henry reaction catalyzed by guanidine-thiourea organocatalyst.

1.6 Summary

Chiral guanidines function as effective Brønsted base catalysts for a variety of reactions. It is best demonstrated in Terada's axially chiral guanidine (*R*)-**70** catalyzed Michael reaction of nitroalkenes, Lipton's dipeptide **13** and Corey's bicyclic guanidine **51** catalyzed Strecker reaction. Chiral guanidinium salts are also effective phase transfer catalysts, as represented by Nagasawa's pentacyclic guanidinium **79** catalyzed phase transfer alkylation of glycinate **15**.

There are less successful examples that utilize acyclic guanidines, which are structurally less rigid than mono-polycyclic guanidines. However, currently available methods for the preparation of chiral bicyclic, tetracyclic and pentacyclic guanidines are generally lengthy, which tends to impede catalyst supply for methodology studies.

Chapter 2

(I) Brønsted-Base Catalyzed Diels-Alder Reaction

(II) Chiral Bicyclic Guanidine Catalyzed Diels–Alder Reactions of Anthrones

2.1 Brønsted-Base Catalyzed Diels-Alder Reaction

2.1.1 Introduction

Diels–Alder reaction provides an important access to complex carbocycles, and represents arguably one of the most powerful approaches in organic chemistry. In particular, the asymmetric variants have received unprecedented attention.[20,21] They have proven to be versatile means to synthesize a large number of important chiral building blocks, e.g. intermediates in the total synthesis of natural products.[22] Many groups have put extensive research effort on the chiral Lewis-acid catalyzed asymmetric Diels–Alder reactions. The state of the art of the asymmetric Lewis-acid catalyzed Diels–Alder reactions has been reviewed.[20c]

Organocatalysts have been shown in recent years to promote a large range of reactions including most C-C bond formation reactions.[23] Organocatalysts are less toxic, easy to handle, generally air and moisture tolerable, and have been applied to large-scale synthesis.

It is common for catalytic Diels–Alder reactions to proceed by using a Lewis acid catalyst to lower the LUMO of the dienophile. However, base-catalyzed Diels–Alder reaction works in a different manner; the base catalytically activates the diene to give a higher HOMO level.[25,35]

2.1.2 Brønsted Base catalyzed reactions of pyrones

Okamura was first to show that Brønsted bases such as Et_3N can promote the Diels–Alder reaction of 3-hydroxy-2-pyrones **85** and electron-deficient dienophiles, giving cycloadducts **86** in nearly quantitative yields (Scheme 2.1).[24a] When

N-methylmaleimide **20a** was used as the dienophile, initial screening of chiral amino alcohols revealed that cinchonidine **87** was an effective promotor; *endo*-**86a** was always formed as the major diastereomer.[24b] Under optimized reaction conditions, this asymmetric reaction afforded *endo*-**86a** in 98% yield with 77% ee, and a diastereomeric ratio (*endo*:*exo*) of 11:1 (Scheme 2.2).[24b] Reducing the amount of catalyst to 10 mol% still gave the desired product in high yield (100% yield) but with lower enantioselectivity (66% ee) and diastereoselectivity. When cinchonine was used as the catalyst, the opposite enantiomer was obtained in 95% yield and with 71% ee.

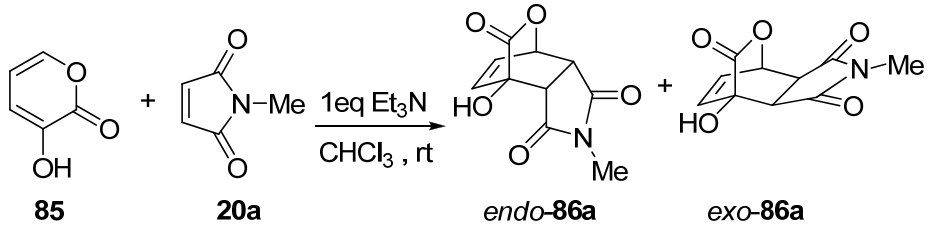

Scheme 2.1. Base catalyzed Diels–Alder reaction of 3-hydroxy-2-pyrone.

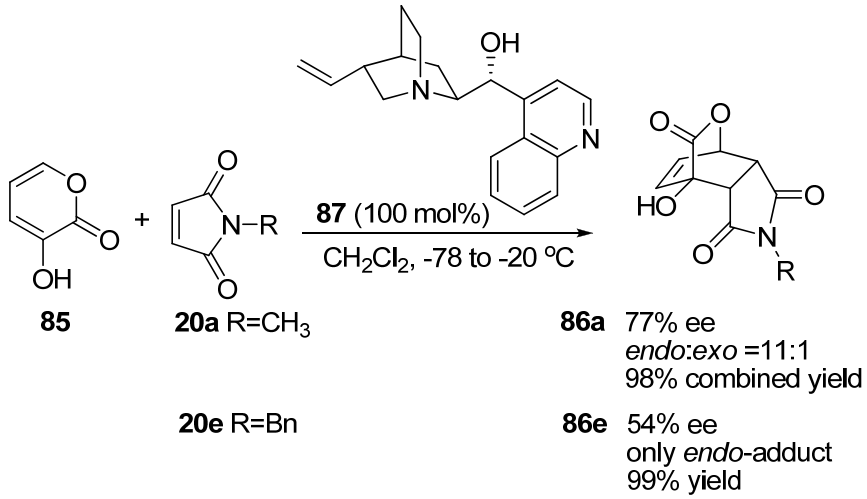

Scheme 2.2. Asymmetric Diels–Alder reaction of 3-hydroxy-2-pyrone.

The reaction with *N*-benzylmaleimide **20e** afforded the *endo*-**86e** in 99% yield with 54% ee when cinchonidine **87** was used as a promotor (Scheme 2.2).[24c] No *exo*-adduct was observed in this reaction. The enantioselectivity was improved to 63%

ee when quinine (1 equiv.) was used. When the catalyst loading was decreased to 30 mol%, nearly comparable enantioselectivity of 59% ee was obtained, but the reaction was slower. The enantioselectivity afforded by natural cinchona alkaloids was modest. Okamura proposed that the mode of action by natural cinchona alkaloids was to activate and orientate **85** in the Diels–Alder reaction.

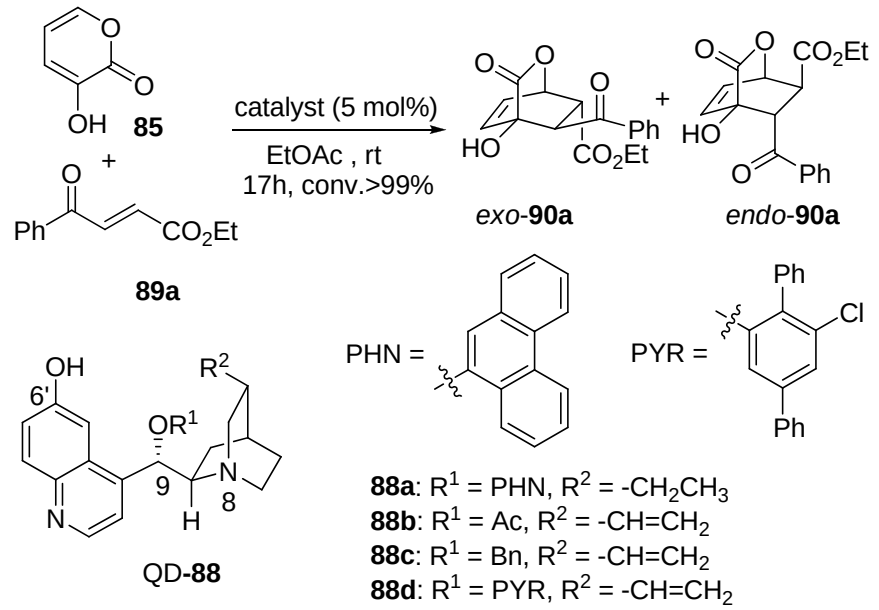

entry	catalyst	dr[a] *exo*:*endo*	ee (%)[a] of *exo*-**95a**	entry	catalyst	dr[a] *exo*:*endo*	ee (%)[a] of *exo*-**90a**
1	quinidine	66:34	5	5	QD-**88c**	87:13	80
2	cinchonine	62:38	-5	6	QD-**88d**	85:15	82
3	DHQD-PHN	66:34	33	7	QD-**88a**	88:12	88
4	QD-**88b**	90:10	57	8[b]	QD-**88a**	93:7	89

[a] In crude reaction mixture. [b] Reaction was run in Et_2O

Scheme 2.3. Cinchona alkaloids catalyzed Diels–Alder reaction of 3-hydroxy-2-pyrone.

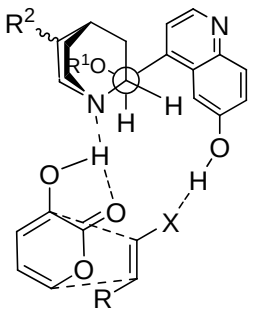

Figure 2.1. Bifunctional catalysis for Diels-Alder reactions of 2-pyrone **85**.

Deng reported the first highly enantioselective and diastereoselective asymmetric Diels–Alder reactions of pyrones with various cinchona alkaloid-based bifunctional catalysts.[25] It was found that 6′-OH cinchona alkaloids **88a-d** afforded significantly better catalytic efficiency than the natural cinchona alkaloids (Scheme 2.3). The structure of the tunable 9-substituent are equally important for high enantioselectivities. The best result was obtained with 5 mol% of catalyst **88a**; the adduct *exo*-**90a** was obtained in 93:7 dr and 89% ee (Scheme 2.3, entry 8). It was proposed that **88a** simultaneously raises the HOMO of the pyrone and lowers the LUMO of the dienophile while orienting the two reagents to exert stereochemistry control (Figure 2.1).

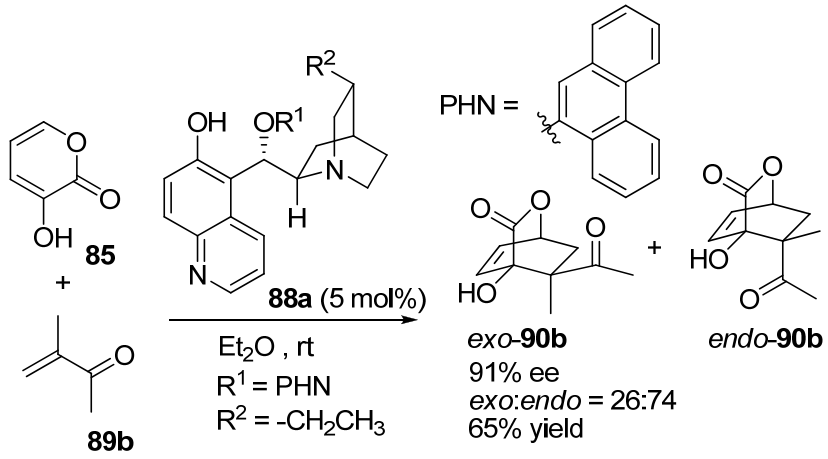

Scheme 2.4. Diels–Alder reaction between 3-hydroxy-2-pyrone with unreactive dienophile catalyzed by **88a**.

Catalyst **88a** was found to tolerate a significant degree of alterations in both pyrones and dienophiles. The reactions between pyrone **85** and dienophiles of different substitution patterns proceeded very well. It is noteworthy that even the relatively unreactive dienophile **89b** could be employed in this reaction, thereby generating optically active chiral building blocks containing two adjacent

tetra-substituted stereocenters (Scheme 2.4).[25] Moreover, catalyst **88a** was able to furnish useful levels of enantioselectivity and diastereoselectivity for reactions between dienophile **89a** and pyrones **85** bearing various substituents.

However, catalyst **88a** was not useful for the reaction of **85** with fumaronitrile **89c**. Although the 9-thiourea cinchona alkaloid **91** was found to be ineffective for the reaction between **85** and **89a**, it greatly improved the enantioselectivity and diastereoselectivity of the reaction between pyrone **85** and fumaronitrile **89c**. The adduct *exo*-**90c** was obtained in 85% yield with 92% ee and >97:3 dr (Scheme 2.5).[25] The reaction also worked well with maleonitrile **89d** which illustrated the ability of **91** to tolerate dienophiles with either an *E*- or a *Z*-double bond. It is remarkable that these reactions are stereospecific with respect to the geometry of the double bond. These results are consistent with a concerted cycloaddition mechanism.[24a]

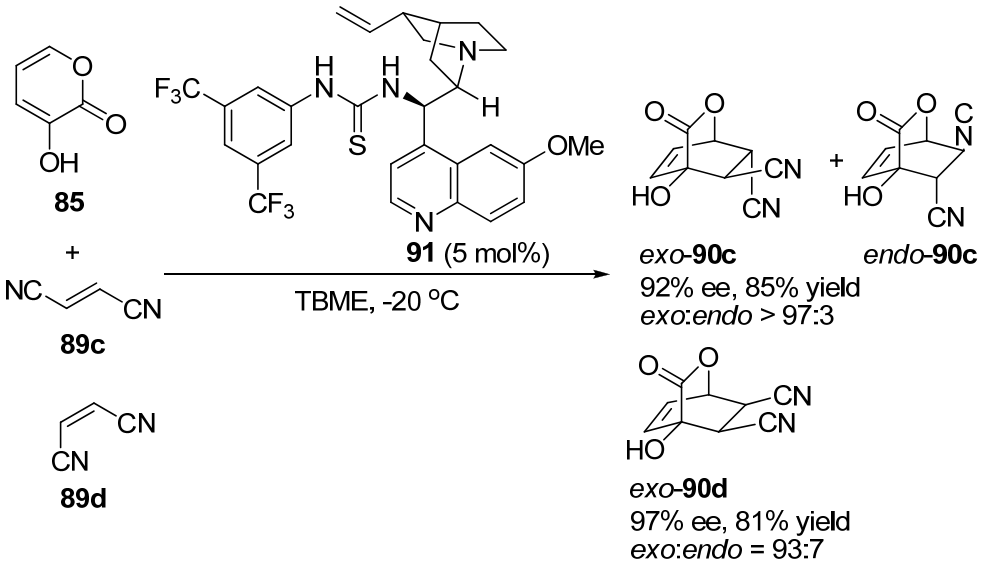

Scheme 2.5. Diels–Alder reaction of 3-hydroxy-2-pyrone catalyzed by **91**.

Okamura reported an asymmetric Diels-Alder reaction between 3-hydroxy-2-pyrone **85** and an optically active acrylate **92**, which afforded a highly

functionalized adduct **93** in almost quantitative yield with >95% de (Scheme 2.6).[26a] The adduct **93** is a useful starting material for the synthesis of various cyclohexene oxides[27b,27c] such as (+)-epiepoformin **98**[27] and (–)-theobroxid **100**[28] (Scheme 2.7).

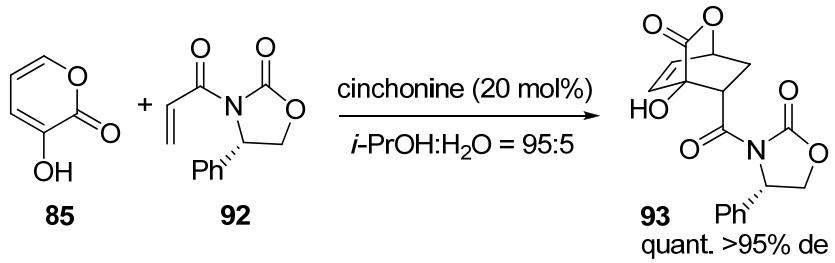

Scheme 2.6. Asymmetric base-catalyzed Diels–Alder reaction of 3-hydroxy-2-pyrone with chiral acrylated derivatives.

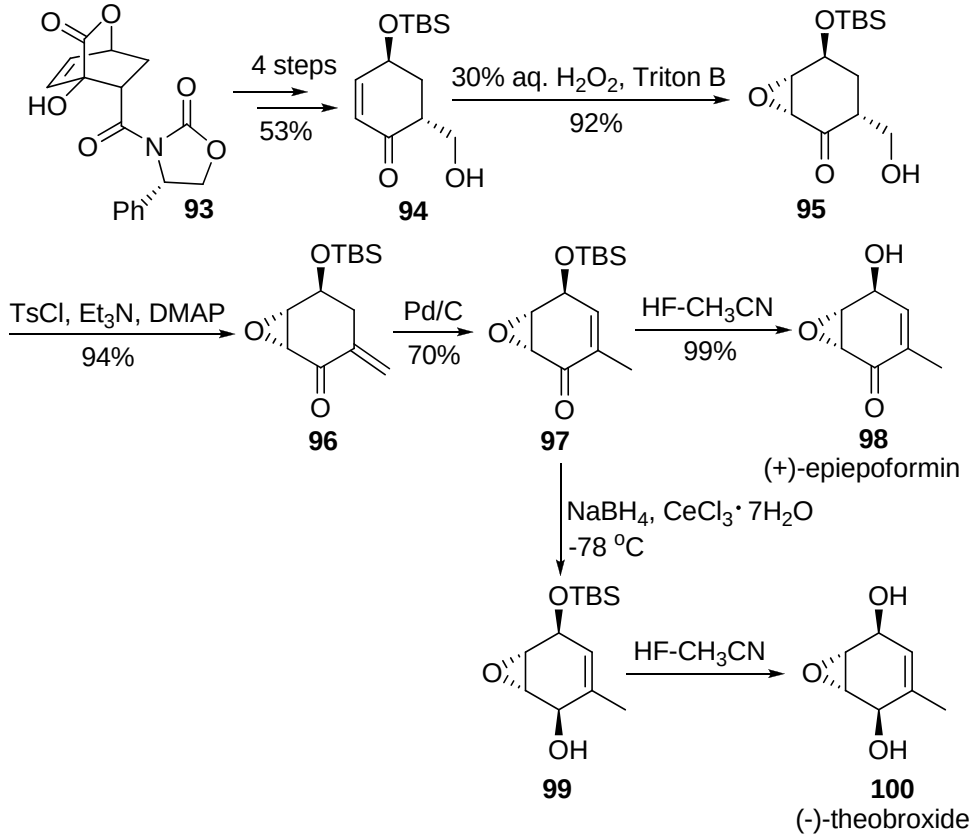

Scheme 2.7. Synthesis of (+)-epiepoformin and (–)-theobroxide.

2.1.3 Brønsted Base-catalyzed reactions of *N*-substituted-3-hydroxy-2-pyridone

In a similar fashion, Diels–Alder reactions between *N*-tosyl-3-hydroxy-2-pyridone **101** and electron deficient dienophile can also be

catalyzed by a base.[29] When Et_3N was used as catalyst, the reaction of **101** and *N*-methylmaleimide **20a** afforded an almost quantitative amount of *endo*-adduct within 0.5 hr (Scheme 2.8). The catalyst was also effective for the reactions with less reactive dienophiles, such as methyl acrylate **102a** and 3-buten-2-one **102b**.

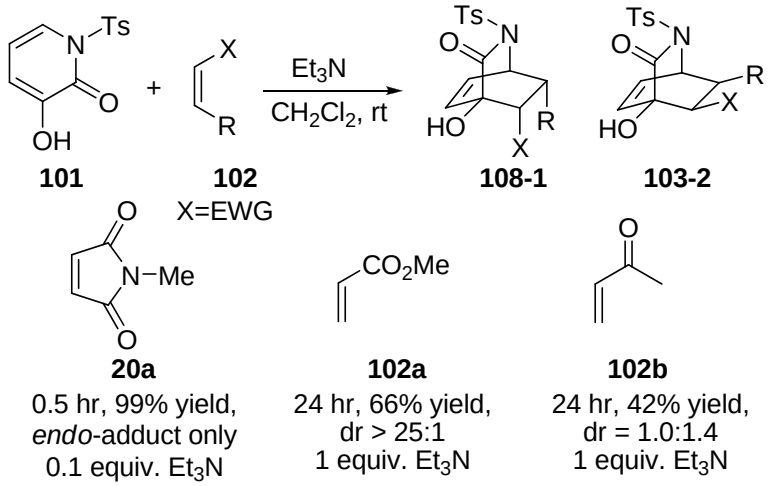

Scheme 2.8. Base-catalyzed reactions of *N*-tosyl-3-hydroxy-2-pyrone.

The *endo* selectivity of these reactions was very high, because the sterically bulky substituent produced an unfavorable interaction with the dienophile during its *exo* approach.[29] The bulkiness of the base catalyst also sterically influenced the approaching dienophile. In fact, a slightly lower *endo* selectivity was observed for the reaction using the sterically less hindered *t*-$BuNH_2$. Stronger inorganic bases such as *n*-BuLi were more effective than the amine catalysts for the reaction with **20a**. Using *n*-BuLi as the catalyst, the reaction was faster and gave higher yield of product. However, *n*-BuLi was not effective for the reactions with olefins such as methyl acrylate **102a** and 3-buten-2-one **102b**, probably due to the base instability of the dienophiles.

The resulting product of the reaction between **101** and **20a** catalyzed by Et_3N is a

highly functionalized bicyclic lactam, and is a useful building block to synthesize *pseudo*-aminosugars. (±)-Validamine is a biologically active *pseudo*-aminosugars, first isolated as a degradation product of a strong antibiotic, validamycin A in 1971.[30] The synthesis of the key intermediate **106** was shown in Scheme 2.9.[31] It was obtained as the exclusive product in good yield. Three validamine type compounds were synthesized *via* the key intermediate **106**. It was easily obtained from the bicyclic lactam **103b**, resulted from a Diels–Alder reaction between pyridone **101** with methyl acrylate **102a** (Scheme 2.9).

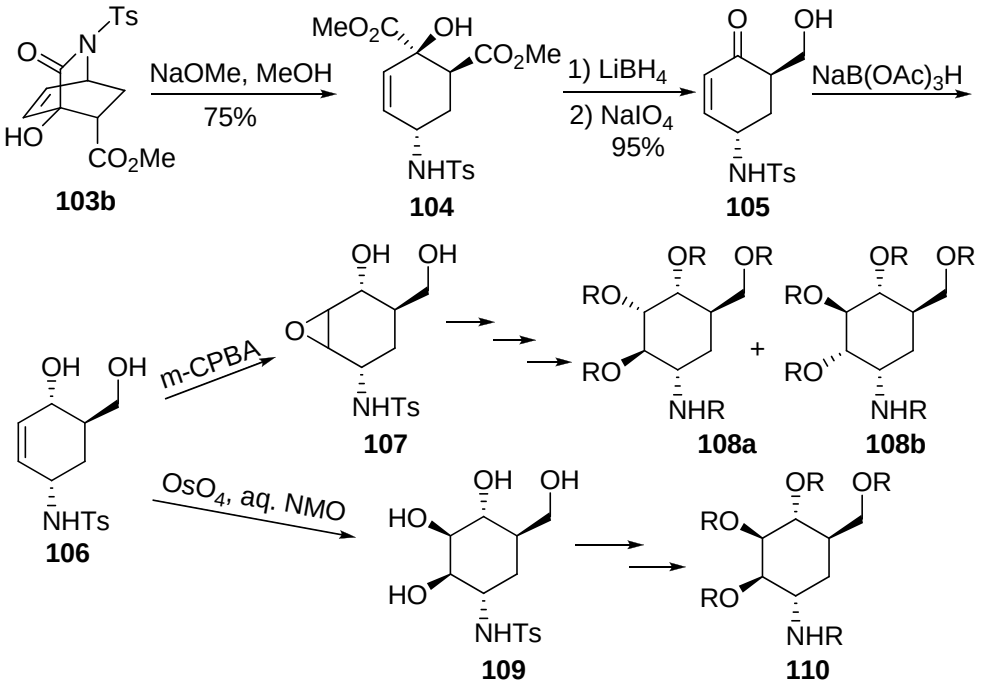

Scheme 2.9. Synthetic route of three validamine type compounds.

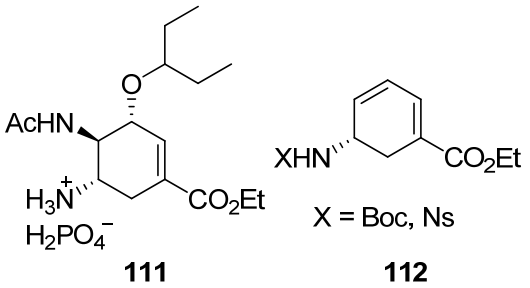

Fig. 2.2. Tamiflu and Corey's intermediate.

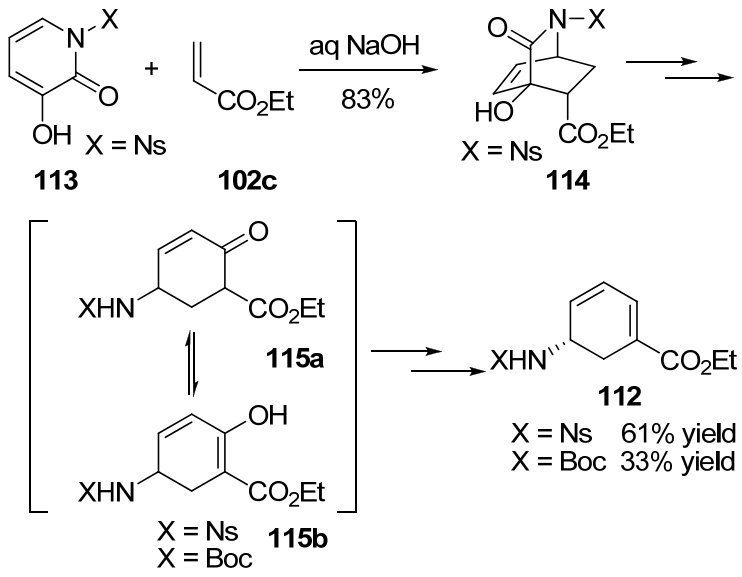

Scheme 2.10. Synthesis of Tamiflu intermediates.

Tamiflu **111** (Fig. 2.2) is a potent neuraminidase inhibitor and the most widely used anti-influenza drug. Influenza viruses with reduced sensitivity to neuraminidase inhibitors have been reported recently.[32] The syntheses of modified tamiflu are thus of high interest. Okamura reported a short and efficient synthesis of Corey's intermediate **112**[33] (Scheme 2.10).[34] The Diels–Alder adduct **114** was easily obtained from an aqueous "green" Diels–Alder reaction that was possible to scale-up to multigram quantity without significant loss of the yield. Only four steps are required to prepare **112** and inexpensive reagents were used (Scheme 2.10).[34]

2.1.4 Brønsted Base catalyzed reactions of anthrones

Rickborn was first to report the base catalyzed reactions between anthrone and various dienophiles (Scheme 2.11).[35] The reactions were believed to follow a concerted mechanism *via* an intermediate oxyanion to give Diels–Alder adducts. 1,8-Dihydroxy-9-anthrone (Dithranol) **116** was observed to favour Michael adducts instead (Scheme 2.11).

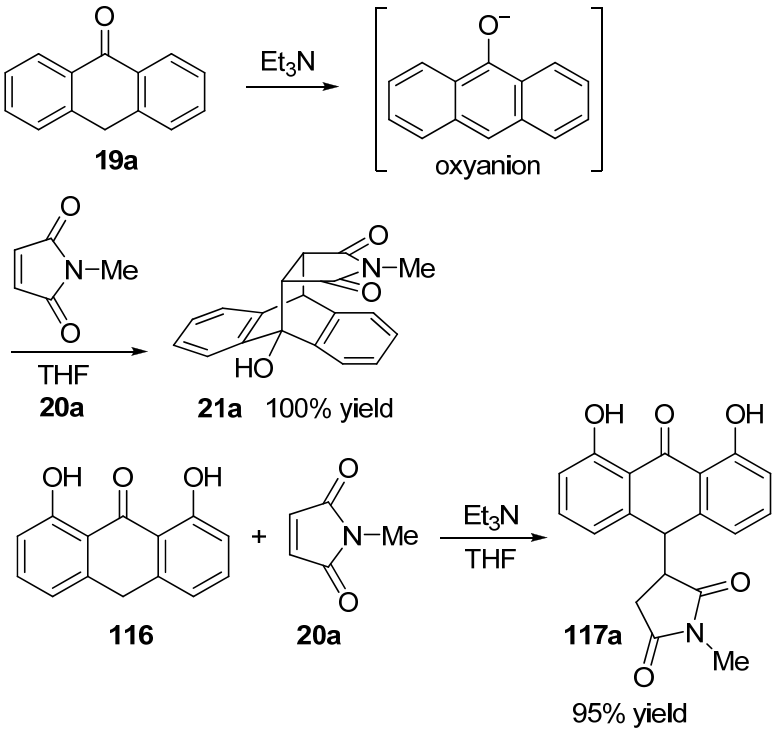

Scheme 2.11. Base catalyzed reactions of anthrones.

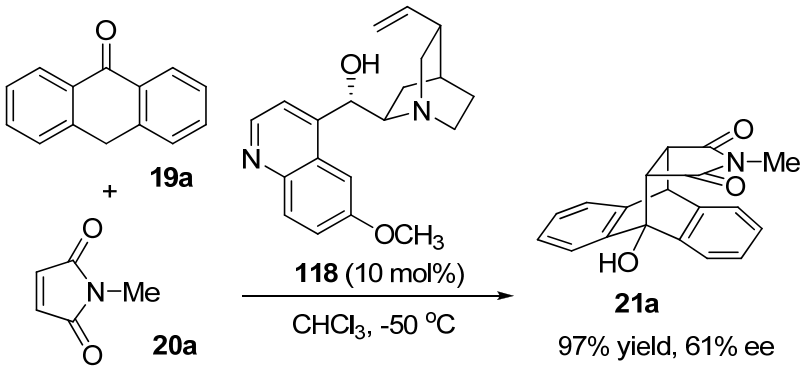

Scheme 2.12. Alkaloid catalyzed Diels–Alder reaction of anthrone.

The first asymmetric catalytic Diels–Alder reaction of anthrones was reported by Kagan in 1989.[36a] Alkaloid bases, prolinol and *N*-methylephedrine were investigated as organocatalysts. In the presence of 1-10 mol% of these chiral catalysts, anthrone **19a** reacted as a masked diene with *N*-methylmaleimide **20a**. The best result was obtained with 10 mol% quinidine **118** in chloroform at -50 °C; the desired product **21a** was obtained in 97% yield and 61% ee (Scheme 2.12). During their study, Kagan also observed that the free hydroxyl group in the alkaloid organocatalyst was essential if

high enantioselectivity was to be achieved.

A detailed study of the reaction conditions was subsequently conducted using different cinchona alkaloids as catalysts.[36b] Lower temperature and less polar solvent would result in better enantioselectivities. The range of dienophile substrates was also studied. Much slower reaction rates were observed when methyl acrylate (0% ee) and methyl fumarate (30% ee) were used. When methyl maleate was used as the dienophile, no reaction was observed.

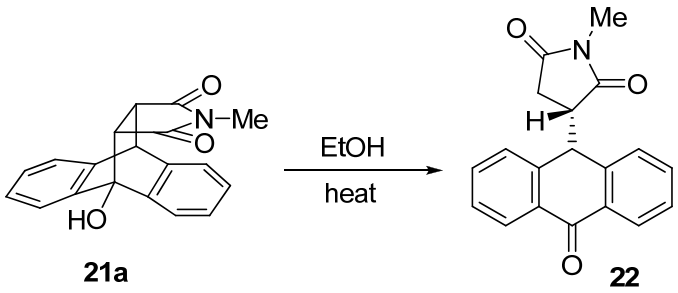

Figure 2.3. Transformation between **21a** and **22**.

In the catalytic reaction of anthrone **19a** with N-methylmaleimide **20a**, the product is almost exclusively the cycloadduct **21a** in the presence of catalytic amount of chiral amines. While a stoichiometric amount of insoluble base (KF) and a catalytic amount of N-benzylquinium chloride (Quibec) provides exclusively the Michael adduct **22**. This raises the possibility of a two-step mechanism for the asymmetric synthesis of **21a** (Michael addition followed by an intramolecular aldolization).[36b] Rickborn and Koerner have demonstrated that cycloadduct **21a** is transformed into Michael adduct **22** under the catalytic influence of Et_3N in methanol.[35] It was also observed by Riant and Kagan that **21a** is converted into **22** by heating in ethanol (Figure 2.3). The formation of Michael adduct **22** in the presence of KF/Quibec is

explained by a further transformation of the initially produced cycloadduct **21a**. When the reaction between **19a** and **20a** catalyzed by KF/Quibec was carried out in dichloromethane at -78 ^{o}C, **21a** is the only product at 40% conversion and there is no Michael adduct formed. The result of the mechanistic studies was in agreement with a concerted [4+2] cycloaddition process. Hydrogen bonding during transition state was proposed to be essential for chiral recognition.

Enantioselectivities of anthrone reactions have been improved with other catalysts such as C_2-symmetrical chiral pyrrolidine **119**.[37] Yamamoto reported a double asymmetric synthetic approach using chiral *N*-substituted maleimides with C_2-chiral pyrrolidine **119** as catalyst. In this reaction, **21b-2** was isolated as the major isomer, and a maximum de of 80% was obtained (Scheme 2.13).[37a]

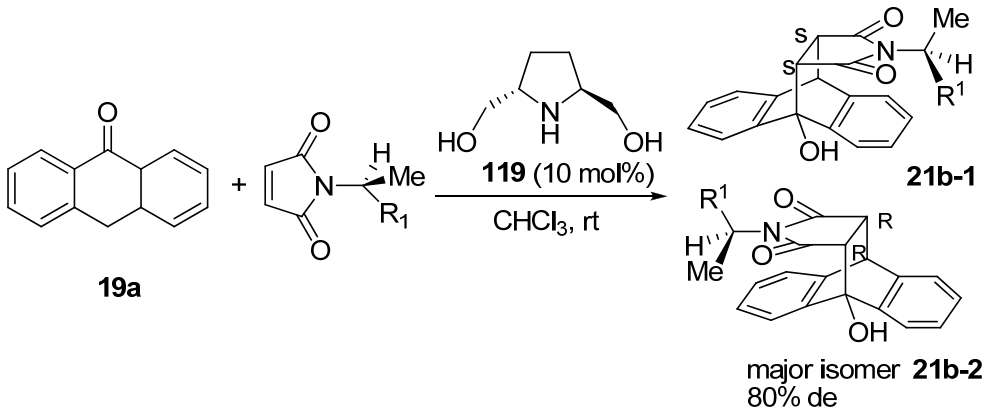

Scheme 2.13. Double asymmetric synthesis with chiral *N*-substituted meleimides and C_2-pyrrolidine.

Various pyrrolidine derivatives were examined for the reaction between anthrone and maleimides. The best asymmetric induction of 87% ee was attained when *N*-4-pyridylmethyl-2,5-bis(hydroxymethyl) pyrrolidine **120** was used in the reaction of anthrone **19a** with 2-*tert*-butyl-phenylmaleimide (Scheme 2.14).[37b] The high

selectivity is partly due to the conformation in which the aromatic ring is perpendicular to the maleimide ring and one face of the latter is shielded by the ^{t}Bu group.

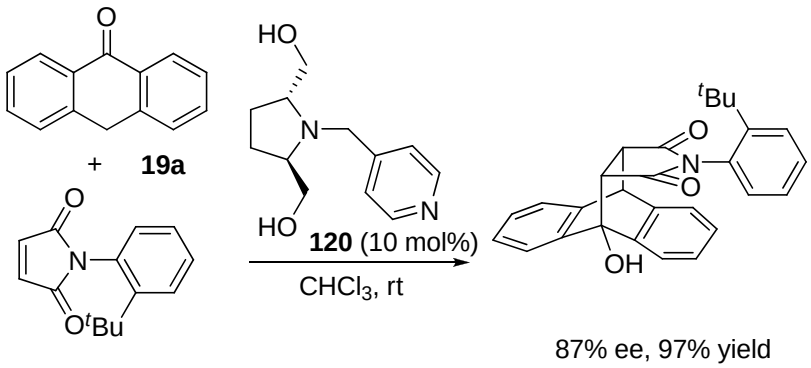

Scheme 2.14. Hydroxy-pyrrolidine catalyzed Diels-Alder reaction between anthrone and phenylmaleimide.

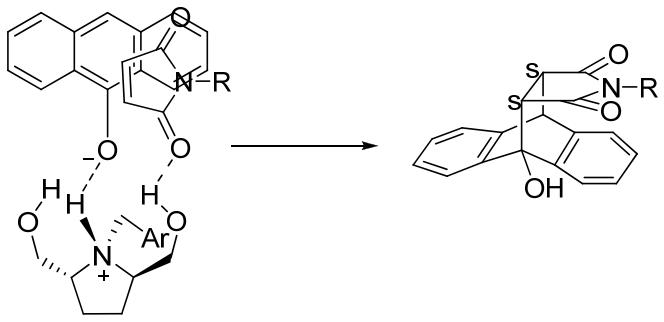

Fig. 2.4. Transition state model for pyrrolidine catalyzed Diels–Alder reaction of anthrones.

Yamamoto presented a tentative transition state model, which affords the (*S,S*)-product (Fig. 2.4).[37b] The protonated pyrrolidine catalyst interacts with the activated diene through ionic interactions and hydrogen bonds.[36b] It is noteworthy that high enantioselectivity is attained only when the catalysts have hydroxyl groups and the reaction is effected in aprotic solvents. This fact indicates the importance of another hydrogen bond in the transition state. When the maleimide approaches from the upper-right direction, the transition state should be stabilized by the hydrogen bond between a carbonyl group of the maleimide and a hydroxyl group of the catalyst.

On the other hand, such stabilization cannot be expected when the maleimide attacks from the upper-left direction. Because the catalysts are of C_2-symmetry, the same stereochemical consideration can be applied to the approach from the lower side. Consequently, the (*S*, *S*)-products are afforded preferentially.

The Diels–Alder adducts obtained could be used as chiral templates to prepare α,β-unsaturated lactams.[38] In addition, dithranol **116** derivatives have been shown to possess antipsoriatic and antiproliferative activity.[39]

2.1.5 Summary

Recent developments in the area of base-catalyzed Diels–Alder reactions have been summarized. The use of Brønsted bases to catalyse the Diels–Alder reactions is a less established approach. Despite several important achievements in this field, the results of Brønsted-base catalyzed reactions of anthrones were not excellent. Therefore, we are interested to investigate the anthrone reactions further and attempt to improve the enantioselectivity.

2.2 Chiral Bicyclic Guanidine Catalyzed Diels–Alder Reactions of Anthrones

2.2.1 Synthesis of anthrone derivatives

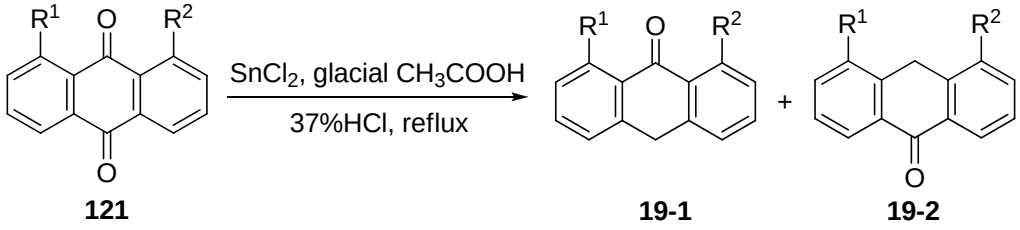

121 **19-1** **19-2**

Scheme 2.15. Standard synthesis of anthrone derivatives.

Many studies have been done on various reduction methods of substituted

anthraquinones, e.g. $Zn/NH_3(aq)$ or $NaBH_4$. Most of them are not selective providing mixture of different products like dihydroanthracenediols or dihydroanthracenes.[40b-d] But $SnCl_2$ mediated reduction was found to be selective towards the formation of anthrones. Thus the required anthrone derivatives were synthesized from their corresponding anthraquinones **121** using an established protocol (Scheme 2.15).[40a]

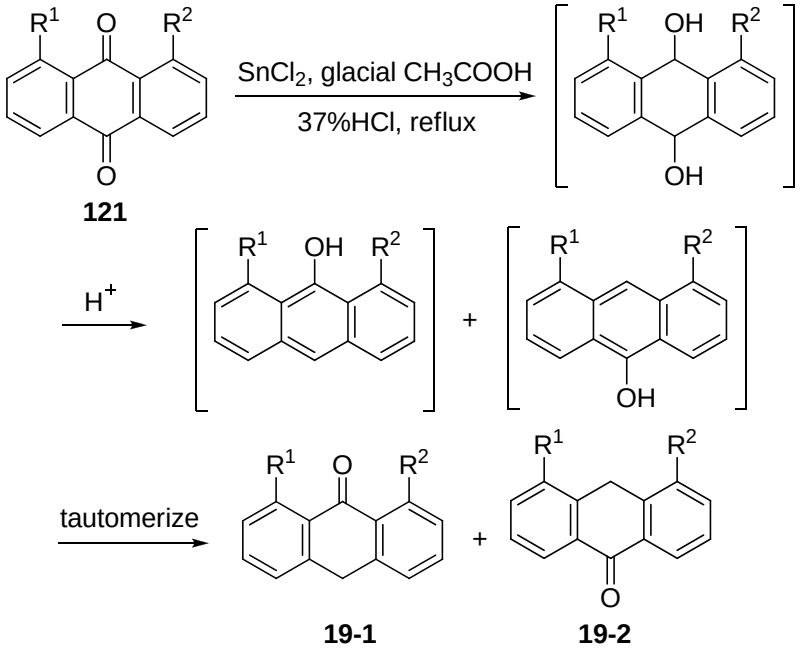

Scheme 2.16. Mechanism for the formation of anthrone derivatives from anthroquinones.[40e]

In this reaction, initially stannous dichloride reduces quinones to diols, followed by *in situ* dehydration of either hydroxyl group with hydrochloric acid. The conjugated enol then tautomerizes to its keto form (Scheme 2.16). It produces two substituted anthrones at a high combined yield of more than 90%. Thin layer chromatography (TLC) shows that the two products spots are quite far apart, thus they could be easily separated by a simple column chromatography. If the substitution groups are electron withdrawing, e.g. chloro, anthrone **19b** is much more polar than anthrone **19c**. Since in anthrone **19c**, the opposite dipole moments of the carbonyl

group and substituents cancel out.

The ratio of anthrones **19-1** and **19-2** depends on the energy differences of the transition states, which means the ability of hydroxyl group to form H-bonding with the neighboring substituents. As hydroxyl group can not form H-bonding with Cl, the energy difference between the transition states of anthrone **19b** and anthrone **19c** are almost the same, as expected, the ratio of anthrone **19b** and **19c** is 1:1 (Table 2.1, entry 1). In the transition state of anthrone **19e**, the hydrogen atom of hydroxyl group forms a hydrogen bond with the nitrogen of amino group. Thus anthrone **19e** is more favourable than anthrone **19f** (no H-bonding) leading to **19e** and **19f** in ratio of 3:1 (Table 2.1, entry 2). In the transition state of anthrone **19g**, the hydroxyl group forms very strong H-bonding with two neighbouring OH groups and hence specifically results in only one product (Table 2.1, entry 3).

Table 2.1. Synthesis of various anthrones.

entry	anthraquinone	R^1	R^2	yield/%[a]	ratio of **19-1:19-2**
1	**121a**	Cl	Cl	91	**19b**:**19c** = 1:1
2	**121b**	HNMe	H	94	**19e**: **19f** = 3:1
3	**121c**	OH	OH	96	**19g**:**19h** = 1:0

[a] Combined and isolated yield.

2.2.2 The effects of the catalyst structure on the enantioselectivity

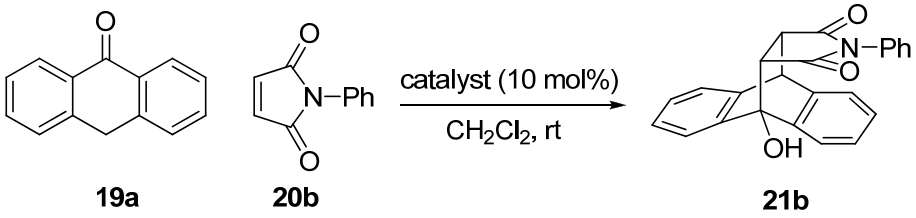

19a **20b** **21b**

Scheme 2.17. Catalytic asymmetric Diels–Alder reaction of anthrone **19a** with *N*-phenylmaleimide **20b**.

Table 2.2. Various chiral catalysts in catalytic asymmetric Diels–Alder reaction of anthrone **19a** with *N*-phenylmaleimide **20b**.

entry	catalyst (mol%)	time/h	yield/%[a]	ee/%[b]
1	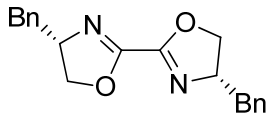 **122a** (10)	7	81	3
2	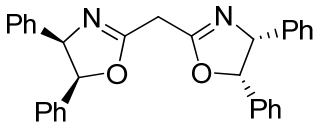 **122b** (10)	7	85	3
3	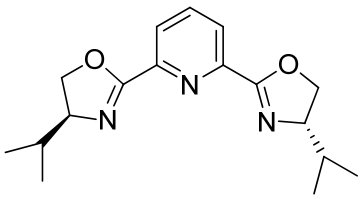 **122c** (10)	7	80	5
4	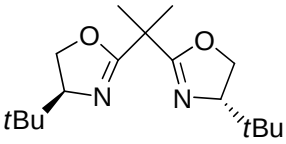 **122d** (10)	7	82	9
5	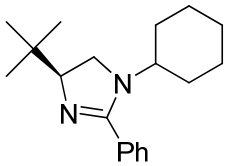 **123a** (10)	1	76	9
6	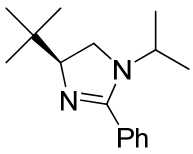 **123b** (10)	1	78	30
7	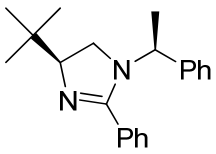 **123c** (10)	1	74	32

8	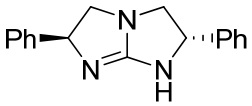 **124a** (10)	1	92	13
9	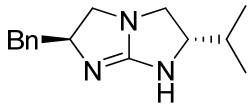 **124b** (10)	1	91	26
10	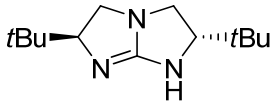 **124c** (10)	1	90	33
11	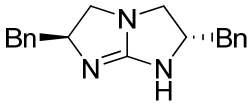 **124d** (10)	0.9	90	52

[a]Isolated yield. [b]Chiral HPLC.

In order to find an efficient catalyst, three categories of catalysts including bis(oxazoline) (BOX), imidazoles, guanidines were screened. We embarked on the study of the Diels–Alder reaction between anthrone **19** and *N*-phenylmaleimide **20b** (Scheme 2.17, Table 2.2).

Compounds containing chiral oxazoline ring have become one of the most successful, versatile, and commonly used classes of ligands for asymmetric catalysis.[41] However, there have been no preliminary results using these ligands in asymmetric Diels-Alder reactions. We were interested to employ this type of catalyst into our proposed Diels–Alder reaction. It was found that with 10 mol% of **122a**, the reaction between anthrone **19a** and *N*-phenylmaleimide **20b** was completed within 7 h at room temperature in CH_2Cl_2 (Table 2.2, entry 1). The product **21b** was obtained in 81% yield and 3% ee. Under the same conditions, the ee of 3%, 5%, 9% (entries 2-4)

were obtained for the reactions catalyzed by **122b**, **122c**, **122d**, respectively. The chiral recognition of this type of catalysts was very low (ee < 10%).

Chiral imidazolidinones were developed by MacMillan and co-workers as highly enantioselective catalysts for a number of reactions, which include Diels–Alder, 1,3-dipolar cycloaddition, and Friedel–Crafts reactions.[42] Jøgensen reported a novel imidazoline catalyst that contains a carboxylic acid. This catalyst was shown to be effective for highly enantioselective Michael reactions.[43] Inspired by these examples, we turned our attention to another class of chiral imidazolines. Their similarity to oxazolines and potential to tune their electronic properties with various 2-substituents make them an appealing type of catalyst. We found that with 10 mol% of **123a**, the reaction between anthrone **19a** and *N*-phenylmaleimide **20b** was completed in 1 h at room temperature in CH_2Cl_2 (Table 2.2, entry 5). The product **21b** was obtained in 76% yield and 9% ee. Under the same conditions, the ee of 30%, 32% (entries 6 and 7) were obtained for the reactions catalyzed by **123b**, **123c**, respectively. The reactions catalyzed by imidazolines were faster than using bis(oxazoline) catalysts. The chiral recognition of this type of catalysts was also much better than bis(oxazoline) catalysts.

Our group has reported an efficient synthesis of chiral bicyclic Brønsted-basic guanidines (Scheme 2.18).[44] Guanidine derivatives with their inherent basic character are widely utilized in synthetic organic chemistry as strong bases in a large variety of reactions. Thus, chiral guanidine catalysts are attractive targets in organocatalysis, they have received unprecedented attention. Accordingly, a series of synthesized chiral

guanidines were screened against the reaction of anthrone **19a** and *N*-phenylmaleimide **20b**. In the reaction catalyzed by guanidine **124a**, the product **21b** was obtained in 92% yield and 13% ee (Table 2.2, entry 8). Catalyst **124b** was also tested and 26% ee (Table 2.2, entry 9) was obtained, which was superior to **124a**. When the reaction was catalyzed by **124c**, the ee was increased to 33% and 90% yield was obtained (Table 2.2, entry 10). Catalyst **124d** with two Bn appendages was found to be the best catalyst; the product **21b** was achieved in 90% yield and 52% ee (Table 2.2, entry 11). The reaction catalyzed by chiral bicyclic guanidines was very fast and completed within 1 h.

2.2.3 An Aziridine-Based Synthesis of Chiral Bicyclic Guanidines

Bicyclic chiral guanidine catalyst **124d** was prepared according to the reported procedure as shown below (Scheme 2.18).[44] Aziridines can undergo regio- and stereoselective ring opening reactions, making them useful synthetic intermediates.[45] *N*-Tosyl aziridine **126** (Scheme 2.18) was readily prepared from its corresponding commercially available α-amino alcohols **125**.[46] Triamine unit **127** was easily obtained by treating **126** with 0.5 equivalent of benzyl amine.[47] The nucleophilic attack occurs preferentially at the sterically least hindered carbon atom. The subsequent removal of tosyl groups was achieved by using sodium in liquid ammonia and was immediately subjected to catalytic hydrogenation without further purification. The crude triamine **129** was then subjected to the final cyclization step, leading to the guanidine **124d** in 71% total yield from its amino alcohol. We have utilized five chemical steps with only three of them requiring chromatographic purification.

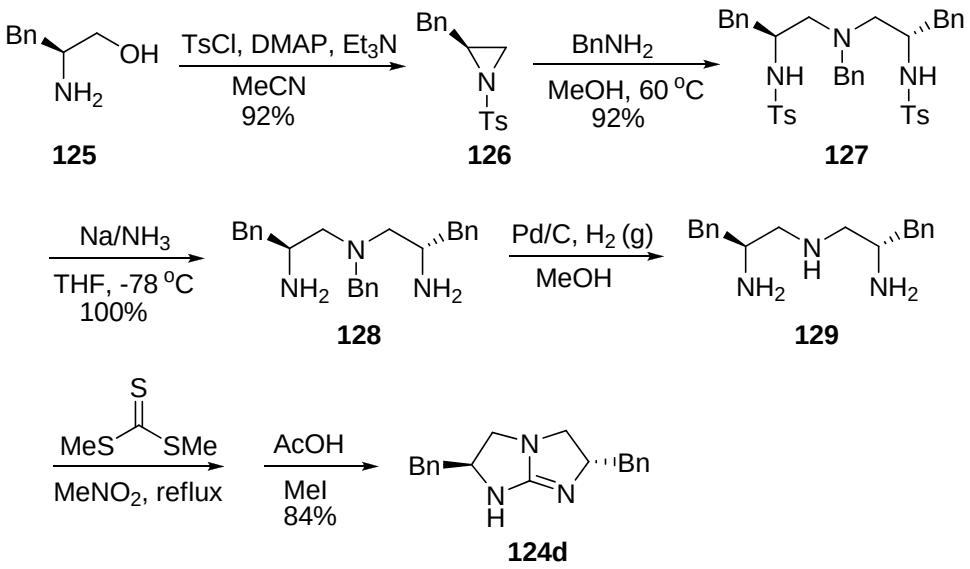

Scheme 2.18. Synthesis of symmetrical chiral bicyclic guanidines.

2.2.4 Optimization studies on the reaction of anthrone and *N*-phenylmaleimides

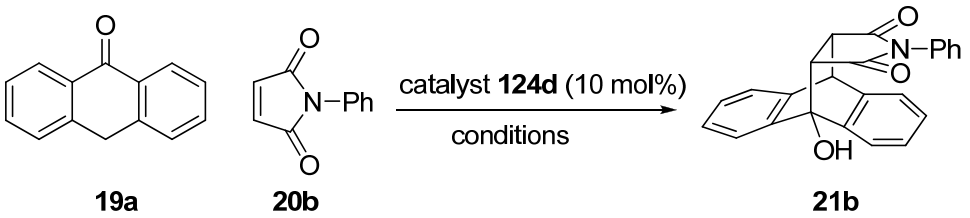

Scheme 2.19. Chiral bicyclic guanidine **124d** catalyzed Diels–Alder reaction of anthrone **19a** with *N*-phenyl maleimide **20b** in different conditions.

Table 2.3. Solvent and temperature effects on the Diels–Alder reaction of anthrone **19a** with *N*-phenylmaleimide **20a** (Scheme 2.19).

entry	Solvent	temp/°C	time/h	yield/%[a]	ee/%[b]
1	THF	rt	1	92	7
2	Toluene	rt	1	88	12
3	CH_2Cl_2	rt	1	91	52
4	$CHCl_3$	rt	1	95	52
5	$ClCH_2CH_2Cl$	rt	1	90	44
6	CH_2Cl_2	0	1.5	90	68
7	CH_2Cl_2	-20	3	90	81[c]
8	CH_2Cl_2	-40	6	91	75

[a] Isolated yield. [b] Chiral HPLC. [c] Absolute configuration of **21b** was determined by comparing with literature reports.

We found that the reaction of anthrone **19** and phenylmaleimide can be efficiently catalyzed using 10 mol% of the bicyclic guanidine **124d** (Scheme 2.19). With **124d** as the optimal catalyst, the reaction was optimized by changing other variables of the reaction conditions (Table 2.3).

Solvent effect was first studied at room temperature (Table 2.3). We found that protic (ef. MeOH) and highly polar solvents (eg. DMSO, DMF) usually resulted in low enantioselectivities. While the reaction worked well in common solvents such as THF and toluene (Table 2.3, entry 1 and 2), only chlorinated solvents such as CH_2Cl_2 (entry 3), $CHCl_3$ (entry 4) and $ClCH_2CH_2Cl$ (entry 5), gave significant levels of enantioselectivity. The best results were achieved using CH_2Cl_2 and $CHCl_3$ as the solvent, 52% ee and more than 90% yield were obtained for both solvents. CH_2Cl_2 was chosen as the optimal solvent, because it has a lower melting point (-96.7 ^oC) than $CHCl_3$ (-63.5 ^oC), and it is a more widely used solvent as compared to $CHCl_3$. Thus, CH_2Cl_2 gives us a chance to lower the reaction temperature to -78 ^oC.

Temperature effects were studied using CH_2Cl_2 as solvent (Table 2.3). When the reaction temperature was lowered to 0 ^oC and -20 ^oC, the reaction rate decreased considerably, however, the enantiomeric excess increased to 81% at -20 ^oC (Table 2.3, entry 7). To our surprise, when the reaction temperature was lowered to -50 ^oC, the ee decreased slightly to 75% (entry 8). It was thus thought that the best reaction condition is in CH_2Cl_2 and at a decreased temperature of -20 ^oC. This condition was used for expanding the substrate scope.

2.2.5 Highly enantioselective Diels-Alder reaction between anthrone and maleimides catalyzed by chiral bicyclic guanidine

With suitable conditions determined, various maleimides were screened as dienophiles for the Diels–Alder reaction to anthrone **19a** (Table 2.4). When *N*-methylmaleimide **20a** was used as the dienophile, moderate enantiomeric excess (16%) was attained (Table 2.4, entries 1). However, when substituted phenylmaleimides were used as the dienophiles, enantiomeric excess was improved up to 98%, and excellent yields were obtained (Table 2.4, entries 3 and 4). It was found that the reaction of anthrone **19a** worked well with arylmaleimides.

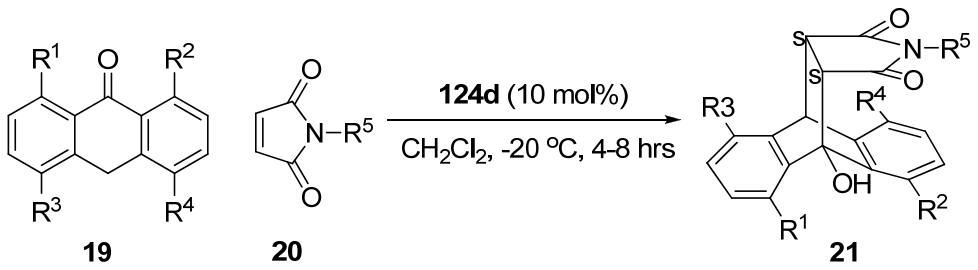

Scheme 2.20. Chiral bicyclic guanidine-catalyzed Diels–Alder reactions between o-substituted anthrones and maleimides.

Table 2.4. Chiral guanidine **124d** catalyzed Diels–Alder reaction of anthrone and various maleimides (Scheme 2.20).

entry	**19** [R^1, R^2, R^3, R^4]	R^5	**21**	yield/%[a]	ee/%[b]
1	**19a** [H, H, H, H]	**20a** [Me]	**21a**	90	16
2	**19a**	**20b** [Ph]	**21b**	90	81
3	**19a**	**20c** [2-$NO_2C_6H_4$]	**21c**	87	98
4	**19a**	**20d** [2,5-diClC_6H_3]	**21d**	88	95
5	**19b** [Cl, Cl, H, H]	**20e** [Bn]	**21e**	92	95
6	**19b**	**20f** [*c*-Hexyl]	**21f**	88	98[c]
7	**19b**	**20g** [*t*-Butyl]	**21g**	87	93
8	**19b**	**20h** [*i*-Butyl]	**21h**	92	91

9	**19b**	**20i** [4-$ClC_6H_5CH_2$]	**21i**	85	98[c]
10	**19c** [H, H, Cl, Cl]	**20j** [Ph]	**21j**	92	99
11	**19c**	**20k** [2,6-$F_2C_6H_3$]	**21k**	92	99
12	**19c**	**20l** [2-$MeOC_6H_4$]	**21l**	90	98
13	**19d** [H, Cl, Cl, H]	**20m** [Ph]	**21m-1**	87	99
14	**19d**	**20n** [2,4,6-$Me_3C_6H_2$]	**21n-1**	85	99
15	**19f** [H, H, NHMe, H]	**20o** [Ethyl]	**21o-1**	95	98
16	**19f**	**20p** [*n*-Hexyl]	**21p-1**	96	85

[a] Isolated yield. [b]Chiral HPLC. [c] Reaction performed at -40 °C.

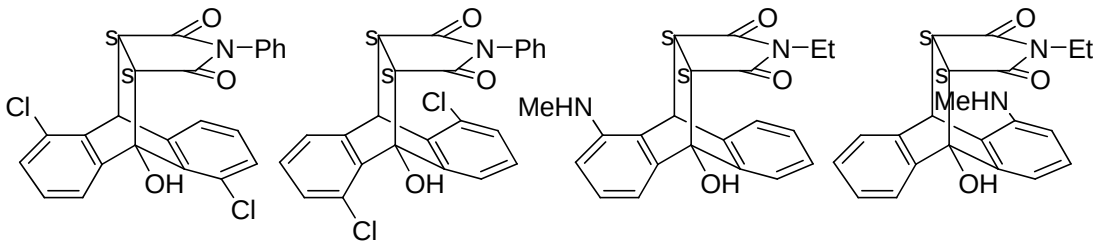

Fig. 2.5. Possible stereoisomers of Diels-Alder products **21m** and **21o**.

High enantiomeric excess was achieved with unsubstituted anthrone **19a**. Hence, we were interested to know whether other types of anthrones could also work well with maleimides in this highly enantioselective Diels–Alder reaction. A series of substituted anthrones **19b-f** (Table 2.4) were prepared from the reduction of their corresponding anthracenediones.[40a] The reaction between 1,8-dichloro-9-anthrone **19b** and phenylmaleimide **20b** gave the desired Diel–Alder product in 45% ee and 80% yield. However, the reaction between 1,8-dichloro-9-anthrone **19b** and benzylmaleimide completed in 5 h and gave the desired Diel–Alder product **21e** in excellent enantioselectivity (95%) and high yield (92%) (Table 2.4, entry 5). 1, 8-dichloro-9-anthrone **19b** was also found to work very well with alkylmaleimides such as *c*-hexylmaleimide, *t*-butylmaleimide, *i*-butylmaleimide (entries 6-9). The

corresponding Diel–Alder products **21f-i** were achieved in 91-98% ee with 85-92% yield. Initially, we speculated that the presence of two Cl substituents next to the oxyanion would prevent close interaction with the chiral guanidinium and result in low enantioselectivity. However, high yields and enantiomeric excesses of Diels–Alder adducts were observed even in this case.

Subsequently, 4,5-dichloro-9-anthrone **19c** was screened against a series of maleimides (Table 2.4, entries 8-10). It was found that 4,5-dichloro-9-anthrone **19c** worked very well with arylmaleimides giving the Diels–Alder products **21j-l** in excellent enantiomeric excess (98-99%) with high yields (90-92%). However, when ethylmaleimides were used as the dienophile, the reaction gave product in 42% ee and 89% yield. Thus it was revealed that 4,5-dichloro-9-anthrone **19c** went well with arylmaleimides. When 1,5-dichloro-9-anthrone **19d** was used as the diene, it also worked well with arylmaleimides, and excellent regioselectivity was observed (entries 11 and 12). For example, Diels–Alder adduct **21m-1** (Figure 2.6) was obtained in a 8:1 ratio with its stereoisomer **21m-2**.[48] We have succeeded in obtaining an X-ray structure of the major product **21m-1** (Figure 2.6), thus solving the regiochemistry analysis. The 4-(*N*-methylamino)-9-anthrone **19f** was also found to give good yields and enantiomeric excess with alkylmaleimides (entries 15 and 16). In the reaction with ethylmaleimide, a small amount of the minor stereoisomer, most likely **21o-2** (Figure 2.7), was detected (entry 15). The regiochemistry was also solved by X-ray crystallographic analysis by obtaining X-ray structure of the major adduct **21o-1** (Figure 2.7).

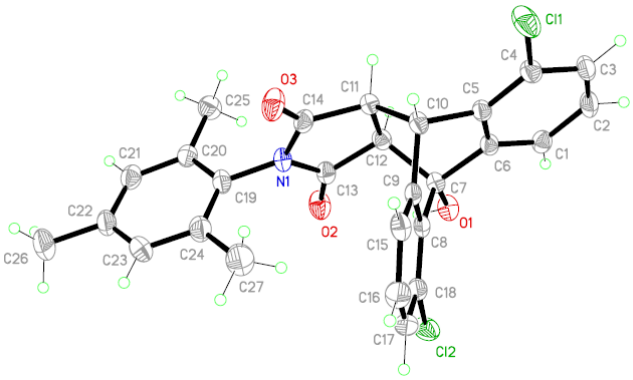

Fig. 2.6. X-ray structure of **21m-1**.

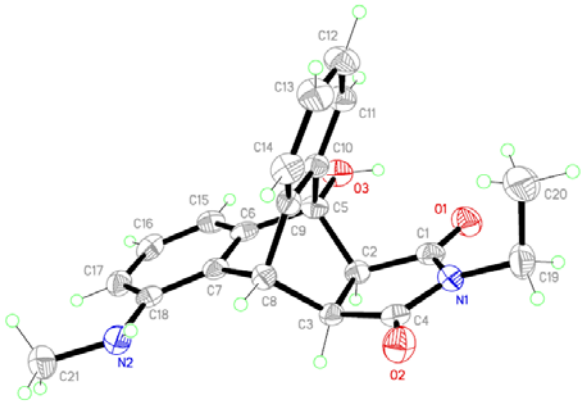

Fig. 2.7. X-ray structure of **21o-1**.

Other anthrones such as 1, 8-dichloro-9-anthrone **19b,** were also able to work well with olefins such as fumaronitrile **89c** and highly enantiopure Diels–Alder adducts **130** were also obtained.

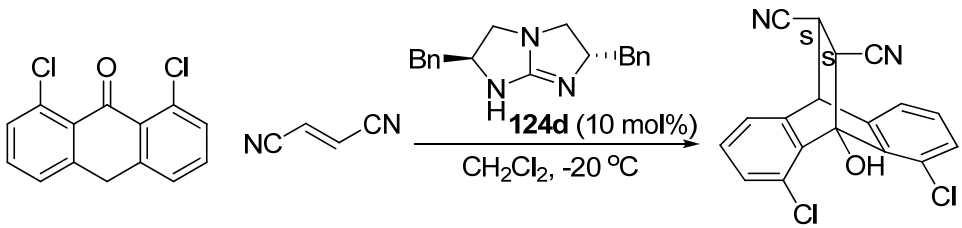

19b **89c** **130**

The above results show that dibenzyl guanidine catalyst **124d** (Table 2.4) can tolerate a wide range of substituents and substitution pattern on the anthrone, and careful optimization should result in high enantioselectivity when suitable maleimides

are used. For example, 1,8-dichloro-9-anthrone **19b** went very well with alkylmaleimides but not very well with arylmaleimides. While 4,5-dichloro-9-anthrone **19c** exhibited high enantioselectivities with arylmaleimides but only gave moderate ee with alkylmaleimides. The choice of maleimides also depends on finding suitable resolution condition. In all, we have achieved excellent enantiomeric excess and high yields in the reactions between both anthrone and substituted anthrones with different maleimides.

2.3 Conjugate addition between anthrones and different dienophiles

2.3.1 Highly enantioselective Conjugate addition between Dithranol and different maleimides catalyzed by chiral bicyclic guanidine

From the above studies, we have developed a highly enantioselective Diels–Alder reaction of anthrones and maleimides. In the case of Michael adducts, they can be obtained by prolonging the reaction time or the treatment of the isolated Diels–Alder adducts under basic conditions. Under these conditions, it could lead to a retro-Aldol ring-opening reaction. Significant racemization was observed for these ring-opening products. The Michael products were unable to be reverted to cycloadducts by guanidine in dichloromethane under the optimized reaction conditions.

Table 2.5. Chiral bicyclic guanidine-catalyzed reactions between dithranol and various maleimides.

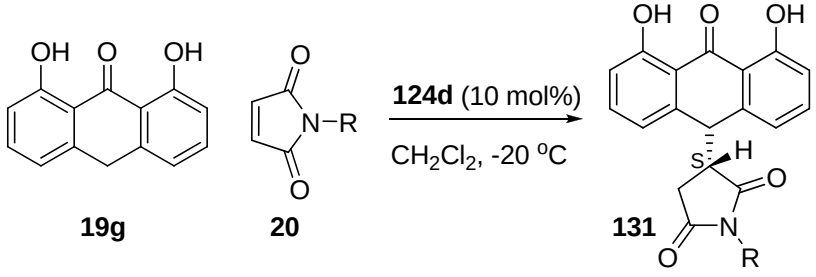

entry	R	adduct	Time/h	yield/%[a]	ee/%[b]
1	Ph	**131a**	7	80	99
2	2-$NO_2C_6H_4$	**131b**	8	87	97
3	3,4-$Cl_2C_6H_3$	**131c**	8	89	98
4	Bn	**131d**	8	86	93

[a] Isolated yield. [b] Chiral HPLC.

With reference to Table 2.5, for certain anthrone derivatives, such as dithranol **19g** (1, 8-dihydroxy-9-anthrone), reactions with dienophiles almost always lead to the exclusive formation of the Michael adducts. No Diels–Alder adduct was observed during the reaction. When dithranol was screened against a series of malemides, including phenylmaleimide **20b** and benzylmaleimide **20e**, using 10 mol% of the bicyclic guanidine catalyst **124d**, it was found that high enantiomeric excess, and yields could be obtained for the Michael adducts **131a** (Table 2.5, 99% ee, entry 1) and **131d** (93% ee, entry 4). When substituted phenylmaleimides were used as the dienophiles, they also reacted well with dithranol **19g**. These reactions were completed within 8 h providing the Michael adducts **131b** and **131c** in 97%, 98% ee, respectively (entries 2 and 3).

2.3.2 Highly enantioselective Conjugate addition between Dithranol and acyclic conjugated olefins catalyzed by chiral bicyclic guanidine

Table 2.6. Chiral bicyclic guanidine-catalyzed Diels–Alder reactions between dithranol and various acyclic conjugated olefins.

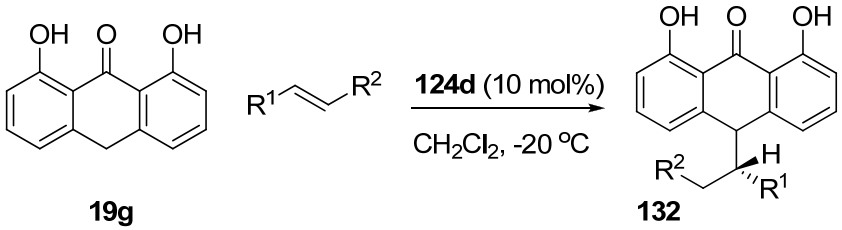

19g **132**

entry	R^1	R^2	adduct	Time/h	yield/%[a]	ee/%[b]
1	CO_2Me	CH_3CO	**132a**	6	92	98
2	CO_2Et	PhCO	**132b**	7	92	95
3	CN	CN	**132c**	7	90	94

[a] Isolated yield. [b] Chiral HPLC.

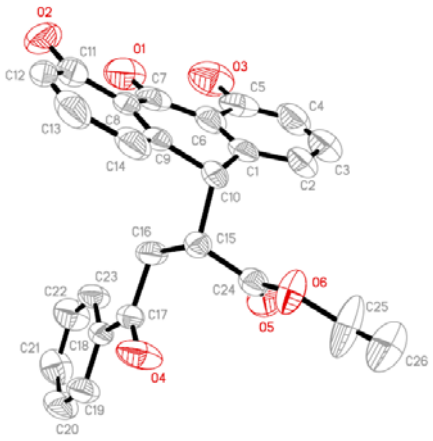

Fig. 2.8. X-ray structure of **132b**.

Dithranol **19g** also worked well with olefins such as methyl *trans*-4-oxo-2-pentenoate and ethyl *trans*-3-benzoylacrylate (Table 2.6, entries 1 and 2). We have previously showed that these olefins are excellent substrates for Michael reaction, and high regioselectivity was observed when 1, 3-dicarbonyls were used in the presence of chiral bicyclic guanidines.[49] These olefins gave Michael products **132a** (entry 1) and **132b** (entry 2)[48] with high regioselectivity, and both were obtained in high yields and enantiomeric excess. The regiochemistry was also solved by X-ray crystallographic analysis by obtaining X-ray structure of the Michael product **132b** (Figure 2.8). Fumaronitrile (entry 3) was also observed to be an excellent substrate for this reaction giving 90% yield and 94% enantiomeric excess. The reaction rate was very fast, completing in 7 h. However, attempts to use diethyl fumarate and diethyl maleates as the dienophiles were not as successful. The reason why dithranol **19g**

works well with olefins is still unclear.

The guanidine catalyst was proposed to generate the active diene *in situ* by deprotonation. The role of the catalyst beyond its function as Brønsted base is still under investigation. It is likely that H-bonding, ion-pairing, and π-interactions all contribute to the organization of a transition state that leads to high enantioselectivity for reactions with maleimides and other electron-deficient dienophiles.

In summary, chiral bicyclic dibenzyl guanidine is an excellent catalyst for Brønsted base catalyzed reactions between anthrone and various dienophiles. The catalyst could tolerate a range of substituents and substitution patterns making several anthrone derivatives suitable for this reaction. As a result, both Diels–Alder and Michael products were obtained in excellent yields, high regioselectivities and high enantioselectivities.

In conclusion, we have developed a highly enantioselective base-catalyzed anthrone Diels–Alder reaction in this chapter.

Chapter 3

Mechanistic and Kinetic Studies of Guanidine Catalyzed Enantioselective Diels–Alder Reactions of Anthrones

3.1 Introduction to Previous Mechanistic Studies on Various Organocatalytic Reactions

Despite the impressive advancement of asymmetric organocatalysis in recent years,[23] the mechanisms of most organocatalytic transformations have not been investigated in detail.[50f] Due to the advantages of organocatalysts, they are particularly well-suited for powerful physical-organic probes to study reaction mechanisms. Mechanistic studies may provide fundamental insights into the structure and function of catalysts, and help improve the existing system to develop new catalysts for new transformations. Many techniques can be employed to elucidate the mechanisms of these organocatalysis, including crystallography, kinetic studies, computational and spectroscopic methods.

Organocatalysts that have been successfully involved in mechanistic study of enantioselective reactions are bifunctional thioureas[50], proline[51], chiral phosphoramides[52], and imidazolidinones.[54] Chiral thioureas represent a versatile and useful class of enantioselective catalysts that function as hydrogen bond donors,[55] and several bifunctional thiourea derivatives have been suggested to operate *via* cooperative mechanisms.[50,56] Bifunctional organocatalysis has evolved which combines H-Bond donors and base functionalities in an asymmetric molecular scaffold. It is exemplified in proline catalyzed enantioselective reactions that involve strong catalyst-substrate interactions *via* enamine formation[51]. H-bonding to the carboxylic acid moiety of proline serves to activate the electrophile towards attack by the enamine.[51] Phosphoramides have been found to be the most effective promoters

for the addition of chlorosilanes to aldehydes. Detailed mechanistic study has been carried out to investigate the origin of activation. It is proposed that either one or two phosphoramides were bound to a siliconium ion organizational center in both the rate and stereochemistry-determining steps.[52] For bulky phosphoramides, they participate *via* a 1:1 phosphoramide/enolate pathway through boatlike transition structures centered around a 5-coordinate cationic siliconate. However, less bulky phosphoramides are able to engage the trichlorosilyl enolate in a 2:1 manner, reacting through a 6-coordinate, chairlike transition structure.[52d] Chiral imidazolidinones have been reported to be an excellent catalyst for the Diels–Alder reactions of cyclopentadiene with α,β-unsaturated aldehydes,[53a] and other reactions.[53] One crucial factor that determines the efficiency of imidazolidione catalysts in their asymmetric enantioselective reactions is the reversible formation of iminium ions from chiral imidazolidinones and α, β-unsaturated carbonyl compounds.[54]

Guanidine has been used for molecular recognition of carboxylate, phosphate and nitrate anions because of its ability to form double hydrogen bonds between the guanidinium cation and the dioxoanion.[57] Moreover, the isolation of the complex formed between the bicyclic guanidine 1,5,7-triazabicyclo[4.4.0]dec-5-ene (TBD) and α-nitrotoluene suggested that this type of intermediates could be a good model for an enantioselective guanidine-catalyzed nitroaldol reaction.[58] The potential of chiral guanidines as catalytic Brønsted bases has also been demonstrated in several reactions including Strecker, epoxidation, and conjugate addition reactions.[59] The use of Brønsted bases to catalyze the Diels–Alder reaction, however, has not been well

studied.[60] We have demonstrated that chiral bicyclic guanidine efficiently catalyzed the cycloaddition of anthrone and *N*-phenylmaleimide to afford Diels–Alder adduct.[59m] Despite the experimental achievements we currently witness in this field, our knowledge about the underlying mechanisms is fairly limited and the role that individual active sites in the catalytic processes is not clearly established. The successful design of a general chiral organocatalyst for the Diels–Alder reaction of anthrones with excellent enantioselectivity is still a challenging task. We are striving to better predict stereoselectivities, suggest promising leads for experimental study, and eventually design new catalyst. Herein, we present the mechanistic and kinetic studies of the guanidine catalyzed reactions of anthrones.

3.2 Kinetic Analysis Using Monofunctional Base

A freshly prepared stock solution of anthrone **19a** and *N*-phenylmaleimide **20b** and CD_2Cl_2 (0.5 ml) was added to the NMR tube. After the addition of the catalyst to the reaction mixture, the reaction was monitored by following the formation of the product and decay of the starting material over 0.25-6 h. Spectra were collected every 30 or 60 seconds, depending on the expected lengths of the experiments. To accurately measure substrate concentrations during the course of the Diels–Alder reaction, it was necessary to employ a non-volatile, unreactive internal standard. Hence, *t*-butylbenzene was chosen as the internal standard in all subsequent NMR kinetic studies. Most reactions were followed till more than 75% conversion and conversion of starting material to product was determined by NMR following the decay of anthrone relative to *t*-butyl benzene internal standard. A series of

experiments between anthrone **19a** and phenylmaleimide **20b** were performed in CD_2Cl_2 and monitored by ^1H NMR spectroscopy.

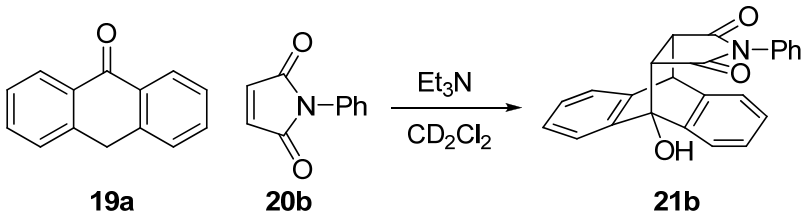

Scheme 3.1. Et_3N catalyzed reaction between anthrone **19a** and *N*-phenylmaleimide **21b**.

Table 3.1. Rate constants of Et_3N catalyzed Diels–Alder reaction of Anthrone.

entry	[**19a**] (M)	[**20b**] (M)	[**Et_3N**] (mM)	k_{obs} (10^{-3} s^{-1})	k [a] (M^{-1} s^{-1})
1	0.200	0.800	2.00	0.37 ± 0.03	0.19 ± 0.02
2	0.100	0.400	2.00	0.43 ± 0.03	0.22 ± 0.02
3	0.200	0.200	2.00	0.43 ± 0.02	0.22 ± 0.01

[a] $k = k_{obs}/[Et_3N]$

To obtain better insight into the nature and mechanism of enantioselective reactions of anthrones catalyzed by bicyclic guanidine catalyst, we selected the Diels–Alder reaction of anthrone **19a** and *N*-phenylmaleimide **20b** catalyzed by Et_3N for comparison. The kinetic experiments were performed by using **19a**, **20b** as the reagents and Et_3N as the catalyst in dicholoromethane-d_2 at -33.3 °C (Scheme 3.1). We need to know the order of the reaction because it tells us the functional relationship between concentration and reaction rate. It determines how the amount of a compound speeds up or retards a reaction. The experimental design is to set the concentration of one substrate much higher, so that this concentration can be treated as approximate constants. Order in anthrone **19a** was established by monitoring the

initial consumption of **19a** using 4 equiv. of **20b** (Table 3.1, entry 1 and 2). Plotting ln [**19a**]^0/ln [**19a**] versus time gave a straight line with zero intercept, thus establishing the first-order dependence on anthrone. Order in **20b** was established indirectly by determining the overall reaction order at equimolar concentration. For this experiment, a plot of ln[**19a**]^0/ln[**19a**] versus time gave a straight line with zero-intercept, indicating that the reaction is overall first order and therefore zero order with respect to **20b** (Table 3.1, entry 3). It implies that the reaction rate is independent of **20b** (zero order) when Et_3N was used as the catalyst.

Table 3.2. Order of Et_3N.

entry	[**19a**] (M)	[**20b**] (M)	[**Et$_3$N**] (mM)	k_{obs} (10^{-3} s^{-1})	k [a] (M^{-1} s^{-1})
1	0.200	0.200	1.00	0.18 ± 0.02	0.18 ± 0.02
2	0.200	0.200	2.00	0.43 ± 0.02	0.22 ± 0.01
3	0.200	0.200	3.00	0.64 ± 0.04	0.21 ± 0.01
4	0.200	0.200	4.00	0.85 ± 0.08	0.21± 0.02
5	0.200	0.200	5.00	1.12 ± 0.1	0.22 ± 0.02

[a] $k = k_{obs}/$ [**Et$_3$N**]

The reaction order in Et_3N was established by determining the kinetic rate constants at various catalyst concentrations. For these experiments equimolar amounts of **19a** and **20b** were used with catalyst loadings of 1.00-5.00 mM (Table 3.2, entry 1-5). A ln[k_{obs}]/ln[Et_3N] plot gave a straight line with a slope of 1 (Figure 3.1). Based on these results, the following rate equation for the Diels–Alder reaction is deduced:

$$-d\,[\mathbf{19a}]/dt = k\,[Et_3N]^1[\mathbf{19a}]^1[\mathbf{20b}]^0$$

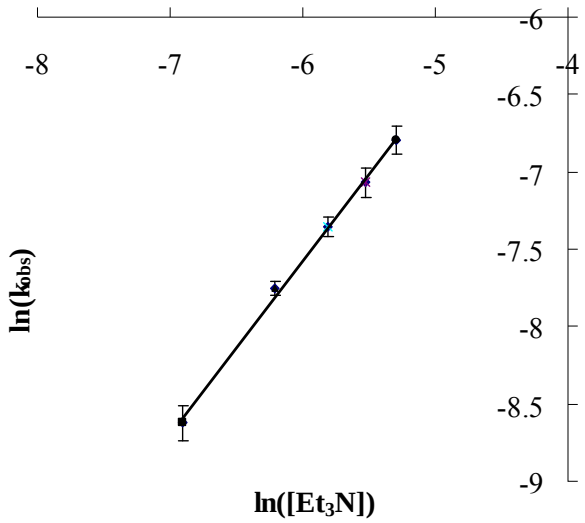

Fig. 3.1. Order of Et_3N.

Determination of Eyring activation parameters was conducted in the usual manner by measuring the rate constants of the catalyzed reactions as a function of temperature between -40.0 ^oC and -10.0 ^oC (Table 3.3, entry 1-5). Eyring equation is as shown below:

$$\ln(kh/k_BT) = -\Delta H^{\ddagger}/RT + \Delta S^{\ddagger}/R$$

The activation parameters reveal a large entropic contribution ($\Delta S^{\ddagger}$ = -32 ± 3 e.u.) and an enthalpic contribution of 7.2 ± 0.8 kcal mol^{-1} to the free energy of activation (Figure 3.2). Large $\Delta S^{\ddagger}$ is consistent with second order rate law. Although a large entropic contribution suggests a highly ordered transition structure, its magnitude does not preclude an unfavorable preequilibrium binding between anthrone and phenylmaleimide.

Table 3.3. VT-NMR Experiments of Et_3N catalyzed Diels–Alder reaction of Anthrone.

entry	t / °C	k_{obs} (10^{-3} s^{-1})	k (M^{-1} s^{-1})
1	-10.0	0.58 ± 0.03	0.58 ± 0.03
2	-20.0	0.38 ± 0.03	0.38 ± 0.03
3	-30.0	0.21 ± 0.03	0.21 ± 0.03
4	-33.3	0.18 ± 0.02	0.18 ± 0.02
5	-40.0	0.10 ± 0.01	0.10 ± 0.01

[a] [**19a**] = 0.200 M, [**20b**] = 0.200 M, [**Et_3N**] = 1.00 mM

[b] $k = k_{obs}/[Et_3N]$

slope ($-\Delta H^{\ddagger}/R$)	intersection ($\Delta S^{\ddagger}/R$)	$\Delta H^{\ddagger}$ [a]	$\Delta S^{\ddagger}$ [b]
-3302.6	-17.3	7.2 ± 0.8	-32 ± 3

[a] Measured in kcal/mol [b] Measured in cal mol^{-1} K^{-1}

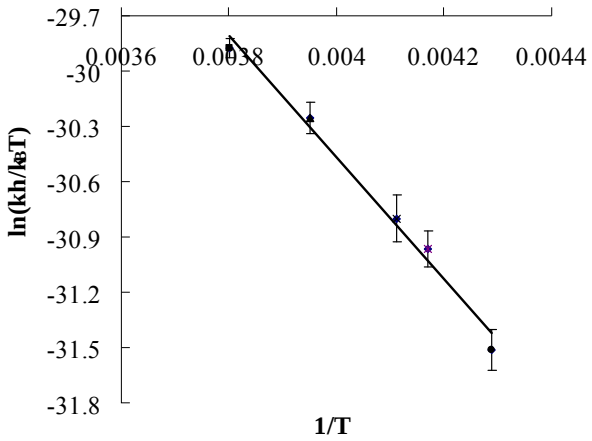

Fig. 3.2. Eyring plot. The rates constant were measured at -10.0, -20.0, -30.0, -33.3, -40.0 °C. k_B = Boltzmann's constant [$1.381 \cdot 10^{-23}$ J K^{-1}] T = absolute temperature in degrees Kelvin (K) h = Plank constant [$6.626 \cdot 10^{-34}$ J s]

Michael adducts can be obtained by prolonging the reaction time or the treatment of the isolated Diels–Alder adducts under basic condition. This also gave good evidence for the formation of Michael adduct by the ring opening of cycloadduct.

Based on experimental observations, the catalytic cycle of Et_3N catalyzed Diels–Alder reaction between anthrone **19a** and *N*-phenylmaleimide **20b** is proposed as in Scheme 3.2. In the first step of the cycle, deprotonation of anthrone **19a** by Et_3N generates an Et_3N-anthronol complex **134**. The second step involves *N*-phenylmaleimide **20b** approaching the complex **134** rapidly to form the intermediate **135**. Finally, the Diels–Alder adduct **21b** was obtained, and Et_3N was released.

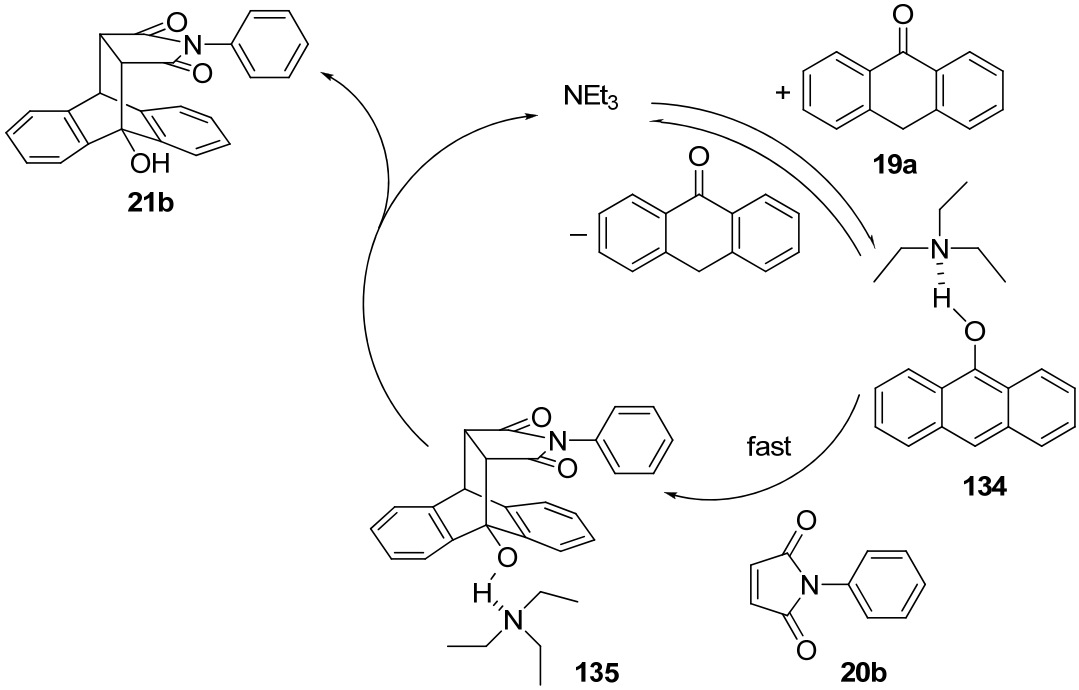

Scheme. 3.2. Proposed non-chiral catalytic cycle.

3.3 Kinetic Analysis Using Bifunctional Chiral Guanidine

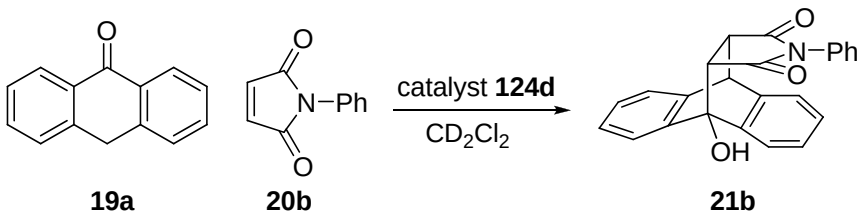

Scheme 3.3. Chiral Bicyclic Guanidine-Catalyzed Diels–Alder Reaction between Anthrone **19a** and Phenylmaleimide **20b**.

For chiral guanidine **124d** catalyzed Diels–Alder reaction between anthrone **19a** and phenylmaleimide **20b.** We also need to know the order of the reaction because it tells us the functional relationship between concentration and reaction rate. It determines how the amount of a compound speeds up or retards the reaction. The experimental design is also to set the concentration of one substrate much higher, so that this concentration can be treated as approximate constants.

Table 3.4. Kinetic study of chiral guanidine catalyzed Diels–Alder reaction of anthrone.

entry	[**19a**] (M)	[**20b**] (M)	[**124d**] (mM)	$^{a}k_{obs1}$ (10^{-3} s^{-1})	$^{b}k_1$ (M^{-1} s^{-1})
1	0.100	0.100	3.00	2.3 ± 0.2	0.77 ± 0.07
2	0.0500	0.0250	3.00	0.79 ± 0.08	0.26 ± 0.03
3	0.125	0.0250	3.00	1.2 ± 0.14	0.40 ± 0.05
4	0.250	0.0250	3.00	1.2 ± 0.08	0.40 ± 0.03
5	0.0500	0.100	5.00		
6	0.0500	0.250	5.00		
7	0.0500	0.500	5.00		

[a] k_{obs1} = slope of the graph: ln([**20b**]^0/[**20b**]) vs t (s) [b] $k_{obs1} = k_1$*[**124d**]

Similar experiments were conducted to determine the order in **20b** by using 0.250M of **19a** and 0.0250 M of **20b** (Table 3.4, entry 3). Plotting ln [**20b**]^0/ln [**20b**] versus time gave a straight line with zero intercept, thus establishing first-order dependence on **20b**. Order in **19a** was established indirectly by determining the overall reaction order at equimolar concentration. For this experiment, a plot of [**19a**]$^{-1}$ versus time gave a straight line with zero intercept, indicating that the reaction

is overall second order and therefore first order in **19a** (Table 3.5, Entry 1-5). The reaction rate displays a straightforward first-order dependence each on [**19a**] and [**20b**]. Interestingly, rate inhibition was observed at high [**20b**] and the reaction became slower. The deviations from simple first-order kinetic behavior at higher concentration of **20b** point to more complicated and potential interactions under certain conditions. The observed inhibition at high [**20b**] is explained through the interaction between the chiral catalyst **123d** and **20b**. To identify the interactions between phenylmaleimide **20b** and chiral guanidine **124d**, we took the ^{1}H NMR spectra of **124d** in the presence of different amount of **20b**. Although there was little change in the ^{1}H NMR spectrum of **124d** by mixing with **20b,** it may reveal some information about the interaction of **124d** and **20b** through hydrogen bonding (Figure 3.3). The chemical shifts of **124d** were gradually shifted downfield with increasing ratio of **20b** to **124d** (Table 3.6). The chemical shift of N-*H* of the catalyst was shifted from 4.14 to 4.26 ppm.

Table 3.5. Order of chiral bicyclic guanidine catalyst **124d**.

entry	[**19a**] (M)	[**20b**] (M)	[**124d**] (mM)	$^{c}k_{obs2}$ (10^{-3} M^{-1} s^{-1})	$^{d}k_2$ (M^{-2} s^{-1})
1	0.100	0.100	3.00	2.3 ± 0.2	0.77 ± 0.07
2	0.100	0.100	5.00	4.8 ± 0.5	1.0 ± 0.1
3	0.100	0.100	8.00	7.6 ± 0.8	0.95 ± 0.1
4	0.100	0.100	10.0	9.5 ± 0.8	0.95 ± 0.08
5	0.100	0.100	12.0	12.4 ± 1	1.0 ± 0.1

^{c} k_{obs2} = slope of the graph: (1/[**19a**]) vs t(s) ^{d} $k_{obs2} = k_2$*[**124d**]

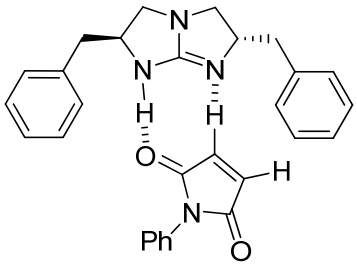

Fig. 3.3. Possible hydrogen bonding between **20b** and **124d**.

Table 3.6. ^{1}H NMR study of **20b**, **124d** and their mixture in CD_2Cl_2.[a]

[20b]:[124d]	δ/ppm	$\Delta\delta^{b}$/ppm
0:1	4.14	0
1:1	4.15	0.01
2:1	4.17	0.03
3:1	4.19	0.05
4:1	4.20	0.06
5:1	4.21	0.07
8:1	4.24	0.10
10:1	4.26	0.12

[a] The concentration of **20b** and **124d** was 0.04M in CD_2Cl_2, the 1:1 mixture of **20b** and **124d** was shaked well before NMR was recorded at -33.3 ^{o}C. [b] Δδ refers to the change of a certain proton's chemical shift when in a mixture form compared with in a pure single component form, eg. $\Delta\delta(H^{a})=\delta(\mathbf{20b}:\mathbf{124d}(1:1)) - \delta(\mathbf{124d})$.

The reaction order in **124d** was established by determining the kinetic rate constants at various catalyst concentrations (at -33.3 ^{o}C). For these experiments equimolar amounts of **19a** and **20b** were used at catalyst loadings of 3-12 mM (Table 3.5, Entry 1-5). An ln/ln plot of the second order rate constants versus the catalyst concentration ($\ln k_{obs}/\ln[\mathbf{124d}]$) gave a straight line with a slope of 1 which showed a clear first-order dependence of the rate on the catalyst concentration (Figure 3.4). On

the basis of these results, the following rate equation for the Diels-Alder reaction is proposed:

$$-d\,(\mathbf{19a})/dt = k\,[\mathbf{124d}]^1[\mathbf{19a}]^1[\mathbf{20b}]^1$$

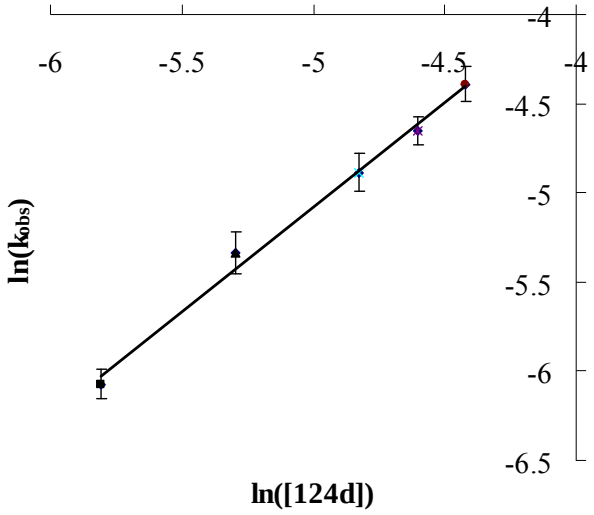

Fig. 3.4. Order of catalyst **124d**.

Table 3.7. VT-NMR Experiments of chiral guanidine catalyzed Diels–Alder reaction of anthrone.

entry	t/ °C	k_{obs} (10^{-3} M^{-1} s^{-1})	k (M^{-2} s^{-1})
1	-10.0	6.3 ± 0.6	2.1± 0.2
2	-15.0	5.2 ± 0.5	1.7 ± 0.1
3	-20.0	4.3 ± 0.5	1.4 ± 0.1
4	-30.0	2.8± 0.2	0.93 ± 0.07
5	-33.3	2.3 ± 0.2	0.77 ± 0.07

[a] [**19a**] = 0.1 M, [**20b**] = 0.1 M, **[124d]** = 0.003 M [b] k_{obs} = slope of the graph 1/[**19a**] vs. time(s)

Determination of Eyring activation parameters was completed in the usual manner by measuring the rate constant of the catalyzed reaction as a function of temperature between -33.3 °C and -10.0 °C. The activation parameters reveal a large entropic contribution ($\Delta S^{\ddagger}$ = -39 ± 3 cal mol^{-1} K^{-1}) and a small enthalpic contribution

($\Delta H^{\ddagger} = 4.7 \pm 0.7$ kcal mol^{-1}) to the free energy of activation.

slope ($-\Delta H^{\ddagger}/R$)	intersection ($\Delta S^{\ddagger}/R$)	$\Delta H^{\ddagger}$ [a]	$\Delta S^{\ddagger}$ [b]
-2356.7	-19.6	4.7 ± 0.7	-39 ± 2.8

[a] Measured in kcal/mol [b] Measured in cal mol^{-1} K^{-1}

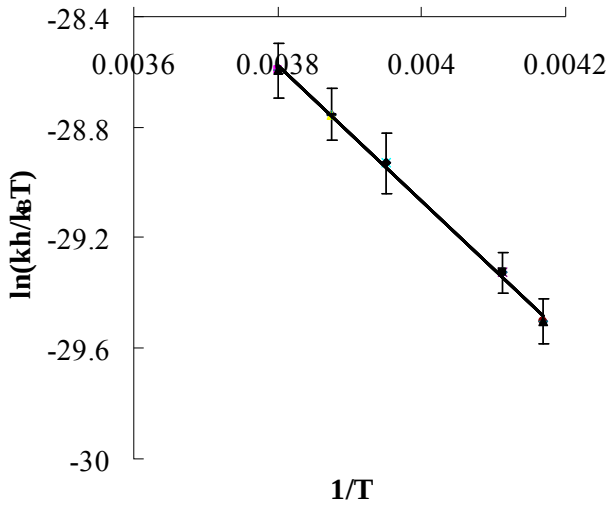

Fig. 3.5. Eyring plot. The rate constant were measured at -10.0, -15.0, -20.0, -30.0, -33.3 ^{o}C. k_B = Boltzmann's constant [$1.381 \cdot 10^{-23}$ J K^{-1}] T = absolute temperature in degrees Kelvin (K) h = Plank constant [$6.626 \cdot 10^{-34}$ J s]

3.4 Mechanistic Possibilities for Chiral Reaction

In collaboration with the Huang Group*, we have succeeded in obtaining an X-ray structure of the salt **136a** of bicyclic guanidine 1,5,7-triazabicyclo[4.4.0]dec-5-ene (TBD) and HCl (Figure 3.6), which shows the double hydrogen bonding between the guanidinium salt and Cl^-. An X-ray structure of the salt **136b** of TBD, HCl and H_2O was also obtained (Figure 3.7). The presence of two hydrogen bonds between guanidinium salt, Cl^- and H_2O reveals that bicyclic guanidine could work as a bifunctional catalyst. The positive charge on the guanidinium is delocalized into the three nitrogens by resonance, with two –NH

* Assistant Professor Huang Guo-Wei (Andy), Department of Chemistry, 3 Science Drive 3, National University of Singapore, Singapore 117543 Email: hkw@nus.edu.sg

groups as potential hydrogen bonding donors.

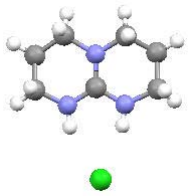

136a

Fig. 3.6. X-ray structure of TBD and HCl. C black, H gray, N blue, Cl^- green.

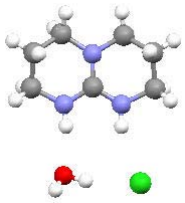

136b

Fig. 3.7. Co-crystal structure of TBD and HCl, H_2O. C black, H gray, O red, N blue, Cl^- green.

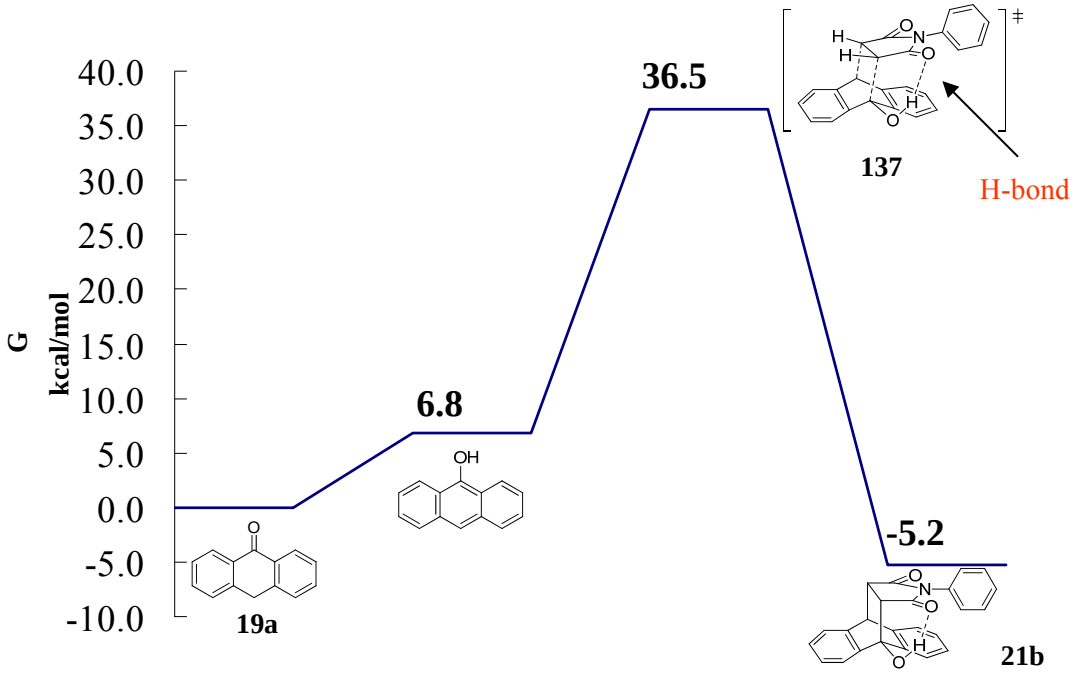

Fig. 3.8. The uncatalyzed Diels–Alder reaction between anthrone **19a** and *N*-phenylmaleimide **20b**. The energies at the B3LYP/6-31G** level relative to the starting material are given in kcal/mol.

In order to support our experimental analysis, DFT computational studies were also carried out in collaboration with the Huang Group using the B3LYP/6-31+G**

level of theory.

In the uncatalyzed Diels–Alder reaction between anthrone **19a** and *N*-phenylmaleimide **20b,** the energy barrier for bringing together anthrone **19a** and *N*-phenylmaleimide **20b** is calculated to be 36.5 kcal/mol in the gas phase (Figure 3.8). The activation energy is very high, which means the reaction does not proceed readily without a proper catalyst.

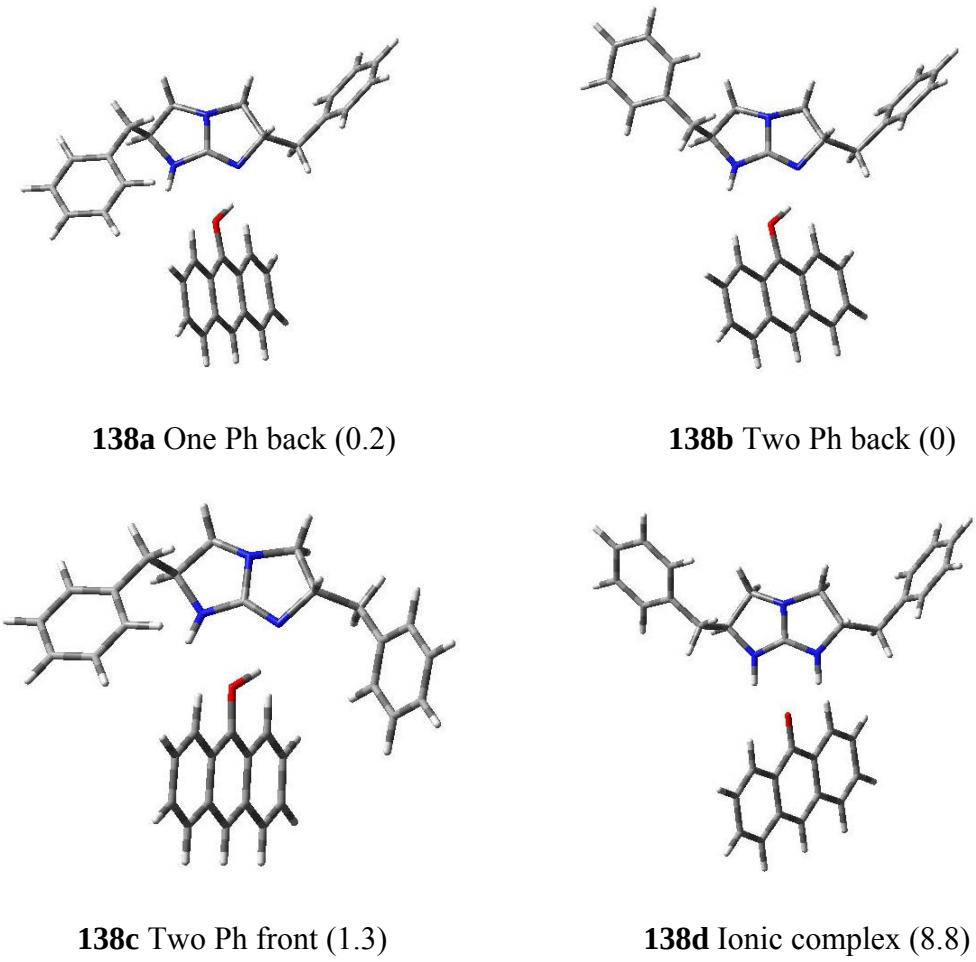

138a One Ph back (0.2) **138b** Two Ph back (0)

138c Two Ph front (1.3) **138d** Ionic complex (8.8)

Fig. 3.9. Calculated relative energy of different anthrone and guanidine complex. Free energies (kcal/mol) are shown.

Figure 3.9 displays four calculated structures of bicyclic anthrone **19a** and guanidine **124d** for the Diels–Alder reaction. First, the guanidine-anthronol complex **138b** is more stable than the guanidinium-enolate complex **138d** by 8.8 kcal/mol.

Therefore, it is likely that guanidine **124d** cooridinates with **19a** through double hydrogen bonding but without formation of zwitterionic intermediate as guanidinium-enolate complex (**138d**). On the other hand, guanidine-anthronol complex **138b** is more stable than **138a** and **138c** by 0.2 and 1.3 kcal/mol, respectively. It is probably due to the steric repulsion by the phenyl group of the guanidine in **138a** and **138c**. Thus the guanidine-anthronol complex **138b** is the optimized transition state in the gas phase. It is thought that anthronol coordinates to guanidine in a bidentate fashion and the proton of hydroxyl group in anthronol is suitably positioned in proximity of the guanidine nitrogen.

The key effect of a catalyst in a chemical reaction is to reduce the reaction barrier. If the catalyst is able to interact with the starting material, the transition structure (TS) and the products, it is necessary that the relative stabilization of the TS is the largest. To validate the efficiency of the catalyst, we compared the gas-phase results of the reaction of anthrone **19a** and *N*-phenylmaleimide **20b** catalyzed by guanidine **124d** (Figure 3.10) with the uncatalyzed reaction (Figure 3.8). As depicted in Figure 3.9, **138b** is the optimized transition state in gas phase. When phenylmaleimide is bound to guanidine-anthronol complex **138b** in the fashion shown in Figure 3.10, there is an energy loss of 4.4 kcal/mol. Compared with uncatalyzed reaction, the transition state **TS140** is stabilized by about 16 kcal/mol. At the stage of the formation of intermediate **139**, one of the hydrogen bonds between anthrone and guanidine is lost in favor of a double hydrogen bonding between the guanidine, anthrone and phenylmaleimide. Thus it can better stabilize the ternary transition structure **TS140**.

124d works as a bifunctional catalyst activating both the diene and dienophile at defined positions simultaneously. The relative stability of the *S*, *S*-product **21b** was obtained from the most stable calculated transition structures, **TS140** and **TS142** (Figure 3.10). Kinetic analysis of the reaction of anthrone **19a** with phenylmaleimide **20b** catalyzed by **124d** showed first order in both substrates and catalyst (see experimental procedures), in agreement with phenylmaleimide **20b** bound to complex **138b** being the rate-determining step.

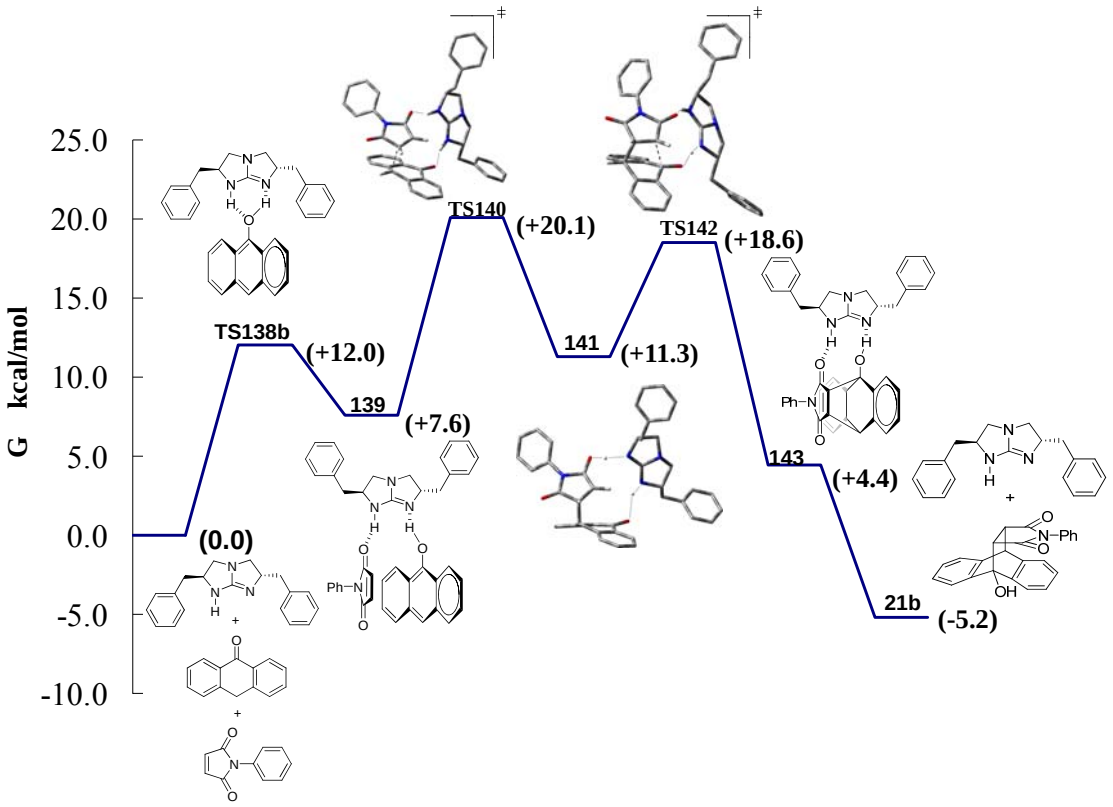

Fig. 3.10. The Diels–Alder reaction between anthrone **19a** and N-phenylmaleimide **20b** catalyzed by guanidine **124d**. The energies at the B3LYP/6-31G** level relative to the starting material are given in kcal/mol.

In the highly enantioselective Diels–Alder reaction catalyzed by chiral bicyclic guanidine, it is believed that two key features of guanidine and guanidinium groups are important: 1) The high basicity of the guanidine group is required to initiate the

base catalyzed Diels–Alder reaction; and 2) The special double hydrogen bonding pattern between the guanidine group **124d**, anthrone **19a** and *N*-phenylmaleimide **20b**. According to the dual activation model proposed by Takemoto[61], **124d** may work as a bifunctional catalyst, by activating both the diene and dienophile at defined positions simultaneously.

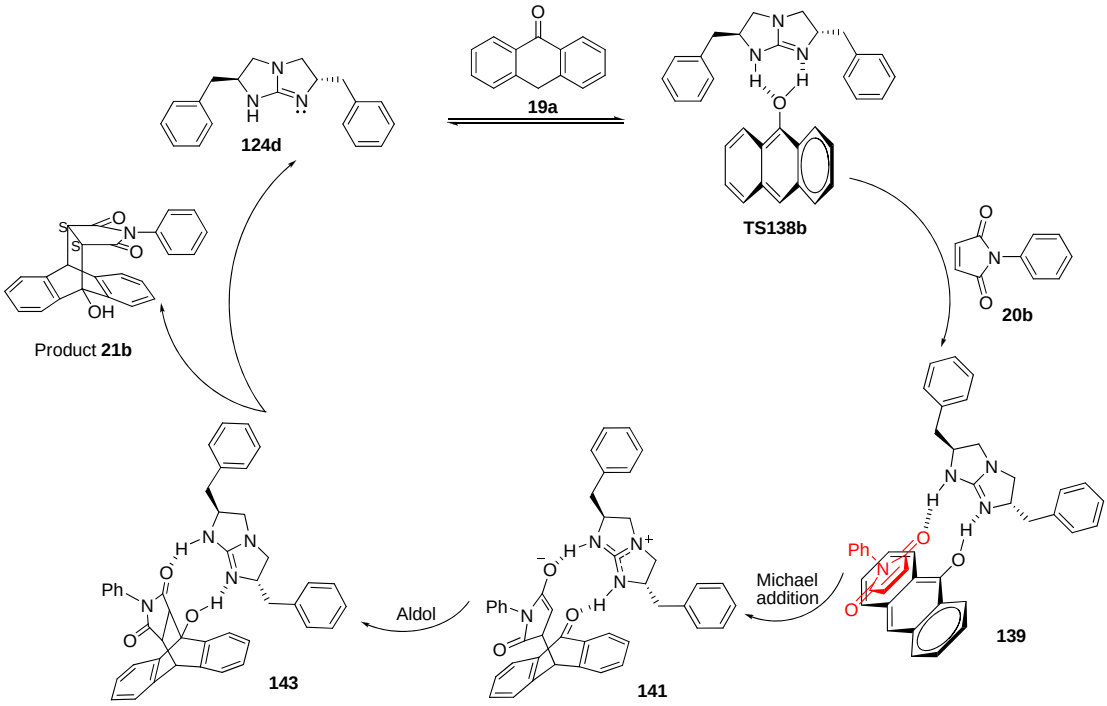

Scheme 3.4. Proposed catalytic cycle in the chiral bicyclic guanidine catalyzed Diels–Alder reaction.

Based on kinetic and computational analysis, the catalytic cycle of the chiral bicyclic guanidine **124d** catalyzed Diels–Alder reaction between anthrone **19a** and *N*-phenylmaleimide **20b** is proposed as in Scheme 3.4. The reaction is likely to proceed *via* a stepwise Michael-aldol mechanism. In the first step of the cycle, hydrogen bond formation between anthrone **19a** and guanidine **124d** generates a guanidine-anthronol complex **138b**. *N*-phenylmaleimide **20b** approaches the complex **138b** to form double hydrogen bonding intermediate **139**. From the previous titration

experiment of **124d** in the presence of different amounts of **20b**, it may also reveal some information about the interaction of **124d** and **20b** through hydrogen bonding. Michael addition reaction occurs to generate the adduct **141**, which coordinates with guanidinium through double hydrogen bonding to avoid the free rotation of the newly formed C-C bond. The complex may also be stabilized by electrostatic attraction between the ion pairs. Consequently, **141** undergoes an intramolecular Aldol reaction to give product-guanidine complex **143**, which readily releases the catalyst **124d** and gives the (*S*, *S*)-**21b**.

The formation of a small amount of Michael adduct also raises the possibility of a two-step mechanism for the asymmetric synthesis of **21b** (Michael addition followed by an intramolecular aldolization). As discussed in the previous chapter, dithranol reacts more rapidly than anthrone and exhibits a strong tendency to give Michael adduct. A possible explanation is that the acidic phenolic hydroxyl groups of dithranol will terminate the Aldol reaction step. The results of dithranol reactions also demonstrate that the reaction of anthrone **19a** and phenylmaleimide **20b** catalyzed by **124d** is likely to proceed through a stepwise Michael-Aldol mechanism.

Conclusion

In conclusion, when using Et_3N as the catalyst, it functions as a normal base to abstract a proton from anthrone. The anthrone works a reactive diene in Diels-Alder reaction. When chiral bicyclic guanidine was used as the catalyst, both kinetic analysis and experimental results support the proposal that the guanidine catalyzed Diels–Alder reaction of anthrones proceeds *via* a mechanism that involves

simultaneous activation of anthrone and of phenyl maleimide by the guanidine at defined positions. Consistent with experimental observations, the calculations predict that ternary transition structure **139** plays an important role in defining the stereochemistry of the product.

Further computational studies and other techniques, such as crystal X-ray diffraction may give greater insights and help elucidate the mechanism of the asymmetric induction.

Chapter 4

Anthrone-Derived NHPI Analogues as Catalysts in Reactions Using Oxygen as an Oxidant

In recent years, *N*-hydroxyphthalimide (NHPI, Fig. 4.1) has been recognized as a valuable catalyst for the aerobic oxidation of organic compounds under mild conditions.[62] Molecular oxygen, which is environmentally benign and economical, would be an ideal oxidant for the oxygenation of hydrocarbons. These oxidations proceed *via* a phthalimide *N*-oxyl (PINO) radical intermediate which is able to abstract hydrogen atom from organic compounds.[63] The newly formed carbon centered radical then readily reacts with molecular oxygen to give oxygenated compounds. However, PINO is not stable under aerobic oxidation conditions.[63c,e]

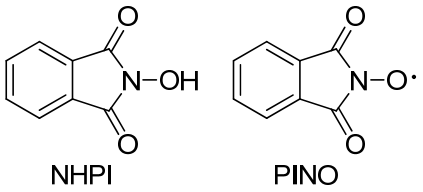

Fig. 4.1. NHPI and PINO.

4.1 Enantioselective Synthesis of Anthrone-Derived NHPI Analogues

It is likely that a suitably designed chiral analogue of NHPI should be of value for asymmetric catalysis. Einhorn reported the synthesis of axially chiral analogues of NHPI.[64a] These analogues gave oxygenated products with moderate enantioselectivities in several catalytic asymmetric oxidation reactions, such as the desymmetrisation of 2-substituted indanes and the kinetic resolution of racemic acetals. A second generation of C_2-symmetrical NHPI analogues based on diphenol was subsequently developed and demonstrated to give moderate to high enantioselectivities for the oxidative ring opening reactions of various *N*-acyl oxazolidines.[64b] The enantioselectivities were highly dependent on the substitution

pattern of the catalysts. Such catalysts could be useful for the synthesis of highly enantiomerically enriched oxazolidines. These experiments represent the first examples of chiral NHPI analogues catalyzed enantioselective aerobic oxidations. Herein, we report a new class of NHPI analogues **145a-d** (Table 4.1), which were derived from anthrones. They were investigated as catalysts for asymmetric aerobic oxidation of various organic compounds.

Table 4.1. Chiral bicyclic guanidine-catalysed Diels–Alder reactions between substituted anthrones and maleimides.

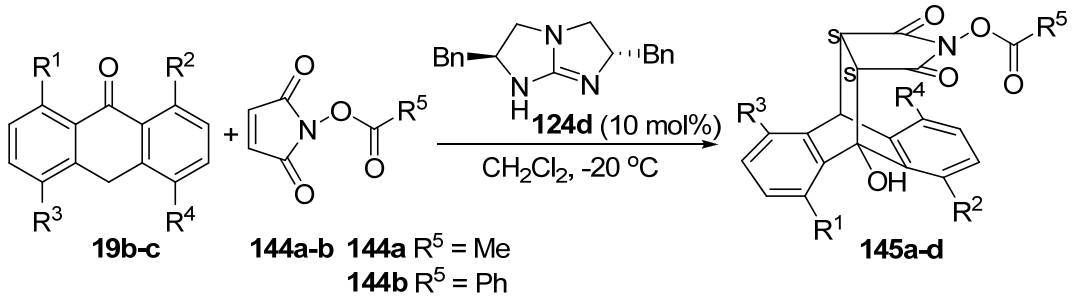

entry	**19** [R^1, R^2, R^3, R^4]	R^5	**145**	yield/%[a]	ee/%[b]
1	**19b** [Cl, Cl, H, H]	Me	**145a**	86	92
2	**19b** [Cl, Cl, H, H]	Ph	**145b**	85	12
3	**19c** [H, H, Cl, Cl]	Me	**145c**	83	64
4	**19c** [H, H, Cl, Cl]	Ph	**145d**	84	87

[a] isolated yield. [b] chiral HPLC.

The Brønsted-basic bicyclic guanidine **124d** has been reported by our group to be an efficient catalyst for the enantioselective Diels–Alder reactions between various anthrones and activated olefins.[65] It led us to evaluate **124d** as catalyst for the reactions of substituted anthrones **19b-c** with protected *N*-hydroxymaleimides **144a-b**. High enantioselectivity and high yield were achieved for adduct **145a** (Table 4.1, entry 1). Substituted anthrones **19b-c** were prepared from the reduction of their corresponding anthracenediones[66] while the *N*-hydroxymaleimides **144a-b** were

prepared from the retro-Diels–Alder reaction of *N*-hydroxy-3,6-epoxy-1,2,3,6-tetrahydro-phthalimide.[67] The subsequent cleavage of the protecting group from 1**45a** was carried out by the treatment with ethylamine in MeOH to yield the anthrone-derived NHPI analogue **146** (Scheme 4.1).

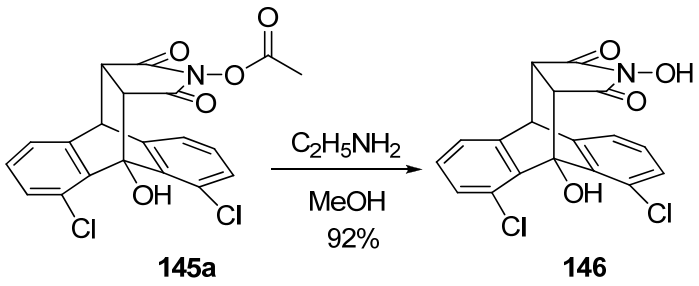

145a **146**

Scheme 4.1. Synthesis of chiral anthrone-derived NHPI analogues.

4.2 Asymmetric Aerobic Oxidation of Benzylic Compounds and Diols Catalyzed by Anthrone-Derived NHPI Analogues with Co(II)

A variety of benzylic compounds can be oxidised to their corresponding oxygenated derivatives by molecular oxygen in the presence of NHPI.[68] When NHPI was replaced by racemic **146** in some preliminary oxidation experiments, very similar results were obtained. This indicated that **146** has the desired catalytic properties. With optically pure **146** in hand, we attempted several asymmetric oxidation reactions of benzylic compounds and diol with **146** and cobalt acetate as the co-catalyst. Cobalt acetate is particular effective in the initiation step because Co(II) activates molecular oxygen to generate a Co(III)-dioxygen complex (Eqn 1). The resulting Co(III)-dioxygen complex assists the formation of a *N*-oxyl radical from anthrone-derived NHPI analogue **146** (Eqn 2).

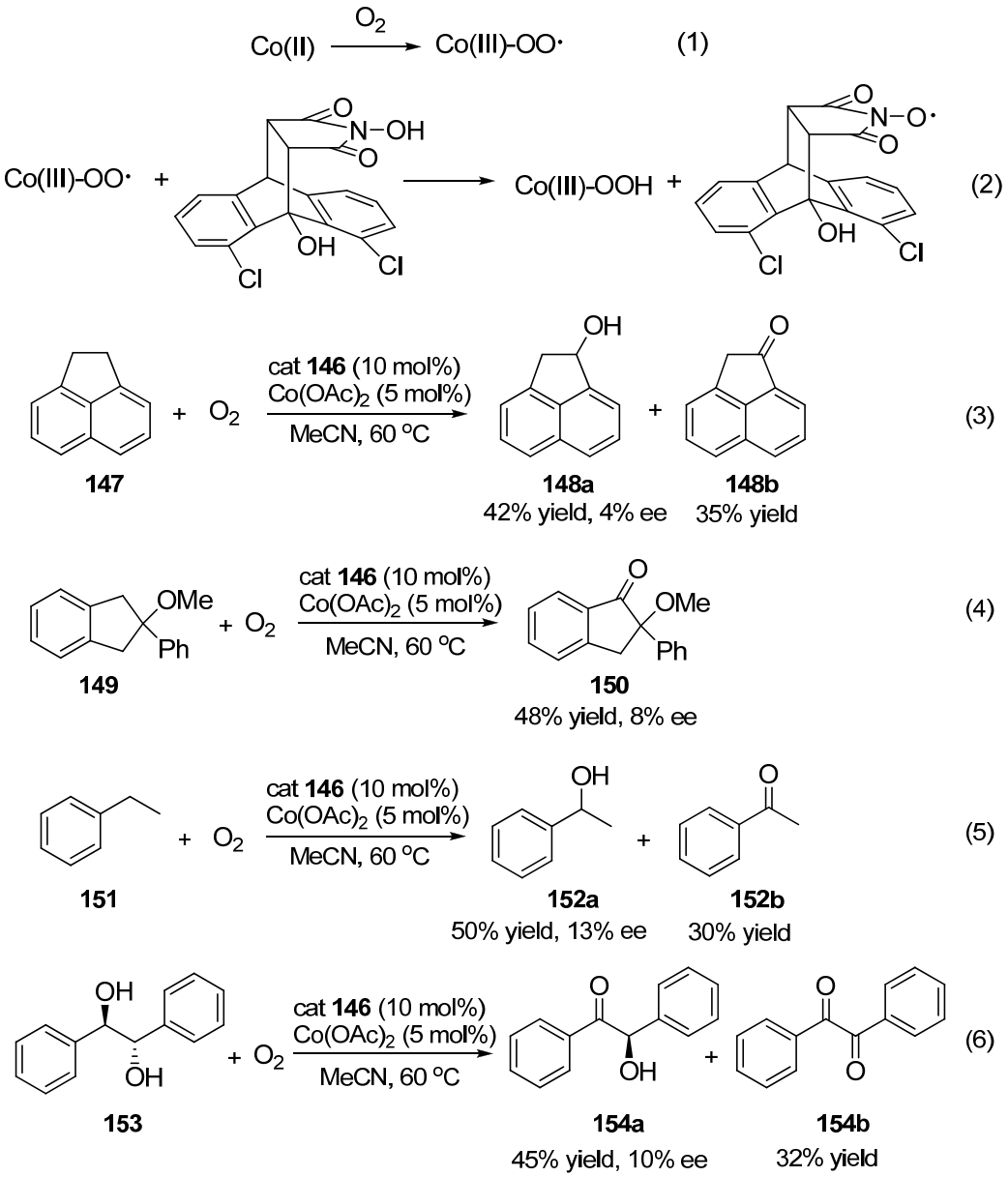

The aerobic oxidation of 0.2 M of acenaphthene **147** in CH_3CN at 60 °C in the presence of 10 mol% of optically pure **146** (92% ee) and $Co(OAc)_2$ (1 mol%) gave alcohol **148a** in 42% yield. Asymmetric induction was negligible (4% ee) (Eqn. 3) and significant over-oxidation was observed, leading to 35% yield of acenaphthylen-1(*2H*)-one **148b**. Indane is readily oxidised to 1-indanone in good yield by NHPI-mediated oxidation.[64,68] Indanes bearing two different substituents on C2 are interesting substrates for asymmetric oxidations as they have two enantiotopic

benzylic carbons. Using similar reaction condition, 2-methoxy-2-phenylindane **149** was oxidised to ketone **150** in 48% yield and 8% ee (Eqn. 4). Slightly better result was observed with ethylbenzene **151**. It was oxidised to 1-phenylethanol **152a** in good yield and 13% ee (Eqn. 5). Over-oxidation was also appreciable and 30% of acetophenone **152b** was obtained.

It has been shown that NHPI in combination with Co(II) salts is also an efficient method for the oxidation of alcohols to their corresponding carbonyl compounds.[69] Our experiments with compounds **147**, **149** and **151** also demostrated that the **146**/Co(II) catalyst system is able to oxidise alcohols with ease under mild conditions. 1,2-Diphenylethanediol **153** was oxidised to benzoin **154a** in 45% yield and 10% ee with 32% of the over-oxidised product, benzil **154b** (Eqn. 6). Optimisation of the reaction may be possible through the variation of reaction temperature and reaction time.

4.3 Aerobic Radical addition of dioxolanes or alcohols to activated alkenes Catalyzed by Anthrone-Derived NHPI Analogues with Co(II)

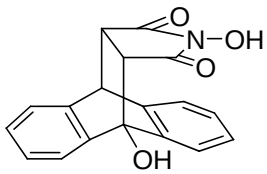

155

Fig. 4.2. Racemic catalyst **155**.

The chiral induction in the previous oxidation reactions was moderate. However, these results clearly indicate that asymmetric catalysis mediated by optically active **146** is possible. We intend to develop several other aerobic oxidation reactions using

our anthrone-derived NHPI analogues as catalysts. Subsequent exploratory work was carried out using racemic catalyst **155** (Fig. 4.2).

Addition of aldehydes to terminal alkenes is an unique method for the preparation of ketones.[71] Direct hydroacylation of terminal alkenes with aldehydes by transition-metal catalysts has been reported (Eqn. 7).[70] The concomitant introduction of acyl or hydroxy moieties to alkenes, referred to as hydroxyacylation, can be achieved by a cascade reaction (Eqn. 8). This provides a novel route to β-hydroxy carbonyl compounds. Acyl radicals[71] can easily decarbonylate and react with O_2 leading to carboxylic acids and other undesired products.[72] To overcome these drawbacks, 1,3-dioxolanes were often employed as masked aldehydes and as the source of the acyl group.[73,74] Deprotection of the product, a β-hydroxy ketal, under acidic conditions will provide the β-hydroxy carbonyl compounds.

***Hydro**acylation*

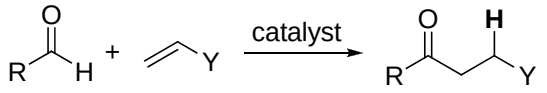

(7)

***Hydroxy**acylation*

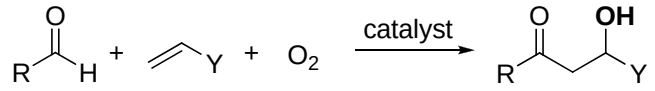

(8)

Table 4.2. Hydroxyacylation of alkenes using 1,3-dioxolanes and dioxygen.

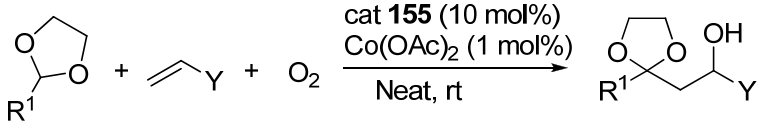

156 **157** **158**

entry	**156** [R^1]	Y	**158**	yield/%[a]
1	**156a** [H]	**157a** [CO_2Me]	**158a**	60
2	**156a** [H]	**157b** [CN]	**158b**	56
3	**156b** [Me]	**157a** [CO_2Me]	**158c**	58
4	**156b** [Me]	**157b** [CN]	**158d**	52

[a] isolated yield.

A mixture of 1,3-dioxolane **156a** and methyl acrylate **157a** was allowed to react under O_2 (1atm) in the presence of catalyst **155** (10 mol%) and a small amount of $Co(OAc)_2$ (1 mol%) at room temperature for 5 hrs (Table 4.2, entry 1). The β-hydroxy ketal **158a** was obtained in 60% yield. Acrylonitrile **157b** was also found to serve as a good acceptor for **156a**, giving cyanohydrin **158b** in good yield (entry 2). 2-Methyl-1,3-dioxolane **156b** also provided the corresponding hydroxy-acylated products **158c-d** in good yields (entries 3 and 4).

α-Hydroxy-γ-lactones are valuable synthetic precursors to compounds such as α,β-butenolides, which have potent biological activities.[75] They are also useful as monomers of biodegradable polymers and as fine chemicals. Ishii reported the catalytic generation of α-hydroxy carbon radical using NHPI in combination with cobalt acetate under O_2 (1 atm).[76] Trapping the generated radicals with α,β-unsaturated esters leads to α-hydroxy-γ-lactones which are difficult to obtain by conventional methods. This new method for the construction of α-hydroxy-γ-lactones is general for a variety of alcohols and α,β-unsaturated esters.

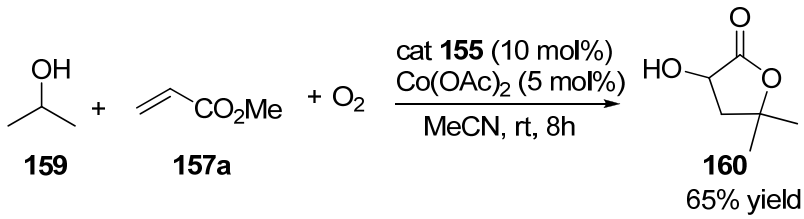

(9)

Catalyst **155**/$Co(OAc)_2$ was employed in the radical reaction between isopropyl alcohol **159** and methyl acrylate **157a** under O_2 (1 atm). This reaction occurred at room temperature to give **160** in 65% yield in 8 hrs (Eqn. 9).

In conclusion, we have developed an enantioselective synthesis of

anthrone-derived NHPI analogues. One of these analogues, in combination with Co salts, was employed to catalyze the aerobic oxidation of benzylic compounds and diols. However, low enantioselectivities were observed. Exploratory studies using a racemic version of the catalyst were also conducted. Radical addition of dioxolanes or alcohols to activated alkenes with molecular oxygen as the terminal oxidant was shown to be catalyzed with the NHPI-analogues.

Chapter 5

Experimental Procedures

5.1 General Procedures

^{1}H and ^{13}C NMR spectra were recorded on a Bruker ACF300 (300 MHz) or AMX500 (500 MHz) spectrometer. Chemical shifts are reported in parts per million (ppm). The residual solvent peak was used as an internal reference. Low resolution mass spectra were obtained on a VG Micromass 7035 spectrometer in EI mode, a Finnigan/MAT LCQ spectrometer in ESI mode, and a Finnigan/MAT 95XL-T mass spectrometer in FAB mode. All high resolution mass spectra were obtained on a Finnigan/MAT 95XL-T spectrometer. Infrared spectra were recorded on a BIO-RAD FTS 165 FTIR spectrometer. Enantiomeric excesses were determined by chiral HPLC analysis on Jasco HPLC units, including a Jasco DG-980-50 Degasser, a LG-980-02 Ternary Gradient Unit, a PU-980 Intelligient HPLC Pump, UV-975 Intelligient UV/VIS Detectors, and an AS-950 Intelligient Sampler. Optical rotations were recorded on a Jasco DIP-1000 polarimeter. Melting points were determined on a BÜCHI B-540 melting point apparatus. Analytical thin layer chromatography (TLC) was performed with Merck pre-coated TLC plates, silica gel 60 F-254, layer thickness 0.25 mm. Flash chromatography separations were performed on Merck 60 (0.040 - 0.063 mm) mesh silica gel. THF was freshly distilled from sodium/benzophenone before use. CH_2Cl_2 were distilled from calcium hydride and stored under N_2 atmosphere. All distilled solvents were stored under N_2. All other reagents and solvents are commercial grade and were used as supplied without further purification, unless otherwise stated.

5.2 Preparation and characterization of dienes and dienophiles

Diene **2b-2e** was prepared using literature protocol.[40a] Aryl maleimides was prepared using literature protocol.[41f] Alkyl maleimides was prepared using literature protocol.[41g]

(19b) 1,8-dichloroanthracen-9(10*H*)-one

Yellow solid. ^{1}H NMR (300 MHz, $CDCl_3$, ppm): δ 4.21 (s, 2H), 7.30-7.46 (m, 6H). LRMS (FAB) m/z 262.9 ($M+H^+$).

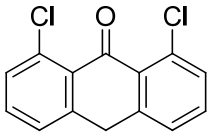

(19c) 4,5-dichloroanthracen-9(10*H*)-one

Yellow solid. ^{1}H NMR (300 MHz, $CDCl_3$, ppm): δ 4.20 (s, 2H), 7.42-8.28 (m, 6H). LRMS (EI) m/z 261.8 (M^+).

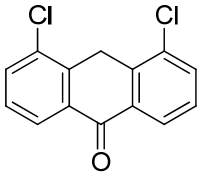

(19d) 1, 5-dichloroanthracen-9(10*H*)-one

Yellow solid. ^{1}H NMR (300 MHz, $CDCl_3$, ppm): δ 4.35 (s, 2H), 7.42-8.23 (m, 6H). LRMS (EI) m/z 261.9 (M^+).

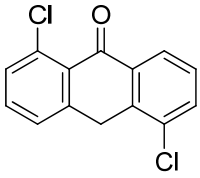

(19f) 4-(methylamino)anthracen-9(10*H*)-one

Yellow solid. ^{1}H NMR (300 MHz, $CDCl_3$, ppm): δ 3.02 (s, 3H), 3.98 (s, 2H),

6.96-8.38 (m, 7H). ^{13}C NMR (300 MHz, $CDCl_3$, ppm): δ 27.8, 31.2, 113.5, 113.8, 116.7, 117.0, 127.1, 127.5, 127.7, 128.6, 131.8, 132.6, 139.3, 145.7, 184.5. LRMS(EI) m/z 223.1 (M^+), HRMS(EI) m/z 223.0995 (M^+), calc. 223.0997 for $C_{15}H_{13}NO$.

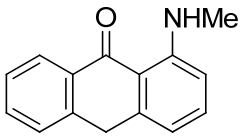

(20c) 1-(2-nitrophenyl)-1*H*-2, 5-dione

Light yellow solid. ^{1}H NMR (300 MHz, $CDCl_3$, ppm): δ 6.93 (s, 2H), 7.42-8.19(m, 4H). LRMS (EI) m/z 218.0 (M^+).

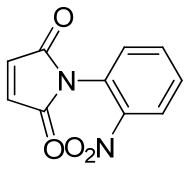

(20d) 1-(2, 5-dichlorophenyl)-1H-pyrrole-2, 5-dione

Yellow solid. ^{1}H NMR (300 MHz, $CDCl_3$, ppm): δ 6.90 (s, 2H), 7.29-7.48 (m, 3H). LRMS (EI) m/z 242.6 (M^+).

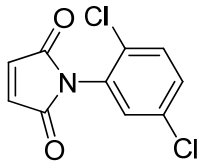

(20h) 1-isobutyl-1*H*-pyrrole-2, 5-dione

White solid. ^{1}H NMR (300 MHz, $CDCl_3$, ppm): δ 0.87 (d, 6H, J = 6.6Hz), 2.00 (m, 1H), 3.32 (d, 2H, J = 7.3Hz), 6.68 (s, 2H). ^{13}C NMR (300 MHz, $CDCl_3$, ppm): δ 19.9, 27.7, 45.1, 133.9, 171.1. LRMS (EI) m/z 152.9 (M^+).

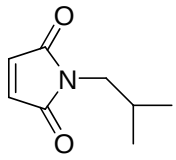

(20i) 1-(4-chlorobenzyl)-1H-pyrrole-2,5-dione

White solid. ^{1}H NMR (300 MHz, $CDCl_3$, ppm): δ 4.67 (d, 2H, J = 3.5Hz), 6.73 (s, 2H), 7. 30-7.32 (m, 4H). LRMS (EI) m/z 220.9 (M^+).

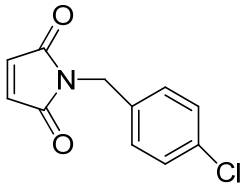

(20k) 1-(2, 6-difluorophenyl)-1*H*-pyrrole-2, 5 -dione

White solid. ^{1}H NMR (300 MHz, $CDCl_3$, ppm): δ 6.93 (s, 2H), 7.02-7.44 (m, 3H). LRMS (EI) m/z 208.9 (M^+).

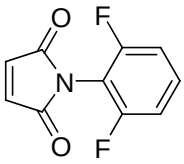

(20l) 1-(2-methoxyphenyl)-1*H*-pyrrole-2, 5- dione

White solid. ^{1}H NMR (300 MHz, $CDCl_3$, ppm): δ 3.83(s, 3H), 6.88 (s, 2H), 7.04-7.45(m, 4H). LRMS (EI) m/z 203.0 (M^+).

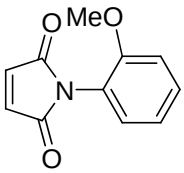

(20n) 1-mesityl-1H-pyrrole-2, 5- dione

White solid. ^{1}H NMR (300 MHz, $CDCl_3$, ppm): δ 2.08 (s, 6H), 2.31 (s, 3H), 6.84 (s,

2H), 6.97 (s, 2H). LRMS (EI) m/z 215.0 (M^+).

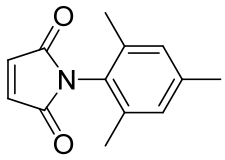

(20p) 1-hexyl-1H-pyrrole-dione

Yellow oil. ^{1}H NMR (300 MHz, $CDCl_3$, ppm): δ 0.87 (m, 3H), 1.27 (s, 6H), 1.56 (m, 2H), 3.50 (t, 2H, J = 7.3Hz), 6.67 (s, 2H). LRMS (EI) m/z 181.0 (M^+).

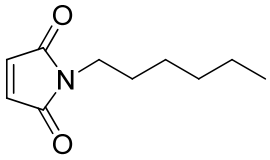

(20q) 1-(3, 4-dichlorophenyl)-1*H*-pyrrole-2, 5- dione

White solid. ^{1}H NMR (300 MHz, $CDCl_3$, ppm): δ 6.88 (s, 2H), 7.27-7.55 (m, 3H). LRMS (EI) m/z 240.8 (M^+).

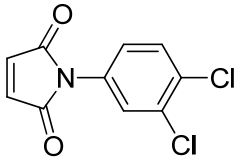

5.3 Procedures for the Synthesis of Chiral Bicyclic Guanidines 124d

5.3.1 Procedure for preparation of aziridine 126

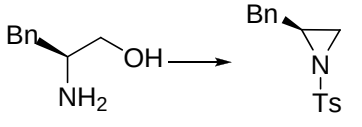

125 **126**

To a flame dried round-bottom flask containing 4Å molecular sieves and a magnetic bar was added L-phenylalaniol (**125**, 128.5 mg, 0.85 mmol), Et_3N (0.48 ml,

3.4 mmol, 4 equiv.), and dry MeCN (2.4 ml). It was cooled to 0 °C and then TsCl (323 mg, 1.7 mmol, 2 equiv.) was added in one portion. After stirring at 0 °C for 20 min, the reaction mixture was brought to room temperature and stirred for another 1 h. The solvent was removed under reduced pressure and ethyl acetate (5 ml) was added. The resulted precipitate and molecular sieves were removed by suction filtration and washed thoroughly with ethyl acetate. After removing the solvent of the filtrate and chromatography on silica gel, **126** was obtained as a white solid (225 mg, 92% yield).

5.3.2 Procedure for ring-opening of *N*-tosyl aziridine using benzylamine

N-Tosyl-aziridine **126** (225 mg, 0.94 mmol,) and benzylamine (50.6 g, 0.47mmol) were dissolved in dry methanol (4.2 mL) and the mixture stirred under reflux for 3 days. The solvent was evaporated under reduced pressure, leaving an off-white oil. Upon trituration with diethyl ether (4.2 mL) the desired product **127** precipitated as colourless crystals, which were recrystallised from ethanol in 92% yield. Mp 119–120°C. $[\alpha]_D^{25}$ −18.0 (*c* 0.5, $CHCl_3$). 1H NMR: δ 7.63 (d, 4H, J = 8.2), 7.20–7.13 (m, 13H), 7.06–7.01 (m, 2H), 6.94–6.91 (m, 4H), 5.22 (bs, 2H), 3.63 (bs, 2H), 3.54 (d, 1H, J = 13.5), 3.10 (d, 1H, J=13.5), 2.71 (dd, 2H, J = 13.9, 5.9), 2.55–2.30 (m, 12H). ^{13}C NMR: δ 143.2, 138.0, 137.5, 129.7, 129.6, 129.4, 128.6, 128.5, 127.4, 127.1, 126.5, 58.3, 58.0, 53.3, 40.1, 21.6. IR (film): 3343, 3219, 1599, 1494, 1450, 1415, 1319, 1149, 1090, 1041, 985, 949, 817, 756, 735, 703, 663, 592, 546 cm $^{-1}$. LRMS(FAB) m/z 682 ($M+H^+$), HRMS(FAB) m/z 682.2750 ($M+H^+$), calc. for $C_{39}H_{44}N_3O_4S_2$ 682.2773.

5.3.3 Procedure for the removal of *p*-toluenesulfonyl (Ts) group

Na (793 mg, 100 equiv.) was washed with hexane and transferred into a 25 ml flame dried two-necked round-bottom flask equipped with a magnetic bar and an ammonium condenser. The reaction flask and the condenser were cooled to -78 ^{o}C. NH_3 gas was condensed through the condenser into the reaction flask until a dark blue solution (around 10 ml) was formed. While stirring, a THF solution (1 ml) of the triamine backbone **127** (235 mg, 0.345 mmol) was added dropwise into the dark blue solution at -78 ^{o}C. Stirring was continued at -78 ^{o}C and more Na was added whenever the dark blue color fades. After 4 h, the reaction flask was opened to the air and brought to room temperature. Solid NH_4Cl was added slowly with vigorous stirring until a white heterogeneous mixture was formed. After all NH_3 evaporated off, CH_2Cl_2 (5 ml) was added to the resulted white solid and stirred for a half hour. The solid was then removed by suction filtration and was washed with CH_2Cl_2 (3 x 5 ml). The filtrate was combined and the solvent was removed under reduced pressure, giving pale yellow oil in quantitative yield. The crude product was used directly for next reaction.

5.3.4 Procedure for Pd/C catalyzed hydrogenation:

After **127** (235 mg, 0.345 mmol) underwent removal of tosyl group in $Na/NH_3(l)$, the crude product was dissolved in dry methanol (3 ml) and added to a dry round-bottom flask containing 10% Pd/C (50 mg, 50% w/w). The reaction mixture was purged with H_2 gas for a half hour and kept stirring under H_2 balloon. The reaction was monitored by TLC. Upon completion of reaction, the Pd/C was removed by suction filtration and the solvent was evaporated off under reduced pressure,

affording **129** as a pale yellow oil, which was used for next step without further purification.

5.3.5 Procedure for final cyclization step:

(This procedure mainly followed the protocol reported by Davis and Dempsey[77] with a slight modification during work-up). The crude free triamine **129** (74 mg, 0.26 mmol) was dissolved in nitromethane (1 ml). Dimethyl trithiocarbonate (36 μl, 0.33 mmol, 1.25 equiv.) in nitromethane (0.1 ml) was added to the mixture slowly, followed by refluxing at 110 °C for 2 h, and then was cooled to room temperature. Acetic acid (61 μl, 1.06 mmol, 4 equiv.) and MeI (49 μl, .53 mmol, 2 equiv.) were added. It was refluxed at 110 °C for 3 h and left stirring at room temperature overnight. CH_2Cl_2 (1 ml) was added to dilute the reaction mixture and the solvent was removed under reduced pressure. CH_2Cl_2 (1 ml) was added and the solution was loaded onto a plug of silica gel. It was eluted with copious CH_2Cl_2 to flush out the dark colored portion and then CH_2Cl_2/MeOH (19:1) to recover the product, which was assumed to be a HI salt. The product was basified with K_2CO_3 in CH_2Cl_2, giving the guanidine **124d** in free amine form as a pale yellow oil (64 mg, 84 % yield from **127**).

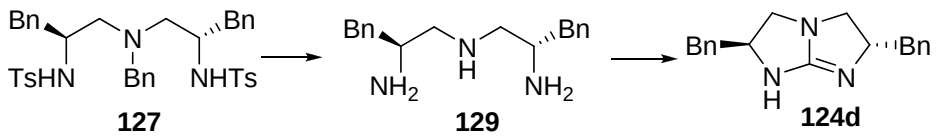

As described above, **127** underwent detosylation and hydrogenolysis, followed by the final cyclization step, to give **124d** as a pale yellow oil in 84% yield (based on **127**). $[\alpha]_D^{25}$ = -22.3 (*c* 1.0, $CHCl_3$). ^{1}H NMR (300 MHz, $CDCl_3$, ppm): δ 2.77 (dd, *J* =

7.5, 13.5 Hz, 2H), 2.83 (dd, *J* = 6.0, 8.0 Hz, 2H), 2.95 (dd, *J* = 7.0, 13.5 Hz, 2H), 3.09 (t, *J* = 7.5 Hz，2H), 4.27 (quintet, *J* = 7.0 Hz, 2H), 7.21-7.33 (m, 10H). ^{13}C NMR (75 MHz, $CDCl_3$, ppm): δ 42.1, 53.6, 65.9, 126.6, 128.7, 129.3, 138.5, 168.3. IR (film): 3069, 3020, 2929, 2857, 1776, 1707, 1667, 1600, 1499, 1459, 1386, 1316, 1187 cm^{-1}. LRMS(ESI) m/z 291.8 ($M+H^+$), HRMS(ESI) m/z 292.1816 ($M+H^+$), calc. for $C_{19}H_{22}N_3$ 292.1814.

5.4 Typical Experimental Protocols for the Reactions of Anthrones

5.4.1 Typical experimental protocols: Standard bicyclic guanidine catalyzed reactions between anthrone, its derivatives and various olefins

To a 5 ml RBF containing catalyst **124d** (0.58 mg, 0.002 mmol, 10 mol %) and a stirring bar, anhydrous CH_2Cl_2 (0.1 ml), 1, 8-dichloro-9-anthrone **19b** (5.8 mg, 0.022mmol) and N-benzylmaleimide **20e** (3.7 mg, 0.02mmol) were added in this sequence. After stirring at room temperature for half an hour, the reaction mixture was load onto a short silica gel column, followed by flash chromatography (gradient elution with hexane/EA mixtures; 9/1 to 4/1). Product **21e** (8.1mg) was obtained as a white solid in 90% yield and 96% ee.

5.4.2 Characterization of Diels-Alder and Michael adducts

(21b) 4-Hydroxy-2-phenyl-3a, 4, 9, 9a-tetrahydro-4, 9[1’, 2’]-benzeno-1*H*-benz[*f*]isoindole-1, 3(2*H*)-dione

White solid. mp 213.4-216.5 ^{o}C. 90% yield, 81% ee. $[\alpha]_D^{25}$ +33.6 (*c* 0.39, $CHCl_3$). ^{1}H NMR (300 MHz, $CDCl_3$, ppm) ： δ 3.27 (d, 1H, *J* = 8.7Hz), 3.49 (dd, 1H, *J* = 3.5,

8.7Hz), 4.55 (s, 1H), 4.84 (d, 1H, J = 3.5Hz), 6.47-7.30 (m, 13H). ^{13}C NMR (75 MHz, $CDCl_3$, ppm): δ 29.6, 44.8, 47.7, 50.8, 120.9, 121.1, 123.7, 124.7, 126.3, 126.8, 126.9, 127.2, 127.3, 128.9, 129.1, 130.9, 136.6, 138.9, 141.0, 142.3, 175.5, 177.1. IR (film): 1215.2, 1704.8, 3019.3 cm^{-1}. LRMS (EI) m/z 367.2 (M^+), HRMS (EI) m/z 367.1203(M^+), calc. for $C_{24}H_{17}NO_3$ 367.1208.

The ee determined by chiral HPLC; CHIRALCEL AD-H (4.6 mm i.d. x 250 mm); hexane/2-propanol 80/20; flow rate 1.0 ml/min; temp 25 °C; detection UV 230 nm; retention time: 24.3 min and 31.8 min.

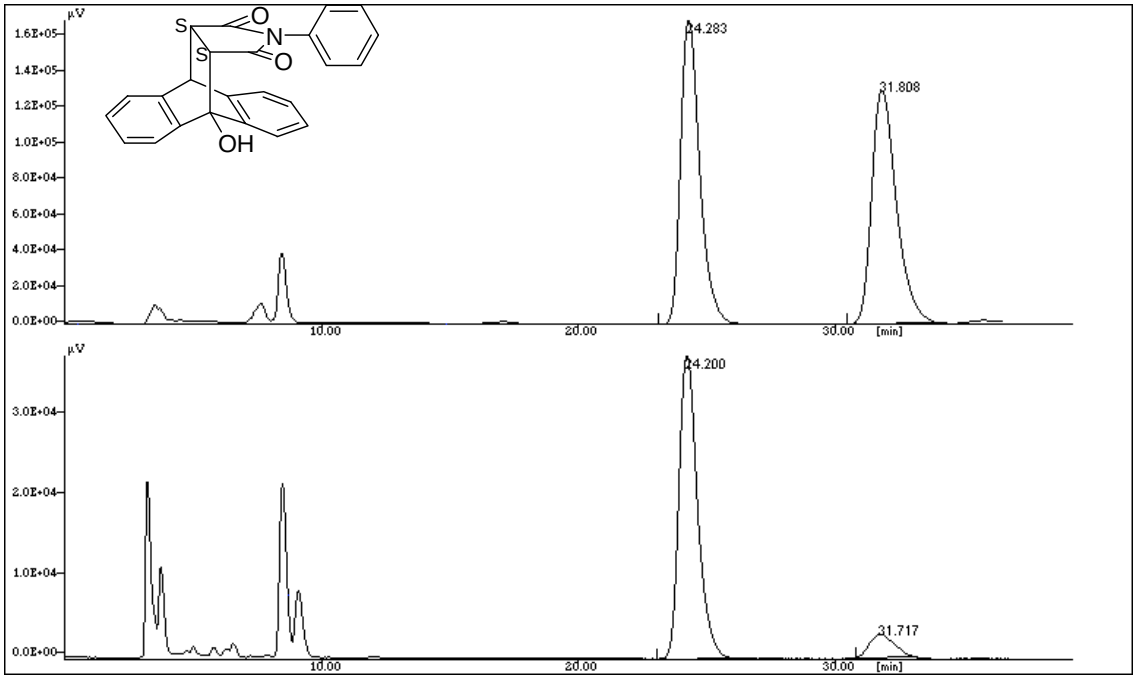

(21c) 4-Hydroxy-2-(2-nitrophenyl)-3a, 4, 9, 9a-tetrahydro-4, 9[1', 2']-benzeno-1*H*-benz[*f*]isoindole-1, 3(2*H*)-dione

White solid. mp 219.4-221.6 ^oC. 90% yield, 96% ee. $[\alpha]_D^{27}$ +58 (c 0.25, $CHCl_3$). ^{1}H NMR (300 MHz, $CDCl_3$, ppm) ： δ 3.38 (d, 1H, J = 8.7Hz), 3.58 (dd, 1H, J = 3.5,

8.7Hz), 4.41 (s, 1H), 4.83 (d, 1H, J = 3.5Hz), 5.87-8.10 (m, 12H). ^{13}C NMR (75 MHz, $CDCl_3$, ppm): δ 44.7, 48.1, 51.3, 77.3, 120.9, 121.1, 123.8, 124.7, 125.0, 125.6, 127.0 (two peaks), 127.2, 127.3, 129.8, 130.3, 134.3, 136.9, 138.5, 141.2, 142.0, 145.0, 174.4, 176.0. IR (film): 1215.6, 1708.1, 3019.5 cm^{-1}. LRMS(EI) m/z 412.0 (M^+), HRMS(EI) m/z 412.1054 (M^+), for $C_{24}H_{16}N_2O_5$ 412.1059.

The ee determined by chiral HPLC; CHIRALCEL AD-H (4.6 mm i.d. x 250 mm); Hexane/2-propanol 60/40; flow rate 1.0 ml/min; temp 25°C; detection UV 230 nm; retention time: 9.0min and 19.8 min.

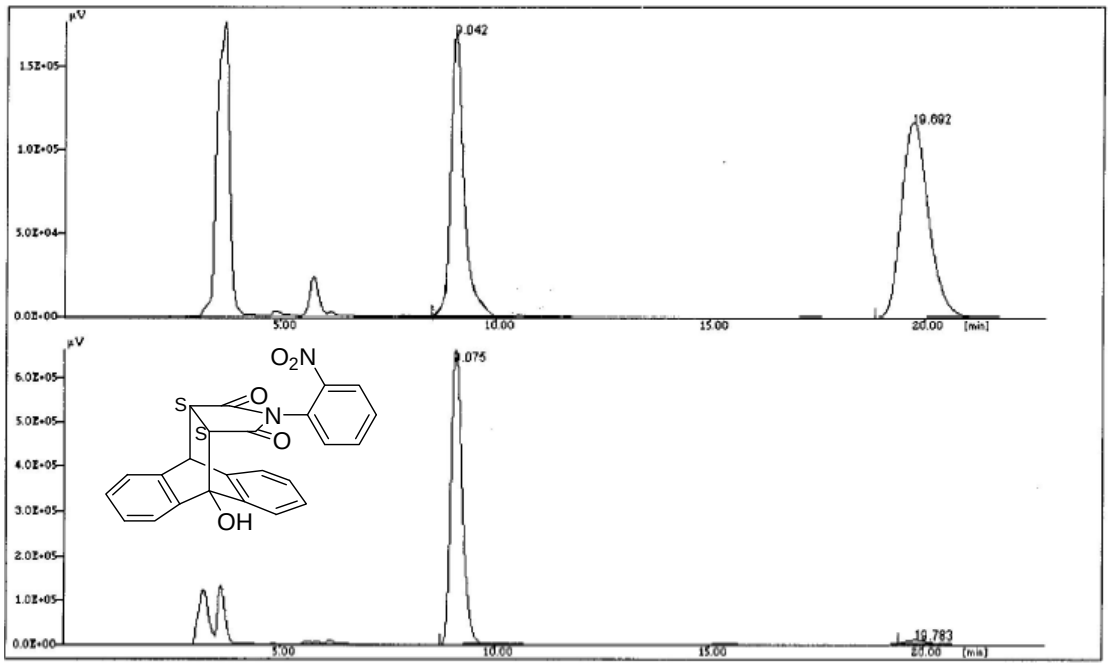

(21d) 2-(2, 5-Dichlorophenyl)-4-hydroxy-3a, 4, 9, 9a-tetrahydro-4, 9[1', 2']-benzeno-1*H*-benz[*f*]isoindole-1, 3(2*H*)-dione

White solid. mp 206.2-207.5. 88% yield, 92% ee. $[\alpha]_D^{28}$ +79 (*c* 0.12, $CHCl_3$). ^{1}H NMR (500 MHz, $CDCl_3$, ppm)：δ 3.35 (d, 1H, J = 8.6Hz), 3.56 (dd, 1H, J = 3.5, 8.6 Hz),

4.46(s, 1H), 4.83 (d, 1H, J = 3.5Hz), 5.57-7.58 (m, 11H). ^{13}C NMR (75 MHz, $CDCl_3$, ppm): δ 44.3, 44.9, 48.1, 51.2, 121.0, 121.3, 123.9, 124.9, 127.0, 127.1, 127.4, 127.5, 129.4, 130.9, 131.0, 133.2, 136.8, 138.5, 141.0, 141.9, 174.4, 176.0. IR (film): 1215.2, 1713.8, 3019.7 cm^{-1}. LRMS (ESI) m/z 434.3 ($M-H^+$), HRMS (EI) m/z 435.0411 (M^+), calc. for $C_{24}H_{15}Cl_2NO_3$ 435.0429.

The ee determined by chiral HPLC; column CHIRALCEL AD-H (4.6 mm i.d. x 250 mm); Hexane/2-propanol 90/10; flow rate 1.0 ml/min; temp 25 °C; detection UV 230 nm; retention time: 10.4 min and 13.4 min.

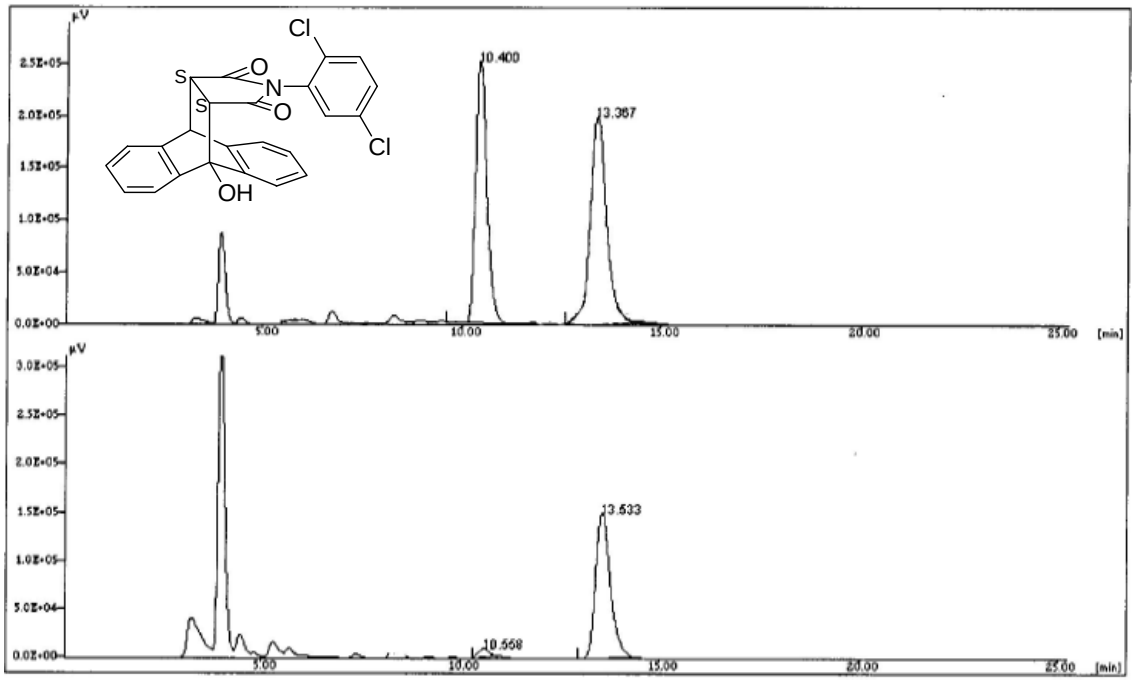

(21e) 2-Benzyl-5, 13-dichloro-4-hydroxy-3a, 4, 9, 9a-tetrahydro-4, 9-[1', 2'] benzene-1*H*-benz[*f*]isoindole-1, 3(2*H*)-dione

White solid. mp 230.0-231.9 °C. 90% yield, 96% ee. $[\alpha]_D^{23}$ +12.8 (*c* 0.036, $CHCl_3$). ^{1}H NMR (500 MHz, $CDCl_3$, ppm)：δ 3.28 (dd, 1H, J = 3.5, 8.8Hz), 3.36 (d, 1H, J = 8.8Hz), 4.35 (dd, 2H, J = 14.2, 29.6Hz), 4.62 (d, 1H, J = 3.5Hz), 4.97 (s, 1H),

6.75-7.18 (m, 11H). ^{13}C NMR (125 MHz, $CDCl_3$, ppm): δ 42.39, 45.25, 45.59, 51.08, 81.31, 122.61, 123.44, 127.71, 128.25, 128.47, 128.64, 129.65, 130.04, 130.91, 131.03, 134.70, 134.96, 137.28, 138.70, 141.94, 175.40, 176.37. IR (film): 1213.7, 1699.0, 3018.8 cm^{-1}. LRMS(FAB) m/z 450.3 ($M+H^+$), HRMS(FAB) m/z 450.0652 ($M+H^+$), calc. for $C_{25}H_{18}Cl_2NO_3$ 450.0664.

The ee determined by chiral HPLC; CHIRALCEL AD-H (4.6 mm i.d. x 250 mm); Hexane/2-propanol 80/20; flow rate 1.0 ml/min; temp 25 °C; detection UV 230 nm; retention time: 13.4 min and 30.3 min.

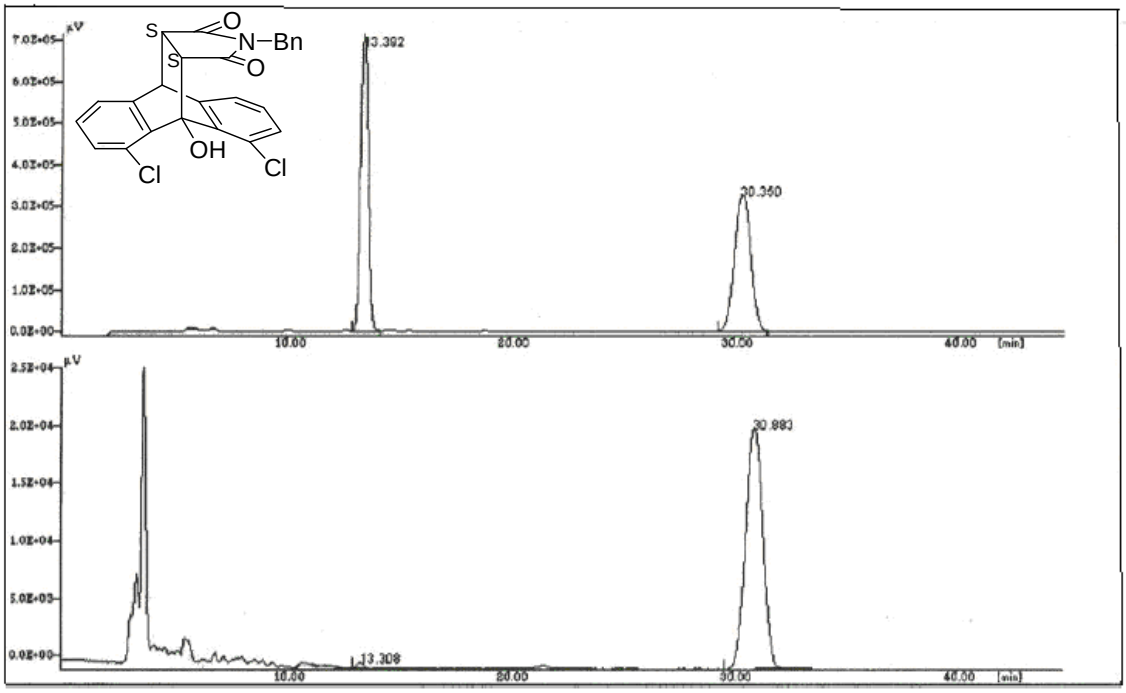

(21f) 2-Cyclohexyl-5, 13-dichloro-4-hydroxy-3a, 4, 9, 9a-tetrahydro-4, 9-[1', 2'] benzeno-1*H*-benz[*f*]isoindole-1, 3(2*H*)-dione

White solid. mp 228.2-230.2 °C. 94% yield, 97% ee. $[\alpha]_D^{23}$ +61.6 (*c* 0.031, $CHCl_3$). ^{1}H NMR (300 MHz, $CDCl_3$, ppm): δ 0.84-1.00 (m, 3H), 1.08-1.18 (m, 3H), 1.68-1.76 (m,

4H), 3.20 (dd, 1H, J = 3.3, 8.9Hz), 3.27 (d, 1H, J = 8.9Hz), 3.57-3.64 (m, 1H), 4.65 (d, 1H, J = 3.3Hz), 5.11 (s, 1H), 7.10-7.35 (m, 6H). ^{13}C NMR (75 MHz, $CDCl_3$, ppm): δ 24.72, 25.53, 27.86, 45.22, 45.52, 50.56, 51.63, 81.43, 122.58, 123.82, 128.19, 128.40, 130.09, 130.20, 130.73, 131.03, 135.70, 137.08, 139.19, 141.81, 175.97, 177.26. IR (film): 1216.2, 1691.0, 3018.9 cm^{-1}. LRMS(FAB) m/z 442.2 ($M+H^+$), HRMS(FAB) m/z 442.0974 ($M+H^+$), calc. for $C_{24}H_{22}Cl_2NO_3$ 442.0997.

The ee determined by chiral HPLC; CHIRALCEL AD-H (4.6 mm i.d. x 250 mm); Hexane/2-propanol = 90/10; flow rate 1.0 ml/min; temp 25 °C; detection UV 230 nm; retention time: 15.5 min and 29.8 min.

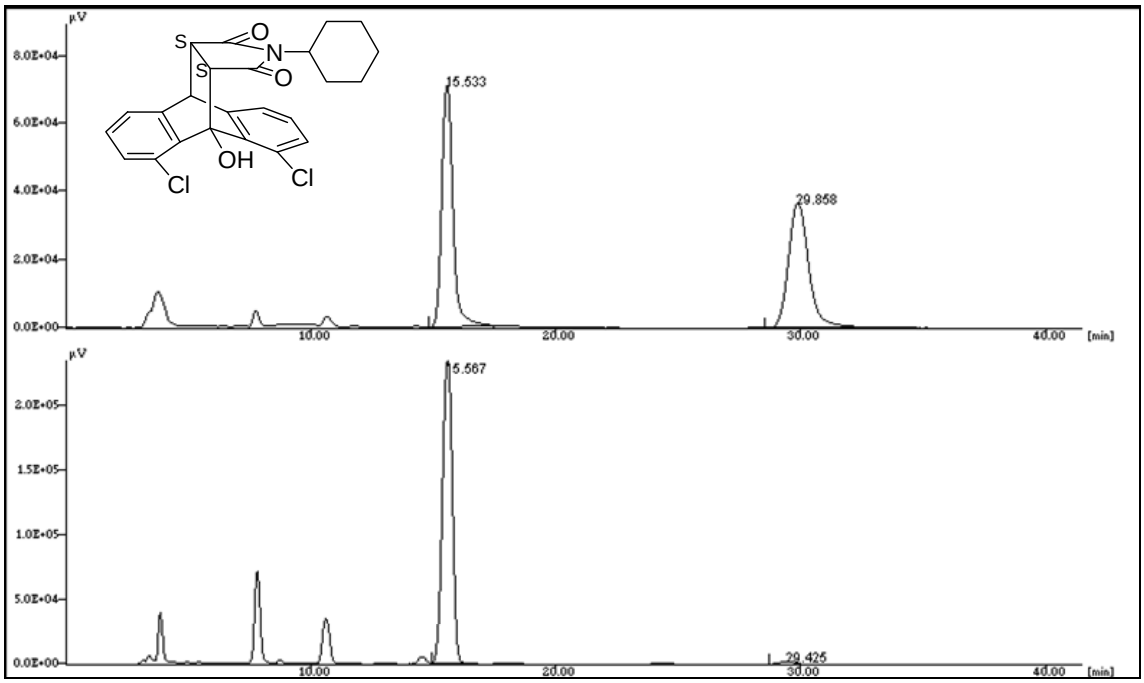

(21g) 2-*tert*-Butyl-5, 13-dichloro-4-hydroxy-3a, 4, 9, 9a-tetrahydro-4, 9-[1', 2'] benzeno-1*H*-benz[*f*]isoindole-1, 3(2*H*)-dione

White solid. mp 254.3-255.8 °C. 90% yield, 93% ee. $[\alpha]_D^{23}$ +17.9 (*c* 0.043**,** $CHCl_3$). ^{1}H

NMR (300 MHz, $CDCl_3$, ppm) ：δ 1.19 (s, 9H), 3.09 (dd, 1H, J = 3.3, 9.1Hz), 3.16 (d, 1H, J = 9.1Hz), 4.06 (d, 1H, J = 3.3Hz), 5.17 (s, 1H), 7.07-7.24 (m, 6H). ^{13}C NMR (125 MHz, $CDCl_3$, ppm): δ 27.71, 45.32, 45.76, 50.44, 58.87, 81.54, 122.56, 123.85, 128.15, 128.34, 130.15, 130.39, 130.74, 131.01, 135.98, 137.21, 139.45, 141.90, 176.96, 178.52. IR (film): 1216.0, 1694.5, 3019.6 cm^{-1}. LRMS(FAB) m/z 416.2 ($M+H^+$), HRMS(FAB) m/z 416.0823 ($M+H^+$), calc. for $C_{22}H_{20}Cl_2NO_3$ 416.082.

The ee determined by chiral HPLC; CHIRALCEL AD-H (4.6 mm i.d. x 250 mm); Hexane/2-propanol = 90/10; flow rate 1.0 ml/min; temp 25 °C; detection UV 230 nm; retention time: 11.1 min and 17.7 min.

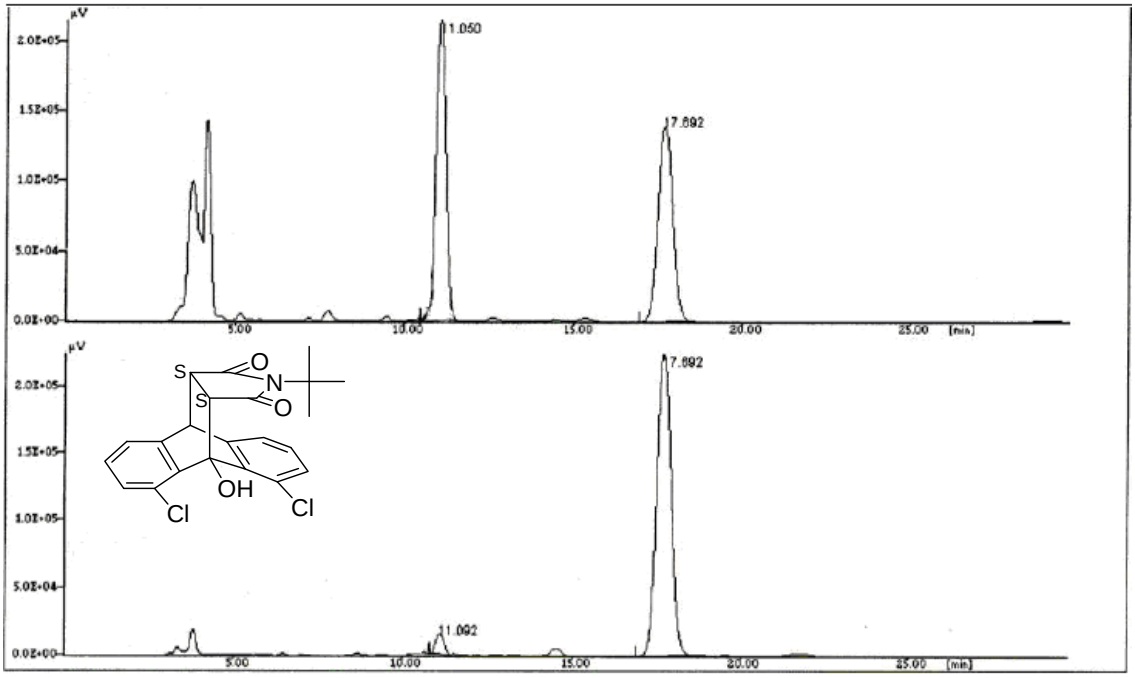

(21h) 2-*iso*-Butyl-5, 13-dichloro-4-hydroxy-3a, 4, 9, 9a-tetrahydro-4, 9-[1', 2'] benzeno-1*H*-benz[*f*]isoindole-1, 3(2*H*)-dione

White solid. mp 202.7-203.8 °C. 86% yield, 92%ee. $[\alpha]_D^{23}$ +584 (*c* 0.4**,** $CHCl_3$). ^{1}H

NMR (500 MHz, $CDCl_3$, ppm)：0.52 (dd, 6H, *J* = 6.9, 15.8Hz), 1.47-1.55(m, 1H), 3.04 (dd, 2H, *J* = 1.3, 6.9Hz), 3.27 (dd, 1H, *J* = 3.8, 8.8Hz), 3.36 (d, 1H, *J* = 8.8Hz), 4.67 (d, 1H , *J* = 3.8Hz), 4.98(s, 1H), 7.07-7.20(m, 6H). ^{13}C NMR (125 MHz, $CDCl_3$, ppm): δ 19.8, 20.0, 27.1, 45.3, 45.6, 46.4, 51.1, 81.3, 122.6, 123.9, 128.3, 128.7, 130.1, 130.2, 131.0, 135.8, 137.4, 139.4, 142.1, 176.1, 177.0. IR (film): 1215.7, 1697.6, 3019.5 cm^{-1}. LRMS(FAB) m/z 415.9($M+H^+$), HRMS(FAB) m/z 416.0832 ($M+H^+$), calc. for $C_{22}H_{20}Cl_2NO_3$ 416.0820.

The ee determined by chiral HPLC: CHIRALPAK ADH (4.6 mm i.d. x 250 mm); Hexane/2-propanol 80/20; flow rate 1.0 ml/min; temp 25 °C; detection UV 230 nm; retention time: 11.2min, 15.7 min.

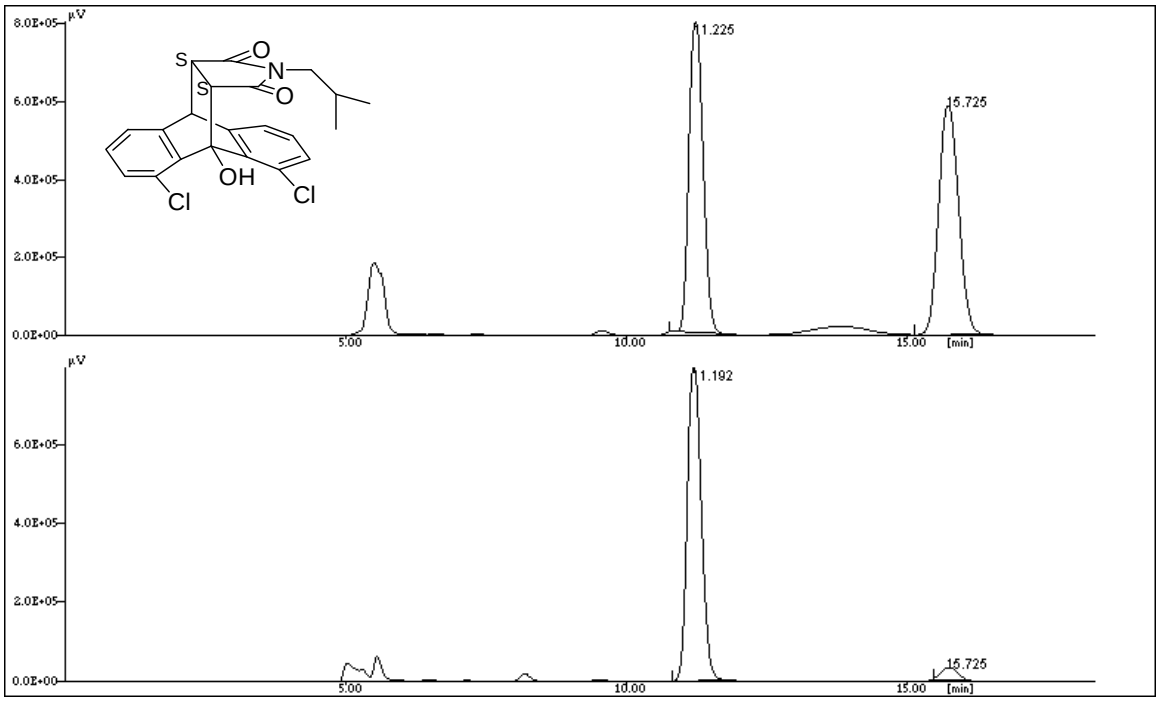

(21i) 2-(4-Chlorobenzyl)-5, 13-dichloro-4-hydroxy-3a, 4, 9, 9a-tetrahydro-4, 9-[1', 2'] benzeno-1*H*-benz[*f*]isoindole-1, 3(2*H*)-dione

White solid. mp 224.0-226.0 °C. 87% yield, 97%ee. $[\alpha]_D^{22}$ +243.1(*c* 0.16, $CHCl_3$). ^1H NMR (300 MHz, $CDCl_3$, ppm)：δ 3.25 (dd, 1H, *J* = 3.5, 8.7Hz), 3.34 (d, 1H, *J* = 8.7Hz), 4.30 (dd, 2H , *J* = 13.6, 24.0Hz), 4.58(d, 1H, *J* = 3.5Hz), 6.71-7.28 (m, 10H). ^{13}C NMR (125 MHz, $CDCl_3$, ppm): δ 41.6, 45.2, 45.5, 51.0, 81.3, 122.6, 123.3, 128.2, 128.3, 128.6, 129.5, 130.0, 130.3, 130.8, 131.0, 133.1, 133.7, 134.8, 137.2, 138.6, 141.8, 175.2, 176.2 ppm. IR (film): 1215.6, 1701.0, 3019.6 cm^{-1}. LRMS(FAB) m/z 484.1 ($M+H^+$), HRMS(FAB) m/z 484.0264 ($M+H^+$), calc. for $C_{25}H_{17}Cl_3NO_3$ 484.0274.

The ee determined by chiral HPLC: CHIRALPAK AD-H (4.6 mm i.d. x 250 mm); Hexane/2-propanol 80/20; flow rate 1.0 ml/min; temp 25 °C; detection UV 230 nm; retention time: 14.6 min and 43.8 min.

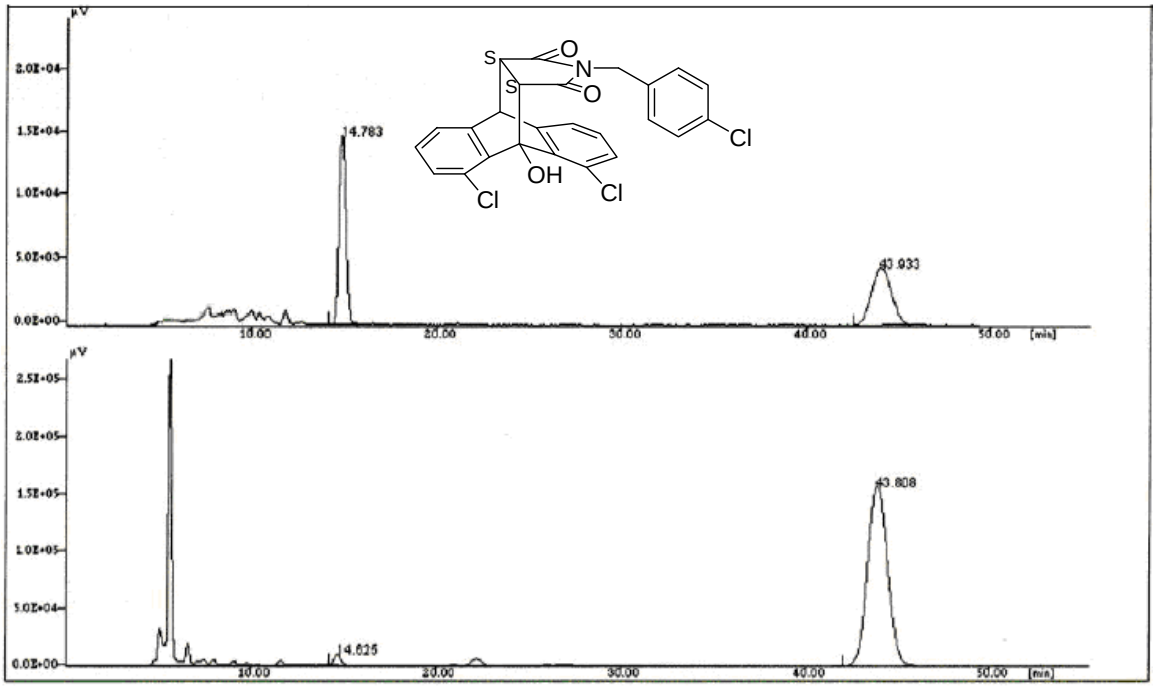

(21j) 8, 10-Dichloro-4-hydroxy-2-phenyl-3a, 4, 9, 9a-tetrahydro-4, 9-[1', 2'] benzeno-1*H*-benz[*f*]isoindole-1, 3(2*H*)-dione

White solid. mp 271.5-273.5 °C. 92% yield, 90%ee. $[\alpha]_D^{25}$ +143.1(*c* 0.16, $CHCl_3$). ^1H

NMR (300 MHz, $CDCl_3$, ppm)：δ 3.26 (d, 1H, J = 8.7 Hz), 3.52 (dd, 1H, J = 3.5, 8.7 Hz), 5.93 (d, 1H, J = 3.5Hz), 6.56-7.33 (m, 11H). ^{13}C NMR (75 MHz, $CDCl_3$, ppm): δ 37.6, 46.1, 50.0, 53.4, 119.6, 120.0, 126.1, 127.6, 128.1, 128.2, 128.3, 129.1, 129.2, 130.1, 130.7, 131.0, 133.9, 135.5, 143.1, 144.5, 174.2, 176.7. IR (film): 1215.6, 1707.5, 3019.6 cm^{-1}. LRMS (FAB) m/z 436.1 ($M+H^+$), HRMS (FAB) m/z 436.0501 ($M+H^+$), calc. for $C_{24}H_{15}Cl_2NO_3$ 436.0507.

The ee determined by chiral HPLC: CHIRALPAK AD-H (4.6 mm i.d. x 250 mm); Hexane/2-propanol 80/20; flow rate 1.0 ml/min; temp 25 °C; detection UV 230 nm; retention time: 13.1 min and 23.4 min.

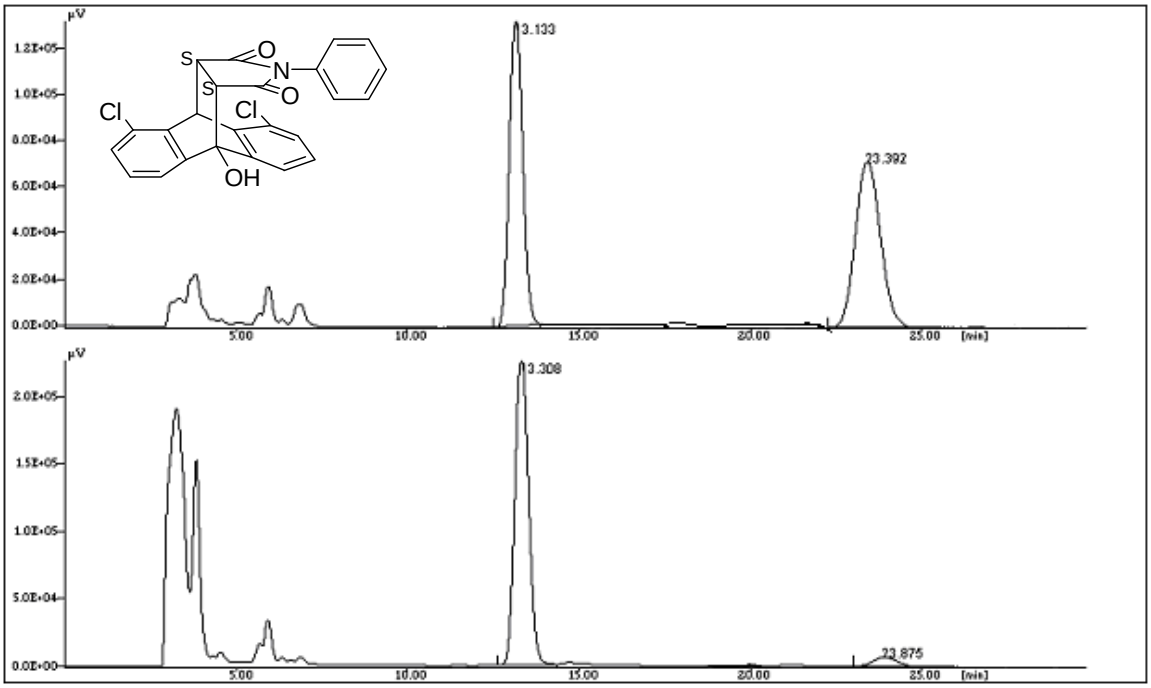

(21k) 8, 10-Dichloro-2-(2, 6-difluorophenyl)-4-hydroxy-3a, 4, 9, 9a-tetrahydro-4, 9-[1', 2'] benzeno-1*H*-benz[*f*]isoindole-1, 3(2*H*)-dione

White solid. mp 284.4-286.0 °C. 95% yield, >99%ee. $[\alpha]_D^{26}$ +170 (*c* 0.2, $CHCl_3$). 1H

NMR (300 MHz, $CDCl_3$, ppm): δ 3.36 (d, 1H, *J* = 9.1Hz), 3.60 (dd, 1H, *J* = 3.5, 9.1Hz), 5.94 (d, 1H, *J* = 3.5Hz), 6.81-7.43 (m, 9H). 13C NMR (75 MHz, $CDCl_3$, ppm): δ 29.6, 37.4, 46.5, 50.3, 111.7(two peaks), 111.9, 112.2(two peaks), 119.5, 119.9, 127.6, 128.1, 128.3, 128.4, 130.0, 131.2, 131.3, 131.5, 135.8, 142.7, 144.7, 172.4, 174.9. IR (film): 1215.6, 1711.8, 3019.7 cm^{-1}. LRMS(FAB) m/z 472.1($M+H^+$), HRMS(FAB) m/z 472.0313 ($M+H^+$), calc. 472.0319 for $C_{24}H_{14}Cl_2F_2NO_3$.

The ee determined by chiral HPLC: CHIRALPAK AD-H (4.6 mm i.d. x 250 mm); Hexane/2-propanol 70/30; flow rate 1.0 ml/min; temp 25 °C; detection UV 230 nm; retention time: 9.8 min and 15.5 min.

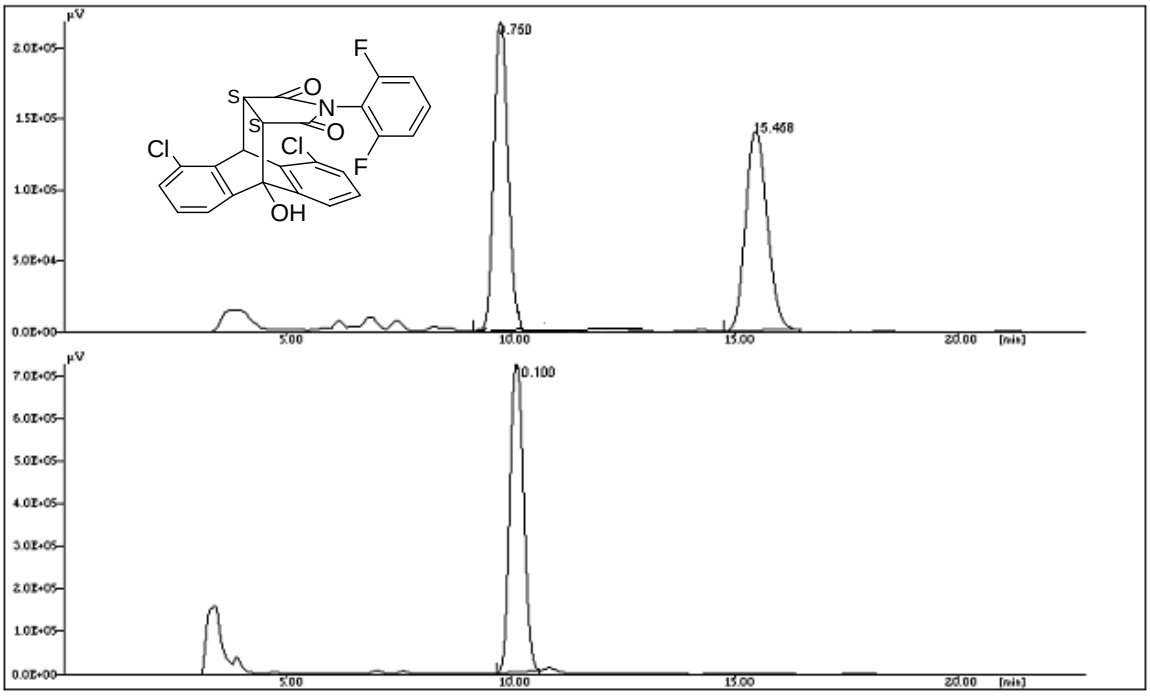

(21l) 8, 10-Dichloro-4-hydroxy-2-(2-methoxyphenyl)-3a, 4, 9, 9a-tetrahydro-4, 9-[1', 2'] benzeno-1*H*-benz[*f*]isoindole-1, 3(2*H*)-dione

White solid. mp 281.8-283.2 °C. 90% yield, >99 % ee. $[\alpha]_D^{24}$ +42.1 (*c* 0.28, $CHCl_3$). ^1H NMR (300 MHz, $CDCl_3$, ppm) ： δ 3.29 (d, 1H, *J* = 8.8Hz), 3.55 (dd, 1H, *J* = 3.5,

8.7Hz), 3.74 (s, 3H), 4.67 (s, 1H), 5.92 (d, 1H, J = 3.5Hz), 6.80-7.63 (m, 10H). ^{13}C NMR (75 MHz, $CDCl_3$, ppm): δ 37.4, 37.7, 46.4, 50.1, 55.8, 112.1, 119.6, 120.1, 120.9, 127.6, 128.0, 128.1, 128.2, 128.6, 130.1, 131.0, 134.2, 135.6, 143.3, 144.6, 154.5, 174.0, 176.6. IR (film): 1215.6, 1681.4, 3019.2 cm^{-1}. LRMS(FAB) m/z 466.1 ($M+H^+$), HRMS(FAB) m/z 466.0598 ($M+H^+$), calc. 466.0613 for $C_{25}H_{18}Cl_2NO_4$.

The ee determined by chiral HPLC: CHIRALPAK AD-H (4.6 mm i.d. x 250 mm); Hexane/2-propanol 70/30; flow rate 1.0 ml/min; temp 25 °C; detection UV 230 nm; retention time: 14.2 min and 22.6 min.

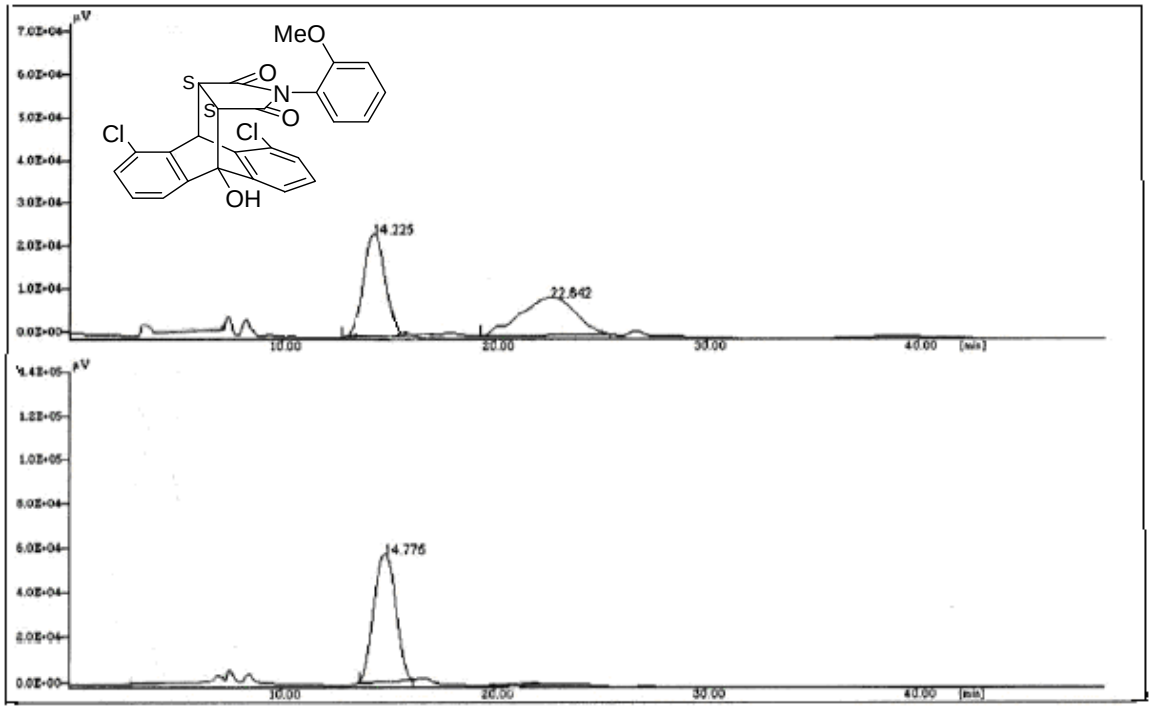

(21m-1) 5, 10-Dichloro-4-hydroxy-2-phenyl-3a, 4, 9, 9a-tetrahydro-4, 9-[1', 2']-benzeno-1*H*-benz[*f*]isoindole-1, 3(2*H*)-dione

White solid. mp 255.7-257.8 °C. 99% yield, 99 % ee. $[\alpha]_D^{23}$ +92.8 (*c* 0.32, $CHCl_3$). ^{1}H NMR (500 MHz, $CDCl_3$, ppm) ： δ 3.18 (d, 1H, J = 9.1Hz), 3.38 (dd, 1H, J = 3.2,

9.1Hz), 5.94 (d, 1H, J = 3.2Hz), 6.52-7.70 (m, 11H). ^{13}C NMR (125 MHz, $CDCl_3$, ppm): δ 41.7, 46.2, 51.2, 79.4, 120.5, 124.5, 126.2, 127.7, 128.1, 128.7, 129.0, 129.2, 129.6, 129.9, 130.8, 130.9, 135.4(two peaks), 139.4, 144.2, 174.8, 176.3. IR (film): 1215.4, 1710.0, 3019.5 cm^{-1}. LRMS(ESI) m/z 458.5 ($M+Na^+$), HRMS(ESI) m/z 458.0326 ($M+Na^+$), calc. 458.0327 for $C_{24}H_{15}Cl_2NNaO_3$.

The ee determined by chiral HPLC: CHIRALPAK AD-H (4.6 mm i.d. x 250 mm); Hexane/2-propanol 80/20; flow rate 1.0 ml/min; temp 25 °C; detection UV 230 nm; retention time: 20.4 min and 28.2 min.

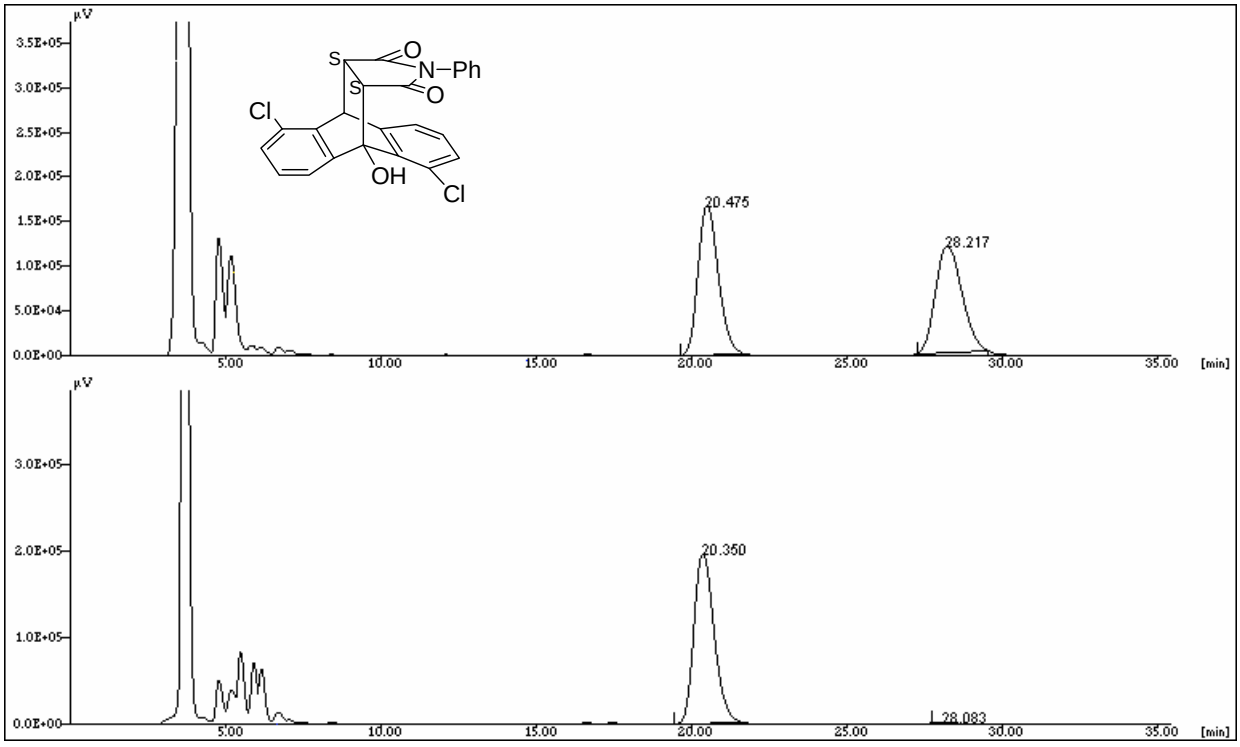

(21n-1)

5,10-Dichloro-4-hydroxy-3a,4,9,9a-tetrahydro-2-(2,4,6-trimethylphenyl)-4,9-[1',2']benzeno-1*H*-benz[*f*]isoindole-1,3(2*H*)-dione

White solid. mp 241.8-243.6 °C. 90%yield, 99%ee. $[\alpha]_D^{25}$ +62.1 (*c* 0.14, $CHCl_3$). ^1H NMR (300 MHz, $CDCl_3$, ppm) ：δ 1.04 (s, 3H), 1.96 (s, 3H), 2.23 (s, 3H), 3.33 (d, 1H, *J* = 9.5Hz), 3.52 (dd, 1H, *J* = 3.2, 9.5Hz), 4.91(s, 1H), 5.33 (d, 1H, *J* = 3.2Hz), 6.78-7.72 (m, 8H). ^{13}C NMR (75 MHz, $CDCl_3$, ppm): δ 16.2, 17.7, 21.0, 41.2, 46.1, 51.1, 79.1, 120.3, 124.7, 126.8, 127.6, 128.0, 128.9, 129.2, 129.3, 129.4, 130.3, 131.1, 134.4, 135.6, 135.9, 139.6, 140.1, 145.0, 174.6, 176.1. IR (film): 1215.6, 1707.4, 3019.7 cm^{-1}. LRMS(EI) m/z 478.9 (M+), HRMS(EI) m/z 477.0880 (M+), calc. 477.0898 for $C_{27}H_{21}Cl_2NO_3$.

The ee determined by chiral HPLC: CHIRALPAK AD-H (4.6 mm i.d. x 250 mm); Hexane/2-propanol 80/20; flow rate 1.0 ml/min; temp 25 °C; detection UV 230 nm; retention time: 19.0 min and 29.7 min.

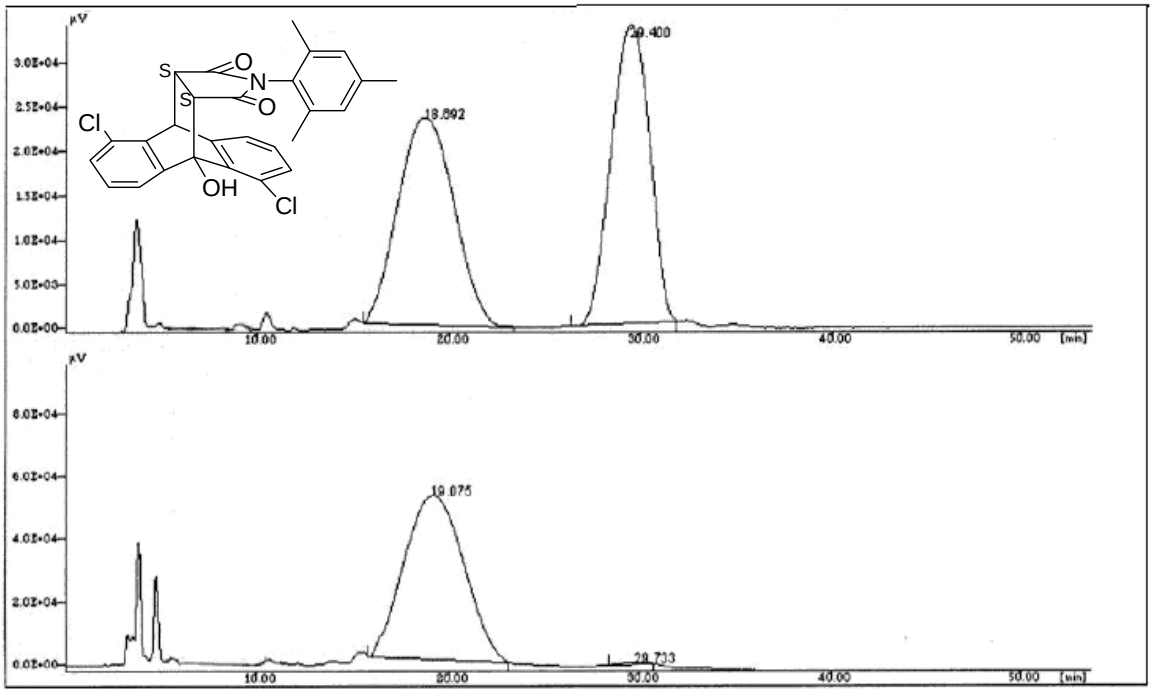

(21o-1) 2-Ethyl-4-hydroxy-8-methylamino-3a, 4, 9, 9a-tetrahydro-4, 9[1',

2']-benzeno-1*H*-benz[*f*]isoindole-1, 3(2*H*)-dione

Yellow solid. mp 209.5-211.0 °C. 90% yield, 98%ee. $[\alpha]_D^{26}$ +195.8 (*c* 0.12, $CHCl_3$)**.** ^1H NMR (500 MHz, $CDCl_3$, ppm) **:** δ 0.38 (t, 3H, *J* = 6.9Hz), 2.92 (s, 3H), 3.07 (d, 1H, *J* = 8.4Hz), 3.13 (dd, 2H, *J* = 2.5, 7.6Hz), 3.25 (dd, 1H, *J* = 3.4, 8.4Hz), 4.46 (s, 1H), 4.77 (d, 1H, *J* = 3.4Hz), 6.57-7.50 (m, 7H). ^{13}C NMR (125 MHz, $CDCl_3$, ppm): δ 11.8, 31.1, 33.3, 38.2, 47.0, 50.3, 121.1, 124.4, 127.0 (two peaks), 127.6, 136.3, 141.3, 143.5, 176.5, 177.9. IR (film): 1215.1, 1693.2, 3019.7 cm^{-1}. LRMS(EI) m/z 348.0 (M^+), HRMS(EI) m/z 348.1464 (M^+), calc. 348.1474 for $C_{21}H_{20}N_2O_3$.

The ee determined by chiral HPLC: CHIRALPAK AD-H (4.6 mm i.d. x 250 mm); Hexane/2-propanol 80/20; flow rate 1.0 ml/min; temp 25 °C; detection UV 230 nm; retention time: 16.2 min and 20.0 min.

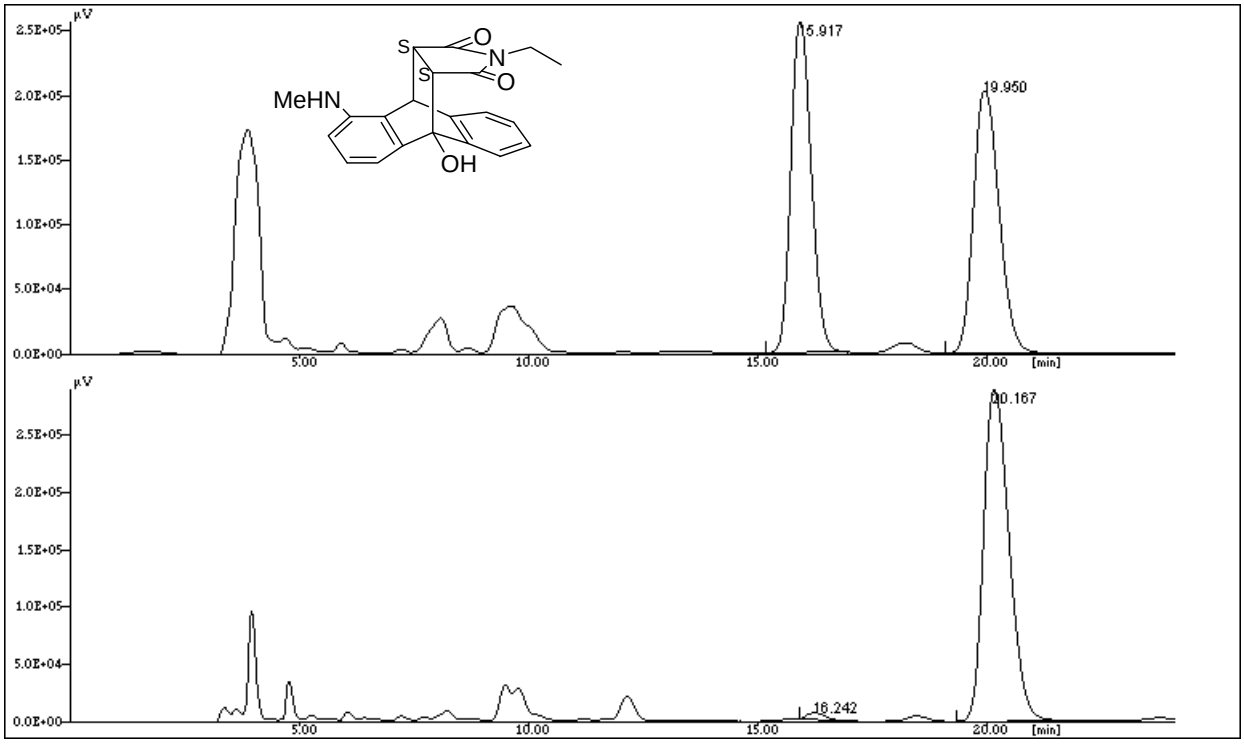

(21p-1) 2-Hexyl-4-hydroxy-8-methylamino-3a, 4, 9, 9a-tetrahydro-4, 9[1', 2']-benzeno-1*H*-benz[*f*]isoindole-1, 3(2*H*)-dione

Yellow solid. mp 193.1-194.6 ^{o}C. 95% yield, 87%ee. ^{1}H NMR (500 MHz, $CDCl_3$, ppm)：δ 0.68-1.23 (m, 11H), 2.93 (s, 3H), 3.04-3.05 (m, 2H), 3.07 (d, 1H, J = 8.2 Hz), 3.25 (dd, 1H, J = 3.2, 8.2Hz), 4.43 (s, 1H), 4.77 (d, 1H, J = 3.2Hz), 6.58-7.50 (m, 7H). ^{13}C NMR (125 MHz, $CDCl_3$, ppm): δ14.0, 22.3, 26.2, 26.9, 31.2, 38.2, 38.6, 47.1, 50.4, 121.1, 124.4, 127.0, 127.1, 127.6, 136.3, 141.3, 143.7, 176.6, 178.0. IR (film): 1216.0, 1693.4, 3020.9 cm^{-1}. LRMS(FAB) m/z 404.1 (M^+), HRMS(FAB) m/z 404.2107 (M^+), calc. 404.2100 for $C_{25}H_{28}N_2O_3$.

The ee determined by chiral HPLC: CHIRALPAK AD-H (4.6 mm i.d. x 250 mm); Hexane/2-propanol 90/10; flow rate 1.0 ml/min; temp 25 °C; detection UV 230 nm; retention time: 13.6 min and 17.6 min.

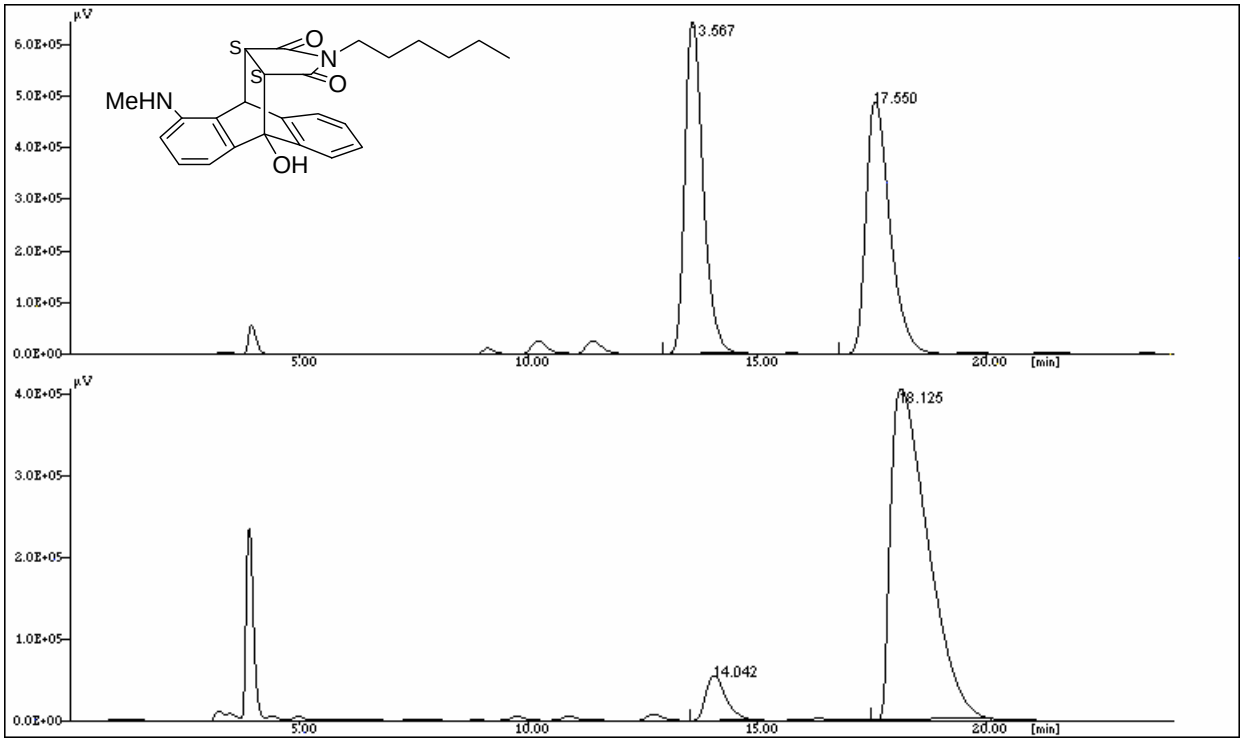

(131a) 1, 8-dihydroxy-10-(1-phenyl-2, 5-dioxopyrrolidin-3-yl)-9-(10*H*)-anthracenone Yellow solid. mp 237.2-239.4 ^{o}C. 90% yield, 99% ee. $[\alpha]_D^{26}$ +44.3 (*c* 0.54, $CHCl_3$). ^{1}H NMR (300 MHz, $CDCl_3$, ppm)：δ 2.21 (dd, 1H, *J* = 5.1, 18.6Hz), 2.52 (dd, 1H, *J* = 9.4,18.6Hz), 3.51 (m, 1H), 5.18 (d, 1H, *J* = 2.8Hz), 6.94-7.61 (m, 11H), 12.15 (s, 1H), 12.19 (s, 1H). ^{13}C NMR (75 MHz, $CDCl_3$, ppm): δ 29.49, 42.25, 51.05, 115.73, 116.47, 117.05, 118.05, 118.67, 119.01, 126.30, 128.92, 129.26, 131.42, 136.70, 137.29, 139.64, 143.79, 163.01, 163.27, 173.96, 176.42, 193.18. IR (film): 1216.2, 1633.4, 1713.6, 3019.7 cm^{-1}. LRMS(ESI) m/z 398.7 ($M-H^+$), HRMS(ESI) m/z 398.1036 ($M-H^+$), calc. 398.1028 for $C_{24}H_{16}NO_5$.

The ee determined by chiral HPLC: CHIRALPAK AD-H (4.6 mm i.d. x 250 mm); Hexane/2-propanol 80/20; flow rate 1.0 ml/min; temp 25 °C; detection UV 230 nm; retention time: 24.6 min, 28.2 min.

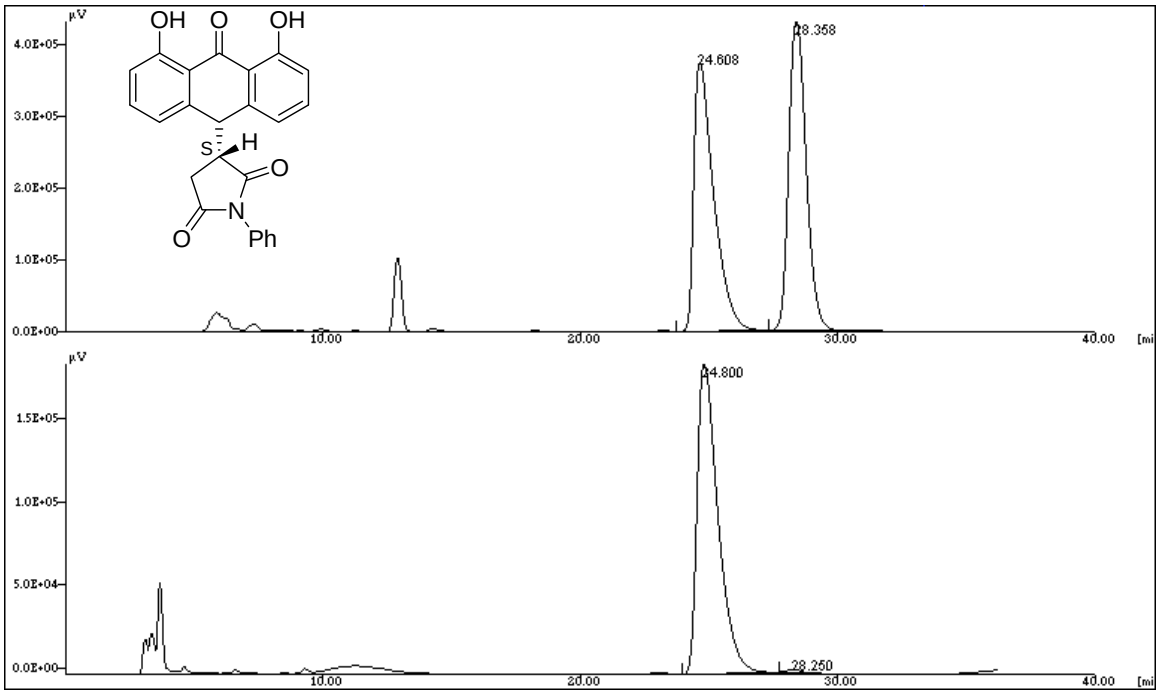

(131b)

1,8-dihydroxy-10-[1-(2-nitrophenyl)-2,5-dioxopyrrolidin-3-yl]-9-(10*H*)-anthracenone Yield solid. mp 236.0-238.2 °C. 86%yield, 96%ee. $[\alpha]_D^{26}$ +106.6 (c, 0.47, $CHCl_3$). ^1H NMR (500 MHz, CDCl3, ppm)：δ2.27 (dd, 1H, *J* = 5.0, 18.6Hz), 2.62 (dd, 1H, *J* = 9.8, 18.6 Hz), 3.61 (m, 1H), 5.17 (d, 1H, *J* = 2.5Hz), 6.94-8.20 (m, 10H), 12.15 (s, 1H), 12.20 (s, 1H). ^{13}C NMR (125 MHz, $CDCl_3$, ppm): δ 29.9, 42.0, 51.5, 115.7, 116.6, 117.3, 118.2, 118.8, 119.0, 126.0, 130.1, 130,4, 134.5, 136.5, 137.5, 163.1, 163.4, 173.1, 193,2. IR (film): 1215.2, 1695.0, 1725.8, 3020.0 cm^{-1}. LRMS(FAB) m/z 445.0 ($M+H^+$), HRMS(FAB) m/z 445.1047 ($M+H^+$), calc. 445.1036 for $C_{24}H_{16}N_2O_7$.

The ee determined by chiral HPLC: CHIRALPAK AD-H (4.6 mm i.d. x 250 mm); Hexane/2-propanol 80/20; flow rate 1.0 ml/min; temp 25 °C; detection UV 230 nm; retention time: 35.3 min, 39.1 min.

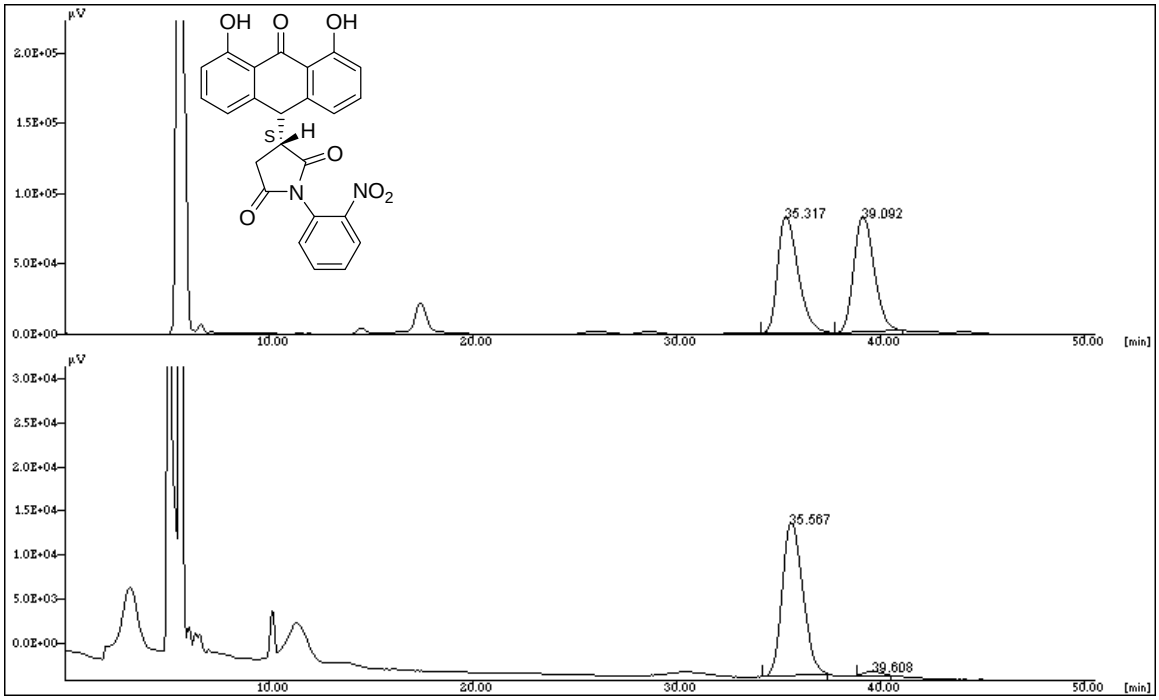

(131c)

1,8-dihydroxy-10-[1-(3,4-dichlorophenyl)-2,5-dioxopyrrolidin-3-yl]-9-(10*H*)-anthrace

none

Yellow solid. mp 239.5-241.6 °C. 92% yield, 97% ee. $[\alpha]_D^{23}$ +79.5 (c, 0.38, $CHCl_3$). ^1H NMR (500 MHz, $CDCl_3$, ppm)：δ 2.25 (dd, 1H, J = 4.7, 18.4Hz), 2.56 (dd, 1H, J = 9.5, 18.4Hz), 3.53 (m, 1H), 5.18 (d, 1H, J = 3.2Hz), 6.90-7.63 (m, 9H), 12.15 (s, 1H), 12.20 (s, 1H). ^{13}C NMR (125 MHz, $CDCl_3$, ppm): δ 29.6, 42.4, 51.1, 115.7, 116.5, 117.3, 118.3, 118.7, 118.9, 125.4, 128.2, 130.6, 130.9, 133.2, 133.3, 136.7, 137.4, 139.5, 143.5, 163.1, 163.4, 173.2, 175.8, 193.1. IR (film): 1214.3, 1720.9, 3019.7 cm^{-1}. LRMS (FAB) m/z 468.0 ($M+H^+$), HRMS (FAB) m/z 468.0387 ($M+H^+$), calc. 467.0406 for $C_{24}H_{16}NO_5$.

The ee determined by chiral HPLC: CHIRALPAK AD-H (4.6 mm i.d. x 250 mm); Hexane/2-propanol 80/20; flow rate 1.0 ml/min; temp 25 °C; detection UV 230 nm; retention time: 25.1 min, 27.6 min.

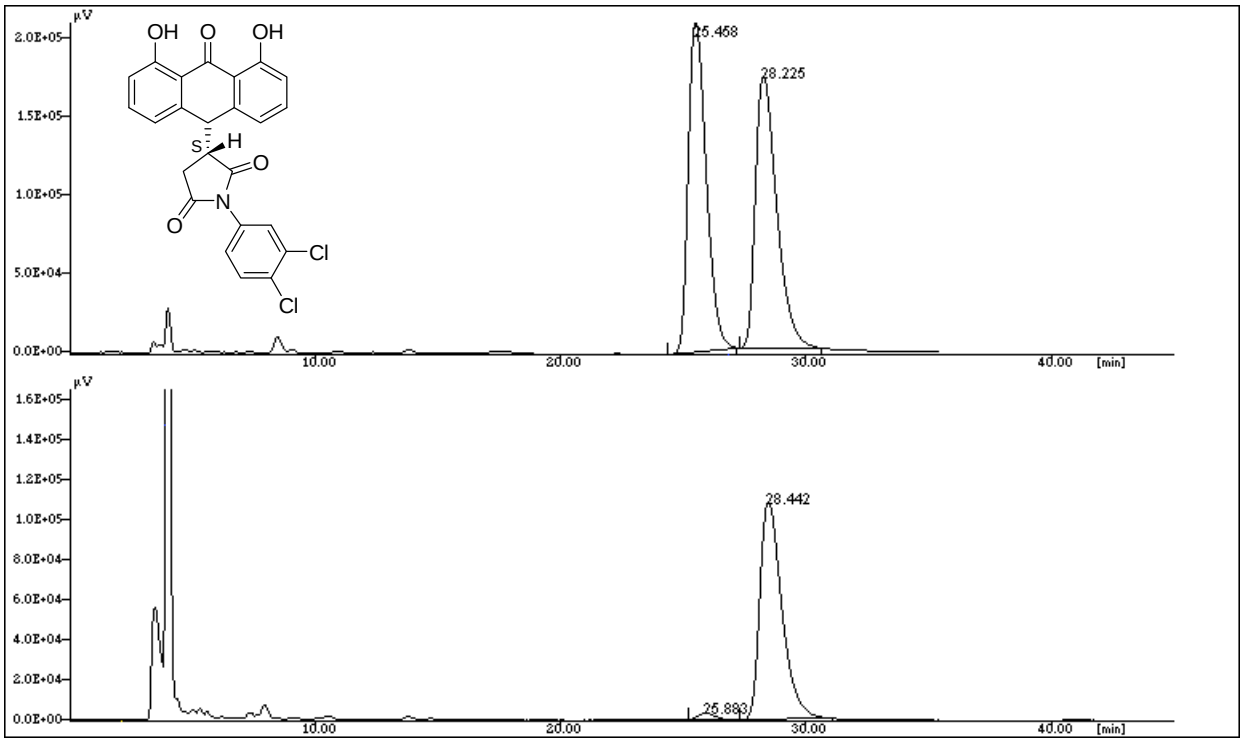

(131d) 1, 8-dihydroxy-10-(1-benzyl-2,5-dioxopyrrolidin-3-yl)-9-(10*H*)-anthracenone Yellow solid. mp 216.5-217.8 ^{o}C. 90% yield, 91% ee. $[\alpha]_D^{26}$ +12.8 (c, 0.036, $CHCl_3$). ^{1}H NMR (300 MHz, $CDCl_3$, ppm)：δ 2.00 (dd, 1H, J = 5.2, 18.5Hz), 2.34 (dd, 1H, J = 9.2, 18.5Hz), 3.32 (m, 1H), 4.57 (dd, 2H, J = 14.1, 21.3 Hz), 5,07 (d, 1H, J = 2.1Hz), 6.56-7.57 (m,11H), 12.13 (s, 1H), 12.14 (s, 1H). ^{13}C NMR (75 MHz, $CDCl_3$, ppm): δ 29.19, 41.78, 42.53, 50.88, 115.62, 116.15, 116.87, 117.53, 118.63, 118.88, 128.02, 128.60, 128.99, 135.25, 136.79, 137.15, 139.36, 144.02, 162.91, 163.04, 174.64, 177.10, 193.12. IR (film): 1215.9, 1634.9, 3019.7, 3424.8 cm^{-1}. LRMS (ESI) m/z 412.3 (M-H$^+$), HRMS (ESI) m/z 412.1188 (M-H$^+$), calc. 412.1185 for $C_{25}H_{18}NO_5$.

The ee determined by chiral HPLC: CHIRALPAK ADH (4.6 mm i.d. x 250 mm); Hexane/2-propanol =90/10; flow rate 1.0 ml/min; temp 25 °C; detection UV 230 nm; retention time: 19.3min and 21.6min.

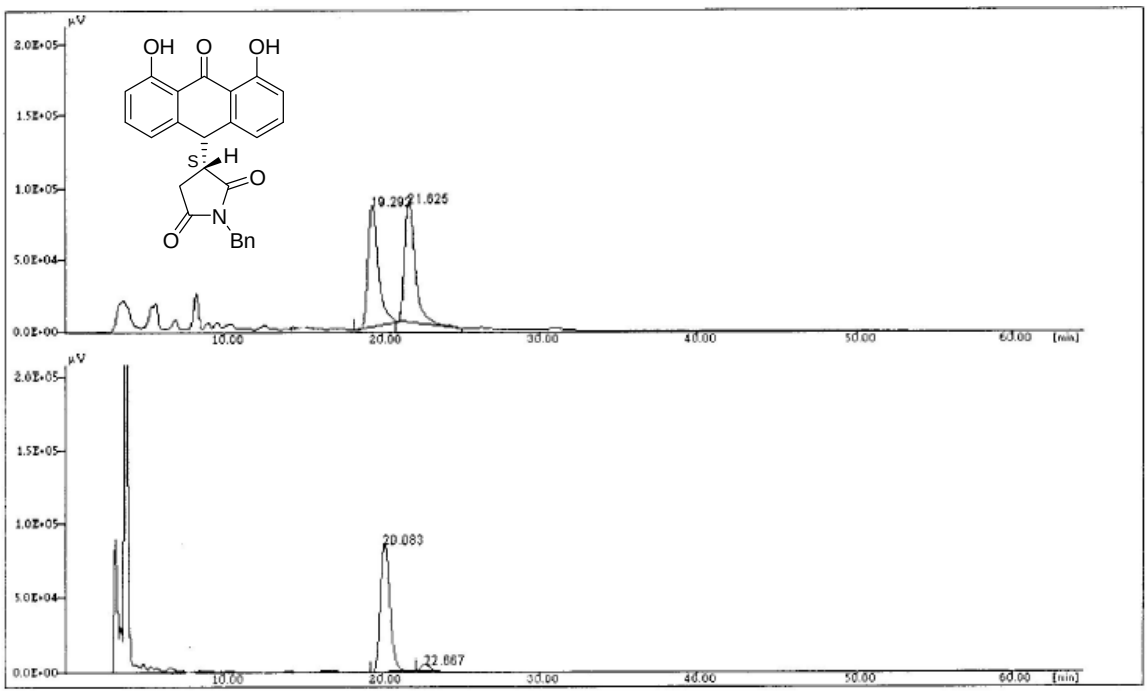

(132a) Methyl 2-(1, 8-dihydroxy-9-oxo-9,

10-dihydroanthracen-10-yl)-4-oxopentanoate

Yellow solid. mp 195.7-196.5 °C. 90% yield, 99% ee. $[\alpha]_D^{26}$ -16.0 (*c* 0.063, $CHCl_3$). ^1H NMR (500 MHz, $CDCl_3$, ppm)：δ 1.86 (dd, 1H, *J* = 3.2, 17.7Hz), 2.40 (dd, 1H, *J* = 10.7, 17.7Hz), 3.42 (m, 1H), 4.80 (d, 1H, *J* = 3.8Hz), 6.63 (d, 1H, J = 7.6), 6.95 (dd, 2H, *J* = 8.2, 12.0Hz), 7.02 (d, 1H, *J* = 7.6Hz), 7.45 (t, 1H, *J* = 7.9Hz), 7.52 (t, 1H, *J* = 7.9Hz), 12.08 (s, 1H), 12.16 (s, 1H). ^{13}C NMR (125 MHz, $CDCl_3$, ppm): δ 30.22, 38.86, 43.86, 51.27, 52.18, 115.94, 116.04, 116.83, 117.22, 118.71, 119.33, 136.47, 136.93, 141.99, 143.95, 162.59, 163.00, 172.39, 193.40, 205.97. IR (film): 1216.0, 1604.5, 1632.2, 3019.0, 3456.3cm^{-1}. LRMS(ESI) m/z 353.5 ($M-H^-$), HRMS(ESI) m/z 353.1013 ($M-H^+$), calc. 353.1025 for $C_{20}H_{17}O_6$.

The ee determined by chiral HPLC: CHIRALPAK ODH (4.6 mm i.d. x 250 mm); Hexane/2-propanol =90/10; flow rate 1.0 ml/min; temp 25 °C; detection UV 230 nm; retention time: 9.4min and 10.3min.

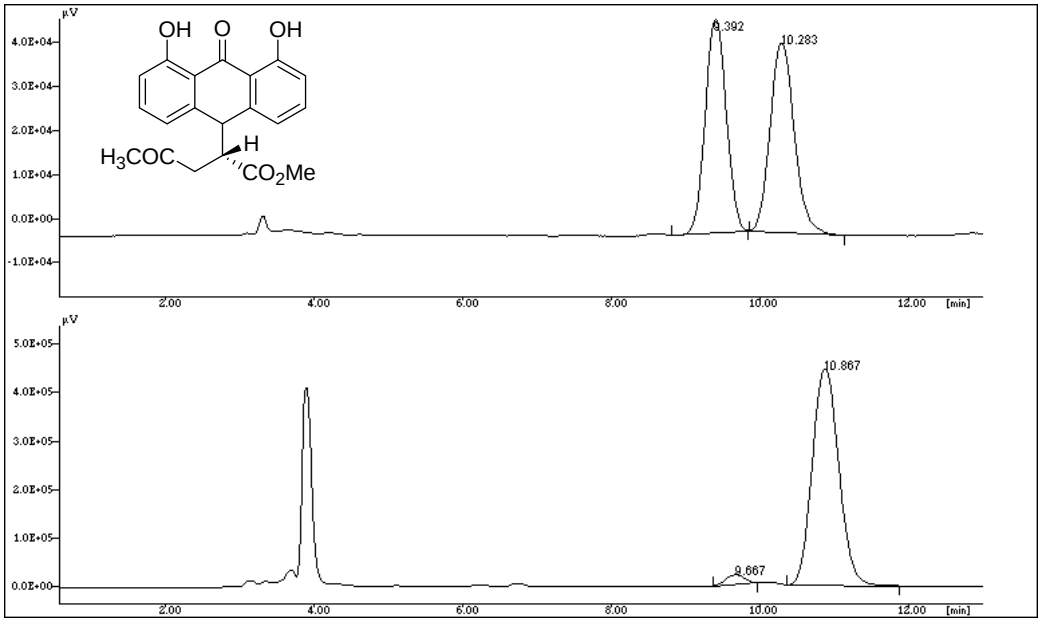

(132b) Ethyl-2-(1,8-dihydroxy-9-oxo-9,10-dihydroanthracen-10-yl)-4-oxo-4-phenylbu

tanoate

Yellow solid. mp 150.5-151.8 °C. 86% yield, 96% ee. $[\alpha]_D^{26}$ +22.3 (c 0.062, $CHCl_3$). ^1H NMR (300 MHz, $CDCl_3$, ppm)：δ 1.21 (t, 3H, J = 7.1Hz), 2.48 (dd, 1H, J = 3.8, 17.4Hz), 3.05 (dd, 1H, J = 10.1, 17.4Hz), 3.61 (m, 1H), 4.14 (m, 2H), 4.86 (d, 1H, J = 3.8Hz), 6.35-7.73 (m, 11H), 12.05 (s, 1H), 12.18 (s, 1H). ^{13}C NMR (75 MHz, $CDCl_3$, ppm): δ 13.98, 34.79, 44.18, 51.62, 56.22, 61.21, 115.97, 116.08, 116.81, 117.12, 119.03, 119.40, 127.88, 128.53, 133.27, 135.62, 136.32, 136.40, 136.74, 142.43, 143.90, 162.60, 162.90, 172.02, 193.43, 197.42. IR (film): 1685.9, 1729.3, 3019.0 cm^{-1}. LRMS(ESI) m/z 429.1 ($M-H^+$), HRMS(ESI) m/z 429.1349 ($M-H^+$), calc. 429.1338 for $C_{26}H_{21}O_6$

The ee determined by chiral HPLC: CHIRALPAK ADH (4.6 mm i.d. x 250 mm); Hexane/2-propanol = 90/10; flow rate 1.0 ml/min; temp 25 °C; detection UV 230 nm; retention time: 15.7 min and 28.1 min.

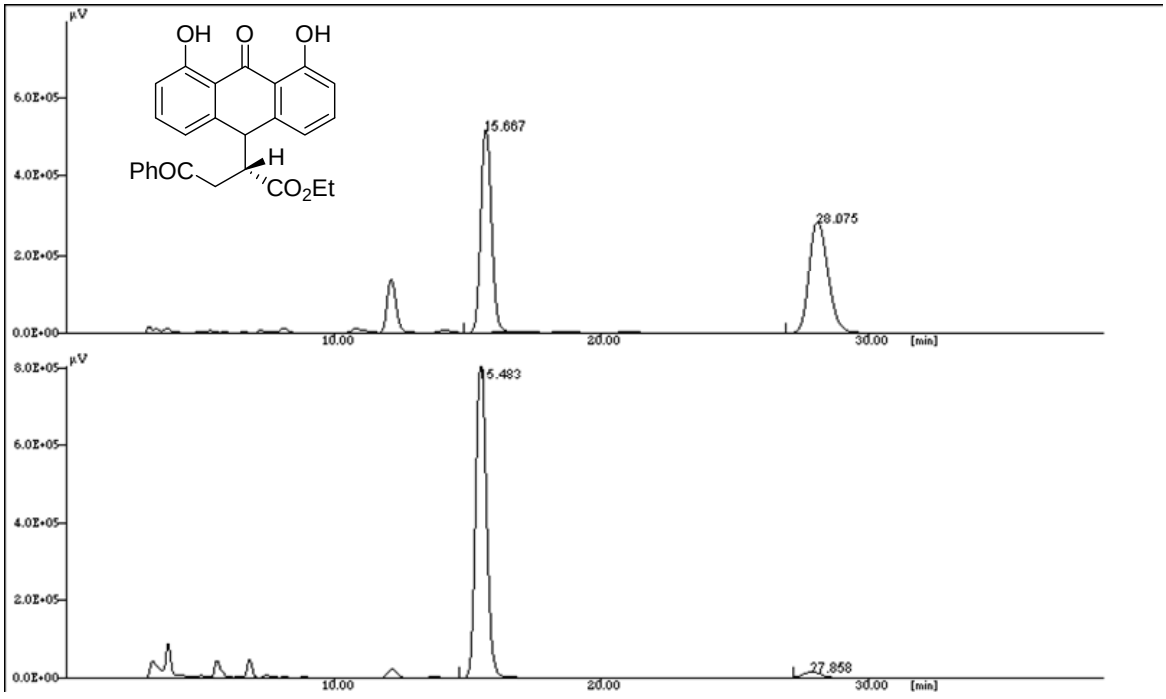

(132c) 2-(1, 8-dihydroxy-9-oxo-9, 10-dihydroanthracen-10-yl)succinonitrile

Yellow solid. mp 209.5-211.4 ^{o}C. 92% yield, 97% ee. $[\alpha]_D^{26}$ +24.5 (*c* 0.076, $CHCl_3$). ^{1}H NMR (300 MHz, $CDCl_3$, ppm)：δ 2.52 (d, 2H, *J* = 7.0Hz), 3.28 (m,1H), 4.56 (d, 1H, *J* = 4.5Hz), 6.98-7.63 (m, 6H),12.04 (s, 1H), 12.06 (s, 1H) ^{13}C NMR (75 MHz, $CDCl_3$, ppm): δ 18.42, 39.93, 43.66 115.18, 115.84, 116.47, 118.82, 118.99, 119.35, 119.47,136.79,137.11,138.59,139.30, 163.39, 163.50, 192.55. IR(film): 1214.7, 1609.6, 1639.6, 3019.5, 3446.7 cm^{-1}. LRMS(ESI) m/z 303.6 (M-H$^+$), HRMS(ESI) m/z 303.0762 (M-H$^-$), calc. 303.077 for $C_{18}H_{11}N_2O_3$.

The ee determined by chiral HPLC: CHIRALPAK ADH (4.6 mm i.d. x 250 mm); Hexane/2-propanol = 90/10; flow rate 1.0 ml/min; temp 25 °C; detection UV 230 nm; retention time: 12.4 min and 14.0 min.

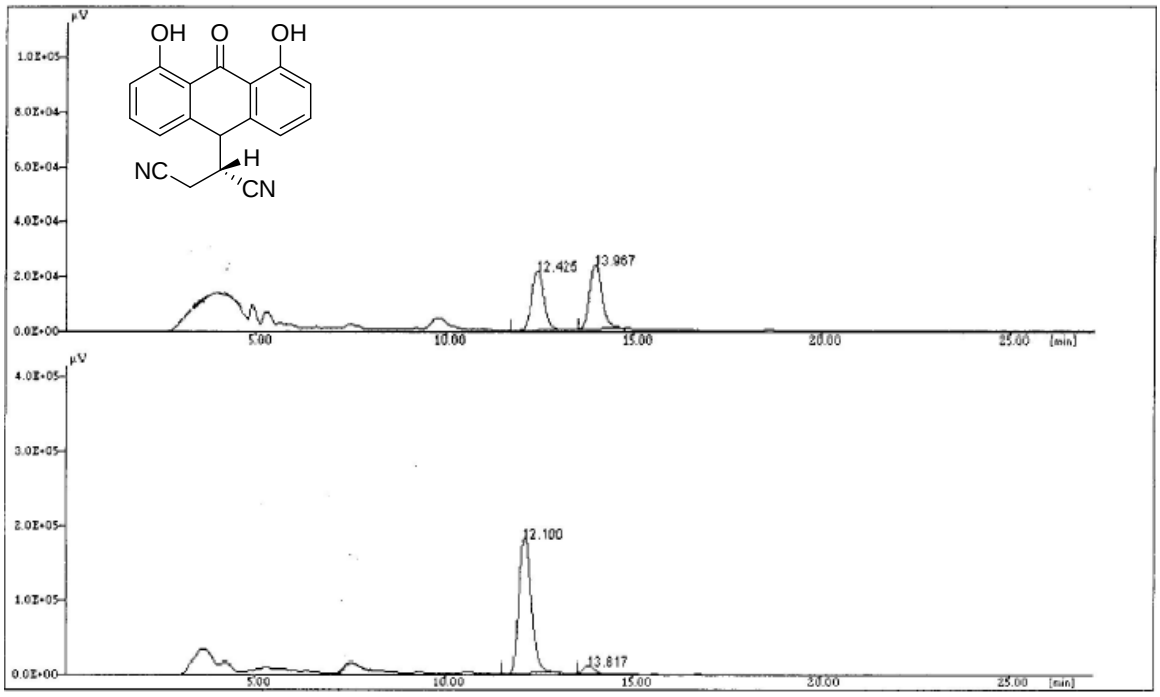

5.5 X-ray ORTEP diagrams

a. *rac*-21m-1 (CCDC 618371)

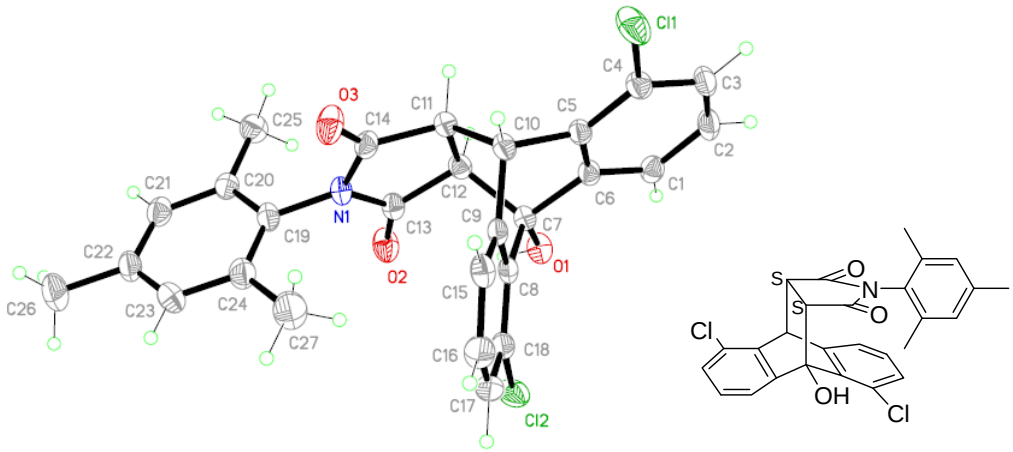

Table 1. Crystal data and structure refinement for 6292.

Identification code	6292	
Empirical formula	C27 H21 Cl2 N O3	
Formula weight	478.35	
Temperature	223(2) K	
Wavelength	0.71073 Å	
Crystal system	Triclinic	
Space group	P-1	
Unit cell dimensions	a = 7.5601(6) Å	a= 86.868(2)°.
	b = 8.2249(7) Å	b= 88.368(2)°.
	c = 18.6639(15) Å	g = 69.562(2)°.
Volume	1085.81(15) $Å^3$	
Z	2	
Density (calculated)	1.463 Mg/m^3	
Absorption coefficient	0.331 mm^{-1}	
F(000)	496	
Crystal size	0.16 x 0.16 x 0.09 mm^3	
Theta range for data collection	2.19 to 27.49°.	
Index ranges	-9<=h<=9, -10<=k<=6, -24<=l<=24	
Reflections collected	7646	
Independent reflections	4917 [R(int) = 0.0247]	
Completeness to theta = 27.49°	98.5 %	
Absorption correction	Sadabs, (Sheldrick 2001)	
Max. and min. transmission	0.9708 and 0.9490	

Refinement method	Full-matrix least-squares on F^2
Data / restraints / parameters	4917 / 0 / 302
Goodness-of-fit on F^2	1.049
Final R indices [I>2sigma(I)]	R1 = 0.0557, wR2 = 0.1338
R indices (all data)	R1 = 0.0676, wR2 = 0.1424
Largest diff. peak and hole	0.429 and -0.285 e.Å^{-3}

b. *rac*-21o-1 (CCDC 618370)

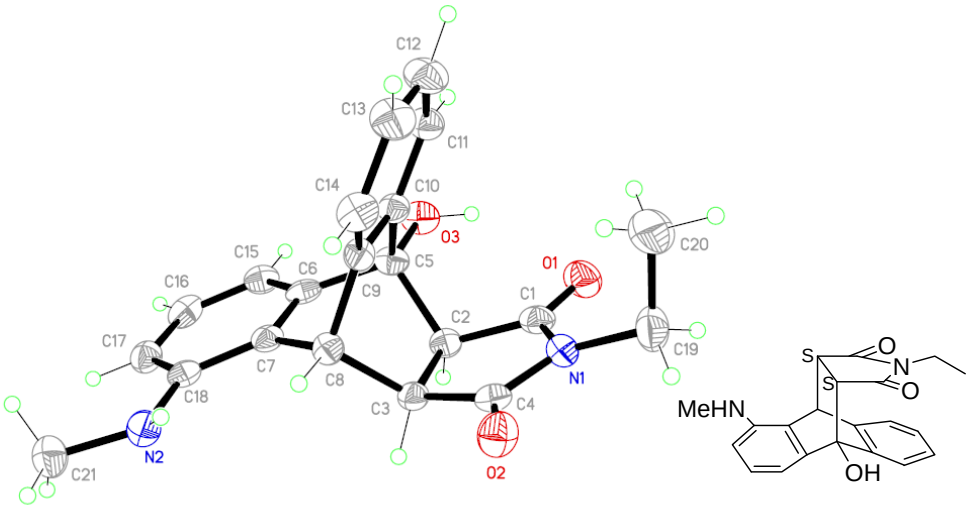

Table 1. Crystal data and structure refinement for 6220.

Identification code	6220	
Empirical formula	C21 H20 N2 O3	
Formula weight	348.39	
Temperature	223(2) K	
Wavelength	0.71073 Å	
Crystal system	Triclinic	
Space group	P-1	
Unit cell dimensions	a = 8.5075(14) Å	a= 73.966(3)°.
	b = 9.0343(15) Å	b= 79.596(4)°.
	c = 12.145(2) Å	g = 73.246(3)°.
Volume	853.9(2) Å^3	
Z	2	
Density (calculated)	1.355 Mg/m^3	

Absorption coefficient	0.092 mm^{-1}
F(000)	368
Crystal size	0.22 x 0.12 x 0.04 mm^3
Theta range for data collection	1.76 to 25.00°.
Index ranges	-10<=h<=10, -10<=k<=10, -14<=l<=14
Reflections collected	9054
Independent reflections	2997 [R(int) = 0.0509]
Completeness to theta = 25.00°	100.0 %
Absorption correction	Sadabs, (Sheldrick 2001)
Max. and min. transmission	0.9963 and 0.9801
Refinement method	Full-matrix least-squares on F^2
Data / restraints / parameters	2997 / 0 / 243
Goodness-of-fit on F^2	1.143
Final R indices [I>2sigma(I)]	R1 = 0.0786, wR2 = 0.1564
R indices (all data)	R1 = 0.1095, wR2 = 0.1689
Largest diff. peak and hole	0.271 and -0.290 $e.Å^{-3}$

c. *rac*-132b (CCDC 618369)

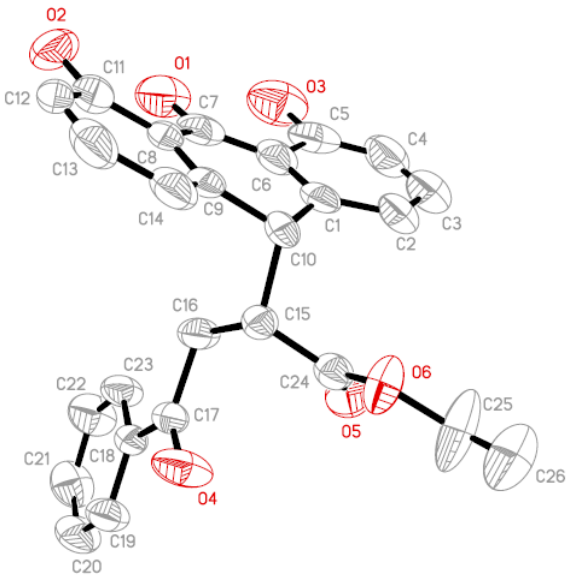

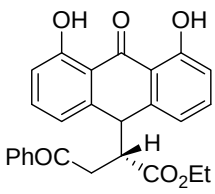

Table 1. Crystal data and structure refinement for 5473.

Identification code	5473
Empirical formula	C26 H22 O6
Formula weight	430.44

Temperature	223(2) K	
Wavelength	0.71073 Å	
Crystal system	Monoclinic	
Space group	P2(1)/c	
Unit cell dimensions	a = 7.7258(17) Å	□= 90°.
	b = 20.075(5) Å	□= 99.342(5)°.
	c = 13.878(3) Å	□ = 90°.
Volume	2123.9(8) $Å^3$	
Z	4	
Density (calculated)	1.346 Mg/m^3	
Absorption coefficient	0.096 mm^{-1}	
F(000)	904	
Crystal size	0.20 x 0.15 x 0.10 mm^3	
Theta range for data collection	1.80 to 24.00°.	
Index ranges	-8<=h<=8, -22<=k<=22, -15<=l<=15	
Reflections collected	20384	
Independent reflections	3323 [R(int) = 0.0565]	
Completeness to theta = 24.00°	100.0 %	
Absorption correction	Sadabs, (Sheldrick 2001)	
Max. and min. transmission	0.9905 and 0.9811	
Refinement method	Full-matrix least-squares on F^2	
Data / restraints / parameters	3323 / 6 / 295	
Goodness-of-fit on F^2	1.105	
Final R indices [I>2sigma(I)]	R1 = 0.1160, wR2 = 0.2453	
R indices (all data)	R1 = 0.1384, wR2 = 0.2588	
Largest diff. peak and hole	0.758 and -0.365 $e.Å^{-3}$	

5.6 Mechanistic and Kinetic Studies of Guanidine Catalyzed Enantioselective Diels-Alder Reactions

5.6.1 General procedures

NMR Spectroscopy: All experiments were performed using instruments equipped with a Bruker magnet. Low temperature experiments were performed using AMX500 MHz instruments equipped with an external thermostat filled with liquid nitrogen. All NMR solvents were purchased from Sigma-Aldrich.

A freshly prepared stock solution of anthrone **1** and *N*-phenylmaleimide **2** and CD_2Cl_2 (0.5 ml) was added to the NMR tube. 0.11 equiv of *t*-butylbenzene was added to the NMR tube as the internal standard. After adding catalyst to the reaction mixture, the reaction was monitored by following the formation of product and the decay of starting material over 0.25-6hrs. Spectra were collected every 30 or 60 seconds, depending on the expected length of the experiment. Most reactions were followed to >75% conversion, conversion of starting material to product was determined by NMR by following the decay of anthrone relative to *t*-butyl benzene internal standard. A series of experiments between anthrone **1** and phenylmaleimide **2** were performed at various temperature in CD_2Cl_2 and monitored at 30 or 60 intervals by ^1H NMR spectroscopy.

5.6.2 Kinetic analysis of monofunctional base

1. 1st Order in Anthrone

Order in anthrone (**19a)** was established by using a large excess of *N*-phenylmaleimide (**20b**) (4 equiv) and 2.00 mM **Et_3N**. The reaction was monitored by following the consumption of anthrone (**19a**). Plotting in ln[**19a**]^0/[**19a**] versus time gives a straight line, thus establishing first-order dependence on anthrone **19a**.

(1) Determination of the order of anthrone **(19a),** [**19a**] =0.200 M, [**20b**] =0.800 M,

[**Et$_3$N**] = 2.00 mM

$y = 0.37x + 36.6 \quad R^2 = 0.9995$

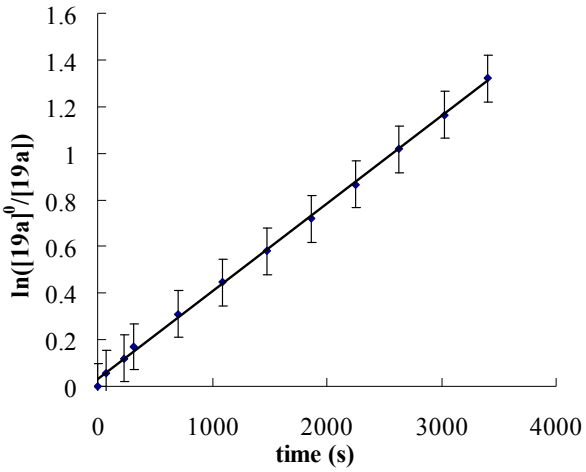

(2) Determination of the order of anthrone **(19a),** [**19a**] =0.100 M, [**20b**] =0.400 M, [**Et$_3$N**] = 2.00 mM

$y = 0.43x - 21.9 \quad R^2 = 0.9997$

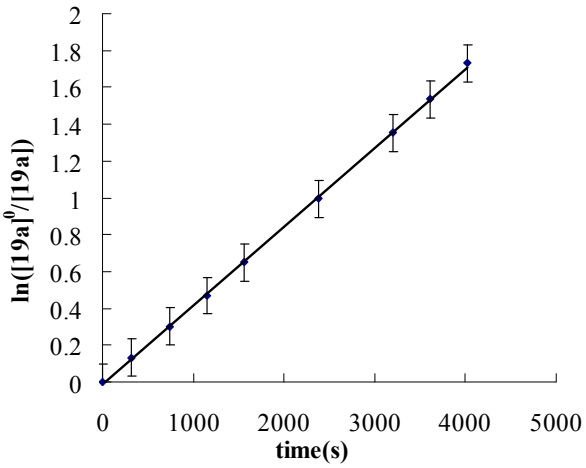

2. Overall Order of Anthrone and *N*-phenylmaleimide

Order in **20b** was established indirectly by determining the overall reaction order at equimolar concentration. For this experiment, a plot of ln [**19a**]$_0$/ln [**19a**] versus time gave a straight line with zero-intercept (R^2= 0.9966), indicating that the reaction is

overall first order and therefore zero order in **20b**.

Determination of the overall order of anthrone **(19a)** and *N*-phenylmaleimide **(20b),** [**19a**] =0.200 M, [**20b**] =0.200 M, [**Et_3N**] = 2.00 mM

$y = 0.43x + 24.64 \qquad R^2 = 0.9966$

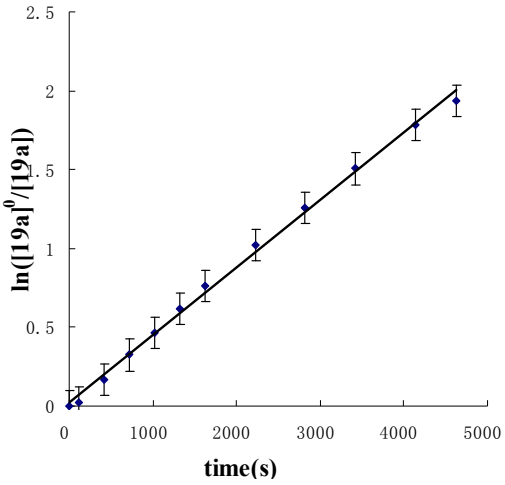

3. 1st Order of Et_3N

The reaction order in catalyst was established by determining the rate constants (kobs) at various catalyst concentrations. A plot of ln[k_{obs}] versus ln[Et_3N] gave a straight line for Et_3N (R^2 = 0.9933), indicating the first-order dependence on Et_3N.

(1). Determination of the rate constants (k_{obs}) with 1.00mM Et_3N, [**19a**] =0.200 M, [**20b**] =0.200 M, [**Et_3N**] = 1.00 mM

$y = 0.18x + 6.99 \quad R^2 = 0.9999$

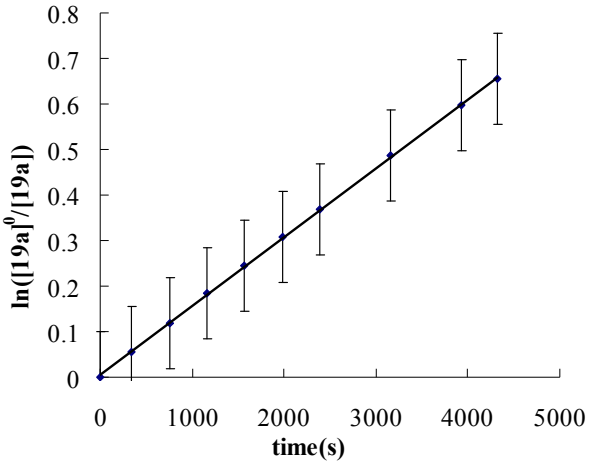

(2). Determination of the rate constants (k_{obs}) with 2.00mM Et_3N, [**19a**] =0.200 M, [**20b**] =0.200 M, [**Et_3N**] = 2.00 mM

$y = 0.43x + 24.64$ $R^2 = 0.9966$

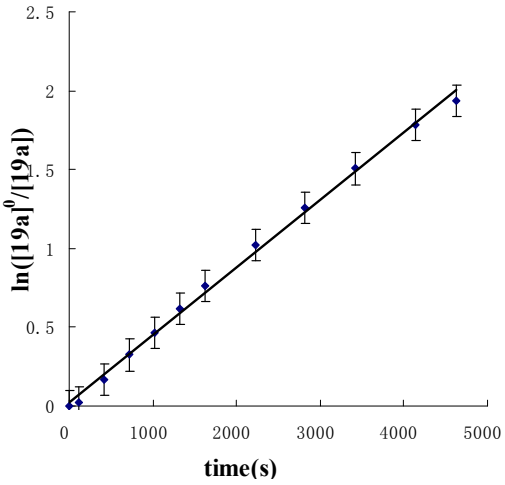

(3). Determination of the rate constants (k_{obs}) with 3.00mM Et_3N, [**19a**] =0.200 M, [**20b**] =0.200 M, [**Et_3N**] = 3.00 mM

$y = 0.64x + 59.8$ $R^2 = 0.9985$

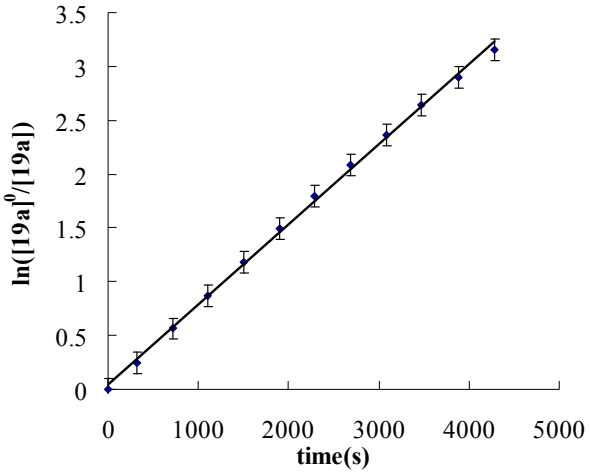

(4). Determination of the rate constants (k_{obs}) with 4.00mM Et_3N, [**19a**] =0.200 M, [**20b**] =0.200 M, [**Et_3N**] = 4.00 mM

$$y = 0.85x + 83.6 \quad R^2 = 0.9975$$

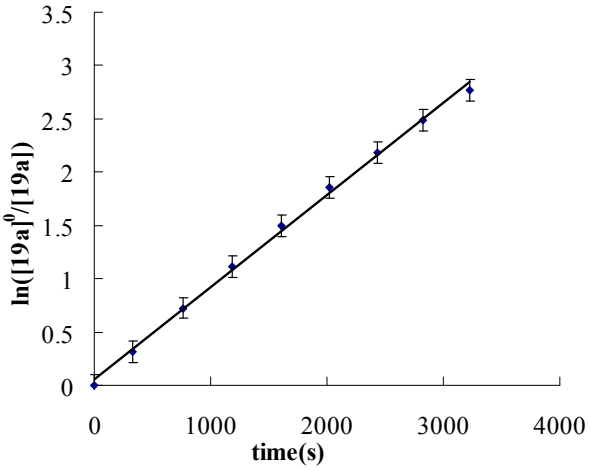

(5). Determination of the rate constants (k_{obs}) with 5.00mM Et_3N, [**19a**] =0.200 M, [**20b**] =0.200 M, [**Et_3N**] = 5.00 mM

$$y = 1.12x + 87.1 \quad R^2 = 0.9976$$

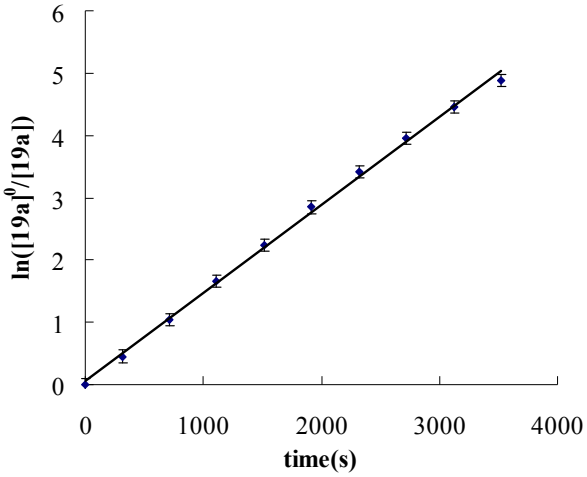

(6) ln[k_{obs}] versus ln[Et_3N]

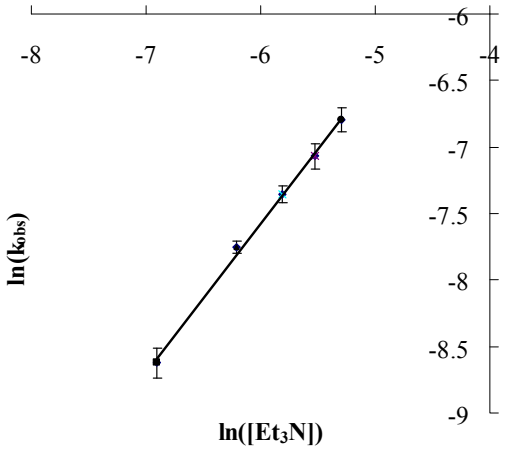

4. Eyring plot

Determination of Eyring activation paramters was conducted in the usual manner by measuring the rate constants of the catalyzed reactions as a function of temperature between -40.0 ^oC and -10.0 ^oC. A plot of ln[kh/k_BT] versus 1/T gave a straight line (R^2 = 0.9872); $\Delta S^{\ddagger}$ and $\Delta H^{\ddagger}$ can be caculated from the slope and intersept. The activation parameters reveal a large entropic contribution ($\Delta S^{\ddagger}$ = -32±3 e.u.) and an enthalpic contribution of 7.2 ±0.8 kcal mol^{-1}.

(1) Determination of the rate constants (k_{obs}) at -10 ^oC, [**19a**] =0.200 M, [**20b**] = 0.200 M, [**Et_3N**] = 1.00 mM, -10.0 ^oC

$y = 0.58x + 29.1$ $R^2 = 0.9969$

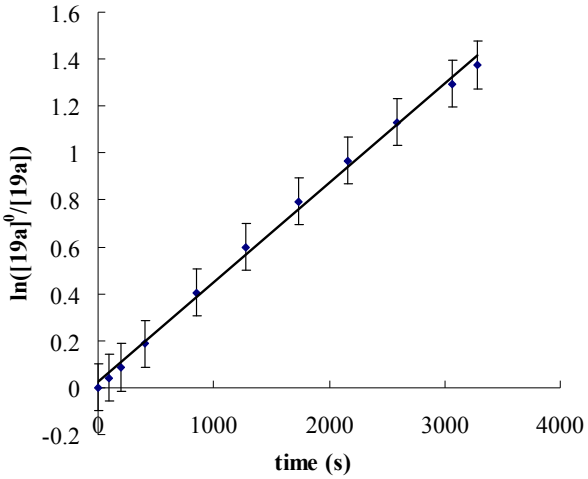

(2) Determination of the rate constants (k_{obs}) at -20 °C, [**19a**] =0.200 M, [**20b**] = 0.200 M, [**Et$_3$N**] = 1.00 mM, -20.0 °C

$y = 0.38x + 14.0$ $R^2 = 0.9994$

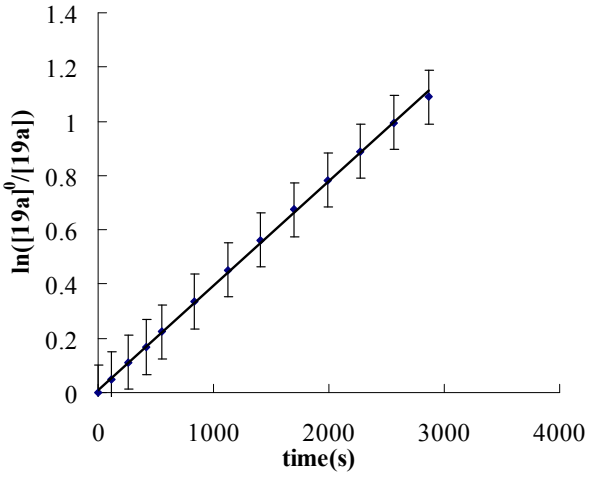

(3) Determination of the rate constants (k_{obs}) at -30.0 °C, [**19a**] =0.200 M, [**20b**] = 0.200 M, [**Et$_3$N**] = 1.00 mM, -30.0 °C

$y = 0.21x + 0.396$ $R^2 = 0.9997$

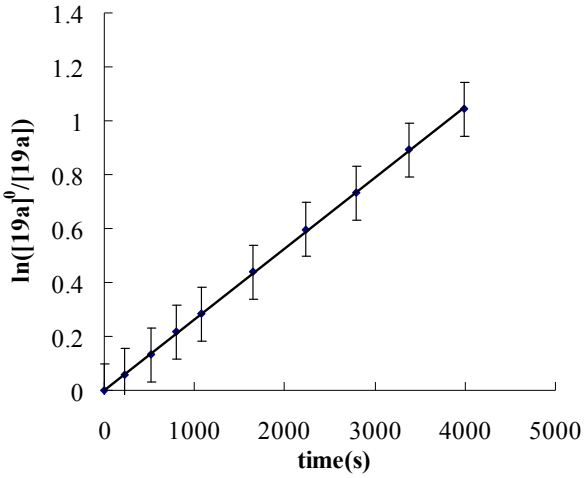

(4) Determination of the rate constants (k_{obs}) at -33.3 °C, [**19a**] =0.200 M, [**20b**] = 0.200 M, [$\mathbf{Et_3N}$] = 1.00 mM, -33.3 °C

$y = 0.18x + 24.97 \qquad R^2 = 0.9996$

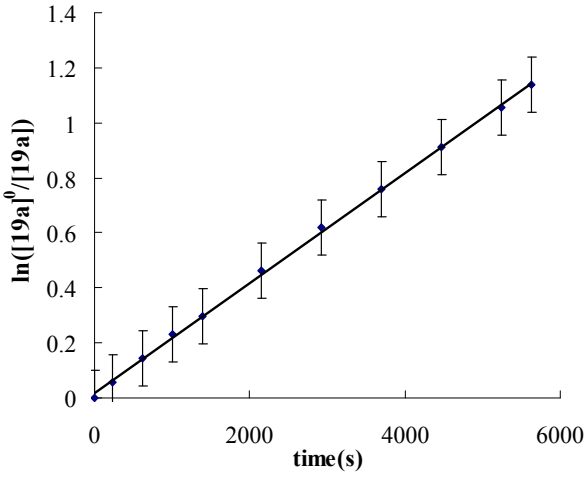

(5) Determination of the rate constants (kobs) at -40.0 °C, [**19a**] =0.200 M, [**20b**] =0.200 M, [$\mathbf{Et_3N}$] = 1.00 mM, -40.0 °C

$y = 0.10x - 6.59 \; R^2 = 0.9998$

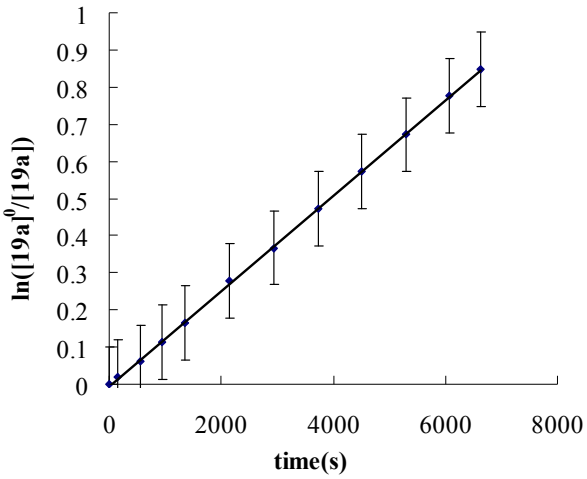

(6) ln[kh/k_BT] versus 1/T

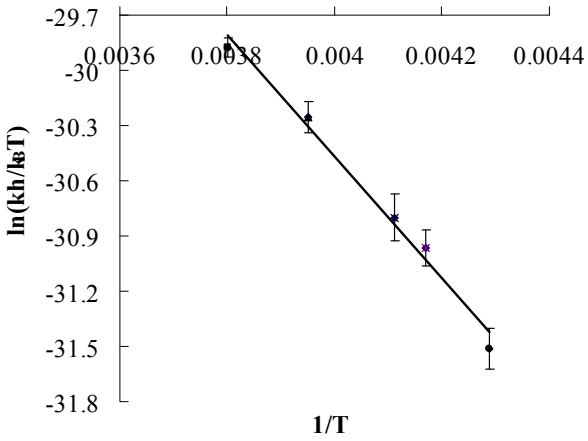

slope	intersection	$\Delta H^{\ddagger}$ [a]	$\Delta S^{\ddagger}$ [b]
-3302.6	-17.3	7.2 ± 0.8	-32 ± 3

[a] Measured in kcal mol^{-1} [b] Measured in cal mol^{-1} K^{-1} [c] R^2 = 0.9872

5.6.3 Kinetic analysis of bifunctional guanidine catalyst

1. Overall Order of Anthrone and *N*-phenylmaleimide

Overall order was established by using equimolar of anthrone **19a** and *N*-phenylmaleimide **20b** and 3.00 mM **124d**. The reaction was monitored by following the consumption of anthrone (**19a**). For this experiment, a plot of ln 1/[**19a**] versus time gave a straight line (R^2= 0.9989), indicating that the reaction is overall

second order.

[**19a**] =0.100 M, [**20b**] =0.100 M, [**124d**] = 3.00 mM

$y = 2.3x + 11092 \qquad R^2 = 0.9989$

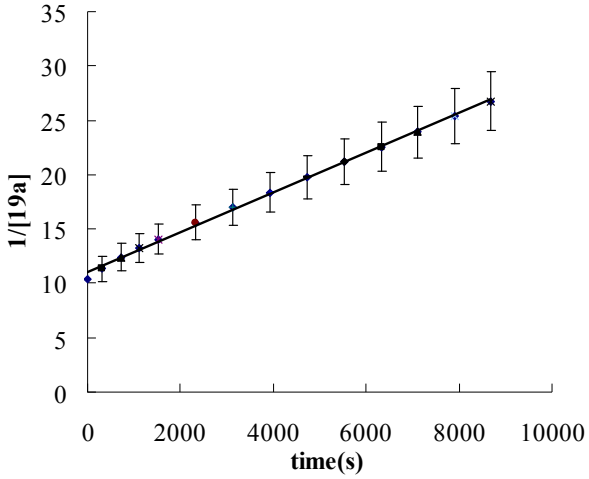

2. 1st Order in *N*-phenylmaleimide

Order in *N*-phenylmaleimide **(20b)** was determined by using a large excess of anthrone (2, 5, 10 equiv) and 3.00 mM **124d**. The reaction was monitored by following the consumption of anthrone (**19a**). Plotting in $\ln[\mathbf{20b}]^0/[\mathbf{20b}]$ versus time gives a straight line, thus establishing first-order dependence on *N*-phenylmaleimide (**20b)**. The reaction is overall second order and therefore first order in **19a**.

(1) Determination of the order of *N*-phenylmaleimide (**20b),** [**19a**] =0.0500 M, [**20b**] = 0.0250 M, [**124d**] = 3.00 mM

$y = 0.79x - 7.75 \quad R^2 = 0.9981$

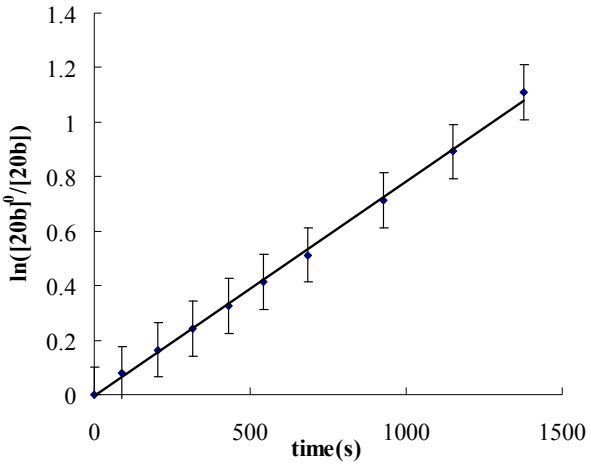

(2) Determination of the order of *N*-phenylmaleimide (**20b)**, [**19a**] =0.125 M, [**20b**] = 0.0250 M, [**124d**] = 3.00 mM

$$y = 1.20x - 27.5 \quad R^2 = 0.9930$$

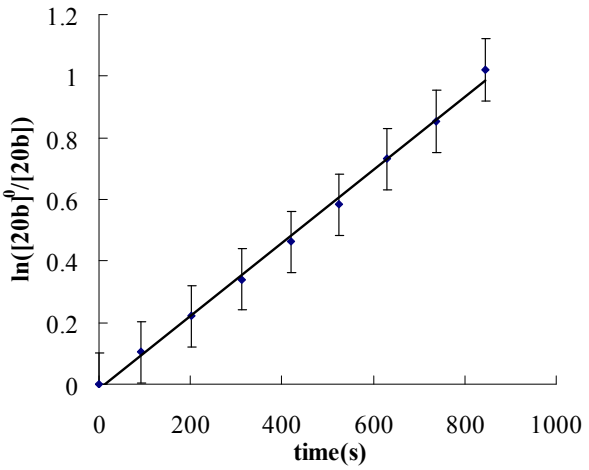

(3) Determination of the order of *N*-phenylmaleimide (**20b),** [**19a**] =0.25 M, [**20b**] = 0.0250 M, [**124d**] = 3.00 mM

$$y = 1.2x - 25.7 \quad R^2 = 0.9939$$

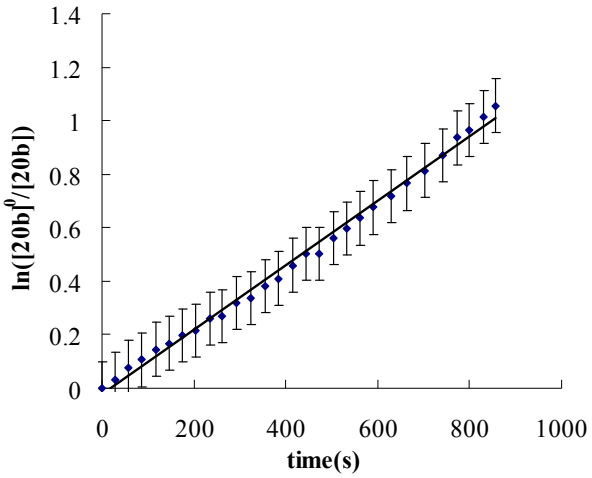

3. Rate inhibition at a high concentraion of 20b

Rate inhibition was observed at high [**20b**]. Plotting in ln[**19a**]^0/[**19a**] versus time at different concentrantion of **20b** gave deviations from simple first-order kinetic behavior at higher concentration of **20b**.

[**19a**] = 0.100 M, [**20b**] =0.100 M, [**124d**] = 5.00 mM

[**19a**]=0.0500 M, [**20b**] =0.100 M, [**124d**] = 5.00 mM

[**19a**]=0.0500 M, [**20b**] =0.250 M, [**124d**] = 5.00 mM

[**19a**]=0.0500 M, [**20b**] =0.500 M, [**124d**] = 5.00 mM

Kinetic profiles for different concentration of **20b**

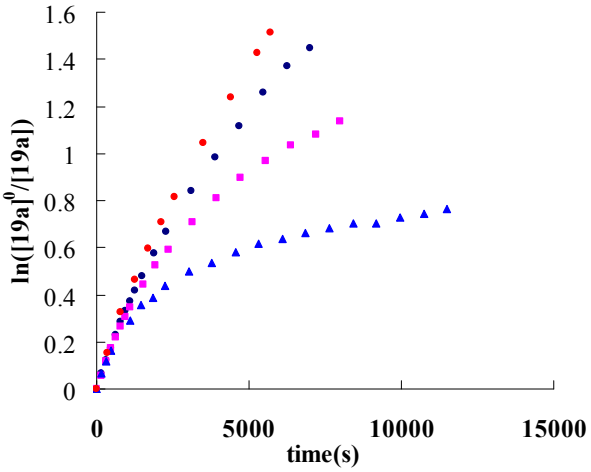

4. 1st Order in chiral guanidine 124d

The reaction order in chiral guanidine **124d** was established by determining the rate

constants (k_{obs}) at various catalyst concentrations. A plot of ln[k_{obs}] versus ln[**124d**] gave a straight line (R^2 = 0.9933), indicating the first-order dependence on **124d**.

(1) Determination of the rate constants (k_{obs}) with 3.00 mM **124d**, [**19a**] =0.100 M, [**20b**] =0.100 M, [**124d**] = 3.00 mM

$y = 2.3x + 11092$ $R^2 = 0.9989$

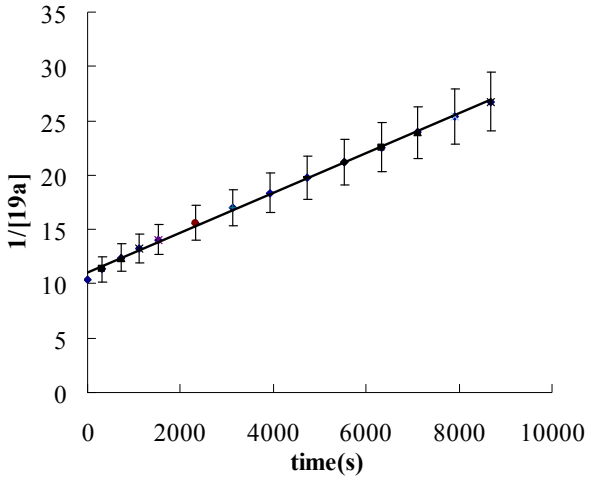

(2) Determination of the rate constants (k_{obs}) with 5.00 mM **124d,** [**19a**] = 0.100 M, [**20b**] = 0.100 M, [**124d**] = 5.00 mM

$y = 4.8x + 10896$ $R^2 = 0.9957$

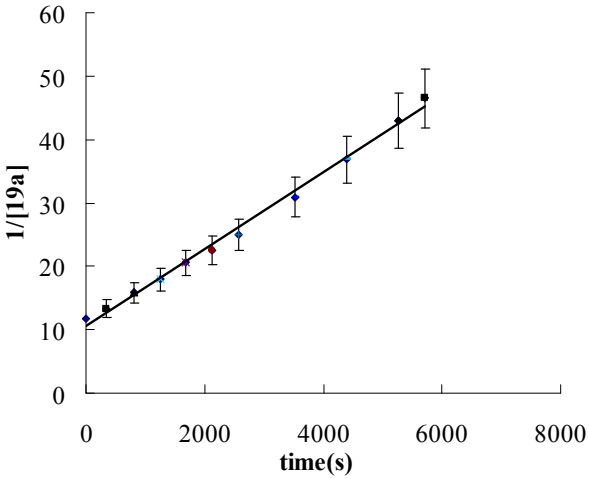

(3) Determination of the rate constants (k_{obs}) with 8.00 mM **124d,** [**19a**] = 0.100 M,

[**20b**] = 0.100 M, [**124d**] = 8.00 mM

$y = 7.6x + 11405 \qquad R^2 = 0.9984$

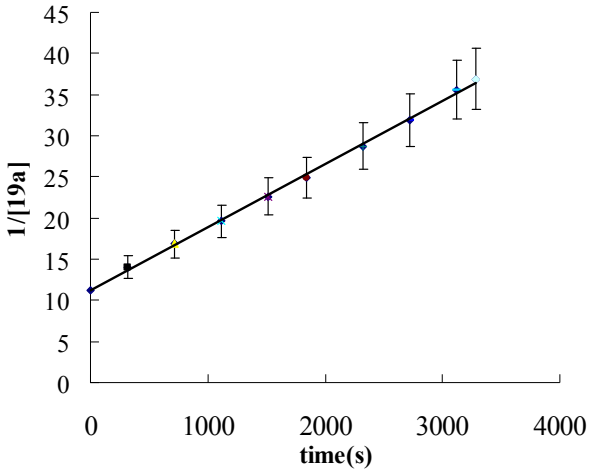

(4) Determination of the rate constants (kobs) with 10.0 mM **124d,** [**19a**] = 0.100 M, [**20b**] = 0.100 M, [**124d**] = 10.0 mM

$y = 9.5x + 11165 \qquad R^2 = 0.9939$

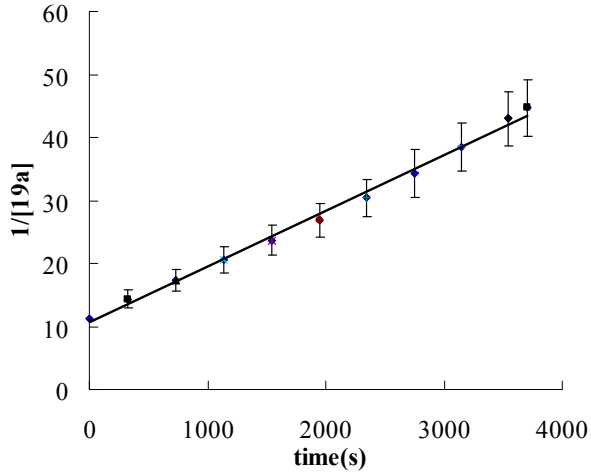

(5) Determination of the rate constants (k_{obs}) with 12.0 mM **124d,** [**19a**] =0.100 M, [**20b**] =0.100 M, [**124d**] = 12.0 mM

$y = 12.4x + 11146 \qquad R^2 = 0.9970$

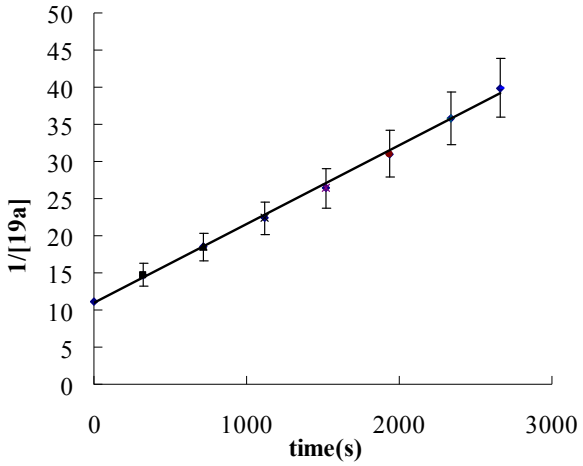

(6) ln[k_{obs}] versus ln[**124d**]

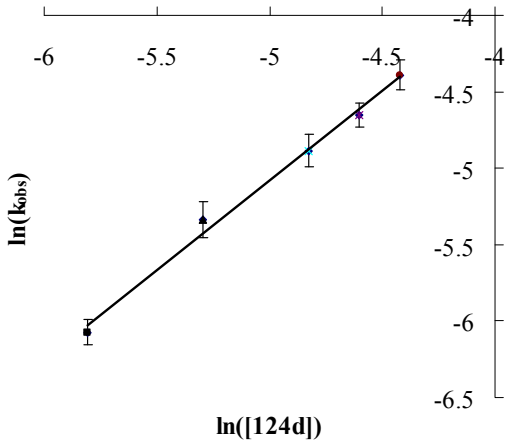

5. Eyring plot

Determination of Eyring activation paramters was conducted in the usual manner by measuring the rate constants of the catalyzed reactions as a function of temperature between -33.3 ^{o}C and -10.0 ^{o}C. A plot of ln[kh/k_BT] versus 1/T gave a straight line (R^2 = 0.9979); $\Delta S^{\ddagger}$ and $\Delta H^{\ddagger}$ can be caculated from the slope and intersept. The activation parameters reveal a large entropic contribution ($\Delta S^{\ddagger}$ = -39± 2.8 e.u.) and an enthalpic contribution of 4.7 ± 0.7 kcal mol^{-1}.

(1) Determination of the rate constants (k_{obs}) at -10.0 ^{o}C, [**19a**] = 0.100 M, [**20b**] =

0.100 M, [**124d**] = 3.00 mM, -10.0 °C

$$y = 6.3x + 12499 \quad R^2 = 0.9998$$

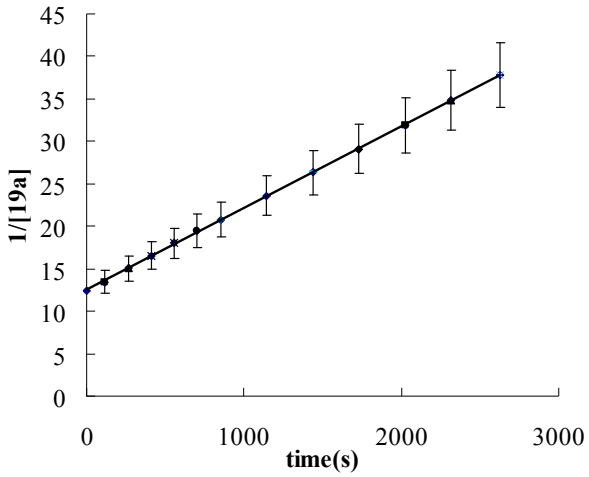

(2) Determination of the rate constants (k_{obs}) at -15.0 °C, [**19a**] =0.100 M, [**20b**] = 0.100 M, [**124d**] = 3.00 mM, -15.0 °C

$$y = 5.2x + 12842 \quad R^2 = 0.9998$$

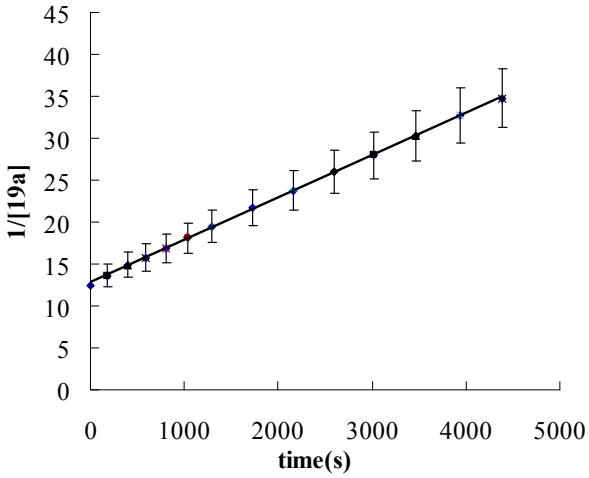

(3) Determination of the rate constants (k_{obs}) at -20.0 °C, [**19a**] =0.100 M, [**20b**] = 0.100 M, [**124d**] = 3.00 mM, -20.0 °C

$$y = 4.3x + 11992 \quad R^2 = 0.9996$$

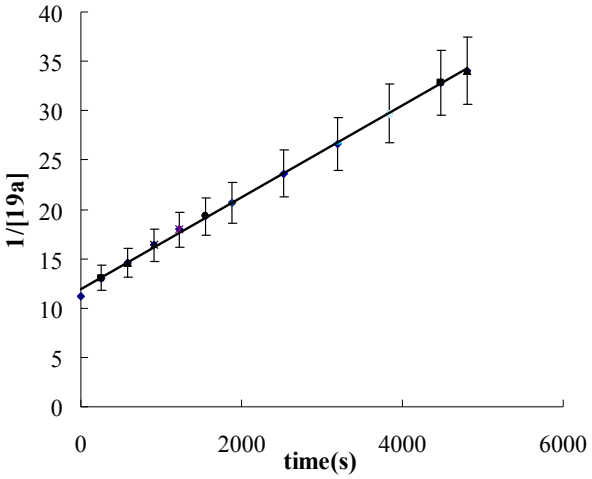

(4) Determination of the rate constants (k_{obs}) at -30.0 ^{o}C, [**19a**] = 0.100 M, [**20b**] = 0.100 M, [**124d**] = 3.00 mM, -30.0 ^{o}C

$$y = 2.8x + 11147 \quad R^2 = 0.9988$$

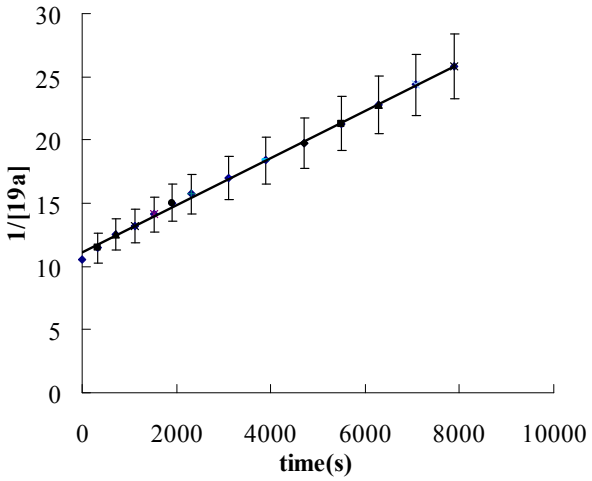

(5) Determination of the rate constants (k_{obs}) at -33.3 ^{o}C, [**19a**] =0.100 M, [**20b**] =0.100 M, [**124d**] = 3.00 mM, -33.3 ^{o}C

$$y = 2.3x + 11092 \quad R^2 = 0.9989$$

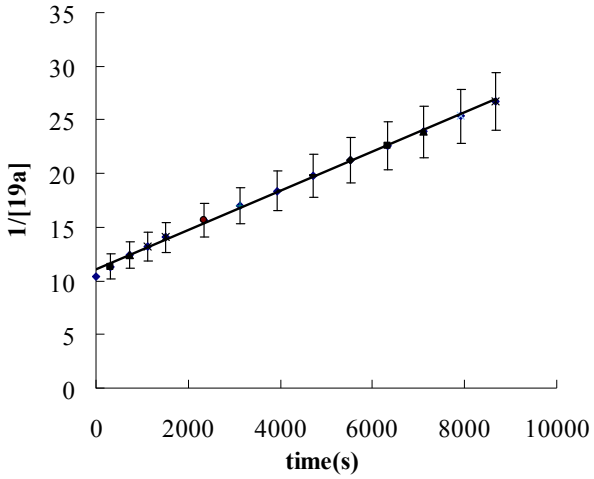

(6) ln[kh/k_BT] versus 1/T

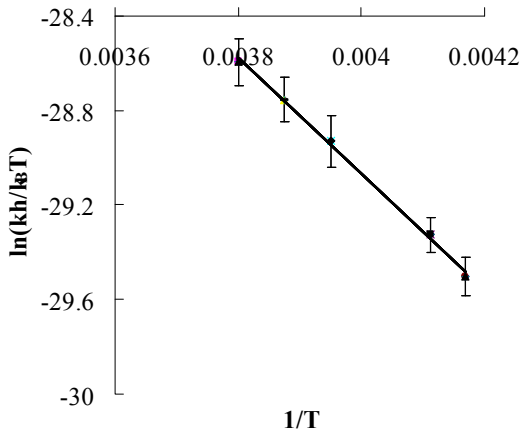

slope	intersection	$\Delta H^{\ddagger}$ [a]	$\Delta S^{\ddagger}$ [b]
-2356.7	-19.6	4.7± 0.7	-39 ± 2.8

[a] Measured in kcal mol^{-1} [b] Measured in cal mol^{-1} K^{-1} [c] R^2 = 0.9979

5.7 Anthrone-Derived NHPI Analogues as Catalysts in Reactions Using Oxygen as an Oxidant

5.7.1 General procedures for bicyclic guanidine catalyzed reactions between substituted anthrone and maleimides.

To a 5 ml RBF containing catalyst **124d** (5.8 mg, 0.02 mmol, 10 mol %) and a stirring bar, anhydrous CH_2Cl_2 (1.0 ml), 1, 8-dichloro-9-anthrone **19b** (58 mg, 0.22mmol) and

N-acetoxymaleimide **144a** (31.0 mg, 0.2mmol) were added in this sequence. After stirring at -20 ^{o}C for 8 hrs, the reaction mixture was loaded onto a short silica gel column, followed by flash chromatography (gradient elution with hexane/EA mixtures; 9/1 to 4/1). Product **145a** (72mg) was obtained as a white solid in 86% yield and 92% ee.

5.7.2 General procedures for the chiral anthrone-derived NHPI analogue mediated oxidations of benzylic compounds and diol.

A solution of substrate **147** (0.2 mmol), catalyst **146** (0.02 mmol), and $Co(OAc)_2$ (0.002 mmol) in anhydrous acetonitrile (1 ml) was placed in a round bottom flask. The flask was equipped with a balloon filled with O_2 (1atm). The mixture was vigorously stirred at 60 ^{o}C for 10h, evaporation of the solvent followed by flash chromatography on silica gel afforded product **148a** as a white solid.

5.7.3 General Procedures for the synthesis of β-hydroxy ketal 158.

A solution of substrate **156a** (1mmol), substrate **157a** (0.2 mmol), catalyst **155** (0.02 mmol), and $Co(OAc)_2$ (0.002 mmol) was placed in a round bottom flask. The flask was equipped with a balloon filled with O_2 (1atm). The mixture was vigorously stirred at rt for 5 h. The recovery of unreacted **156a** under a reduced pressure followed by flash chromatography on silica gel (*n*-hexane–AcOEt = 1:2) afforded product **158a** (60% yield) as a colorless liquid.

5.7.4 Procedures for the synthesis of α-hydroxy-γ-lactone 160.

To a solution of alcohol **159** (2 mmol), catalyst **155** (0.02 mmol), $Co(OAc)_2$ (0.002 mmol) in acetonitrile (0.5 ml) placed in a round bottom flask, **157a** (0.2 mmol) was

was added. The flask was equipped a ballon filled with O_2 (1atm). After the mixture was stirred at rt for 8 h, rotary evaporation of the solvent and unreacted alcohol followed by flash chromatography on silica gel afforded product **160** in 65 % yield.

5.7.5 Characterization of the oxidation products

(**145a**) 2-Acetoxy-5, 13-dichloro-4-hydroxy-3a, 4, 9, 9a-tetrahydro-4, 9-[1', 2'] benzeno -1*H*-benz[*f*]isoindole-1, 3(2*H*)-dione

White solid. mp 251.9-252.7 ^{o}C. 86% yield, 92% ee. $[\alpha]_D^{25}$ +58 (*c* 0.25, $CHCl_3$). ^{1}H NMR (500 MHz, $CDCl_3$, ppm)：δ 2.15 (s, 3H), 3.32 (dd, 1H, *J* = 3.1, 8.8Hz), 3.43 (d, 1H, *J* = 9.5Hz), 4.69 (d, 1H, *J* = 3.2Hz), 4.86 (s, 1H), 7.12-7.27 (m, 6H). ^{13}C NMR 125 MHz, $CDCl_3$, ppm): 17.3, 43.0, 44.9, 48.6, 81.3, 122.7, 124.2, 128.5, 129.1, 130.0, 130.1, 131.3, 134.8, 138.7, 141.5, 168.4, 168.6. IR (film): 1215.4, 1637.8, 3019.0 cm^{-1}. LRMS(FAB) m/z 417.8 (M^+), HRMS(FAB) m/z 418.0249 ($M+H^+$), calc. for $C_{20}H_{14}Cl_2NO_5$ 418.0249.

The ee determined by chiral HPLC; CHIRALCEL AD-H (4.6 mm i.d. x 250 mm); hexane/2-propanol 80/20; flow rate 1.0 ml/min; temp 25 °C; detection UV 230 nm; retention time: 18.1 min and 22.2 min.

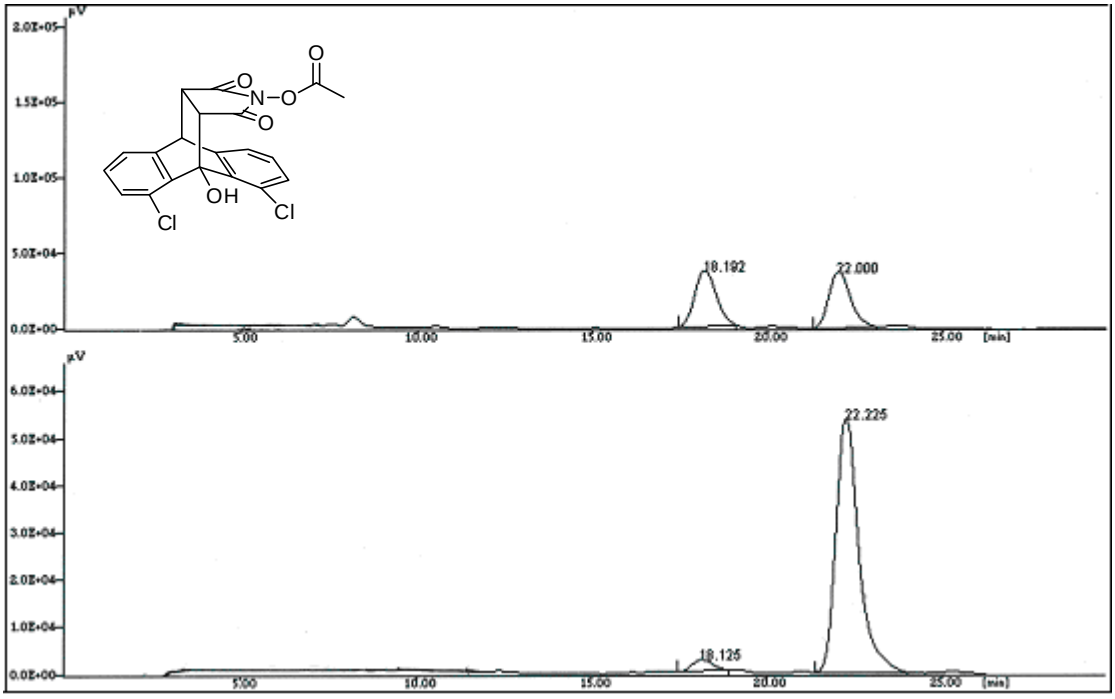

(**145b**) 8, 10-Dichloro-2-acetoxy-4-hydroxy-3a, 4, 9, 9a-tetrahydro-4, 9-[1', 2'] benzeno-1*H*-benz[*f*]isoindole-1, 3(2*H*)-dione

White solid. mp 244.1-245.0 ^{o}C. 85% yield, 12% ee. ^{1}H NMR (300 MHz, $CDCl_3$, ppm) ： δ 2.16 (s, 3H), 3.20 (d, 1H, J = 8.7Hz), 3.42 (dd, 1H, J = 3.1, 8.4Hz), 4.33 (s, 1H), 5.87 (d, 1H, J = 3.1Hz), 7.20-7.60 (m, 6H). ^{13}C NMR (75 MHz, $CDCl_3$, ppm): δ 14.1, 17.3, 36.9, 43.4, 47.1, 119.5, 119.9, 127.7, 128.2, 128.4, 128.6, 130.0, 131.1, 133.3, 142.4, 144.3, 167.7, 169.9. IR (film): 1216.0, 1643.3, 3019.5 cm^{-1}. LRMS(FAB) m/z 418.0 (M^+), HRMS(FAB) m/z 418.0248 ($M+H^+$), calc. for $C_{20}H_{14}Cl_2NO_5$ 418.0249.

The ee determined by chiral HPLC; CHIRALCEL AD-H (4.6 mm i.d. x 250 mm); hexane/2-propanol 80/20; flow rate 1.0 ml/min; temp 25 °C; detection UV 230 nm; retention time: 27.0 min and 32.1 min.

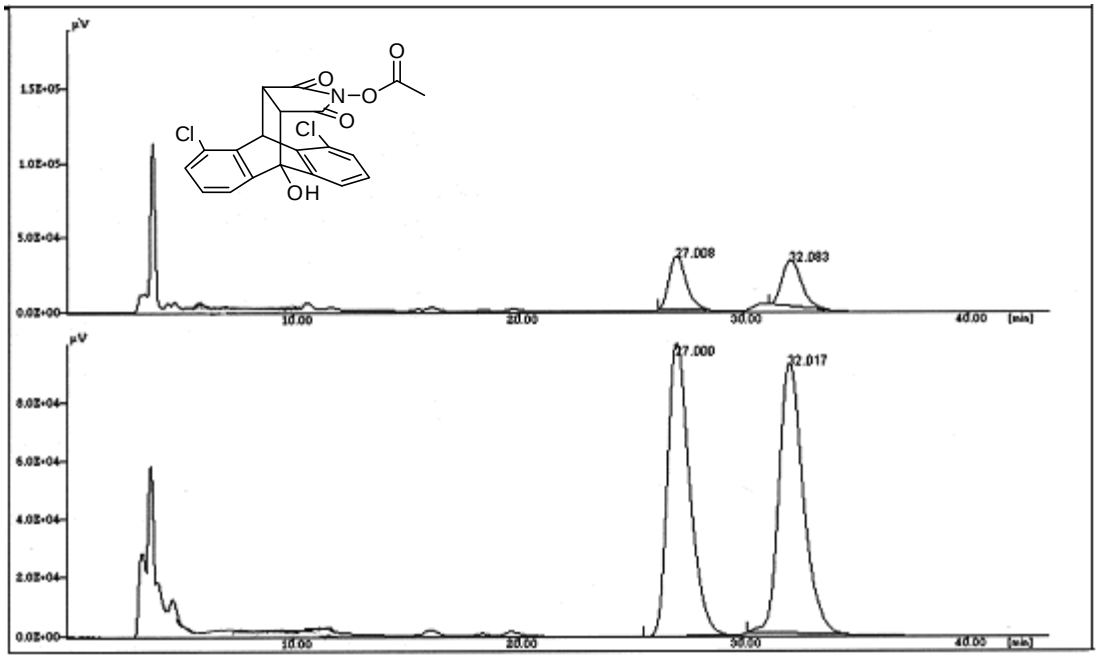

(**145c**) 2-benzoyloxy-5, 13-dichloro-4-hydroxy-3a, 4, 9, 9a-tetrahydro-4, 9-[1', 2'] benzeno -1*H*-benz[*f*]isoindole-1, 3(2*H*)-dione

White solid. mp 176.5 -177.2 ^{o}C. 83% yield, 64% ee. ^{1}H NMR (500 MHz, $CDCl_3$, ppm)： δ 3.40 (dd, 1H, J = 3.1, 8.8Hz), 3.51 (d, 1H, J = 8.8Hz), 4.74 (d, 1H, J = 3.2Hz), 4.90 (s, 1H), 7.14-7.97 (m, 11H). ^{13}C NMR (75 MHz, $CDCl_3$, ppm): δ 41.8, 43.6, 47.4, 80.0, 121.4, 122.9, 123.4, 127.2, 127.4, 127.8, 128.6, 128.7, 129.2, 129.9, 130.0, 133.5, 137.3, 140.2, 167.2, 167.5. IR (film): 1216.0, 1641.9, 3018.7 cm^{-1}. LRMS(FAB) m/z 479.9 (M^+), HRMS(FAB) m/z 480.0400 ($M+H^+$), calc. for $C_{20}H_{13}Cl_2NO_5$ 480.0406.

The ee determined by chiral HPLC; CHIRALCEL AD-H (4.6 mm i.d. x 250 mm); hexane/2-propanol 80/20; flow rate 1.0 ml/min; temp 25 °C; detection UV 230 nm; retention time: 12.3 min and 14.8 min.

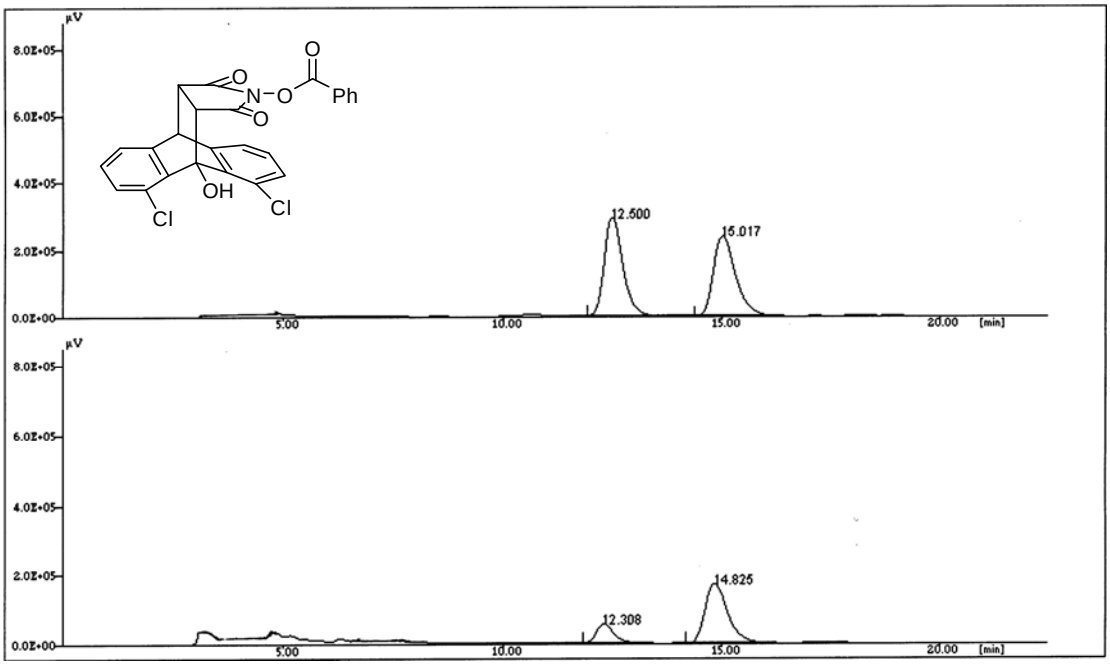

(**145d**) 8, 10-Dichloro-2-benzoyloxy-4-hydroxy-3a, 4, 9, 9a-tetrahydro-4, 9-[1', 2'] benzeno-1*H*-benz[*f*]isoindole-1, 3(2*H*)-dione

White solid. mp 253.3-254.2 ^{o}C. 84% yield, 87% ee. ^{1}H NMR (500 MHz, $CDCl_3$, ppm)：δ 3.26 (d, 1H, J = 8.8Hz), 3.49 (dd, 1H, J = 3.7, 8.8Hz), 4.35 (s, 1H), 5.92 (d, 1H, J = 3.2Hz), 7.22-7.97 (m, 11H). ^{13}C NMR (125 MHz, $CDCl_3$, ppm): δ 37.0, 43.6, 47.2, 77.2, 119.5, 120.0, 124.7, 127.7, 128.3, 128.6 (two peaks), 128.7, 130.1, 130.5, 131.2, 133.4, 134.9, 142.5, 144.5, 167.8, 170.1. IR (film): 1216.0, 1735.4, 3018.2 cm^{-1}. LRMS (FAB) 480.0 m/z (M^+), HRMS (FAB) m/z 480.0378 ($M+H^+$), calc. for $C_{25}H_{16}Cl_2NO_5$ 480.0406.

The ee determined by chiral HPLC; CHIRALCEL AD-H (4.6 mm i.d. x 250 mm); hexane/2-propanol 80/20; flow rate 1.0 ml/min; temp 25 °C; detection UV 230 nm; retention time: 15.6 min and 19.4 min.

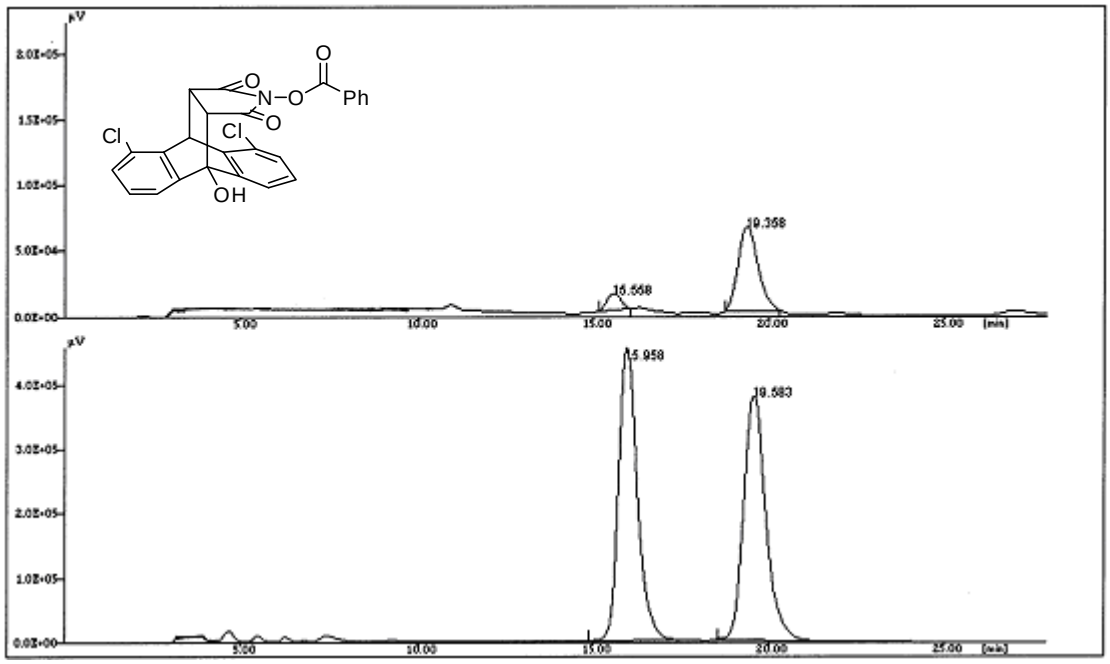

(**146**) 2-Hydroxy-5, 13-dichloro-4-hydroxy-3a, 4, 9, 9a-tetrahydro-4, 9-[1', 2'] benzeno -1*H*-benz[*f*]isoindole-1, 3(2*H*)-dione

White solid. mp 191.0 -191.8 ^{o}C. 92% yield. ^{1}H NMR (500 MHz, $(CD_3)_2CO$, ppm): δ 3.40 (dd, 1H, J = 3.1, 8.8Hz), 3.43 (d, 1H, J = 8.8Hz), 4.82 (d, 1H, J = 2.5Hz), 4.97 (s, 1H), 7.16-7.49 (m, 6H). ^{13}C NMR (125 MHz, $(CD_3)_2CO$, ppm): δ 42.7, 44.8, 48.3, 81.2, 123.3, 124.2, 128.5, 128.8, 129.3, 129.4, 130.6 (two peaks), 135.9, 137.5, 140.2, 142.7, 170.6, 172.2. IR (film): 1215.9, 1642.0, 3018.2, 3433.0 cm^{-1}. LRMS(ESI) m/z 376.3 (M^+), HRMS(ESI) m/z 397.9957 ($M+Na^+$), calc. for $C_{18}H_{11}Cl_2NO_4Na$ 397.9963.

(**148a**) 1-Acenaphthenol

Yellow solid. 42% yield. ^{1}H NMR (300 MHz, $CDCl_3$, ppm): δ 1.98 (d, 1H, J = 7.5Hz), 3.27 (d, 1H, J = 17.8Hz), 3.82 (dd, 1H, J = 7.4, 17.8Hz), 5.75 (t, 1H, J = 6.3 Hz),

7.31-7.78 (m, 6H). LRMS (FAB) m/z 170.1 (M^+).

The ee determined by chiral HPLC; CHIRALPAK IA (4.6 mm i.d. x 250 mm); hexane/2-propanol 95/5; flow rate 0.5 ml/min; temp 25 °C; detection UV 230 nm; retention time: 21.8 min and 23.2 min.

(**150**) 2-Methoxy-2-phenylindan-1-one

White solid. 55% yield. ^{1}H NMR (300 MHz, $CDCl_3$, ppm)：δ 3.34 (s, 3H), 3.59 (s, 2H), 7.29-7.79 (m, 9H). LRMS (FAB) m/z 237.0 ($M-H^+$).

The ee determined by chiral HPLC; CHIRALPAK IA (4.6 mm i.d. x 250 mm); hexane/2-propanol 97/3; flow rate 0.3 ml/min; temp 25 °C; detection UV 230 nm; retention time: 27.5 min and 28.9 min.

(**152a**) 1-Phenylethanol

The ee determined by chiral HPLC; CHIRALPAK IA (4.6 mm i.d. x 250 mm); hexane/2-propanol 95/5; flow rate 0.5 ml/min; temp 25 °C; detection UV 230 nm; retention time: 11.0 min and 15.1 min.

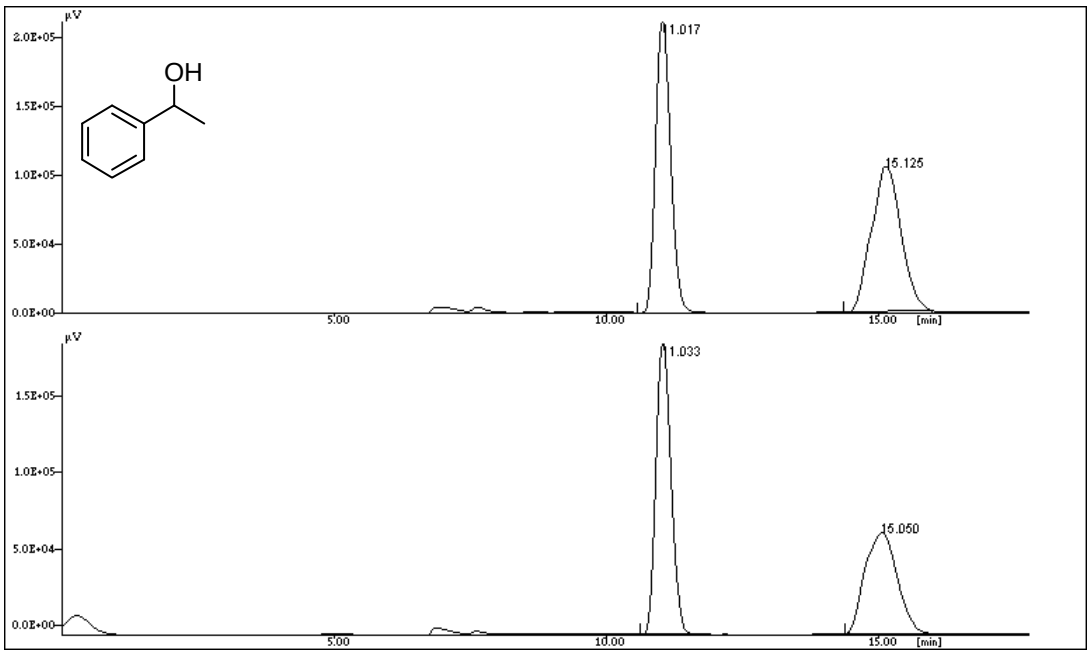

(**154a**) Benzoin

White solid. 35% yield. ^{1}H NMR (300 MHz, $CDCl_3$, ppm) ：δ 4.57 (d, 1H, J = 6.0Hz), 5.96 (d, 1H, J = 6.3Hz), 7.26-7.93 (m, 10H). LRMS (FAB) m/z 213.0 ($M+H^+$).

The ee determined by chiral HPLC; CHIRALPAK IA (4.6 mm i.d. x 250 mm); hexane/2-propanol 95/5; flow rate 1.0 ml/min; temp 25 °C; detection UV 230 nm; retention time: 40.0 min and 46.5 min.

(**155**) 4-Hydroxy-2-hydroxy -3a, 4, 9, 9a-tetrahydro-4, 9[1’, 2’]-benzeno-1*H*-benz[*f*]isoindole-1, 3(2*H*)-dione

White solid. mp 225.0 -225.9 ^{o}C. 92% yield. ^{1}H NMR (500 MHz, $(CD_3)_2CO$, ppm)：δ 3.14 (d, 1H, J = 8.8Hz), 3.34 (dd, 1H, J = 3.2, 8.2Hz), 4.76 (d, 1H, J = 3.2Hz), 7.13-7.66 (m, 8H). ^{13}C NMR (125 MHz, $(CD_3)_2CO$, ppm): δ 44.0, 44.7, 47.8, 76.9, 120.5, 121.0, 123.7, 124.5, 126.3, 126.5, 126.6, 126.8, 137.4, 139.9, 141.3, 144.0,

170.9, 171.2. IR (film): 1215.7, 1638.2, 3018.0, 3429.3 cm^{-1}. LRMS(ESI) m/z 306.2 ($M-H^+$), HRMS(ESI) m/z 330.0734 ($M+Na^+$), calc. for $C_{18}H_{13}NO_4Na$ 330.0742.

(**158a**) Methyl 2-hydroxy-3-(2-methyl-1,3-dioxolan-2-yl)propanoate

Colorless liquid. 60% yield. ^1H NMR (300 MHz, $CDCl_3$, ppm) ： δ 1.38 (s, 3H), 2.14 (dd, 1H, J = 7.6, 14.8Hz), 2.27 (dd, 1H, J = 3.3, 14.8Hz), 3.77 (s, 3H), 3.99 (m, 4H), 4.40 (m, 1H). LRMS(ESI) m/z 213.0 ($M+Na^+$)

(**158b**) Methyl 3-(1,3-dioxolan-2-yl)-2-hydroxypropanoate

Colorless liquid. 56% yield. ^1H NMR (300 MHz, $CDCl_3$, ppm)：δ 2.85 (dd, 1H, J = 6.3, 16.4Hz), 2.92 (dd, 1H, J = 4.4, 16.4Hz), 3.66 (s, 3H), 3.81 (m, 4H), 4.26 (m, 1H), 4.52 (t, 1H, J = 5.4Hz). LRMS(FAB) m/z 177.0 ($M+H^+$)

(**158c**) 2-Hydroxy-3-(2-methyl-1,3-dioxolan-2-yl)propanenitrile

Colorless liquid. 58% yield. ^1H NMR (500 MHz, $CDCl_3$, ppm)：δ 1.39 (s, 3H), 2.26 (dd, 1H, J = 5.7, 15.1Hz), 2.44 (dd, 1H, J = 7.6, 15.1Hz), 4.01 (m, 4H), 4.92 (dd, 1H, J = 5.6, 7.6Hz). LRMS(ESI) m/z 176.1 ($M+NH_4^+$)

(**158d**) 3-(1,3-Dioxolan-2-yl)-2-hydroxypropanenitrile

Colorless liquid. 52% yield. ^1H NMR (300 MHz, $CDCl_3$, ppm)：δ 2.21 (m, 1H), 2.32 (m, 1H), 3.67 (1H, d, 1H, J = 6.6Hz), 3.92-4.09 (m, 4H), 4.74 (dd, 1H, J = 3.8, 6.6Hz), 5.18 (dd, 1H, J = 3.5, 5.2Hz). LRMS(EI) m/z 142.1 ($M–H^+$)

(**160**) Dihydro-3-hydroxy-5,5-dimethyl-2(3*H*)-furanone

Colorless liquid. 65% yield. ^{1}H NMR (300 MHz, $CDCl_3$, ppm)：δ 1.39 (s, 3H), 1.50 (s, 3H), 2.04 (dd, 2H, J = 2.8, 9.1Hz), 2.50(dd, 1H, J = 8.7, 12.9Hz), 4.65 (t, 4H, J = 9.1). LRMS(FAB) m/z 147.1 ($M+NH_4^+$)

References

1 C. L. Hannon, E. V. Anslyn, *Bioorganic Chemistry Frontiers*, Springer-Verlag: Berlin, Heidelberg, **1993**, vol 3, 193–255.

2 Y. Yamamoto, S. Kojima, In *The Chemistry of Amidines and Imidates*; S. Patai, Z. Rappoport, Eds, John Wiley & Sons Inc.: New York, **1991**, vol 2, pp 485.

3 (a) E. van Aken, H. Wynberg, F. van Bolhuis, *J. Chem. Soc., Chem. Commun.* **1990**, 55–57; (b) E. van Aken, H. Wynberg, F. van Bolhuis, *J. Chem. Soc., Chem. Commun.* **1992**, 239–242; (c) E. van Aken, H. Wynberg, F. van Bolhuis, *J. Chem. Soc., Chem. Commun.* **1992**, 629–630; (d) E. van Aken, H. Wynberg, F. van Bolhuis, *Acta. Chem. Scand.* **1993**, *47*, 122–124.

4 R. Chinchilla, C. Nájera, P. Sánchez-Agulló, *Tetrahedron: Asymmetry* **1994**, *5*, 1393–1402.

5 D. Ma, Q. Pan, F. Han, *Tetrahedron Lett.* **2002**, *43*, 9401–9403.

6 M. S. Iyer, K. M. Gigstad, N. D. Namdev, M. Lipton, *J. Am. Chem. Soc.* **1996**, *118*, 4910–4911.

7 D. Ma, K. Cheng, *Tetrahedron: Asymmetry* **1999**, *10*, 713–719.

8 B. Peng, K. Cheng, D. Ma, *Chin. J. Chem.* **2000**, *18*, 411–413.

9 (a) T. Ishikawa, Y. Araki, T. Kumamoto, H. Seki, K. Fukuda, T. Isobe, *Chem. Commun.* **2001**, 245–246; (b) T. Ishikawa, T. Isobe, *Chem. Eur. J.* **2002**, *8*, 552–557; (c) T. Isobe, K. Fukuda, Y. Araki, T. Ishikawa, *Chem. Commun.* **2001**, 243–244.

10 J. C. McManus, T. Genski, J. S. Carey, R. J. K. Taylor, *Synlett* **2003**, 369–371.

11 M. Martín-Portugués, V. Alcázar, P. Prados, J. de Mendoza, *Tetrahedron* **2002**, *58*, 2951–2955.

12 M. T. Allingham, A. Howard-Jones, P. J. Murphy, D. A. Thomas, P. W. R. Caulkett, *Tetrahedron Lett.* **2003**, *44*, 8677–8680.

13 A. P. Davis, K. J. Dempsey, *Tetrahedron: Asymmetry* **1995**, *6*, 2829–2840.

14 E. J. Corey, M. J. Grogan, *Org. Lett.* **1999**, *1*, 157–160.

15 W. Ye, Z. Jiang, Y. Zhao, S. L. M. Goh, D. Leow, Y.-T. Soh, C.-H. Tan, *Adv. Synth. Catal.* **2007**, *349*, 2454–2458.

16 X. Fu, Z. Jiang, C.-H. Tan, *Chem. Commun.* **2007**, 5058–5060.

17 (a) M. Terada, H. Ube, Y. Yaguchi, *J. Am. Chem. Soc.* **2006**, *128*, 1454–1455; (b) M. Terada, M. Nakano, H. Ube, *J. Am. Chem. Soc.* **2006**, *128*, 16044–16045; (c) M. Terada, T. Ikehara, H. Ube, *J. Am. Chem. Soc.* **2007**, *129*, 14112–14113.

18 T. Kita, A. Georgieva, Y. Hashimoto, T. Nakata, K. Nagasawa, *Angew. Chem. Int. Ed.* **2002**, *41*, 2832–2834.

19 (a) Y. Sohtome, N. Takemura, T. Iguchi, Y. Hashimoto, K. Nagasawa, *Synlett* **2006**, 144–146; (b) Y. Sohtome, Y. Hashimoto, K. Nagasawa, *Adv. Synth. Catal.* **2005**, *347*, 1643–1648.

20 Recent reviews of enantioselective Diels–Alder reaction, see: (a) H. B. Kagan, O. Riant, *Chem. Rev.* **1992**, *92*, 1007–1019; (b) D. A. Evans, J. S. Johnson, in: E. N. Jacobsen, A. Pfaltz, H. Yamamoto (Eds.), *Comprehensive Asymmetric Catalysis*, Vol. 3, Springer, New York, **1999**; (c) E. J. Corey, *Angew. Chem., Int. Ed.* **2002**, *41*, 1650–1667.

21 For the original work on the Diels–Alder reaction, see: (a) O. Diels, K. Alder, *Justus Liebigs Ann. Chem.* **1926**, *450*, 237–254; (b) O. Diels, K. Alder, *Justus Liebigs Ann. Chem.* **1927**, *460*, 98–122.

22 K. C. Nicolaou, Scott. A. Snyder, T. Montagnon, G. Vassilikogiannakis, *Angew. Chem., Int. Ed*. **2002**, *41*, 1668–1698.

23 Reviews on enantioselective organocatalysis: (a) P. I. Dalko, L. Moisan, *Angew. Chem. Int. Ed*. **2001**, *40*, 3726–3748; (b) P. I. Dalko, L. Moisan, *Angew. Chem, Int. Ed*. **2004**, *43*, 5138–5175; (c) *Acc. Chem. Res.* **2004**, *37*, 487–631, ed. K. N. Houk, B. List, special issue on organocatalysis; (d) *Adv. Synth. Catal*. **2004**, *346*, 1021–1249, ed. B. List, C. Bolm, Special issue on organocatalysis; (e) J. Seayad, B. List, *Org. Biomol. Chem.* **2005**, *3*, 719–724; (f) A. Berkessel, H. Gröger, *Asymmetric Organocatalysis*, Wiley-VCH, Weinheim, **2005**; (g) B. List, *Chem. Commun.* **2006**, 819–824; (h) B. List, J. W. Yang, *Science* **2006**, *313*, 1584–1586; (i) P. I. Dalko, *Enantioselective Organocatalysis*, Wiley-VCH, Weinheim, 2007.

24 (a) H. Okamura, T. Iwagawa, M. Nakatani, *Tetrahedron Lett.* **1995**, *36*, 5939–5942; (b) H. Okamura, Y. Nakamura, T. Iwagawa, M. Nakatani, *Chem. Lett.* **1996**, 193–194; (c) H. Okamura, H. Nagaike, T. Iwagawa, M. Nakatani, *Tetrahedron Lett*. **2000**, *41*, 4147–4150.

25 Y. Wang, H. Li, Y.-Q. Wang, Y. Liu, B. M. Foxman, L. Deng, *J. Am. Chem. Soc*. **2007**, *129*, 6364–6365.

26 (a) H. Okamura, K. Morishige, T. Iwagawa, M. Nakatani, *Tetrahedron Lett*. **1998**, *39*, 1211–1214; (b) H. Shimizu, H. Okamura, N. Yamashita, T. Iwagawa, M. Nakatani, *Tetrahedron Lett*. **2001**, *42*, 8649–8651; (c) T. Kamikubo, K. Ogasawara, *Tetrahedron Lett*. **1995**, *36*, 1685–1688.

27 H. Nagasawa, A. Suzuki, S. Tamura, *Agric. Biol. Chem.* **1978**, *42*, 1303–1304.

28 (a) K. Nakamori, H. Matsuura, T. Yoshihara, A. Ichihara, Y. Koda, *Phytochemistry* **1994**, *35*, 835–839; (b) T. Yoshihara, F. Ohmori, K. Nakamori, M. Amanuma, T. Tsutsumi, A. Ichihara, H. Matsuura, *J. Plant Growth Regul.* **2000**, *19*, 457–461.

29 H. Okamura, H. Nagaike, T. Iwagawa, M. Nakatani, *Tetrahedron Lett*. **2000**, *41*, 8317–8321.

30 (a) S. Horii, T. Iwasa, E. Mizuta, Y. Kameda, *J. Antibiot.* **1971**, *24*, 59–63; (b) T. Iwasa, H. Yamamoto, M. Shibata, *J. Antibiot.* **1970**, *23*, 595–602; (c) K. Kamiya, Y. Wada, S. Horii, M. Nishikawa, *J. Antibiot.* **1971**, *24*, 317–318.

31 H. Okamura, H. Nagaike, N. T. Kipassa, T. Iwagawa, M. Nakatani, *Heterocycles* **2006**, *68*, 2587–2594.

32 P. A. Reece, *J. Med. Virol.* **2007**, *79*, 1577–1586.

33 Y.-Y. Yeung, S. Hong, E. J. Corey, *J. Am. Chem. Soc.* **2006**, *128*, 6310–6311.

34 N. T. Kipassa, H. Okamura, K. Kina, T. Hamada, T. Iwagawa, *Org. Lett.* **2008**, *10*, 815–816.

35 (a) M. Koerner, B. Rickborn, *J. Org. Chem*. **1989**, *54*, 6–9; (b) M. Koerner, B. Rickborn, *J. Org. Chem*. **1990**, *55*, 2662–2672.

36 (a) O. Riant, H. B. Kagan, *Tetrahedron Lett*. **1989**, *30***,** 7403–7406; (b) O. Riant, H. B. Kagan, L. Ricard, *Tetrahedron*, **1994** *50*, 4543–4554.

37 (a) K. Tokioka, S. Masuda, T. Fujii, Y. Hata, Y. Yamamoto, *Tetrahedron: Asymmetry* **1997**, *8*, 101–107; (b) K. Uemae, S. Masuda, Y. Yamamoto, *J. Chem. Soc., Perkin Trans. I* 2001, 1002–1006.

38 a) A. Sanyal, Q. Yuan, J. K. Snyder, *Tetrahedron Lett.* **2005**, *46*, 2475–2478; (b) K. L. Burgess, N. J. Lajkiewicz, A. Sanyal, W. Yan, J. K. Snyder, *Org. Lett.* **2005**, *7*, 31–34.

39 (a) K. Müller, H. Prinz, I. Gawlik, K. Ziereis, H.-S. Huang, *J. Med. Chem.* **1997**, *40*, 3773–3780; (b) K. Müller, H. Reindl, K. Breu, *J. Med. Chem.* **2001**, *44*, 814–821; (c) F. Diaz, H.-B. Chai, Q. Mi, B.-N. Su, J. S. Vigo, J. G. Graham, F. Cabieses, N. R. Farnsworth, G. A. Cordell, J. M. Pezzuto, S. M. Swanson, A. D. Kinghorn, *J. Nat. Prod.* **2004**, *67*, 352–356.

40 (a) H. Prinz, W. Wiegrebe, K. Müller, *J. Org. Chem.* **1996**, *61*, 2853–2856; (b) T. R. Criswell, B. H. Klanderman, *J. Org. Chem.* **1974,** *39*, 770–774; (c) N. Shyamasundar, P. Caluwe, *J. Org. Chem.* **1981**, *46*, 1552–1557; (d) N. Shyamasundar, P. Caluwe, *J. Org. Chem.* **1981**, *46*, 809–811; (e) H. O. House, N. I. Ghali, J. L. Hack, D. VanDerveer, *J. Org. Chem.* **1980**, *45*, 1807–1817; (f) M. R. Fielding, R. Grigg, V. Sridharan, M. Thornton-Pett, C. J. Urch, *Tetrahedron* **2001**, *57*, 7737-7748; (g) Z. Y. Wang, *Syn. Comm.* **1990**, *20*, 1607-1610.

41 (a) A. K. Ghosh, P. Mathivanan, J. Cappiello, *Tetrahedron: Asymmetry* **1998**, *9*, 1–45; (b) G. Helmchen, A. Pfaltz, *Acc. Chem. Res.* **2000**, *33*, 336–345; (c) O. B. Sutcliffe, M. R. Bryce, *Tetrahedron: Asymmetry* **2003**, *14*, 2297–2325; (d) H. A. McManus, P. J. Guiry, *Chem. Rev.* **2004**, *104*, 4151–4202.

42 (a) K. A. Ahrendt, C. J. Borths, D. W. C. MacMillan, *J. Am. Chem.Soc.* **2000**, *122*, 4243–4244; (b) W. S. Jen, J. J. M. Wiener, D. W. C. MacMillan, *J. Am. Chem. Soc.* **2000**, *122*, 9874–9875; (c) N. A. Paras, D. W. C. MacMillan, *J. Am. Chem. Soc.* **2001**, *123*, 4370–4371.

43 (a) N. Halland, R. G. Hazell, K. A. Jøgensen, *J. Org. Chem.* **2002**, *67*, 8331–8338; (b) N. Halland, P. S. Aburel, K. A. Jøgensen, *Angew. Chem. Int. Ed.* **2003**, *42*,

661–665; (c) N. Halland, T. Hansen, K. A. Jøgensen, *Angew. Chem. Int. Ed.* **2003**, *42*, 4955–4957.

44 W. Ye, D. Leow, S. L. M. Goh, C.-T. Tan, C.-H. Chian, C.-H. Tan, *Tetrahedron Lett.* **2006**, *47*, 1007–1010

45 a) W. McCoull, F. A. Davis, *Synthesis* **2000**, *10*, 1347–1365; (b) D. Tanner, *Angew. Chem. Int. Ed.* **1994**, *33*, 599–619.

46 M. B. Berry, D. Craig, *Synlett* **1992**, 41–44.

47 (a) B. M. Kim, S. M. So, H. J. Choi, *Org. Lett.* **2002**, *4*, 949–952; (b) J. E. W. Scheuermann, G. Ilyashenko, D. V. Grioffiths, M. Watkinson, *Tetrahedron: Asymmetry* **2002**, *13*, 269–272; (c) F. Lake, C. Moberg, *Eur. J. Org. Chem.* **2002**, *18*, 3179–3188; (d) M. Cernerud, A. Skrinning, I. Bérgère, C. Moberg, *Tetrahedron: Asymmetry* **1997**, *8*, 3437–3441.

48 Regiochemistry was determined by X-ray crystallographic analysis of *rac*-**21m-1**, *rac*-**21o-1**, and *rac*-**132b**.

49 W. Ye, J. Xu, C.-T. Tan, C.-H. Tan, *Tetrahedron Lett.* **2005**, *46*, 6875–6878.

50 Mechanistic studies of thiourea-catalyzed reactions: (a) P. Vachal, E. N. Jacobsen, *J. Am. Chem. Soc.* **2002**, 1*24*, 10012–10014; (b) T. Okino, Y. Hoashi, T. Furukawa, X. Xu, Y. Takemoto, *J. Am. Chem. Soc.* **2005**, 1*27*, 119–125; (c) A. Hamza, G. Schubert. T. Soó, I. Pápai, *J. Am. Chem. Soc.* **2006**, 1*28*, 13151–13160; (d) D. A. Yalalov, S. B. Tsogoeva, S. Schmatz, *Adv. Synth. Catal.* **2006**, *348*, 826–832; (e) S. J. Zuend, E. N. Jacobsen, *J. Am. Chem. Soc.* **2007**, 1*29*, 15872–15883; (f) P. Hammar, T. Marcelli, H. Hiemstra, F. Himo, *Adv. Synth. Catal.* **2007**, *349*, 2537–2548.

51 Mechanistic studies of proline-catalyzed reactions: (a) S. Bahmanyar, K. N. Houk, *J. Am. Chem. Soc.* **2001**, 1*23*, 11273–11283; (b) S. Bahmanyar, K. N. Houk, *J. Am. Chem. Soc.* **2001**, 1*23*, 12911–12912; (c) L. Hoang, S. Bahmanyar, K. N. Houk, B. List, *J. Am. Chem. Soc.* **2003**, 1*25*, 16–17; (d) S. Bahmanyar, K. N. Houk, H. J. Martin, B. List, *J. Am. Chem. Soc.* **2003**, 1*25*, 2475–2479; (e) S. Bahmanyar, K. N. Houk, *Org. Lett.* **2003**, *5*, 1249–1251; (f) F. R. Clemente, K. N. Houk, *Angew. Chem. Int. Ed.*. **2004**, *43*, 5766–5768; (g) C. Allemann, R. Gordillo, F. R. Clemente, P. H. Cheong, K. N. Houk, *Acc. Chem. Res.* **2004**, *37*, 558–569; (h) B. List, L. Hoang, H. J. Martin, *Proc. Natl. Acad. Sci. U.S.A.* **2004**, *101*, 5839–5842; (i) F. R. Clemente, K. N. Houk, *J. Am. Chem. Soc.* **2005**, 1*27*, 11294–11302; (j) A. Fu, B. List, W. Thiel, *J. Org. Chem.* **2006**, *71*, 320–326; (k) C. B. Shinisha, R. B. Sunoj, *Org. Biomol. Chem.* **2007**, *5*, 1287–1294.

52 Mechanistic studies of phosphoramide-catalyzed reactions: (a) S. E. Denmark, J. Fu, *J. Am. Chem. Soc.* **2000**, 1*22*, 12021–12022; (b) S. E. Denmark, T. Bui, *J. Org. Chem.* **2005**, *70*, 10393–10399; (c) S. E. Denmark, J. Fu, D. M. Coe, X. Su, N. E. Pratt, B. D. Griedel, *J. Org. Chem.* **2006**, *71*, 1513–1522; (d) S. E. Denmark, S. M. Pham, R. A. Stavenger, X. Su, K. T. Wong, Y. Nishigaichi, *J. Org. Chem.* **2006**, *71*, 3904–3922.

53 (a) K. A. Ahrendt, C. J. Borths, D. W. C. MacMillan, *J. Am. Chem. Soc.* **2000**, *122*, 4243–4244; (b) W. S. Jen, J. J. M. Wiener, D. W. C. MacMillan, *J. Am. Chem. Soc.* **2000**, *122*, 9874–9875; (c) N. A. Paras, D. W. C. Macmillan, *J. Am. Chem. Soc.* **2001**, 123, *4370–4371*; (d) J. F. Austin, D. W. C. Macmillan, *J. Am.*

54 Mechanistic studies of imidazolidinone -catalyzed reactions: (a) R. Gordillo, K. N. Houk, *J. Am. Chem. Soc.* **2006**, *128*, 3543–3553; (b) A. B. Northrup, D. W. C. MacMillan, *J. Am. Chem. Soc.* **2002**, *124*, 2458–2460.

55 For review, see: (a) Y. Takemoto, *Org. Biomol. Chem.* **2005**, *3*, 4299–4306; (b) M. S. Taylor, E. N. Jacobsen, *Angew. Chem. Int. Ed.* **2006**, *45*, 1520–1543; (c) S. J. Connon, *Chem. Eur. J.* **2006**, *12*, 5418–5427; (d) A. G. Doyle, E. N. Jacobsen, *Chem. Rev.* **2007**, *107*, 5713–5743.

56 Primary amino-thioureas: (a) M. P. Lalonde, Y. Chen, E. N. Jacobsen, *Angew. Chem. Int. Ed.* **2006**, *45*, 6366–6370 and refs cited therein. Secondary amino-thioureas: (b) T. P. Yoon, E. N. Jacobsen, *Angew. Chem. Int. Ed.* **2005**, *44*, 466–468; Sulfinamino thioureas: (c) K. L. Tan, E. N. Jacobsen, *Angew. Chem. Int. Ed.* **2007**, *46*, 1315–1317; Hydroxyl thioureas: (d) R. P. Herrera, V. Sgarzani, L.

Bernardi, A. Ricci, *Angew. Chem. Int. Ed.* **2005**, *44*, 6576–6579; Amino-hydrocyl thioureas: (e) Y. Yamaoka, H. Miyabe, Y. Takemoto, *J. Am. Chem. Soc.* **2007**, *129*, 6686–6687; Guanidino thioureas: (f) Y. Sohtome, Y. Hashimoto, K. Nagasawa, *Adv. Synth. Catal.* **2005**, *347*, 1643–1648.

57 (a) C. L. Hannon, E. V. Anslyn, *Bioorganic Chemisty Frontiers*; Springer-Verlag: Berlin, 1993, Vol. 3, pp 193–255; (b) F. P. Schmidtchen, M. Berger, *Chem. Rev*. **1997**, *97*, 1609–1646.

58 (a) A. Gleich, F. R. Schmidtchen, P. Mikulcik, G. Müller, *J. Chem. Soc., Chem. Commun.* **1990**, 55–57; (b) E. van Aken, H. Wynberg, F. van Bolhuis, *J. Chem. Soc., Chem. Commun.* **1992**, 239–242; (c) E. van Aken, H. Wynberg, F. van Bolhuis, *J. Chem. Soc., Chem. Commun.* **1992**, 629–630; (d) E. van Aken, H. Wynberg, F. van Bolhuis, *Acta. Chem. Scand.* **1993**, *47*, 122–124.

59 (a) M. S. Iyer, K. M. Gigstad, N. D. Namdev, M. Lipton, *J. Am. Chem. Soc*. **1996**, *118*, 4910–4911; b) E. J. Corey, M. J. Grogan, *Org. Lett.* **1999**, *1*, 157–160; c) T. Ishikawa, Y. Araki, T. Kumamoto, H. Seki, K. Fukuda, T. Isobe, *Chem. Commun.* **2001**, 245–246; d) T. Kita, A. Georgieva, Y. Hashimoto, T. Nakata, K. Nagasawa, *Angew. Chem. Int. Ed.* **2002**, *114*, 2956–2958; (e) T. Kita, A. Georgieva, Y. Hashimoto, T. Nakata, K. Nagasawa, *Angew. Chem. Int. Ed.* **2002**, *41*, 2832–2834; (f) T. Ishikawa, T. Isobe, *Chem. Eur. J.* **2002**, *8*, 553–557; (g) M. T. Allingham, A. Howard-Jones, P. J. Murphy, D. A. Thomas, P. W. R. Caulkett, *Tetrahedron Lett.* **2003**, *44*, 8677–8680; (h) Y. Sohtome, Y. Hashimoto, K. Nagasawa, *Adv. Synth. Catal.* **2005**, *347*, 1643–1648; (i) M. Terada, H. Ube, Y.

Yaguchi *J. Am. Chem. Soc.* **2006**, *128*, 1454–1455; (j) M. Terada, M. Nakano, H. Ube, *J. Am. Chem. Soc.* **2006**, *128*, 16044–16045; (k) M. Terada, T. Ikehara, H. Ube, *J. Am. Chem. Soc.* **2007**, *129*, 14112–14113; Contributions from our group, see: (l) W. Ye, D. Leow, S. L. M. Goh, C.-T. Tan, C.-H. Chian, C.-H. Tan, *Tetrahedron Lett.* **2006**, *47*, 1007–1010; (m) J. Shen, T. T. Nguyen, Y.-P. Goh, W. Ye, X. Fu, J. Xu, C.-H. Tan, *J. Am. Chem. Soc.* **2006**, *128*, 13692–13693; (n) X. Fu, Z. Jiang, C.-H. Tan, *Chem. Commun.* **2007**, 5058–5060; (o) W. Ye, Z. Jiang, Y. Zhao, S. L. M. Goh, D. Leow, Y.-T. Soh, C.-H. Tan, *Adv. Synth. Catal.* **2007**, *349*, 2454–2458.

60 (a) H. Okamura, H. Nagaike, T. Iwagawa, M. Nakatani, *Tetrahedron Lett*. **2000**, *41*, 8317–8321; (b) H. Okamura, T. Iwagawa, M. Nakatani, *Tetrahedron Lett.* **1995**, *36*, 5939–5942.

61 T. Okino, Y. Hoashi, Y. Takemoto, *J. Am. Chem. Soc.* **2003**, *125*, 12672–12673.

62 (a) Y. Ishii, S. Sakaguchi, T. Iwahama, *Adv. Synth. Catal.* **2001**, *343*, 379–427; (b) F. Recupero, C. Punta, *Chem. Rev.* **2007**, *107*, 3800–3842.

63 (a) R. Arnaud, A. Milet, C. Adamo, D. Einhorn, J. Einhorn, *J. Chem. Soc., Perkin Trans. 2* **2002**, 1967–1972; (b) R. Amorati, M. Lucarini, V. Mugnaini, G.-F. Pedulli, F. Minisci, F. Recupero, F. Fontana, P. Astolfi, L. Greci, *J. Org. Chem.* **2003**, 68, 1747–1754; (c) N. Koshino, B. Saha, J. H. Espenson, *J. Org. Chem.* **2003**, *68*, 9364–9370; (d) N. Koshino, Y. Cai, J. H. Espenson, *J. Phys. Chem. A* **2003**, *107*, 4262–4267; (e) B. Saha, N. Koshino, J. H. Espenson, *J. Phys. Chem. A* **2004**, *108*, 425–431.

64 (a) C. Einhorn, J. Einhorn, C. Marcadal-Abbadi, J.-L. Pierre, *J. Org. Chem.* **1999**, *64*, 4542–4546; (b) M. Nechab, D. N. Kumar, C. Philouze, C. Einhorn, J. Einhorn, *Angew. Chem, Int. Ed.* **2007**, *46*, 3080–3083.

65 J. Shen, T. T. Nguyen, Y.-P. Goh, W. Ye, X. Fu, J. Xu, C.-H. Tan, *J. Am. Chem. Soc.* **2006**, *128*, 13692–13693.

66 H. Prinz, W. Wiegrebe, K. Müller, *J. Org. Chem.* **1996**, *61*, 2853–2856.

67 M. Akiyama, K. Shimizu, S. Aiba, F. Banba, *J. Chem. Soc., Perkin Trans. I* **1980**, 2122–2125.

68 (a) Y. Ishii, K. Nakayama, M. Takeno, S. Sakaguchi, T. Iwahama, Y. Nishiyama, *J. Org. Chem.* **1995**, *60*, 3934–3935; (b) C. Einhorn, J. Einhorn, C. Marcadal, J. L. Pierre, *Chem. Commun.* **1997**, 447–448; (c) M. Nechab, C. Einhorn, J. Einhorn, *Chem. Commun.* **2004**, 1500–1501; (d) G. Yang, Q. Zhang, H. Miao, X. Tong, J. Xu, *Org. Lett.* **2005**, *7*, 263–266.

69 (a) T. Iwahama, S. Sakaguchi, Y. Nishiyama, Y. Ishii, *Tetrahedron Lett.* **1995**, *36*, 6923–6926; (b) T. Iwahama, Y. Yoshino, T. Keitoku, S. Sakaguchi, Y. Ishii, *J. Org. Chem.* **2000**, *65*, 6502–6507; (c) F. Rajabi, B. Karimi, *J. Mol. Catal. A* **2005**, *232*, 95–99.

70 C.-H. Jun, J.-B. Hong, D.-Y. Lee, *Synlett* **1999**, *1*, 1–12.

71 C. Chatgilialoglu, D. Crich, M. Komatsu, I. Ryu, *Chem. Rev.* **1999**, *99*, 1991–2070.

72 T. Punniyamurthy, B. Bhatia, J. Iqbal, *J. Org. Chem.* **1994**, *59*, 850–853

73 (a) H.-S. Dang, B. P. Roberts, *Tetrahedron Lett.* **1999**, *40*, 8929–8933; (b) A.

Gross, L. Fensterbank, S. Bogen, R. Thouvenot, M. Malacria, *Tetrahedron* **1997**, *53*, 13797–13810.

74 (a) K. Hirano, T. Iwahama, S. Sakaguchi, Y. Ishii, *Chem. Commun.* **2000**, 2457–2458; (b) T. Kagayama, S. Sakaguchi, Y. Ishii, *Tetrahedron Lett.* 2005, *46*, 3687–3689

75 (a) Y. S. Rao, Chem. *Rev.* **1976**, *76*, 625–694; (b) H. M. R. Hoffman, J. Rabe, *Angew. Chem. Int. Ed.* **1985**, *24*, 94–110.

76 T. Iwahama, S. Sakaguchi, Y. Ishii, *Chem. Commun.* **2000**, 613–614.

77 A.P. Davis, K. J. Dempsey, *Tetrahedron: Asymmetry*, **1995**, *6*, 2829.

Appendices

(21b)

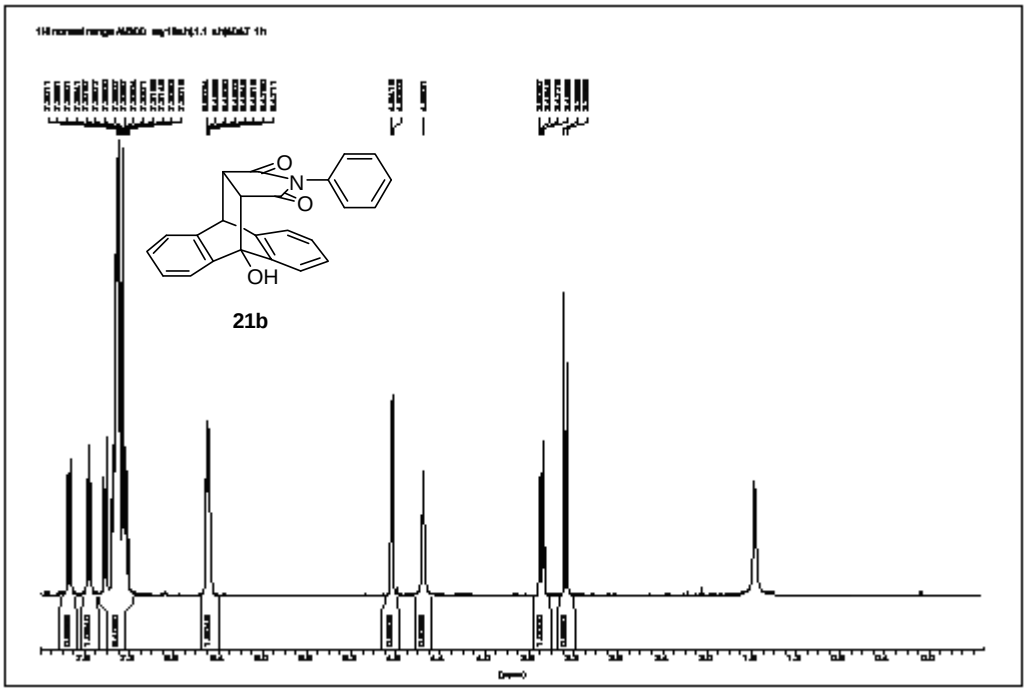

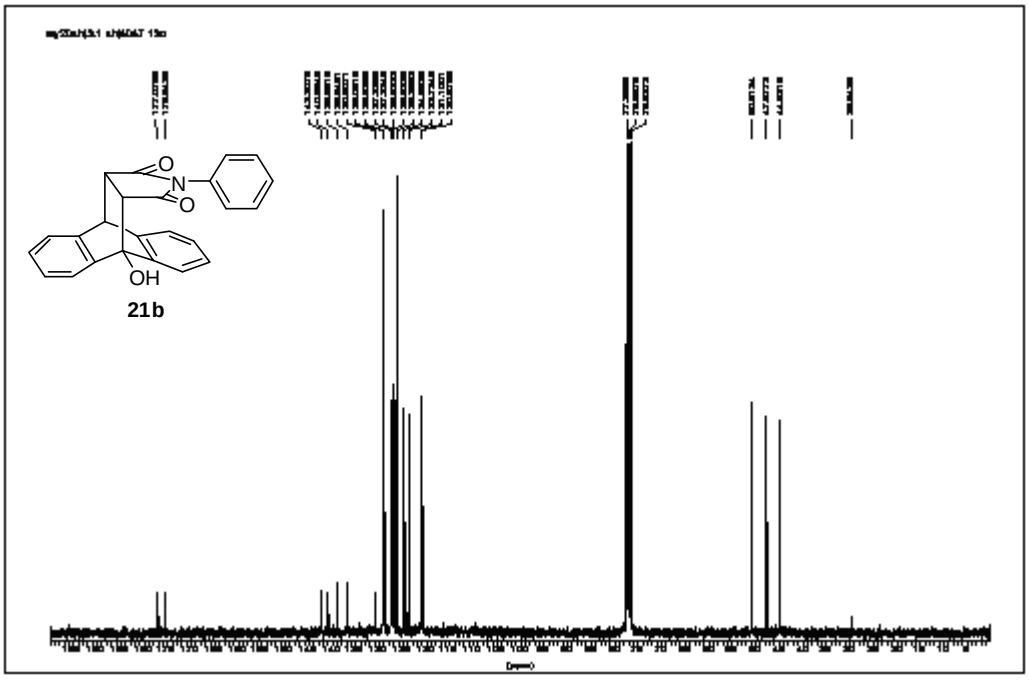

(**21c**)

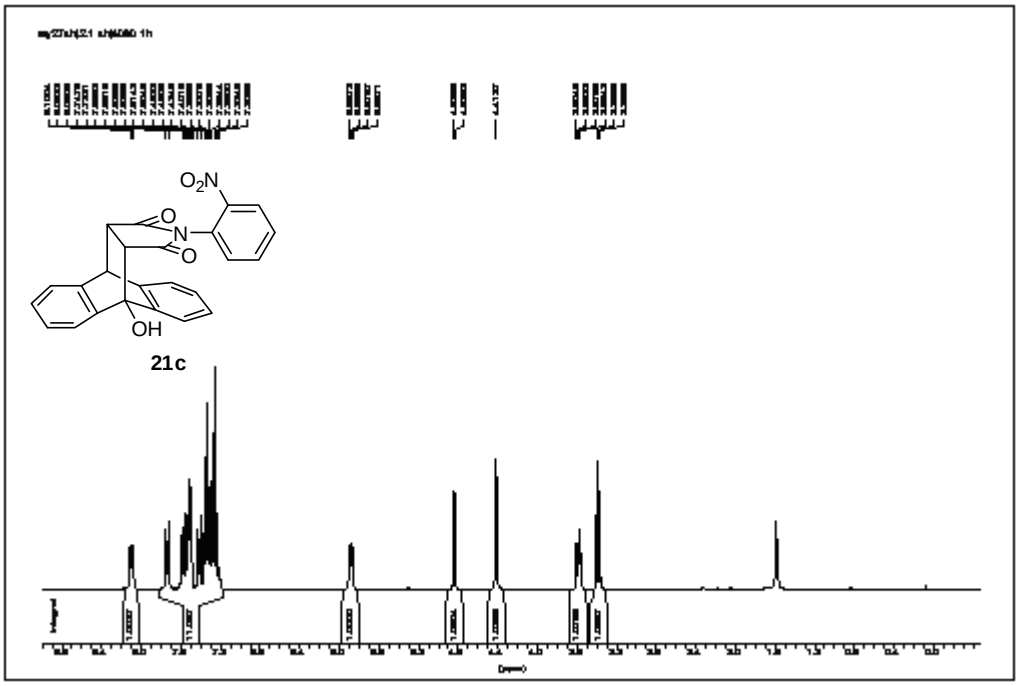

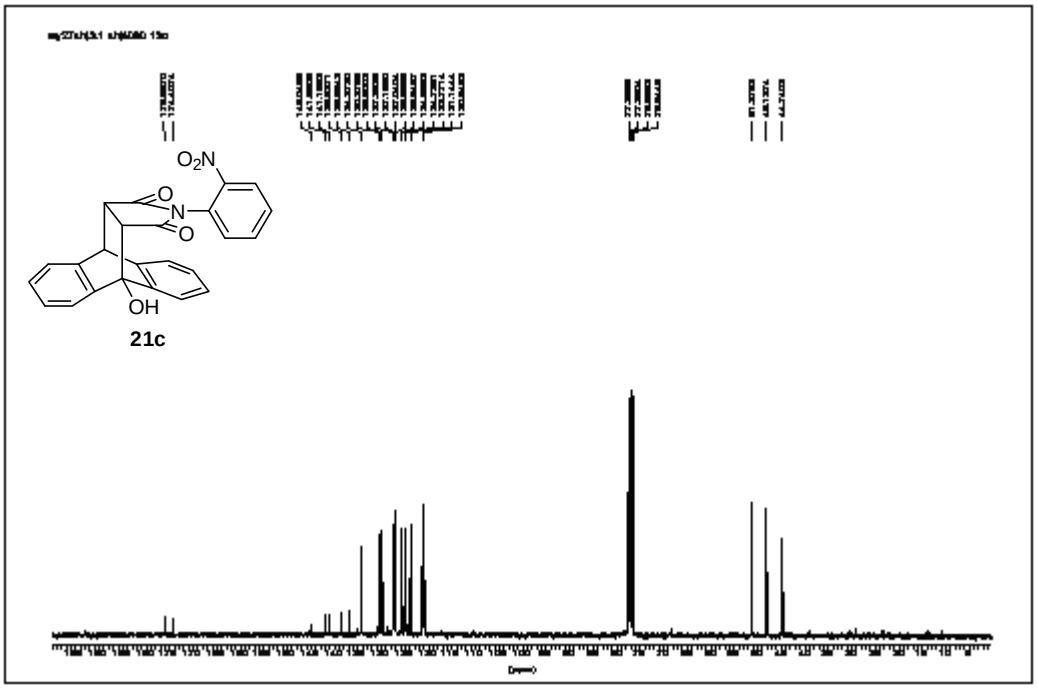

(21d)

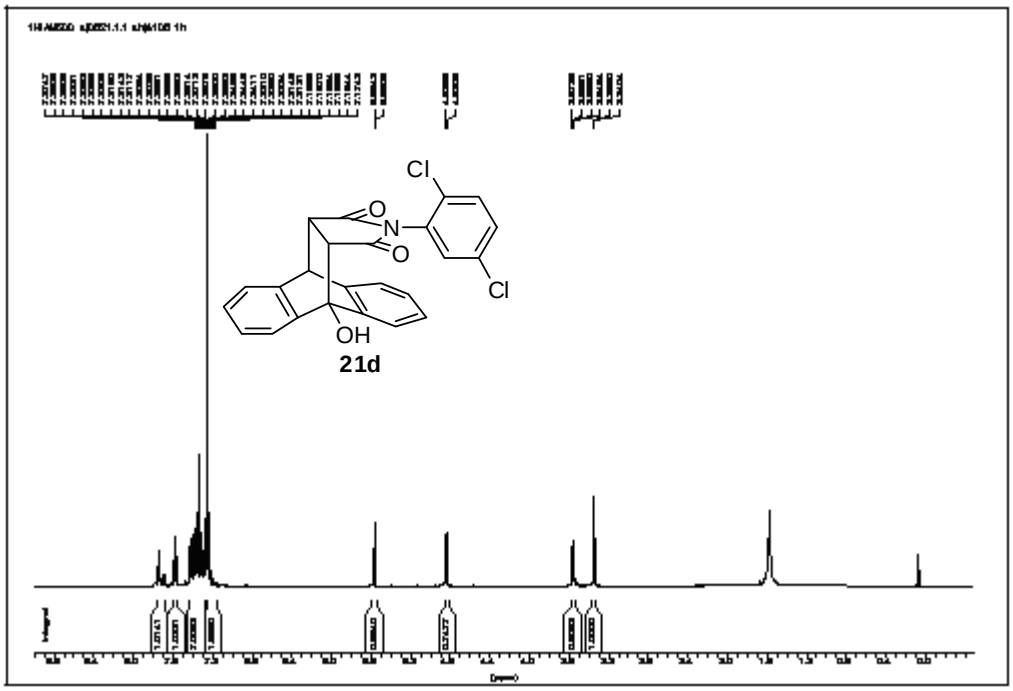

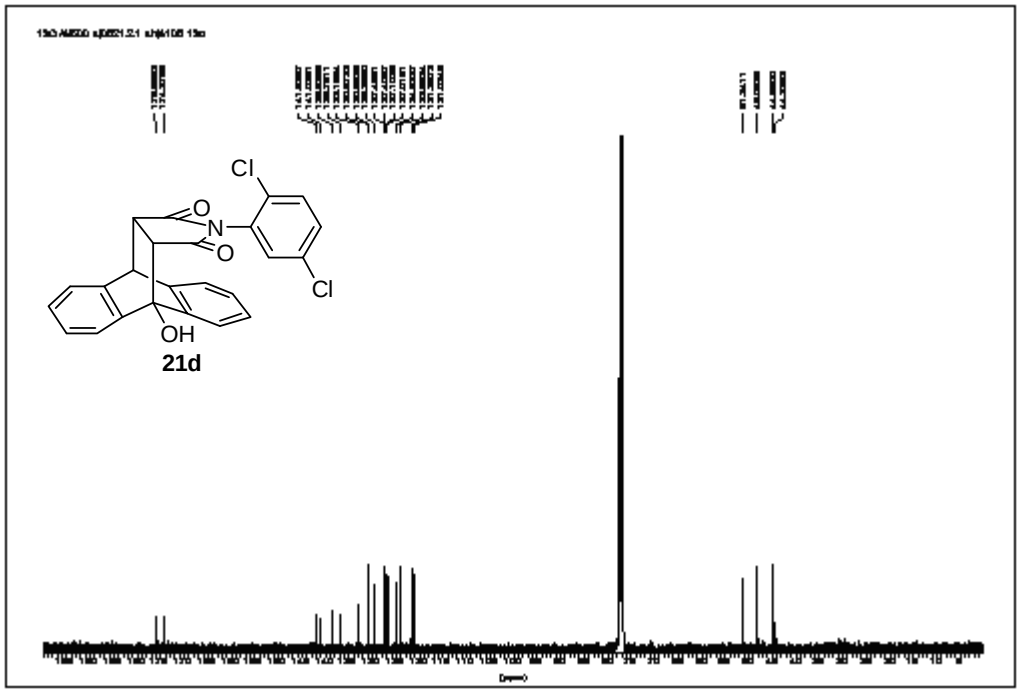

(**21e**)

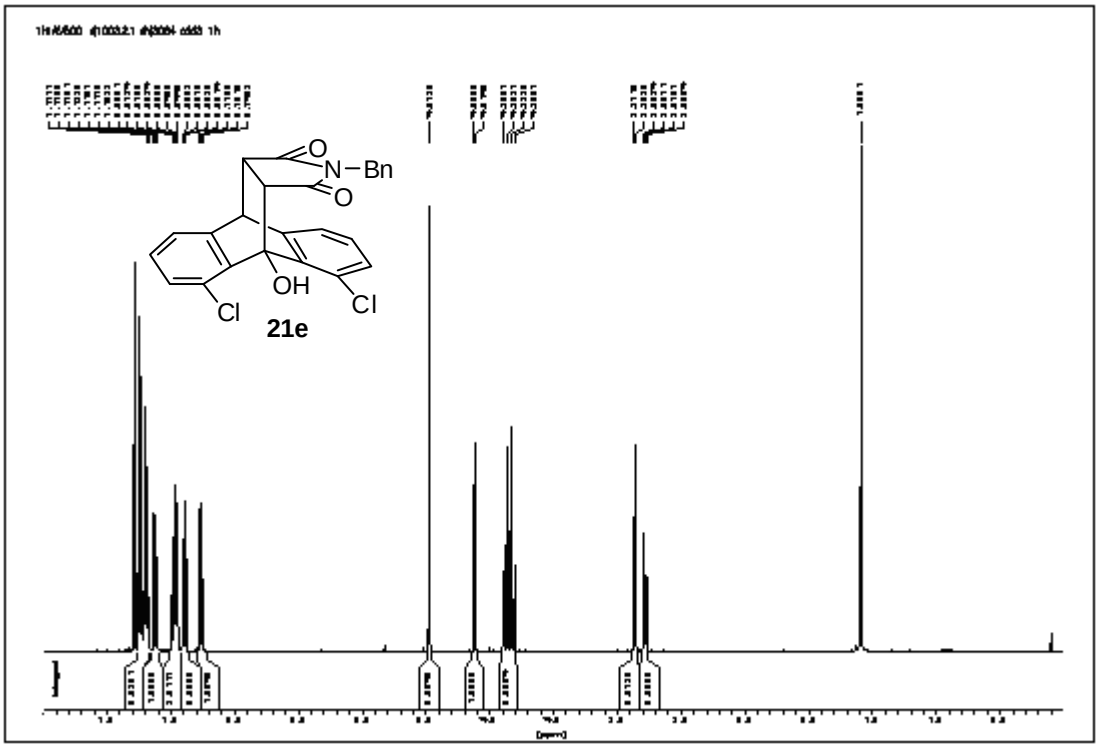

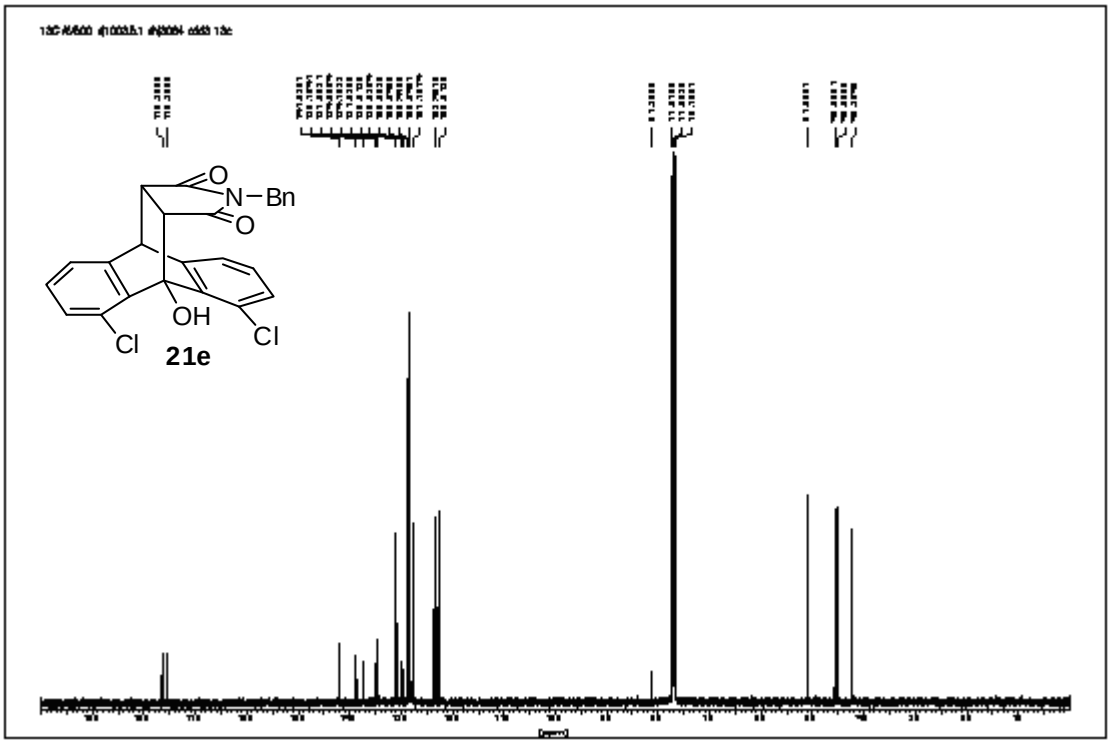

(21f)

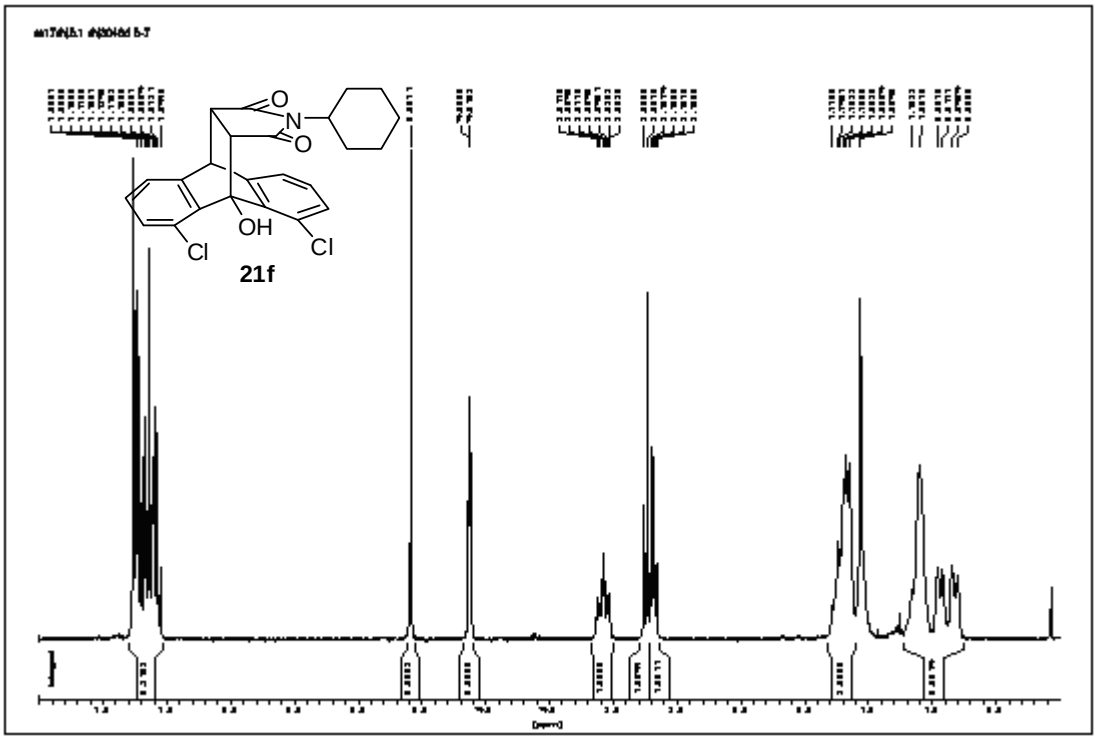

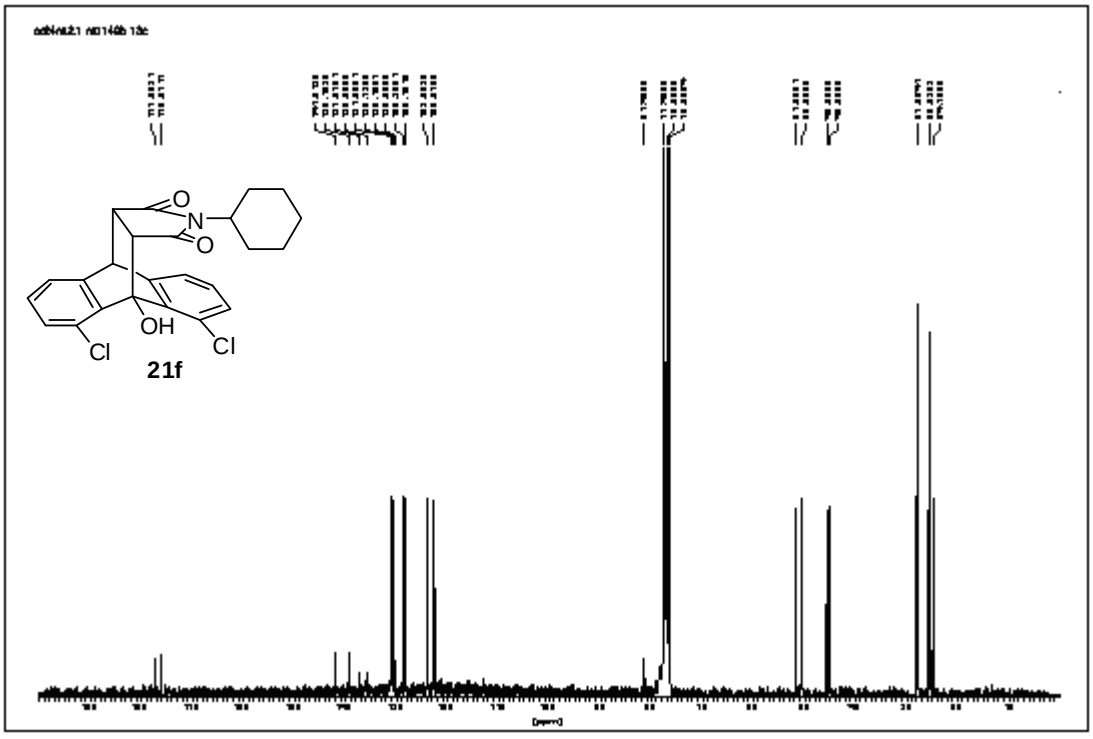

(**21g**)

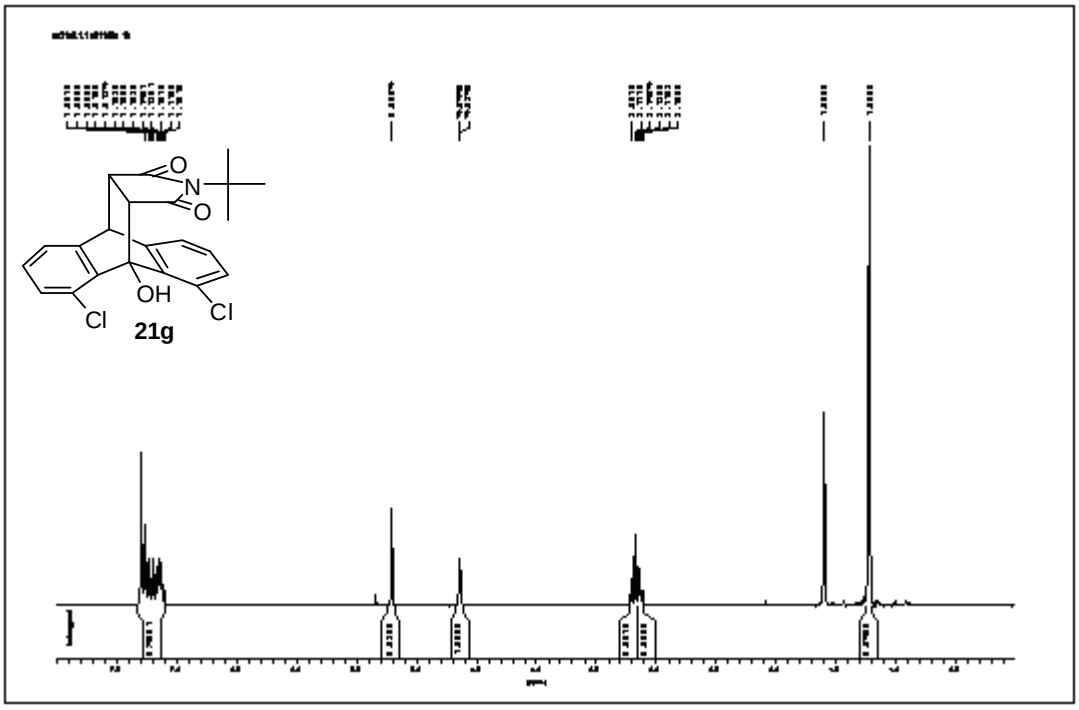

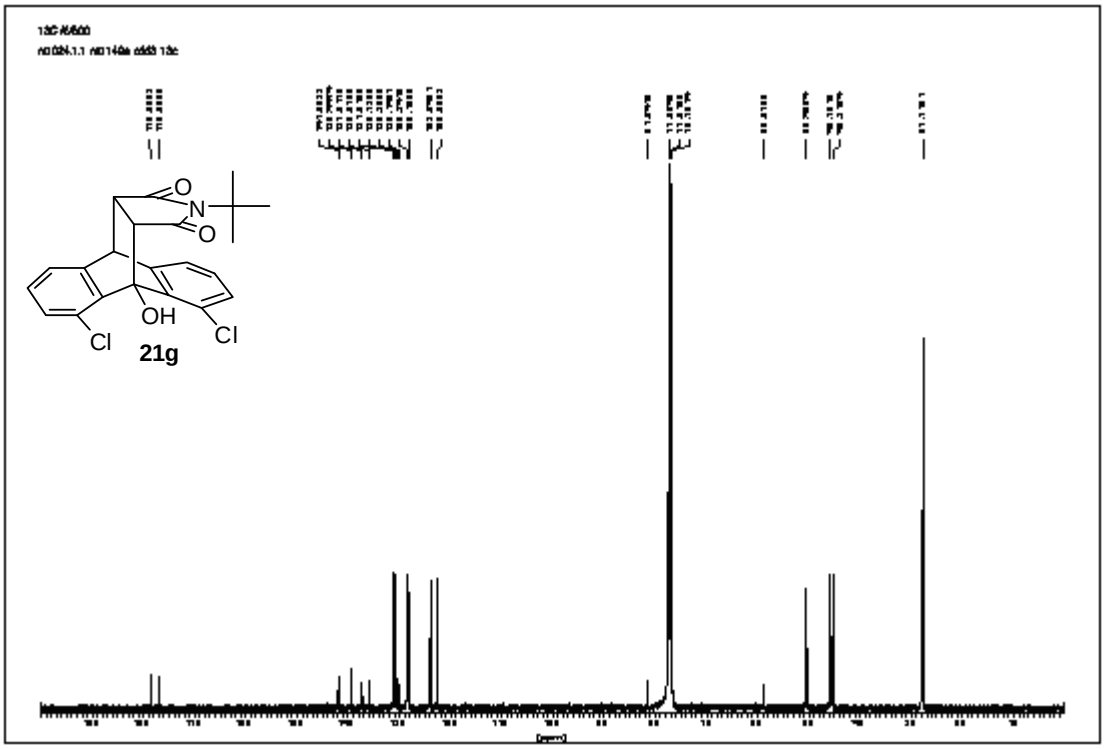

(21h)

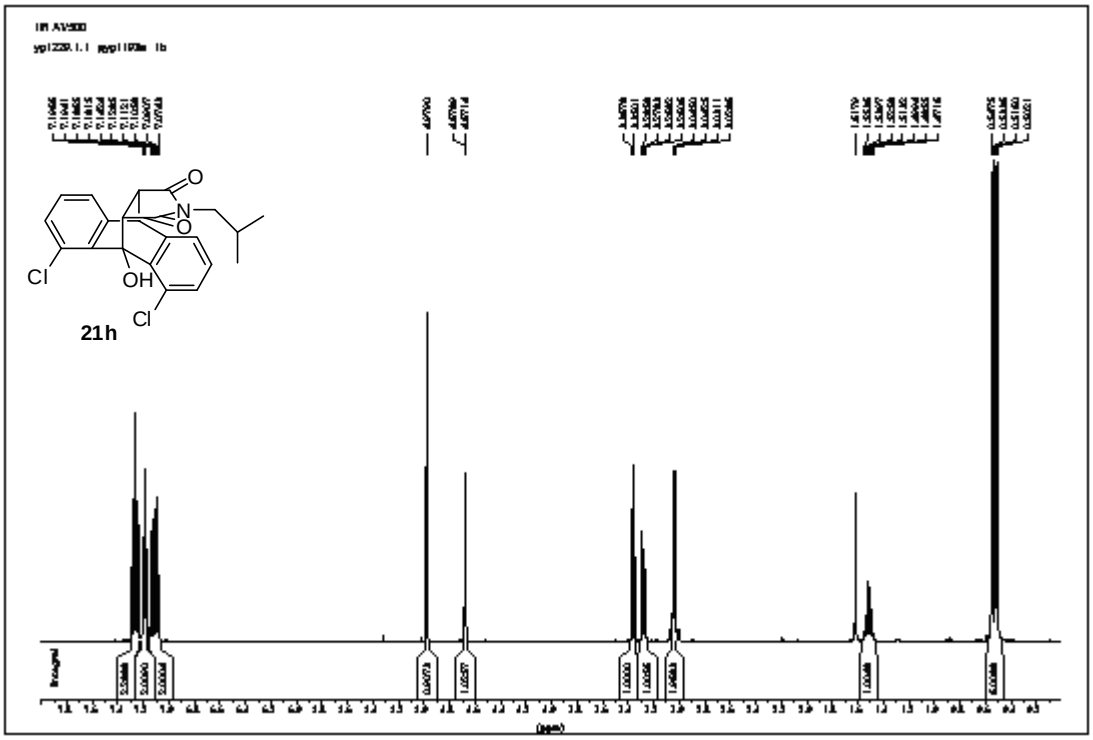

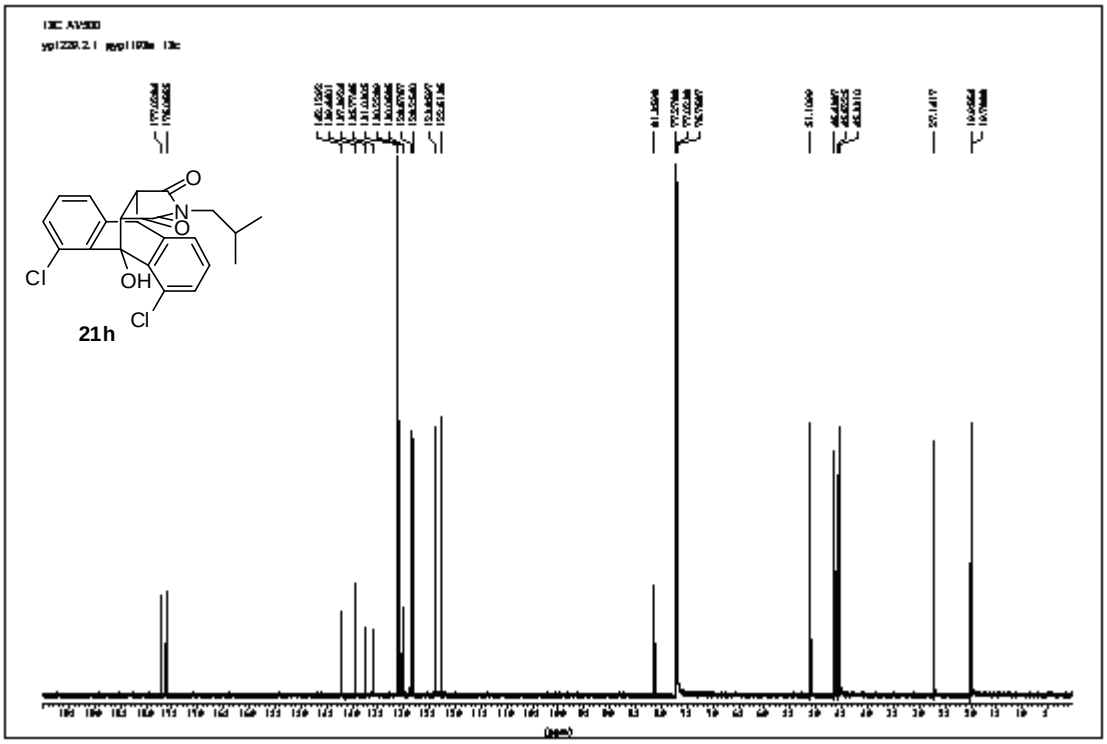

(21i)

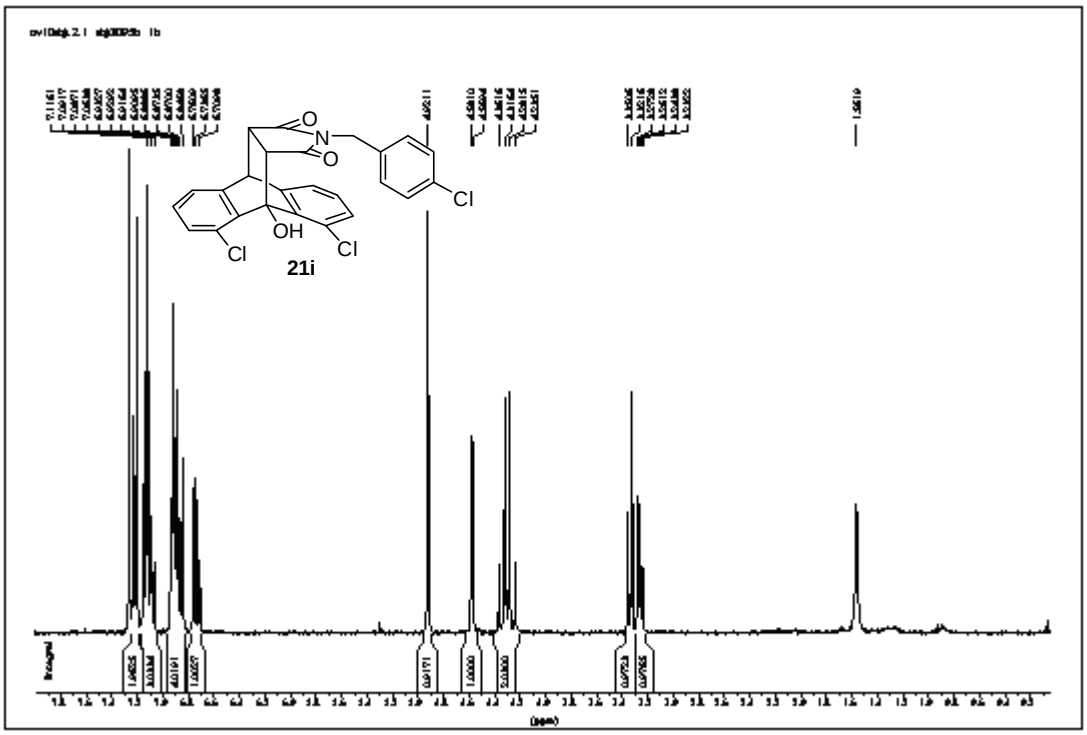

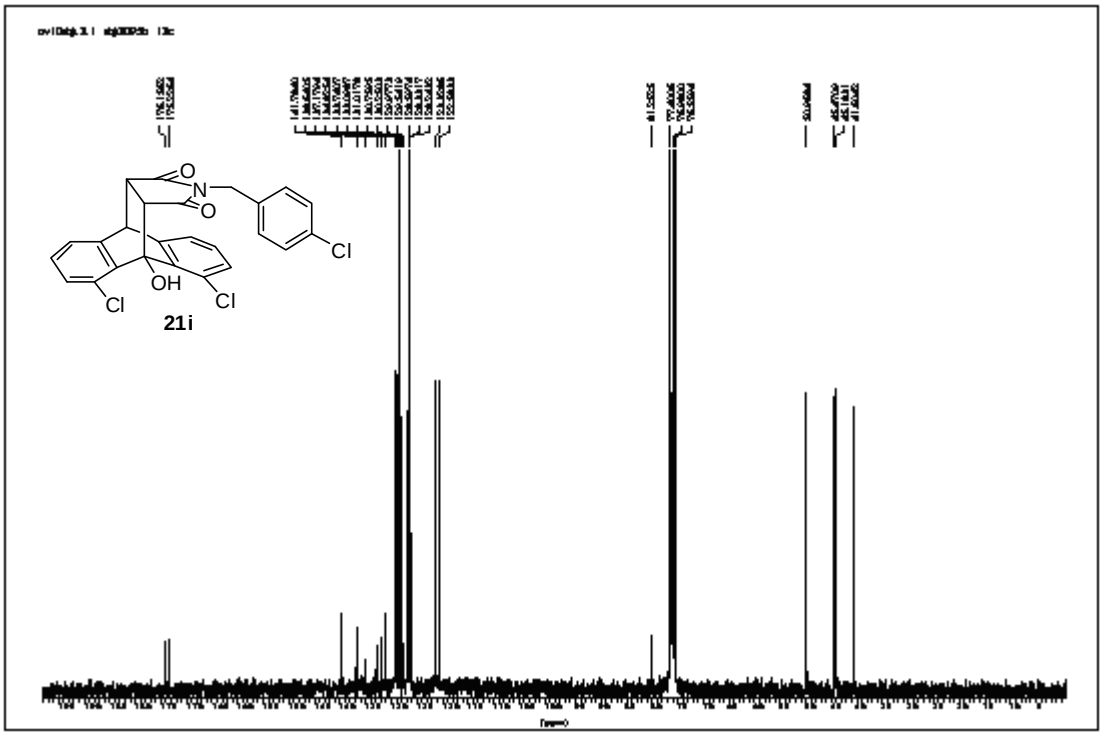

(21j)

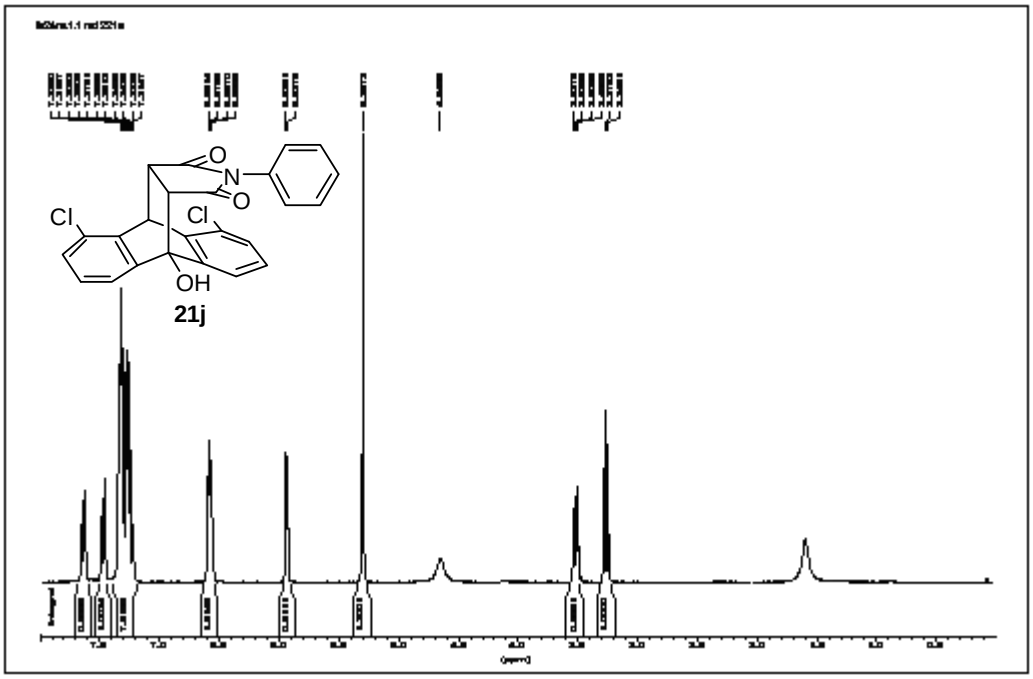

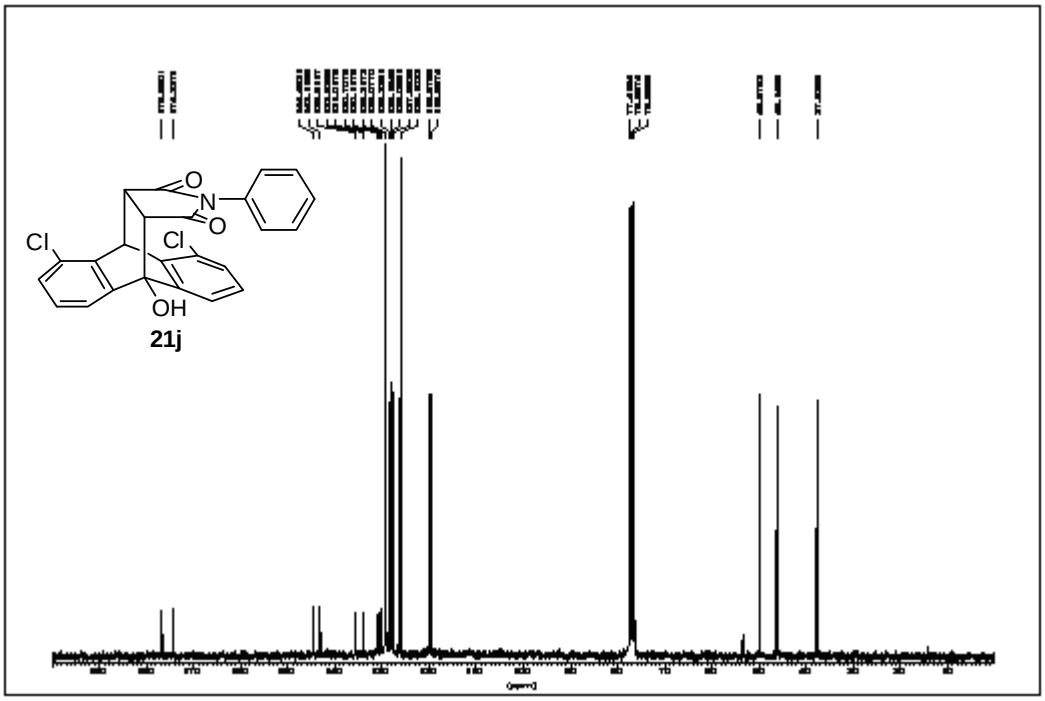

(21k)

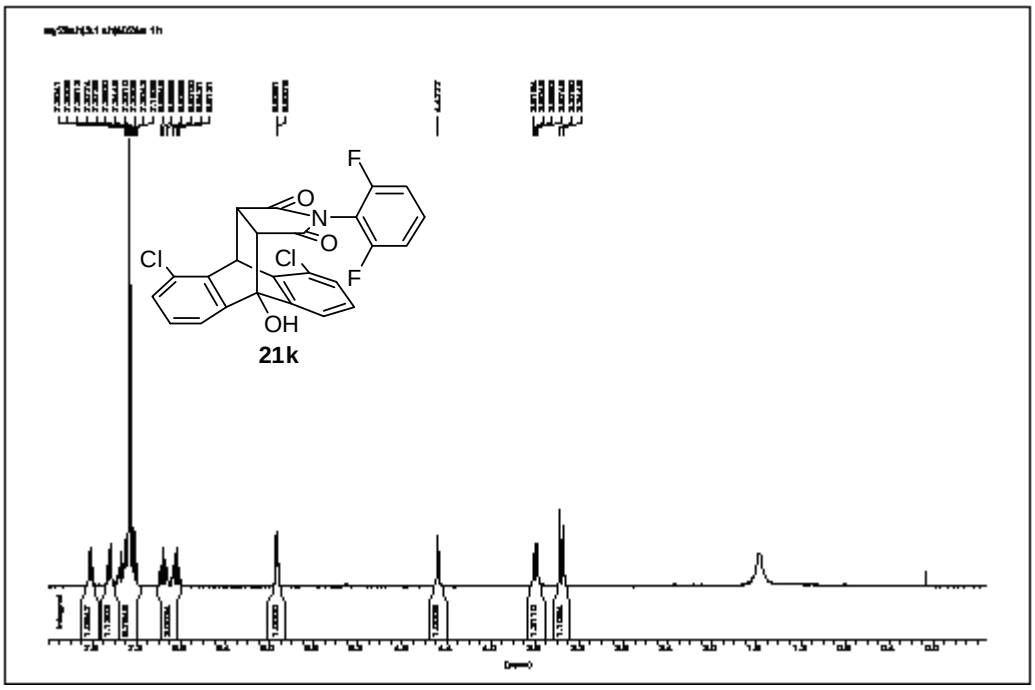

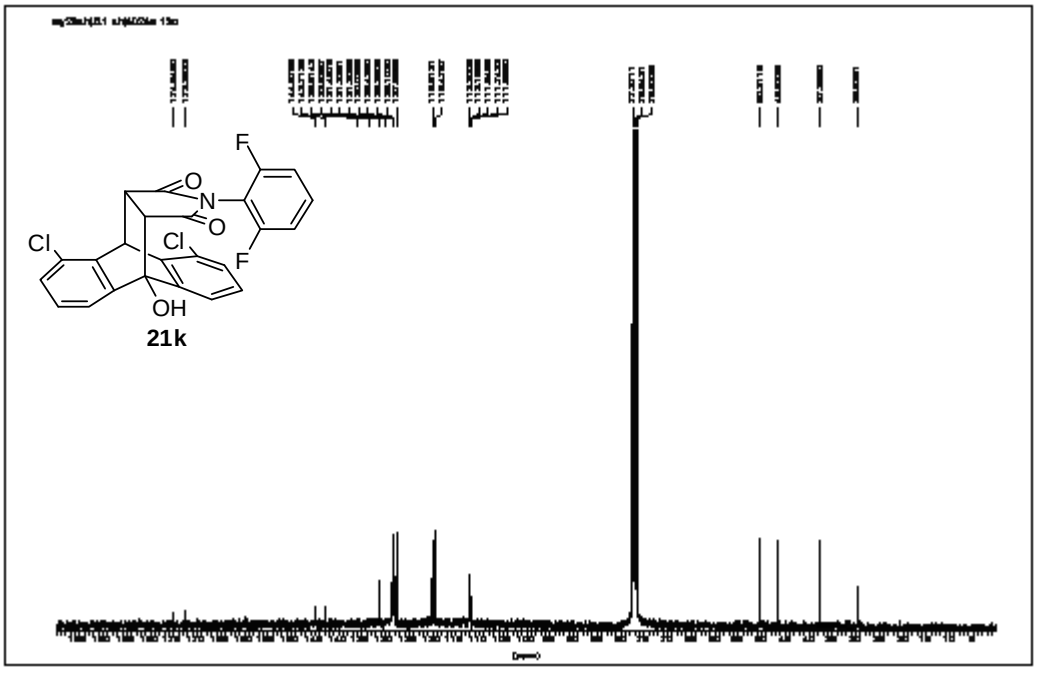

(21l)

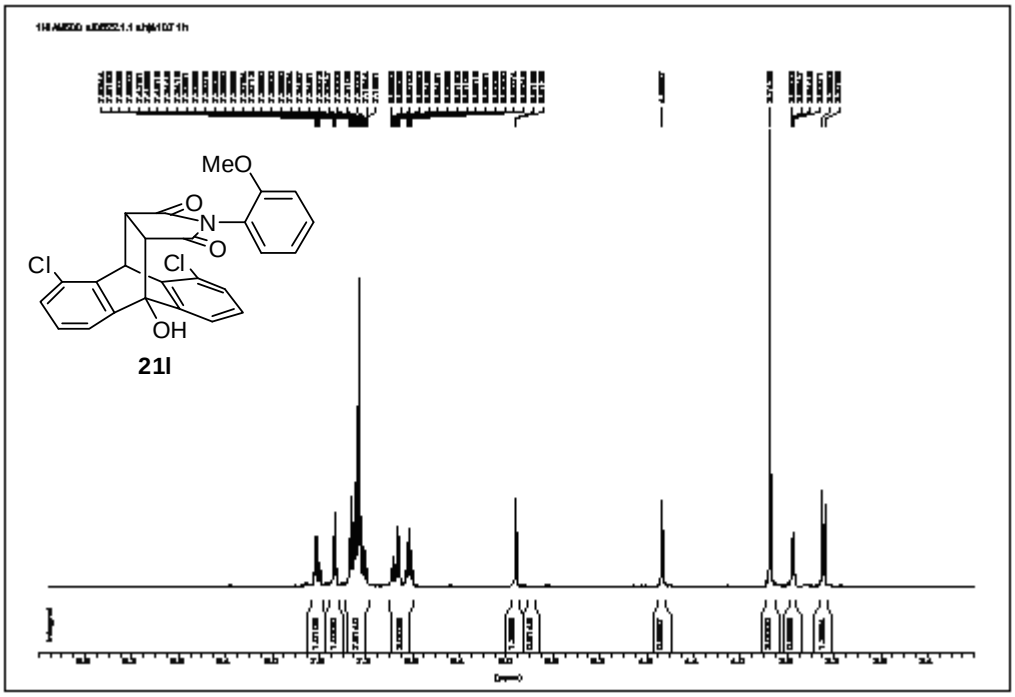

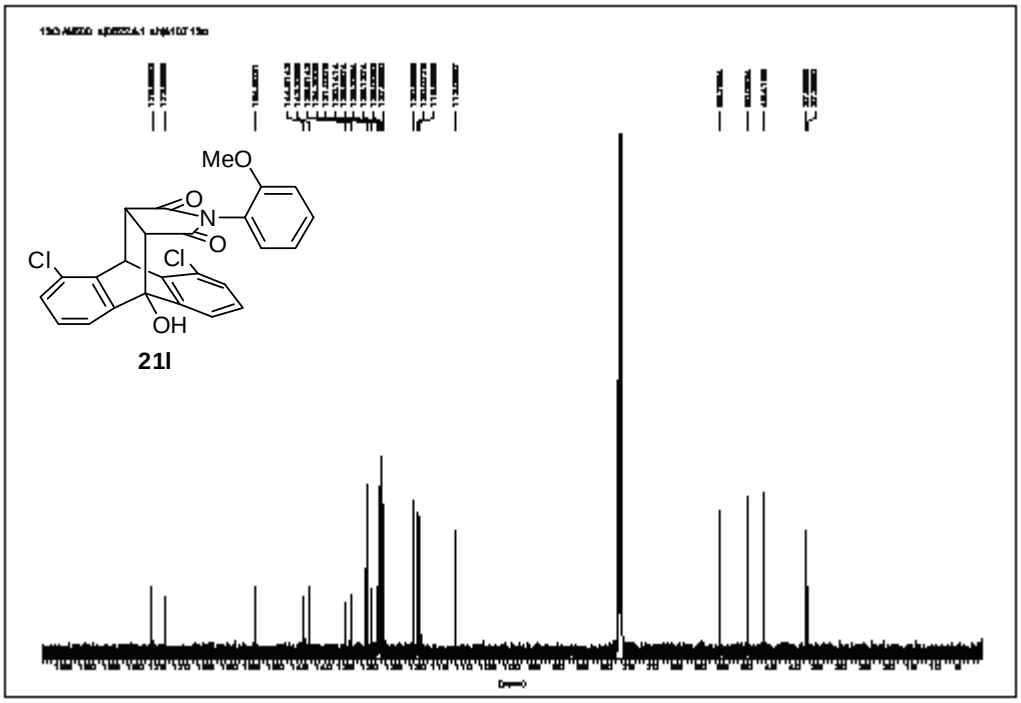

(21m-1)

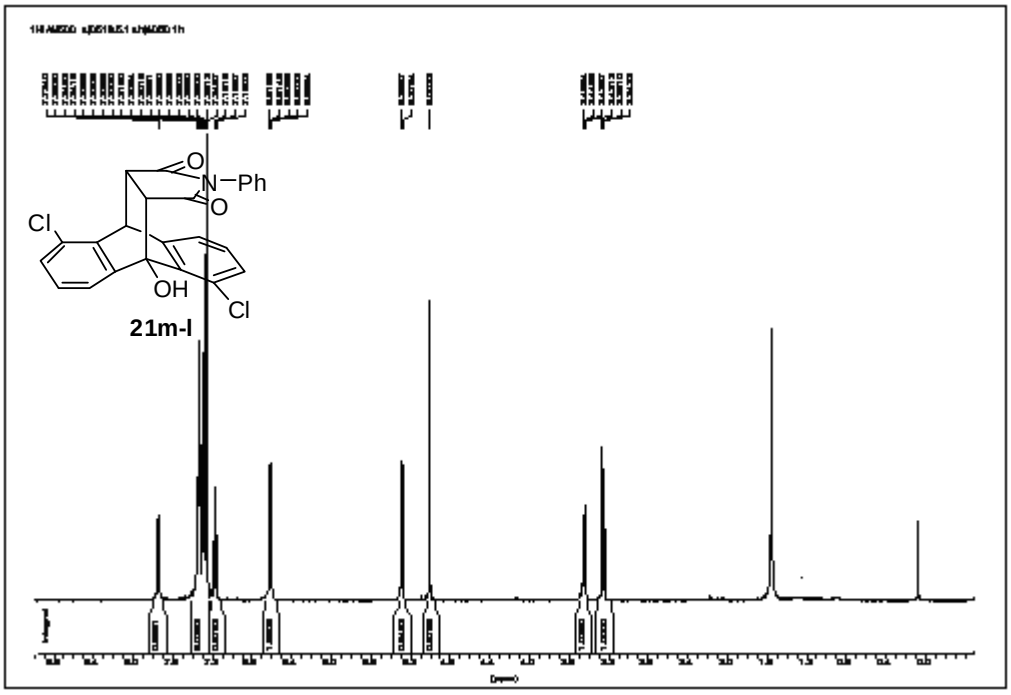

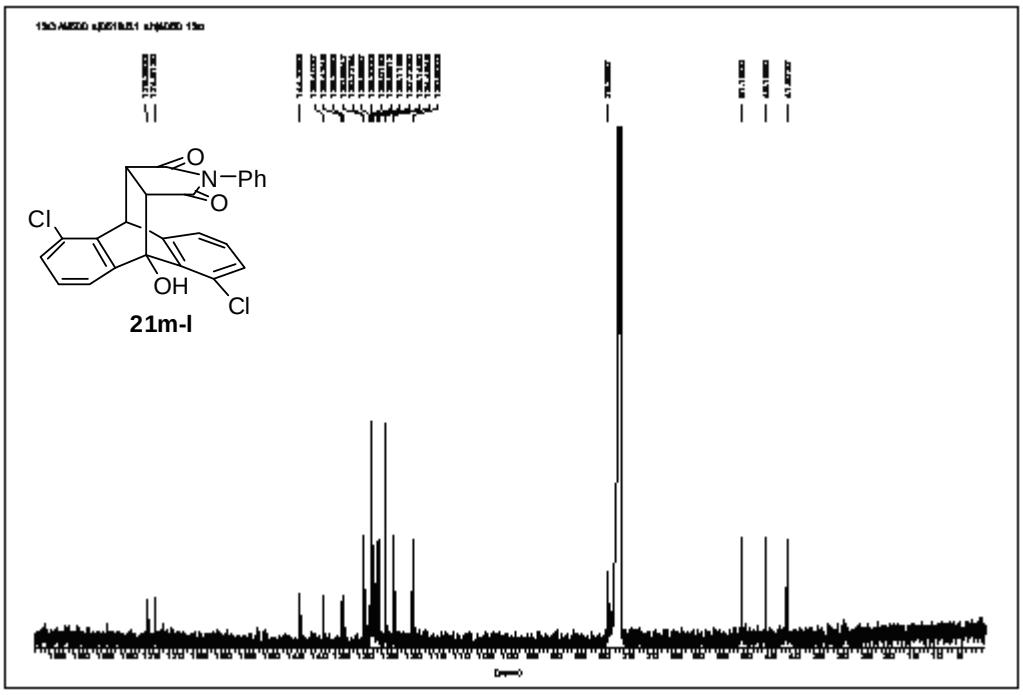

(**21n-1**)

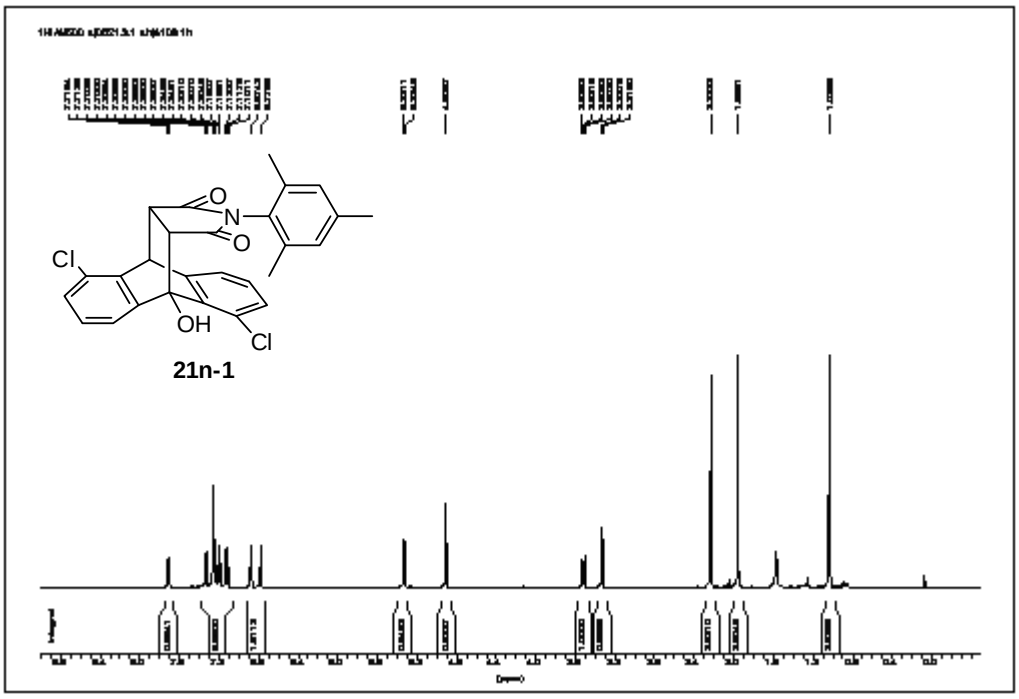

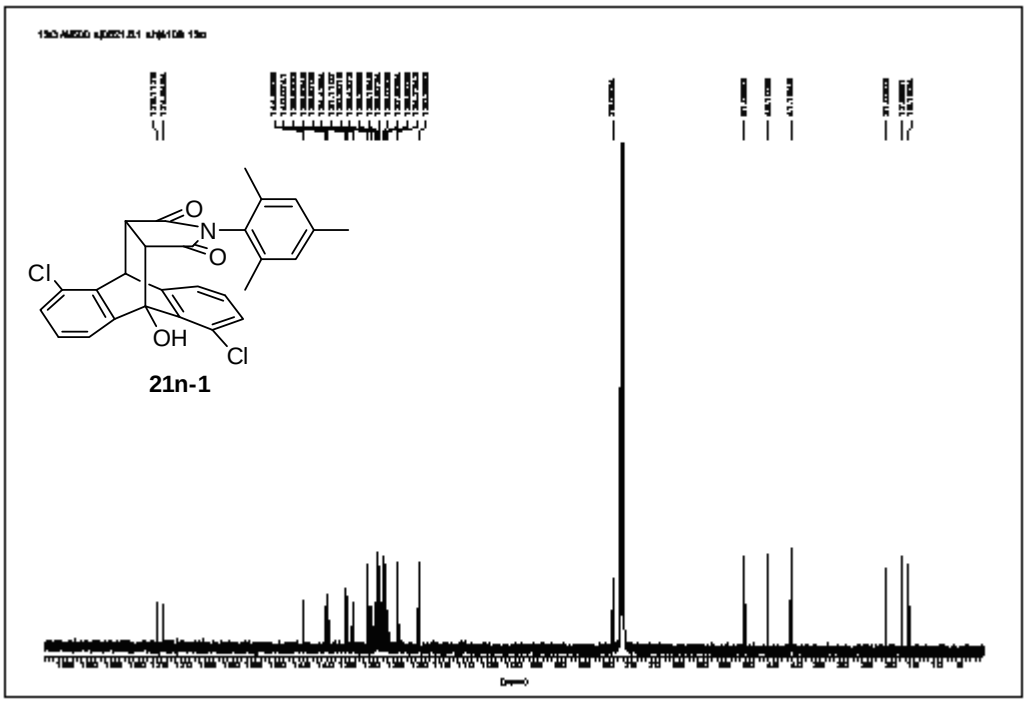

(**21o-1**)

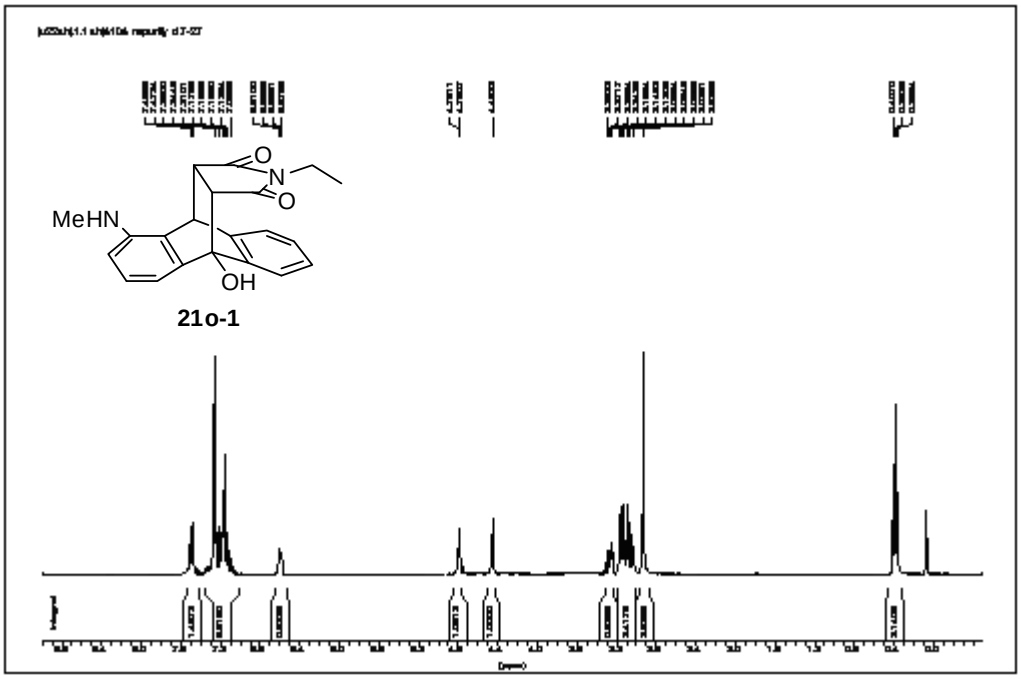

21o-1

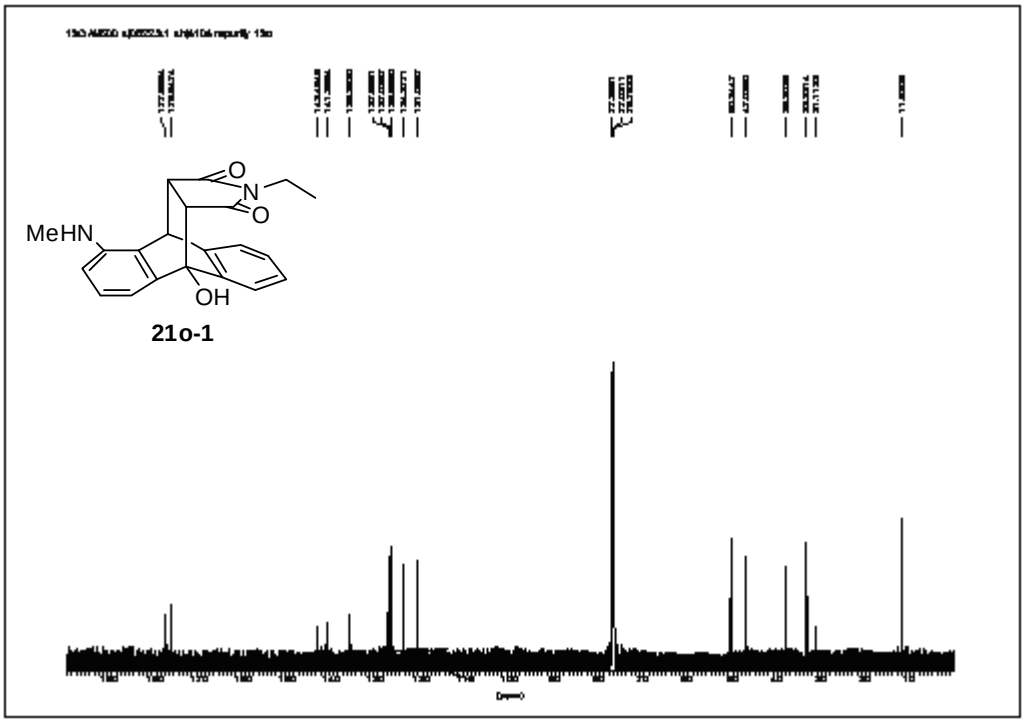

21o-1

(**21p-1**)

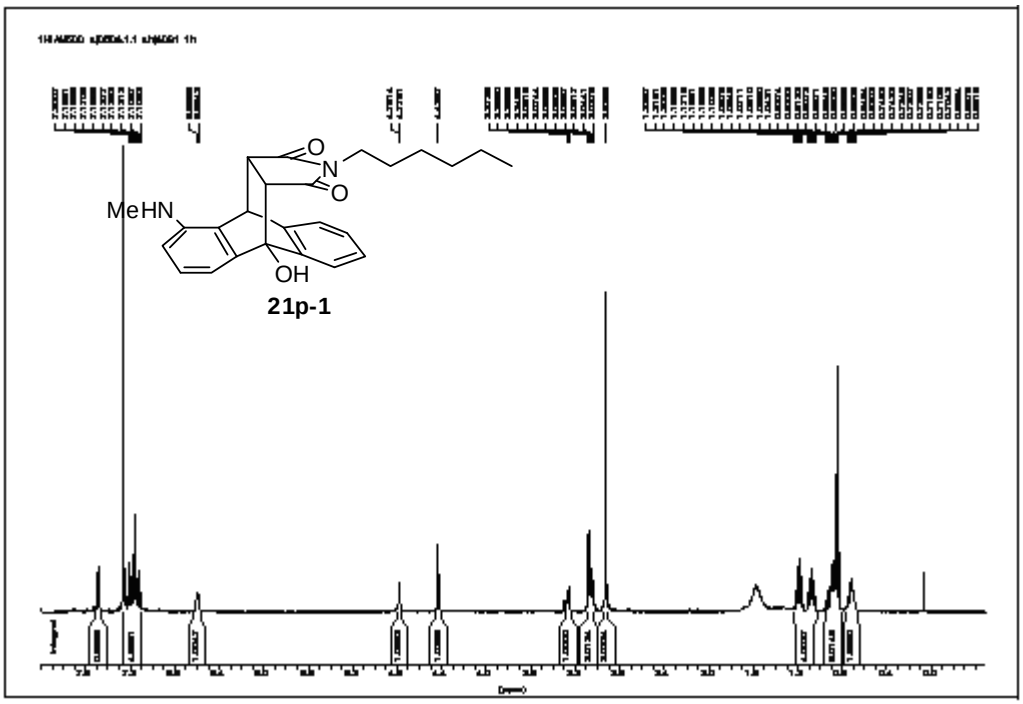

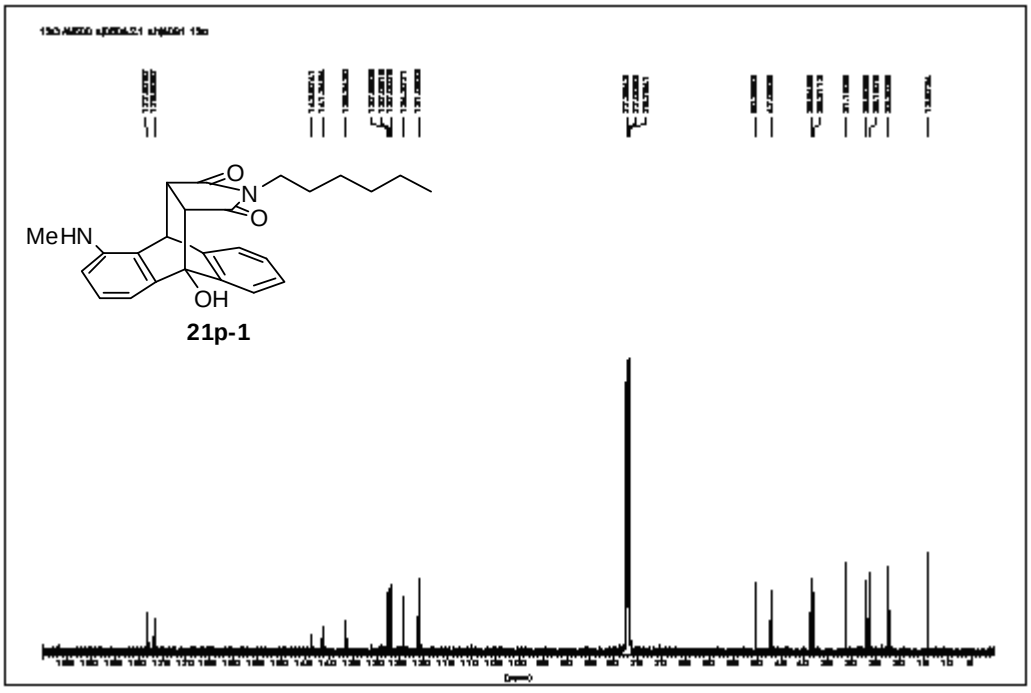

(131a)

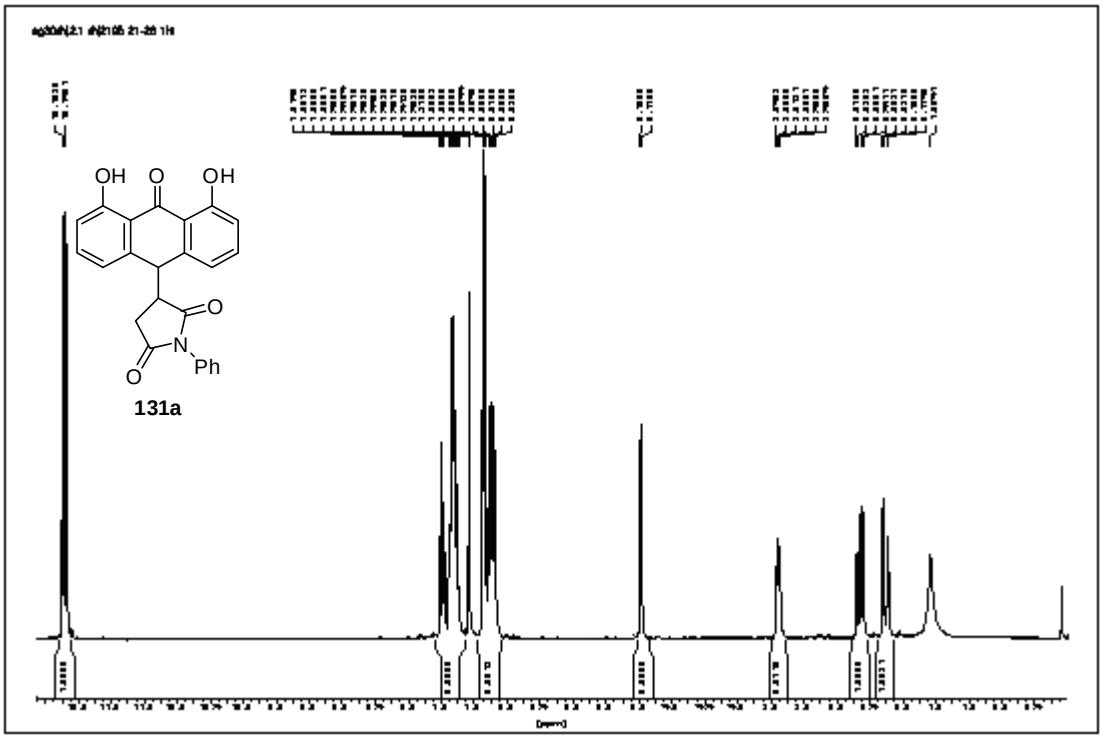
OH
O
OH
O
N
Ph
O
131a

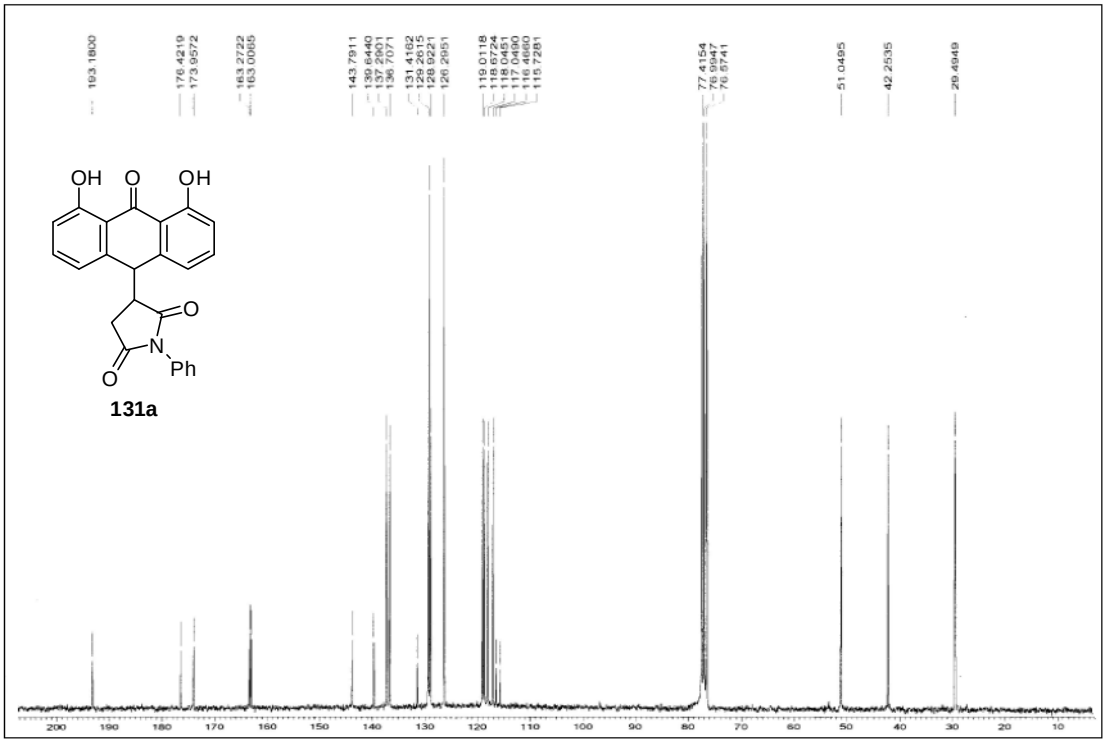
193.1800
176.4219
173.9572
163.2722
163.0065
143.7911
139.6440
137.2901
136.7071
131.4162
129.2615
128.9221
126.2951
119.0118
118.6724
118.0451
117.0490
116.4660
115.7281
77.4154
76.9947
76.5741
51.0495
42.2535
29.4949
OH
O
OH
O
N
Ph
O
131a
200
190
180
170
160
150
140
130
120
110
100
90
80
70
60
50
40
30
20
10

(**131b**)

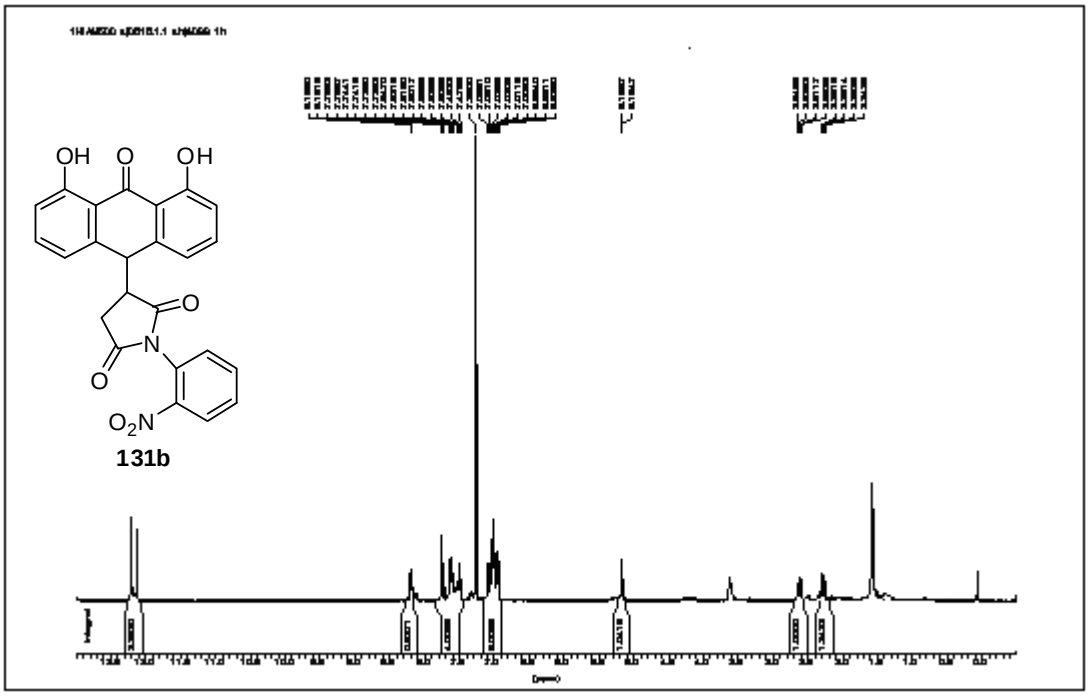

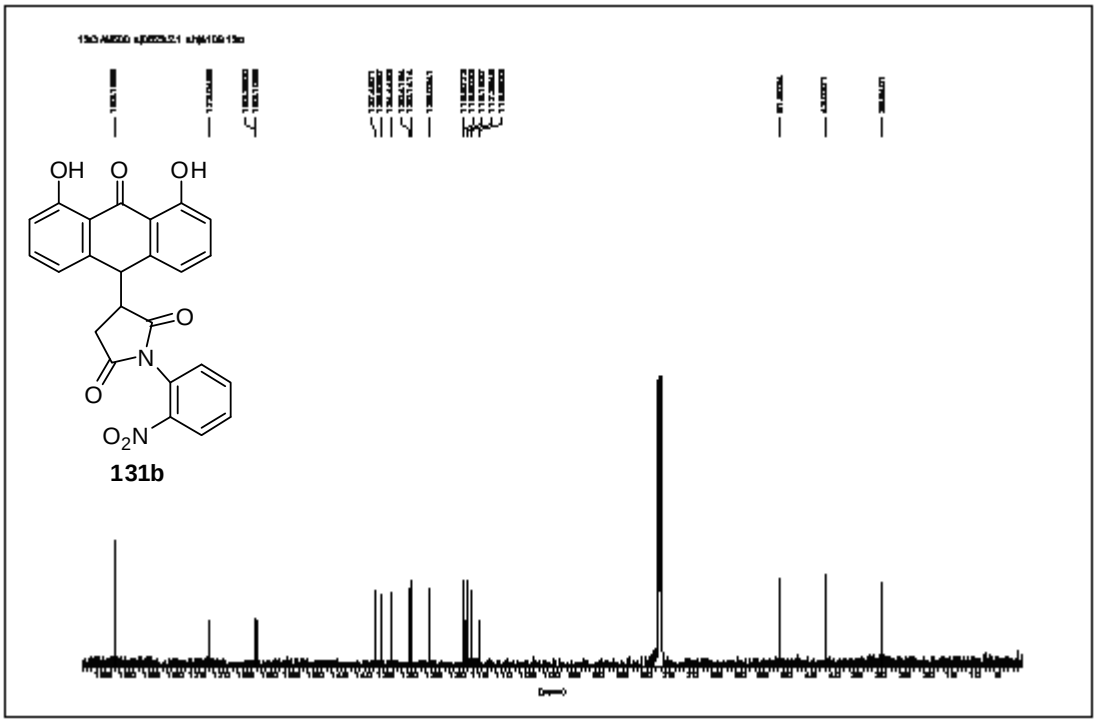

(131c)

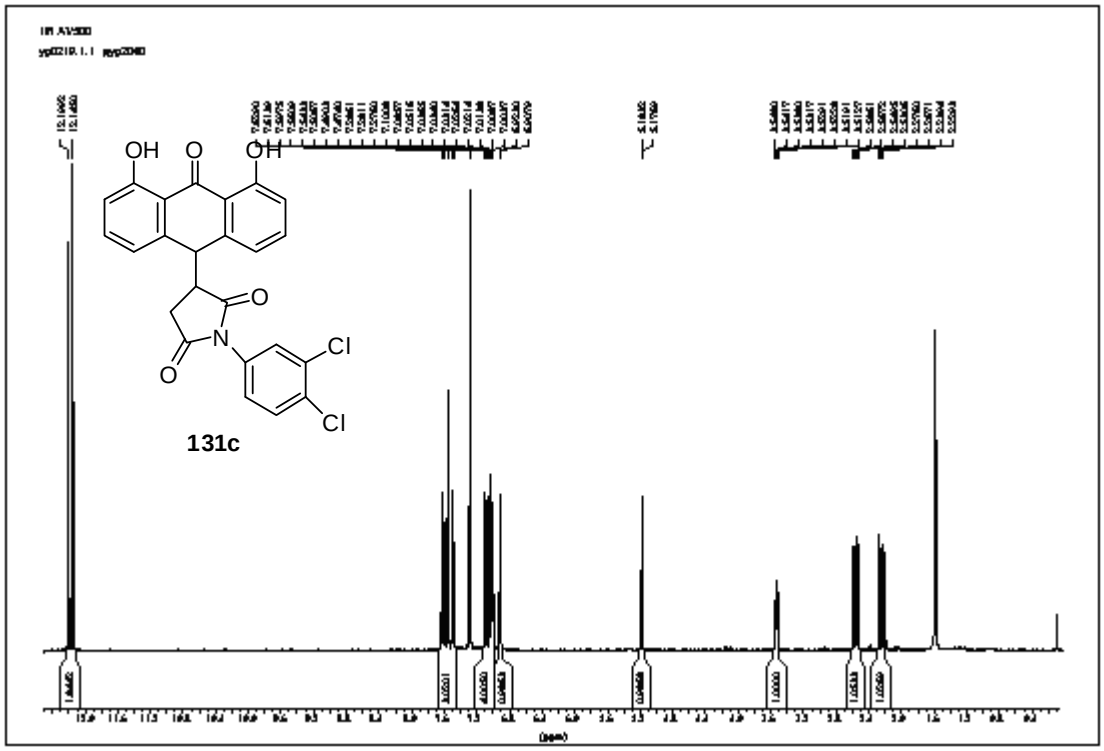

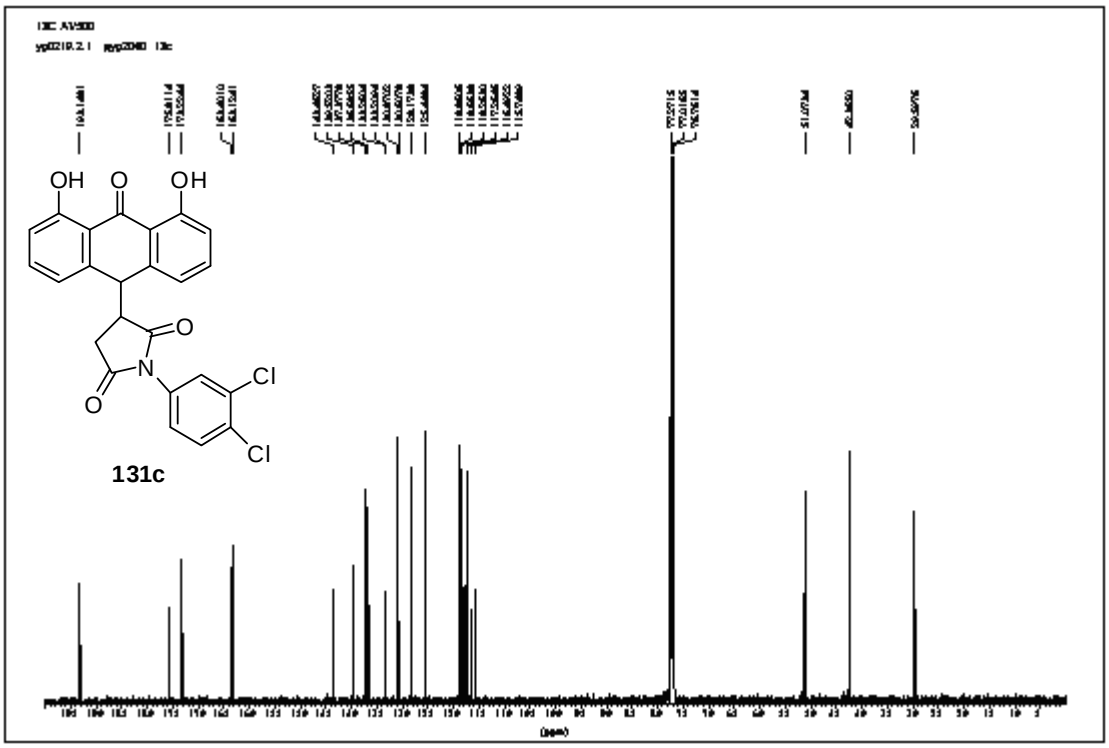

(131d)

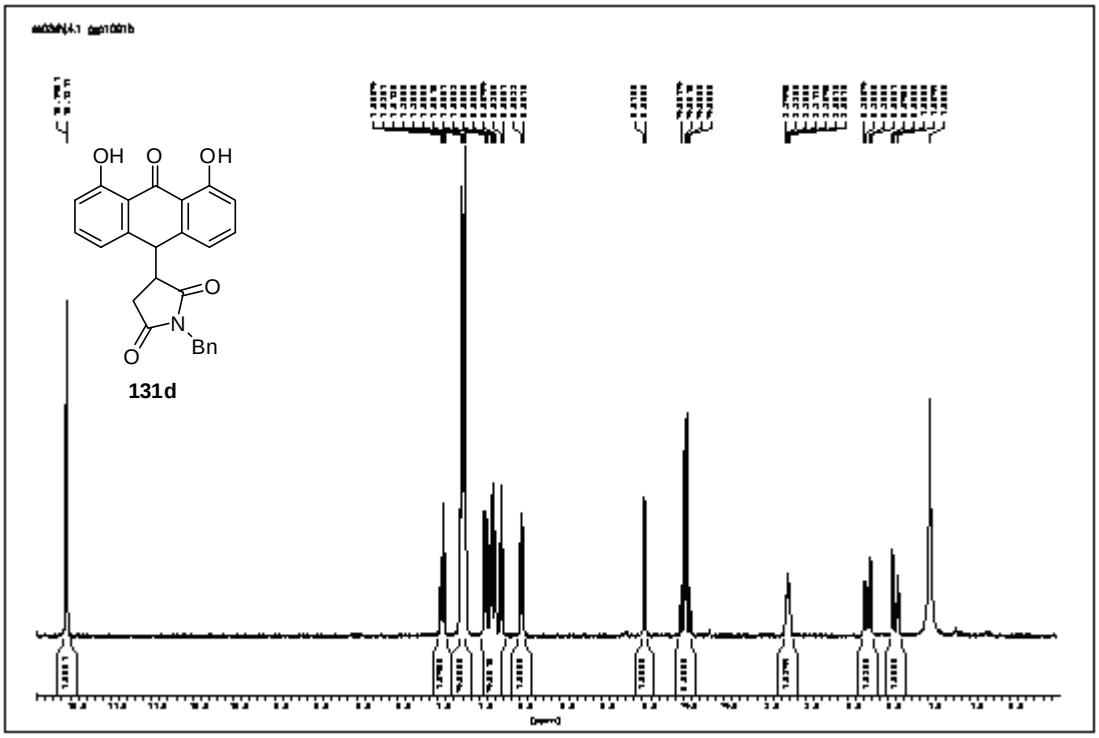

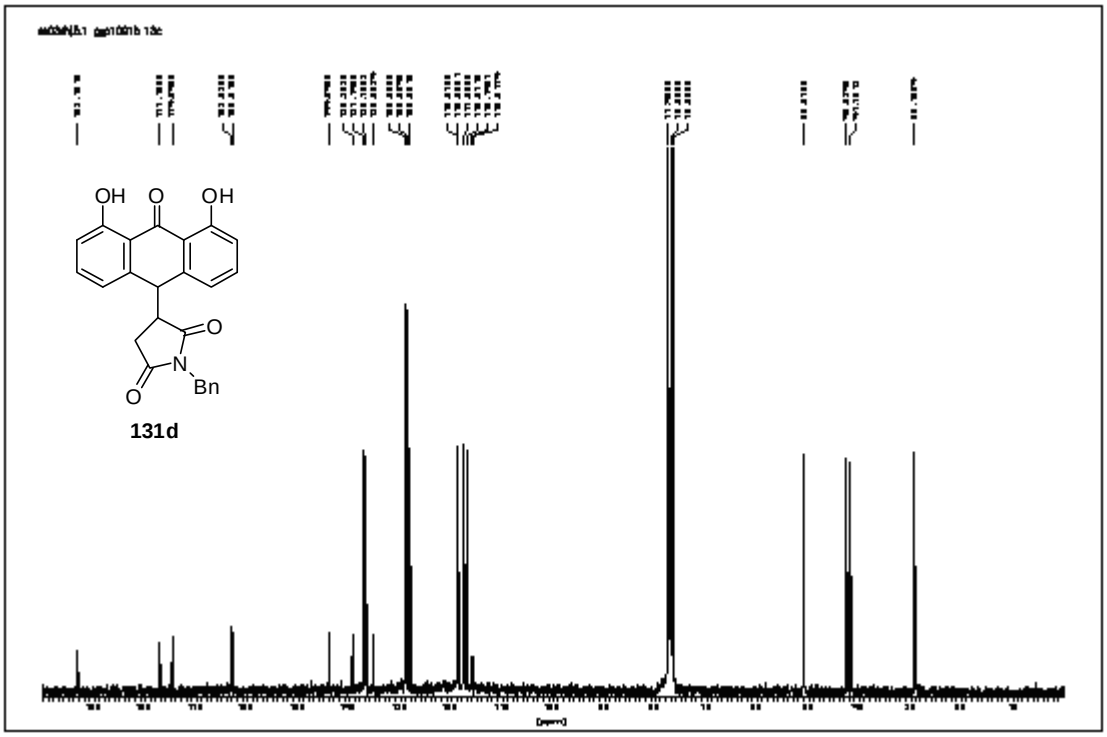

(**132a**)

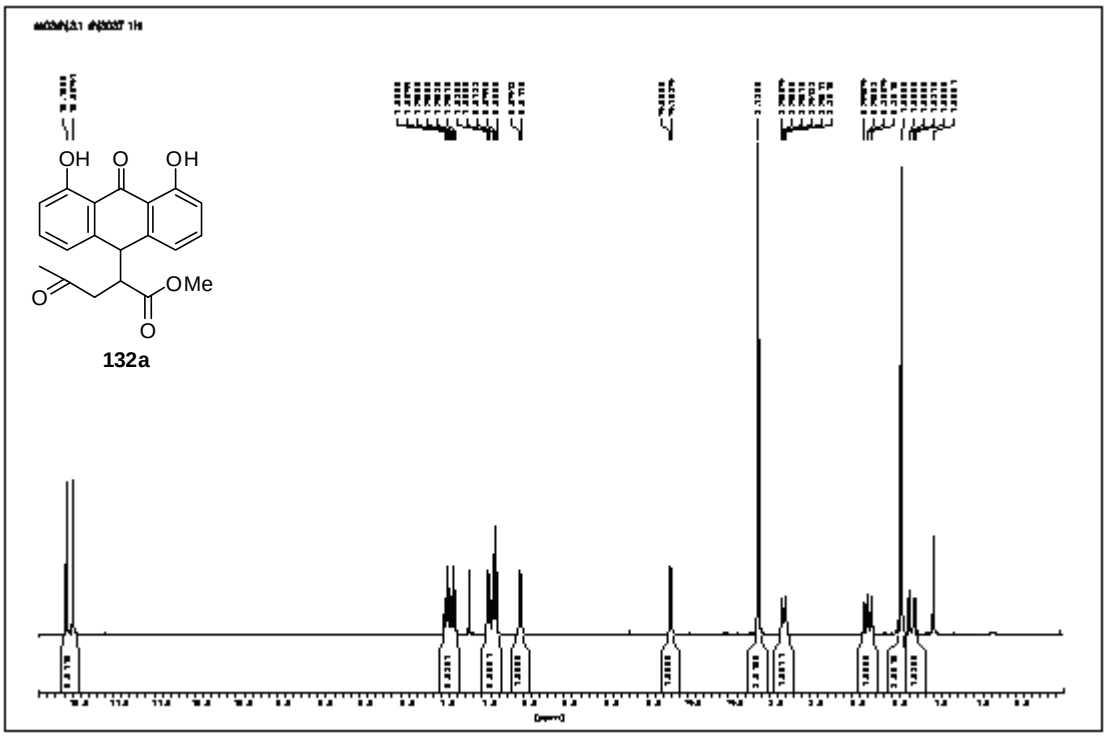
OH
O
OH
OMe
O
O
132a

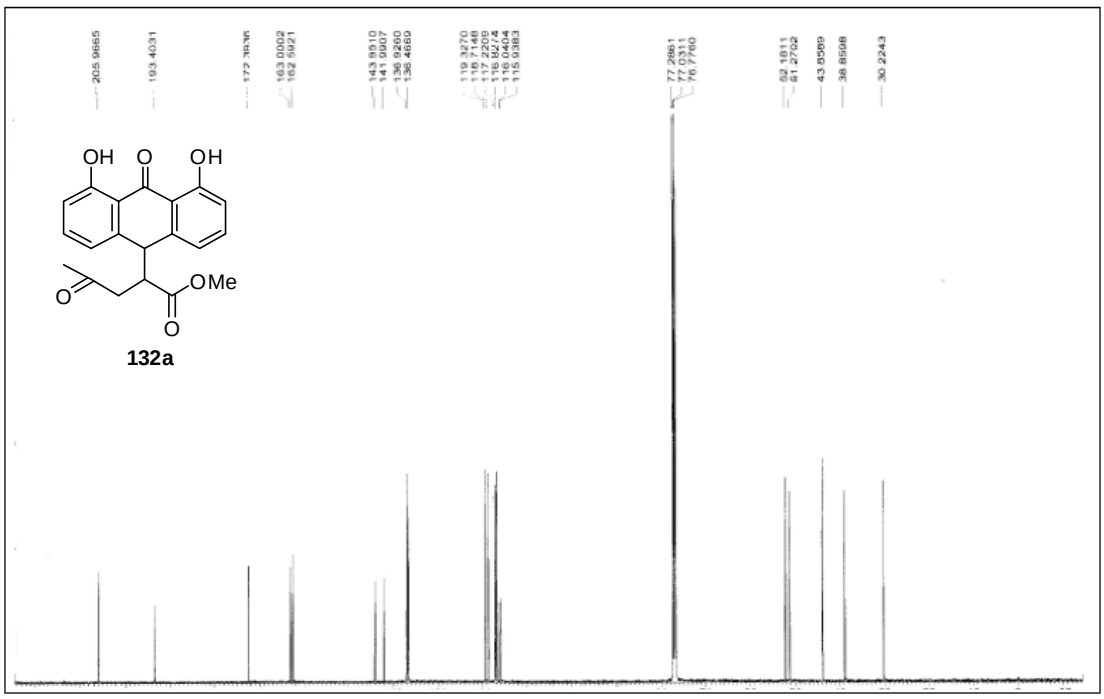
205.9865
193.4031
183.0002
162.5921
143.9910
143.6007
136.9260
136.4689
119.3270
118.7148
117.2209
116.0404
115.9383
77.2861
77.0311
76.7760
62.1811
61.2702
43.6569
38.8598
30.2243
OH
O
OH
OMe
O
O
132a

(**132b**)

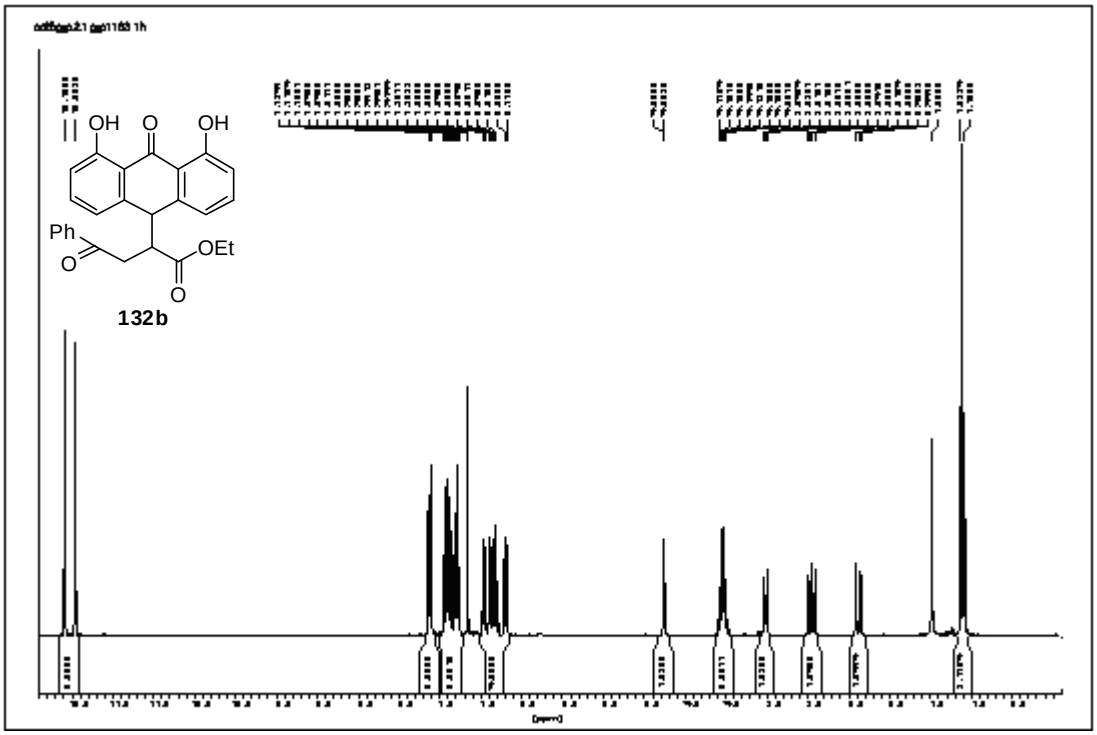

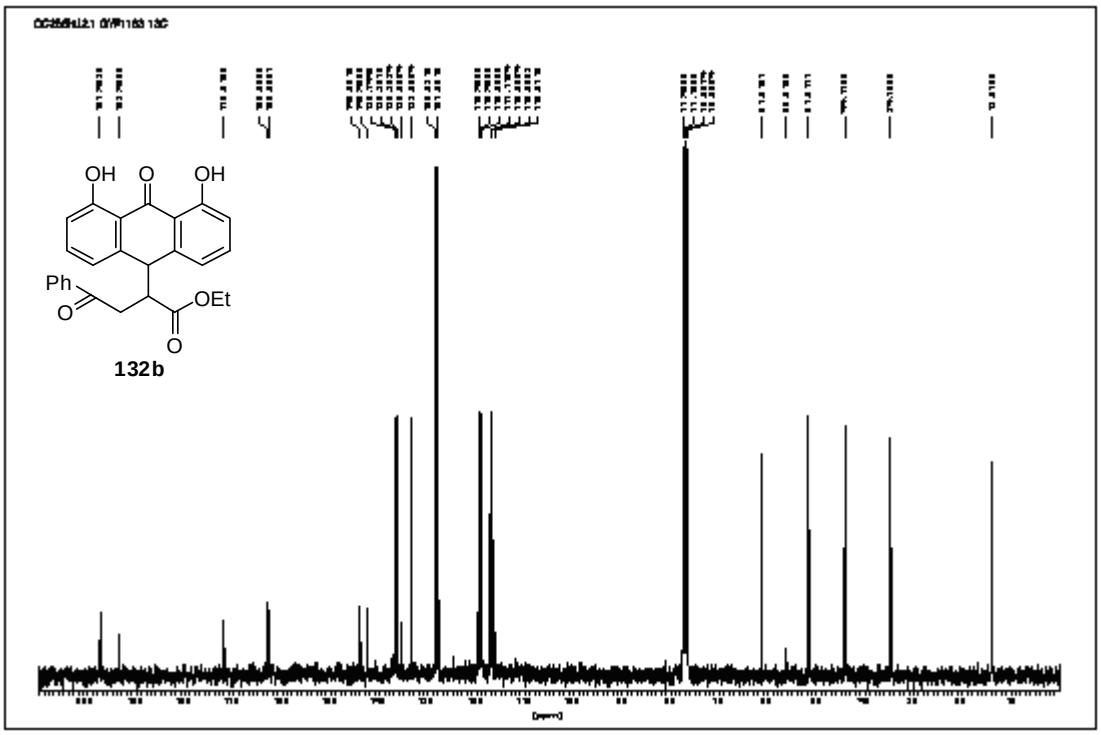

(132c)

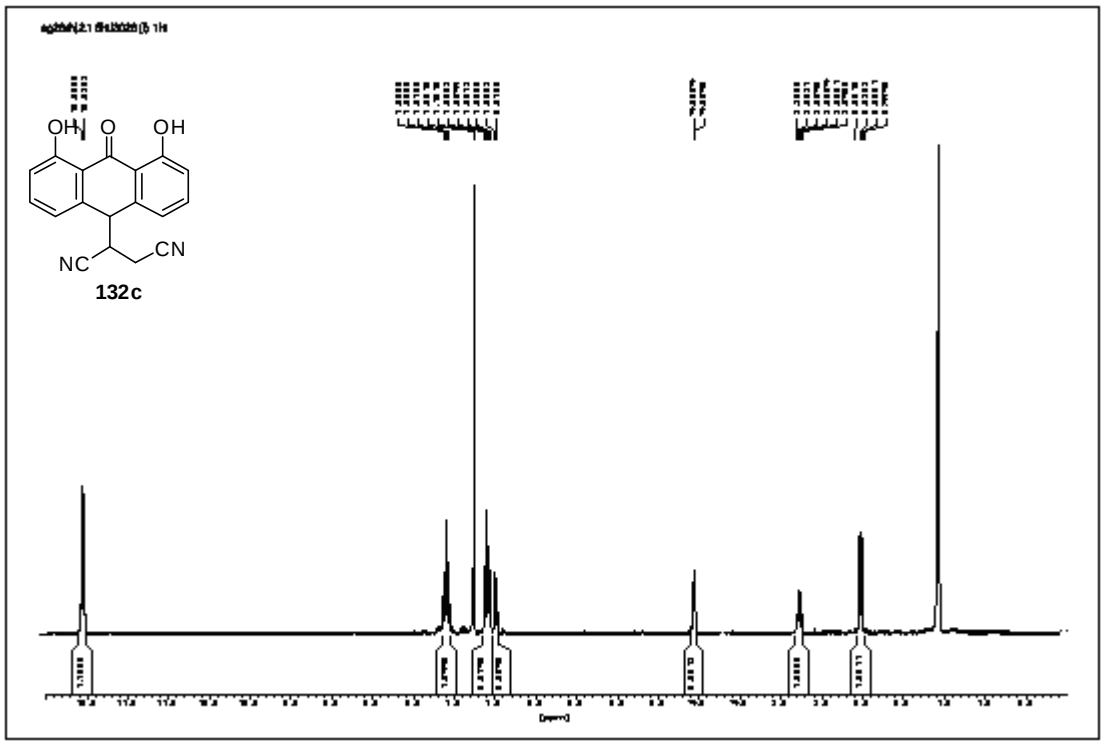

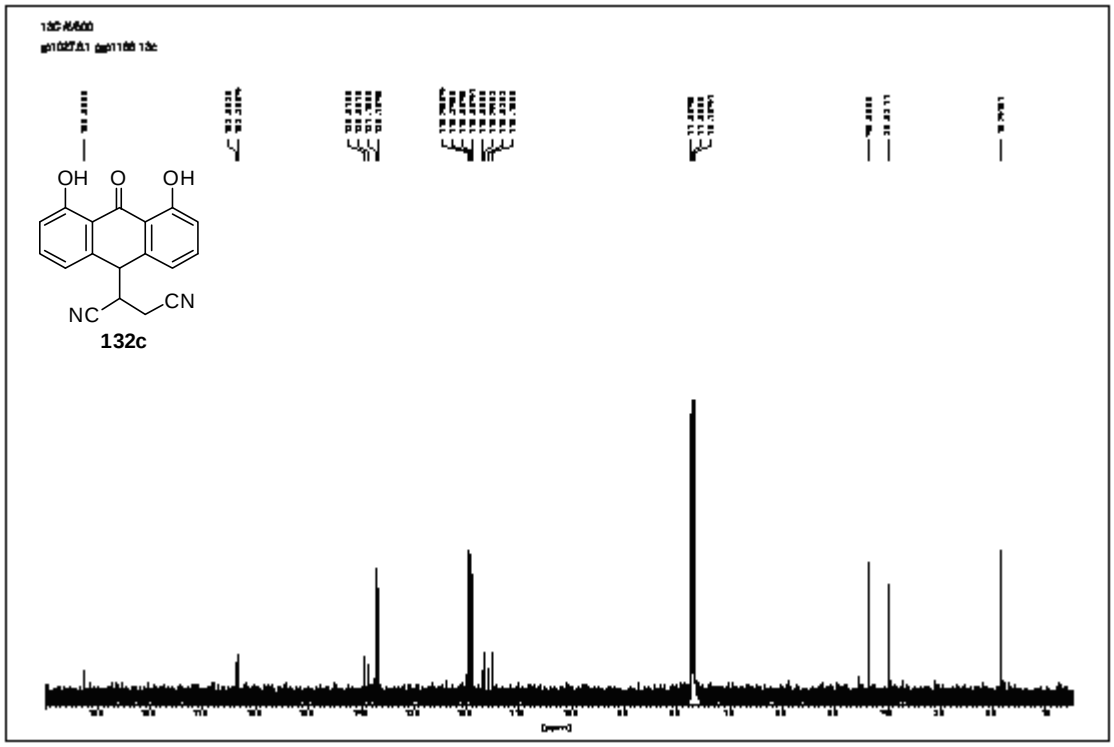

(145a)

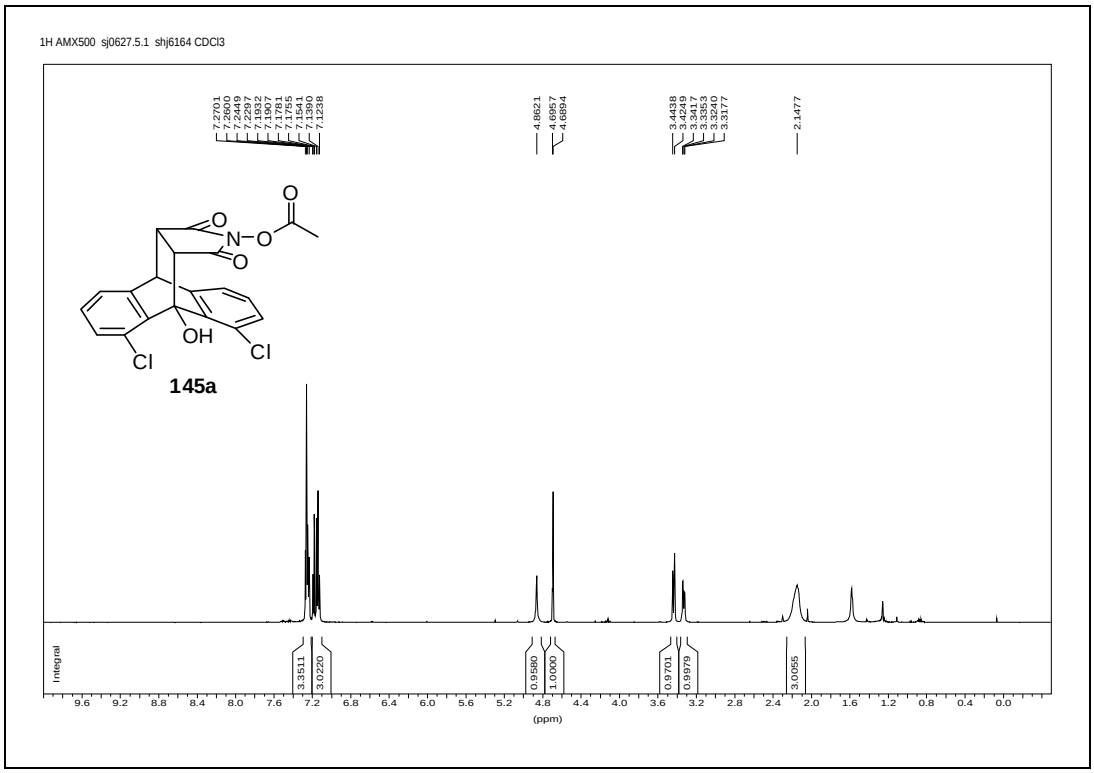
1H AMX500 sj0627.5.1 shj6164 CDCl3
7.2701
7.2600
7.2449
7.2297
7.1932
7.1907
7.1781
7.1755
7.1541
7.1390
7.1238
4.8621
4.6957
4.6894
3.4438
3.4249
3.3417
3.3353
3.3240
3.3177
2.1477
O
O
N
O
O
OH
Cl
Cl
145a
Integral
3.3511
3.0220
0.9580
1.0000
0.9701
0.9979
3.0055
9.6 9.2 8.8 8.4 8.0 7.6 7.2 6.8 6.4 6.0 5.6 5.2 4.8 4.4 4.0 3.6 3.2 2.8 2.4 2.0 1.6 1.2 0.8 0.4 0.0
(ppm)

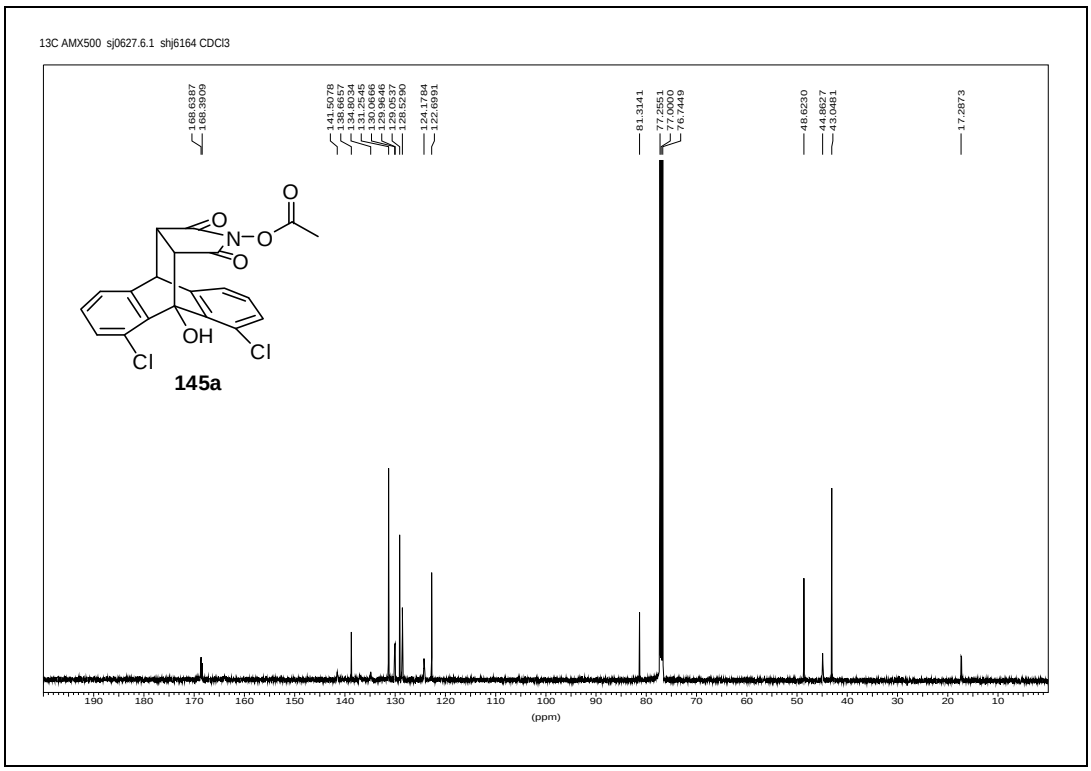
13C AMX500 sj0627.6.1 shj6164 CDCl3
168.6387
168.3909
141.5078
138.8657
134.8034
131.2545
130.0666
129.9646
129.0537
128.5290
124.1784
122.6991
81.3141
77.2551
77.0000
76.7449
48.6230
44.9627
43.0481
17.2873
O
O
N
O
O
OH
Cl
Cl
145a
190 180 170 160 150 140 130 120 110 100 90 80 70 60 50 40 30 20 10
(ppm)

(**145b**)

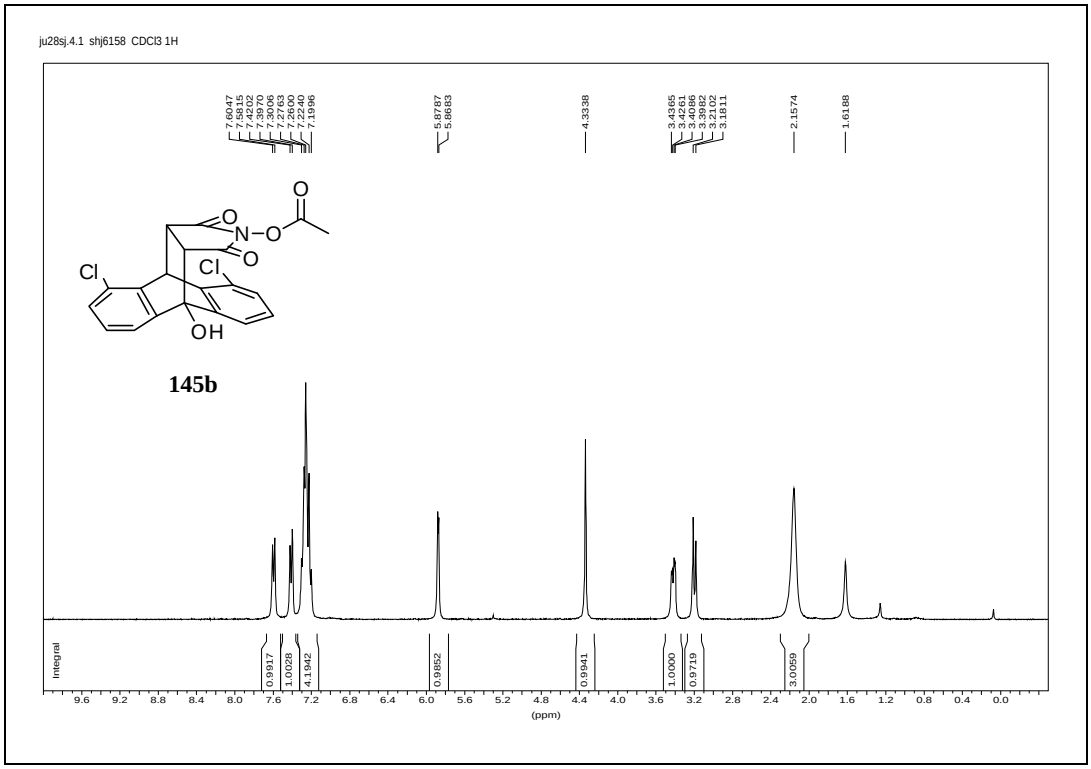
ju28sj.4.1 shj6158 CDCl3 1H
7.6047
7.5815
7.4832
7.4670
7.3006
7.2763
7.2650
7.2240
7.1996
5.8787
5.8683
4.3338
3.4365
3.4051
3.4086
3.3982
3.2102
3.1811
2.1574
1.6188
Cl
Cl
OH
145b
Intégral
0.9917
1.0028
4.1942
0.9852
0.9941
1.0000
0.9719
3.0059
(ppm)

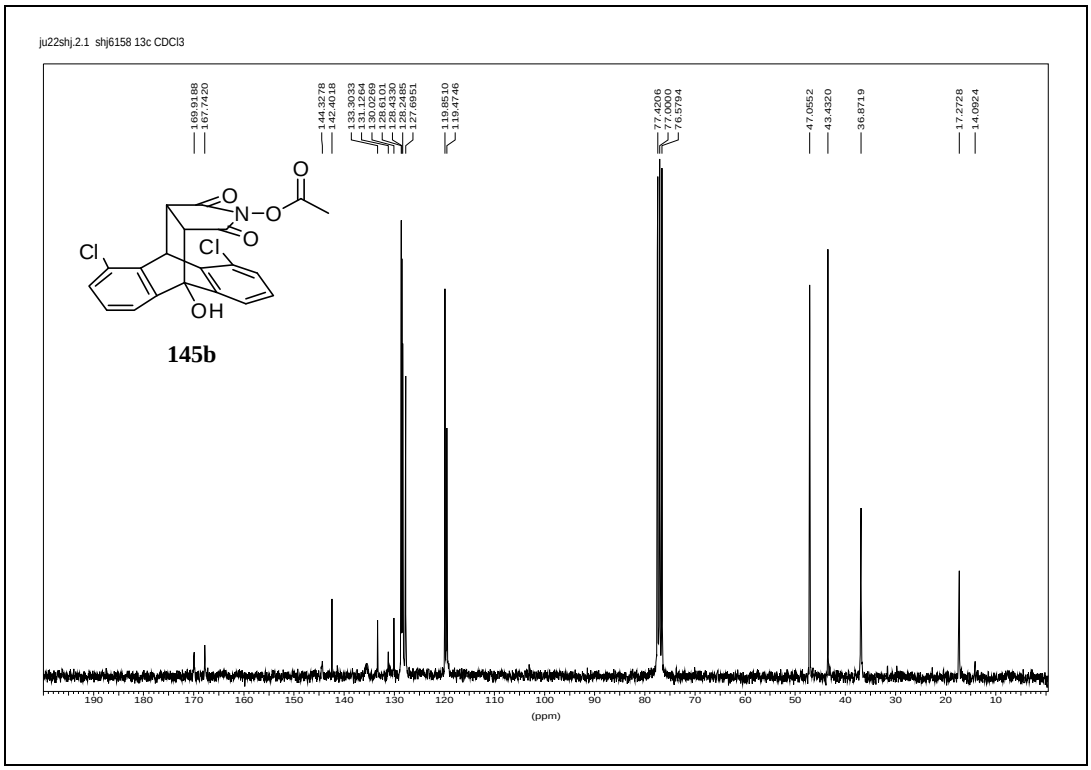
ju22shj.2.1 shj6158 13c CDCl3
169.9188
167.7420
144.3278
142.4018
133.3033
131.1264
130.0068
128.6101
128.4330
127.9285
127.6951
119.9510
119.4746
77.4206
77.0000
76.5794
47.0552
43.4320
36.8719
17.2728
14.0924
Cl
Cl
OH
145b
(ppm)

(**145c**)

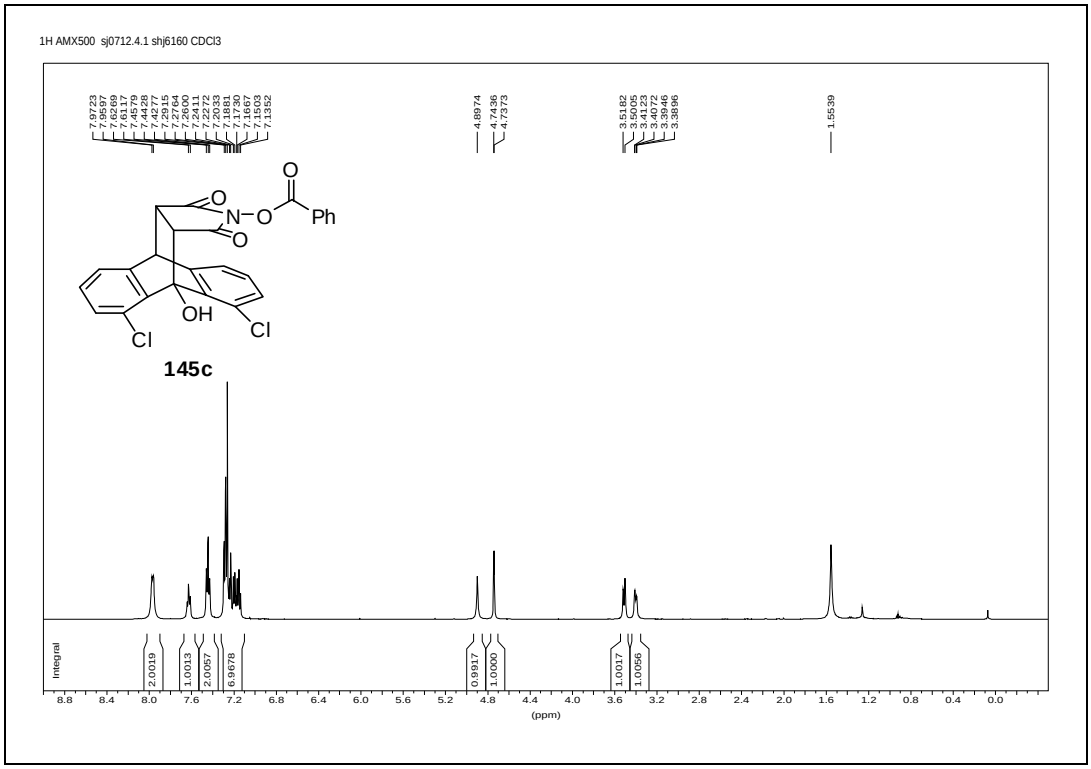
1H AMX500 sj0712.4.1 shj6160 CDCl3
7.9723
7.9597
7.6269
7.6117
7.4578
7.4428
7.4277
7.2915
7.2764
7.2600
7.2411
7.2272
7.2033
7.1881
7.1730
7.1567
7.1503
7.1352
4.8974
4.7436
4.7373
3.5182
3.5005
3.4123
3.3972
3.3946
3.3896
1.5539
O
N−O
Ph
O
OH
Cl
Cl
145c
Intégral
2.0019
1.0013
2.0057
6.9678
0.9917
1.0000
1.0017
1.0056
8.8 8.4 8.0 7.6 7.2 6.8 6.4 6.0 5.6 5.2 4.8 4.4 4.0 3.6 3.2 2.8 2.4 2.0 1.6 1.2 0.8 0.4 0.0
(ppm)

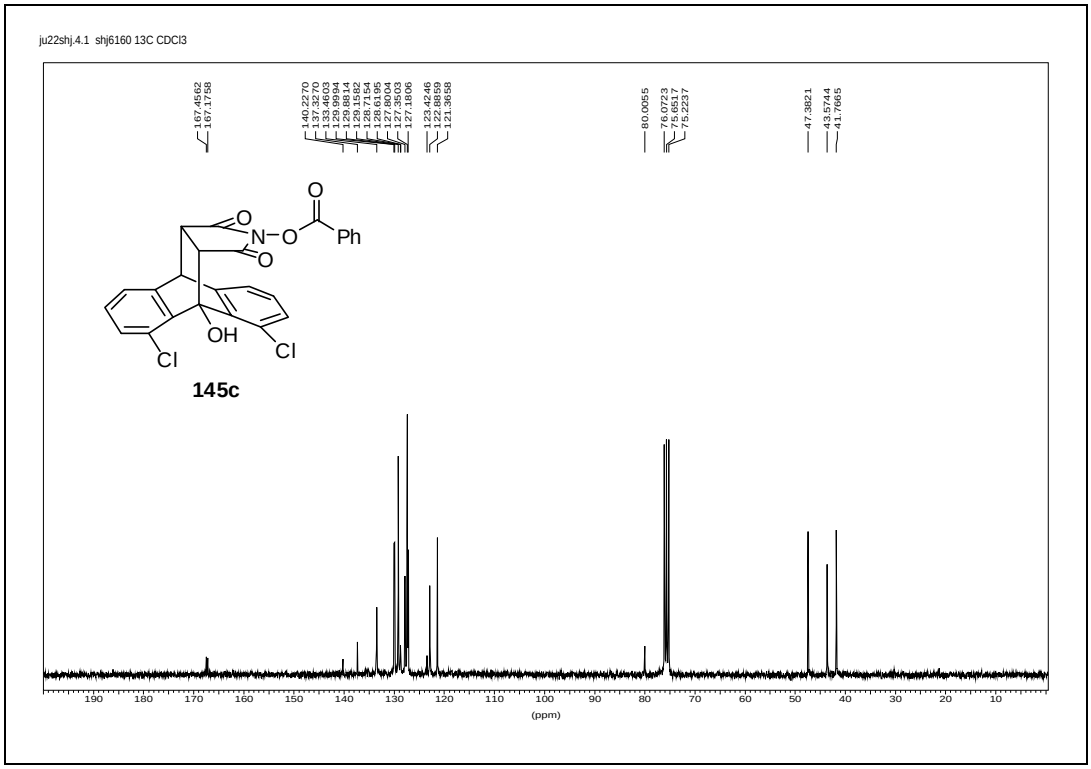
ju22shj.4.1 shj6160 13C CDCl3
167.4562
167.1758
140.2270
137.2270
133.4603
129.9994
129.8814
129.1582
128.7154
128.6195
128.3904
127.3503
127.1806
123.4246
122.8859
121.3658
80.0055
76.0723
75.6517
75.2237
47.3821
43.5744
41.7665
O
N−O
Ph
O
OH
Cl
Cl
145c
190 180 170 160 150 140 130 120 110 100 90 80 70 60 50 40 30 20 10
(ppm)

(145d)

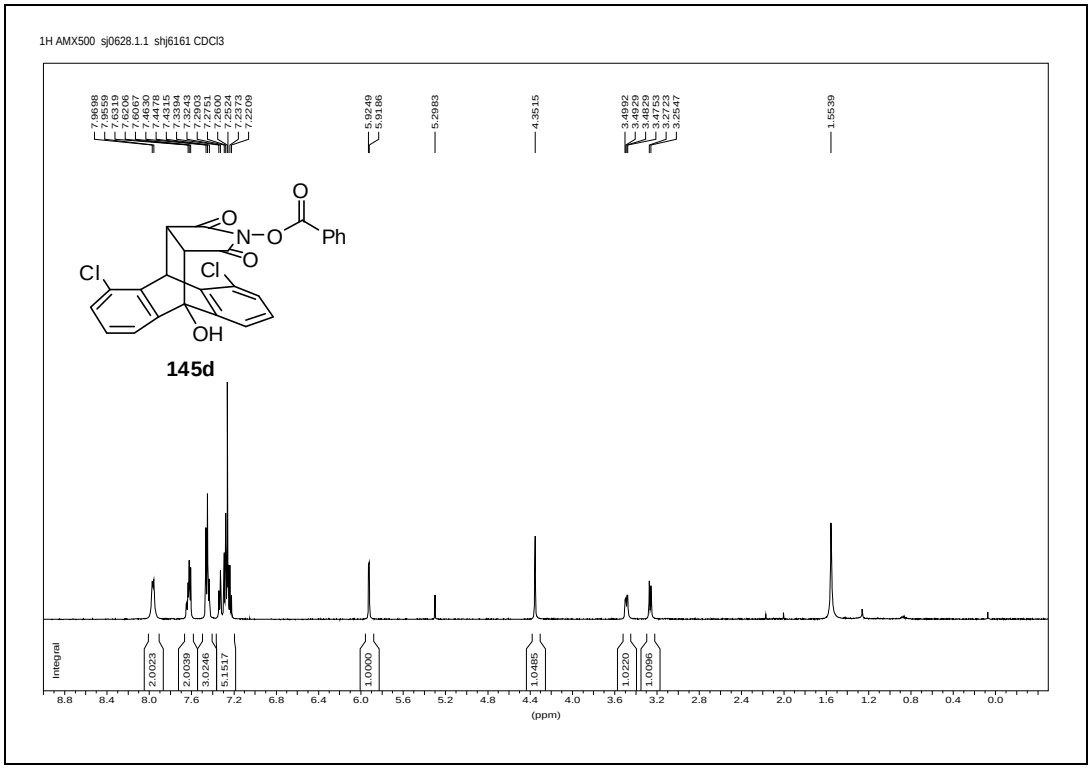
1H AMX500 sj0628.1.1 shj6161 CDCl3
7.9698
7.9559
7.6319
7.6206
7.6067
7.4630
7.4478
7.4315
7.3964
7.3243
7.2903
7.2751
7.2600
7.2524
7.2373
7.2209
5.9249
5.9186
5.2983
4.3515
3.4992
3.4929
3.4829
3.4753
3.2723
3.2547
1.5539
O
O
N
O
Ph
O
Cl
Cl
OH
145d
Intégral
2.0023
2.0039
3.0246
5.1517
1.0000
1.0485
1.0220
1.0096
(ppm)

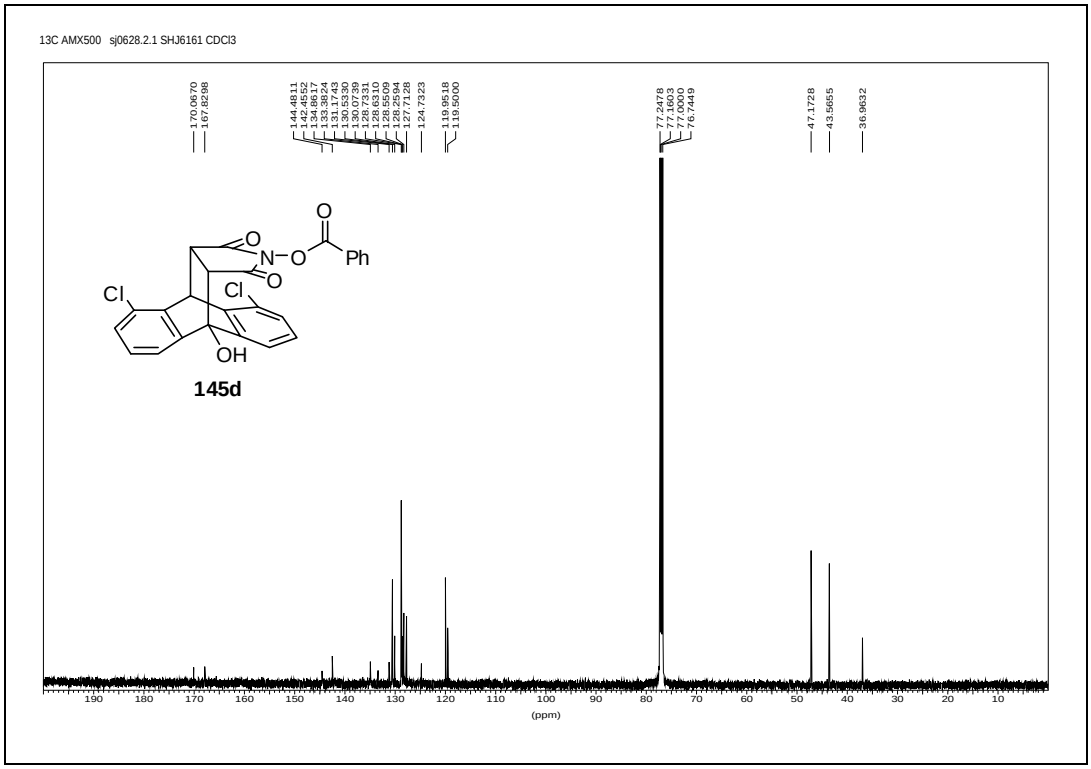
13C AMX500 sj0628.2.1 SHJ6161 CDCl3
170.0670
167.0298
144.4811
142.4552
134.8617
133.3824
131.1743
130.5530
130.0739
128.7331
128.6310
128.5509
128.2594
127.7128
124.7323
119.9518
119.9000
77.2478
77.1603
77.0000
76.7449
47.1728
43.5655
36.9632
O
O
N
O
Ph
O
Cl
Cl
OH
145d
(ppm)

(**146**)

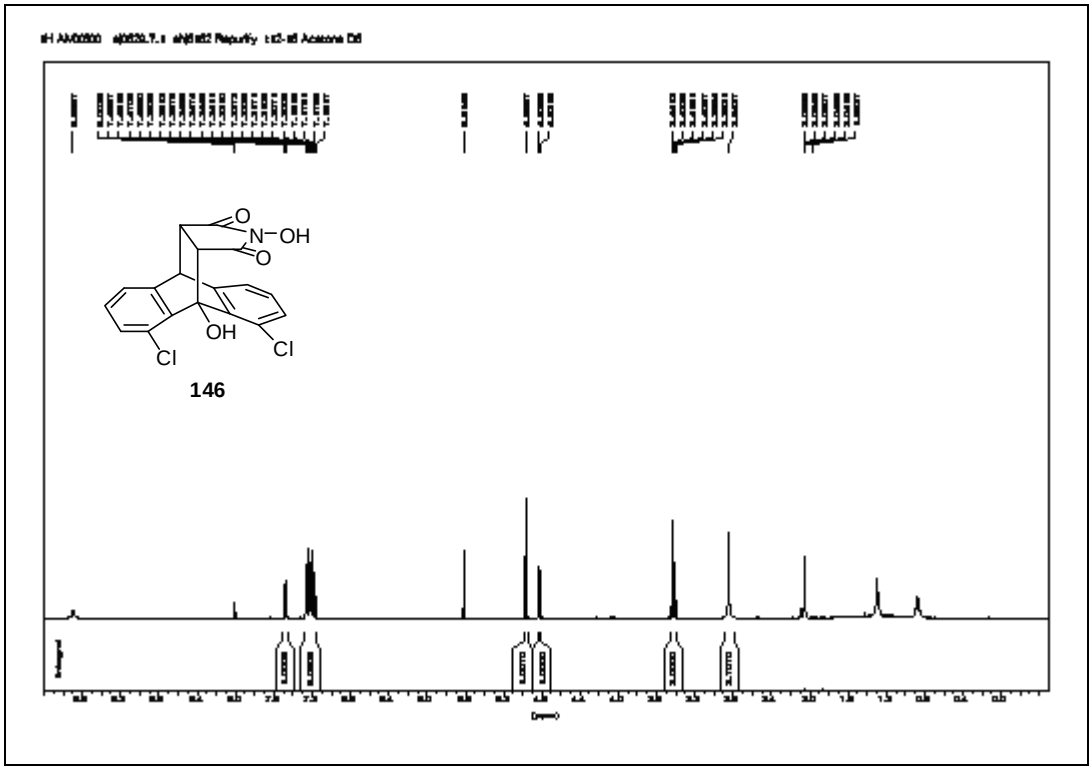
O
N−OH
O
OH
Cl
Cl
146

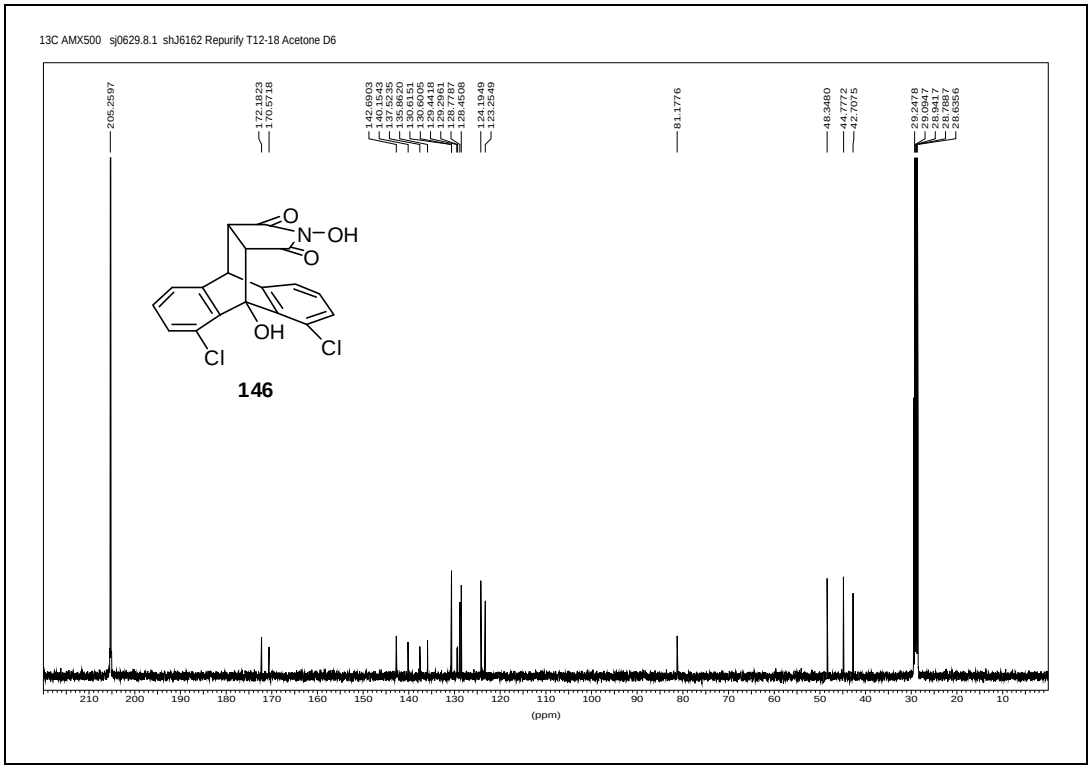
13C AMX500 sj0629.8.1 shJ6162 Repurify T12-18 Acetone D6
205.2597
172.1823
170.5718
142.6903
140.1543
137.8235
135.8620
130.6151
130.6005
129.4418
129.2961
128.7787
128.4508
124.1949
123.2549
81.1776
48.3480
44.7772
42.7075
29.2478
29.0947
28.9417
28.7887
28.6356
O
N−OH
O
OH
Cl
Cl
146
(ppm)

(**148a**)

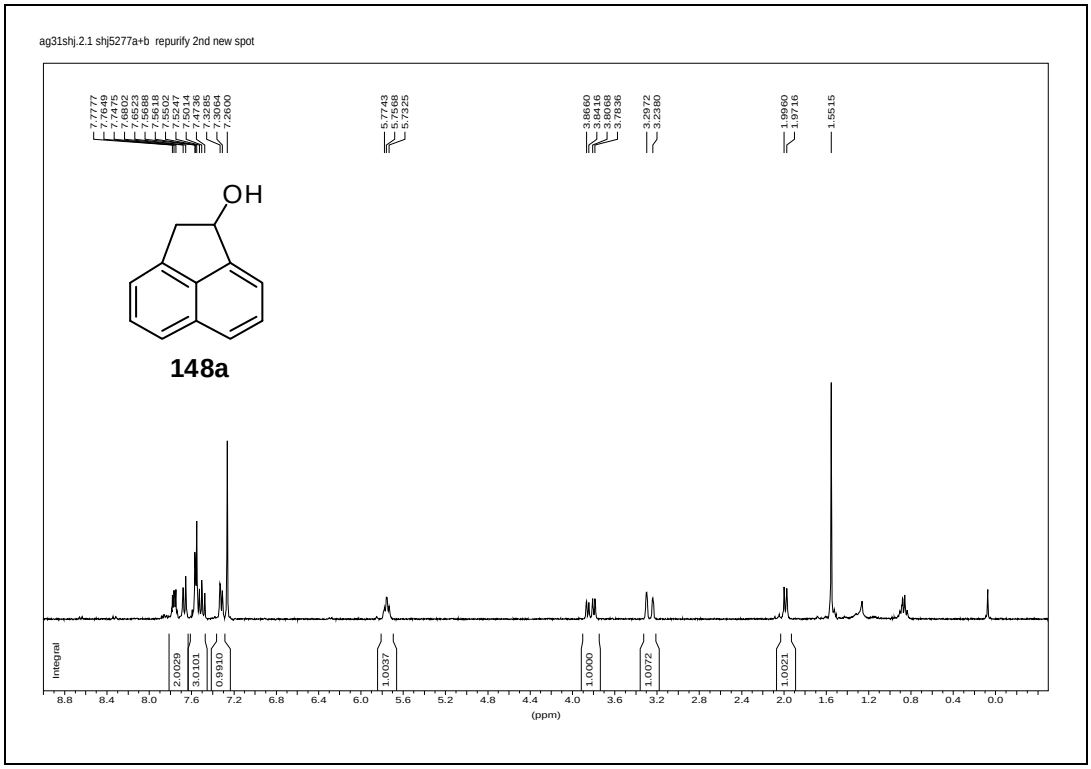
ag31shj.2.1 shj5277a+b repurify 2nd new spot
7.7777
7.7649
7.7475
7.6802
7.6623
7.5688
7.5618
7.5502
7.5047
7.5014
7.4736
7.3085
7.3064
7.2600
5.7743
5.7568
5.7325
3.8660
3.8515
3.8068
3.7836
3.2972
3.2380
1.9960
1.9716
1.5515
OH
148a
Integral
2.0029
3.0101
0.9910
1.0037
1.0000
1.0072
1.0021
(ppm)

(**150**)

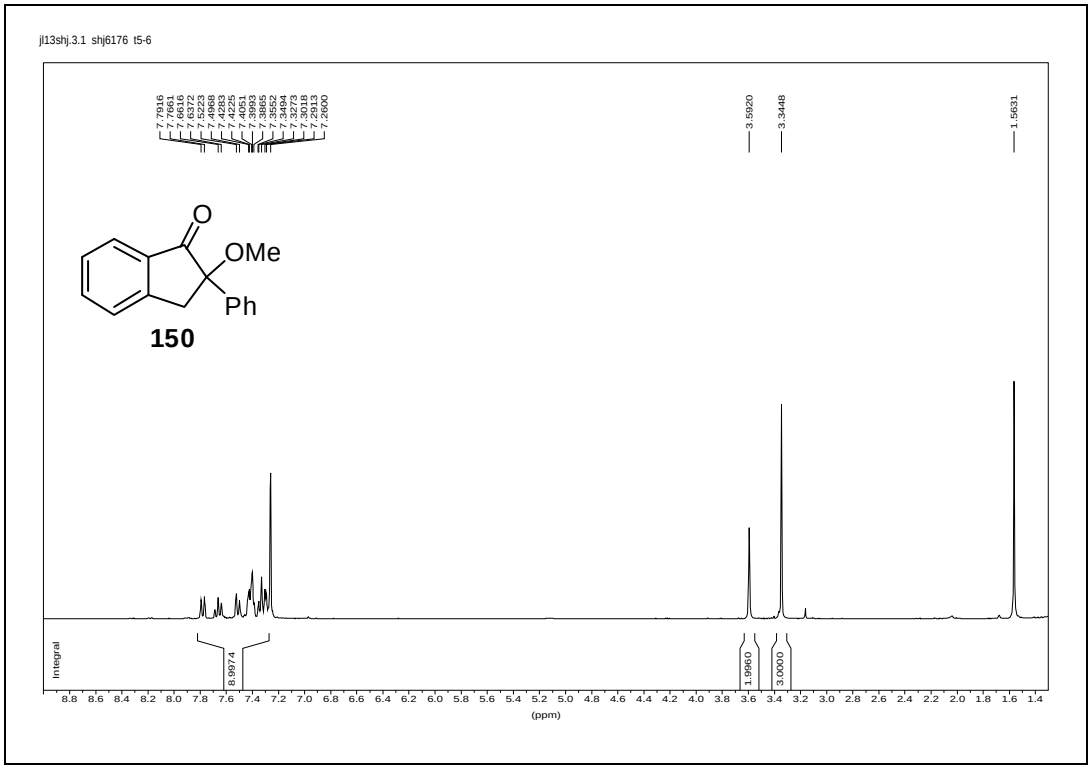
jl13shj.3.1 shj6176 t5-6
7.7916
7.7661
7.6616
7.6572
7.5223
7.4968
7.4283
7.4225
7.4051
7.3993
7.3965
7.3852
7.3494
7.3273
7.3018
7.2913
7.2600
3.5920
3.3448
1.5631
O
OMe
Ph
150
Integral
8.997
1.996
3.000
(ppm)

(154)

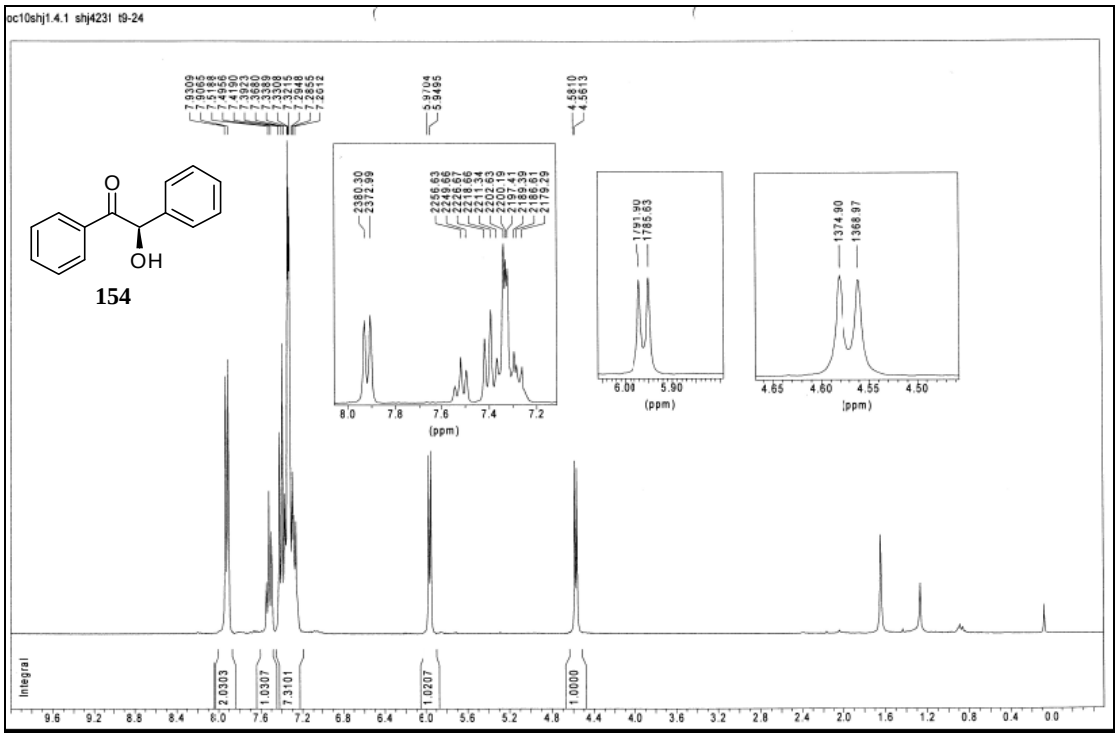

(155)

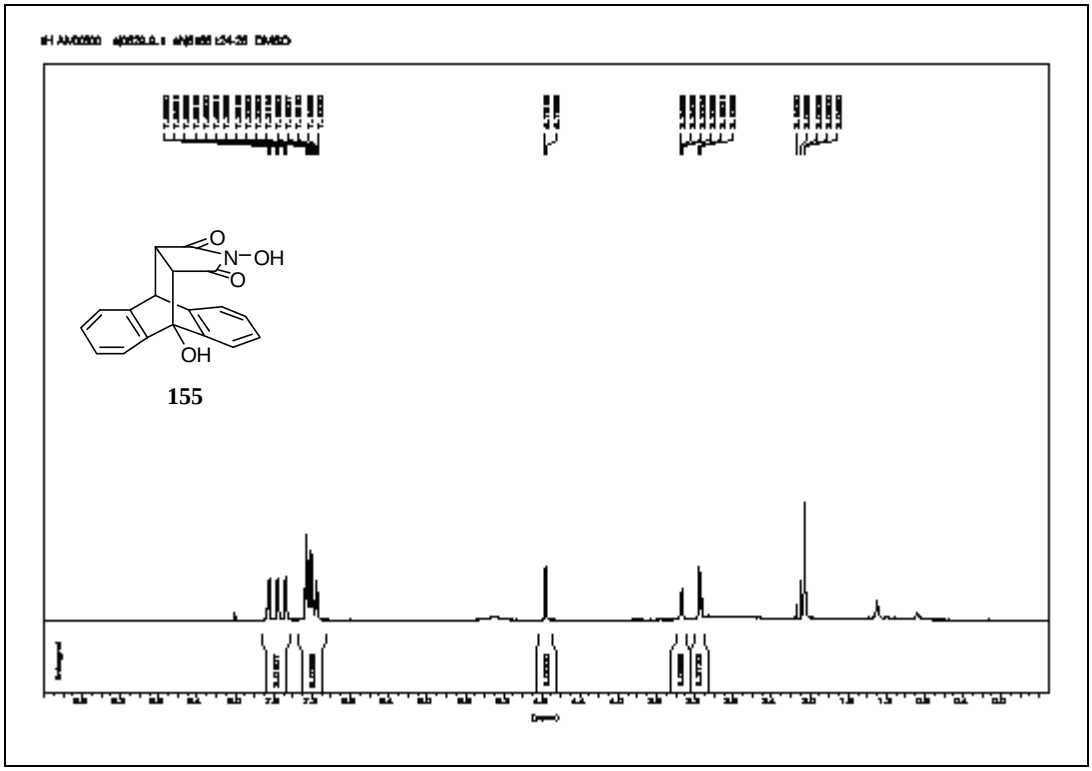

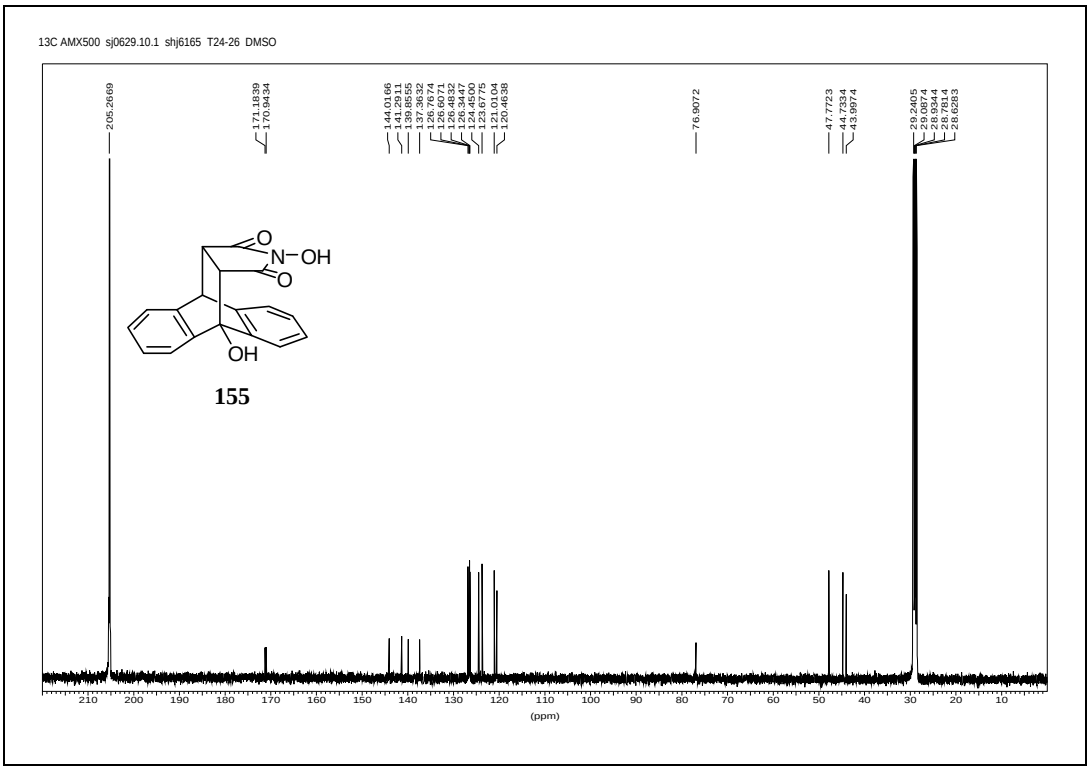
13C AMX500 sj0629.10.1 shj6165 T24-26 DMSO
205.2669
171.1839
170.9434
144.0166
141.2911
139.8555
137.3632
126.7674
126.6071
126.4832
126.3447
124.4609
123.6775
121.0104
120.4638
76.9072
47.7723
44.7334
43.9974
29.2405
29.0874
28.8934
28.7414
28.6283
O
N−OH
O
OH
155
(ppm)

(**158a**)

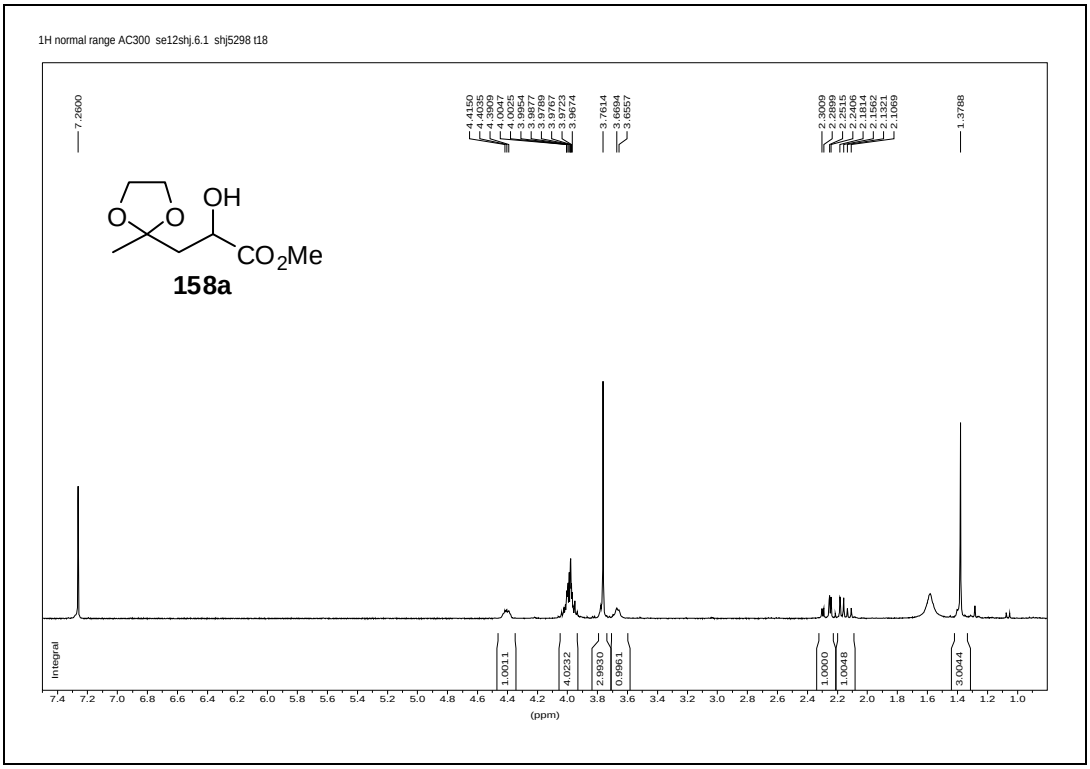
1H normal range AC300 se12shj.6.1 shj5298 t18
7.2600
4.4150
4.4035
4.3909
4.0047
4.0025
3.9954
3.9877
3.9768
3.9767
3.9723
3.9674
3.7614
3.6694
3.6557
2.3009
2.2899
2.2515
2.2406
2.2314
2.1562
2.1321
2.1069
1.3788
O
O
OH
CO2Me
158a
integral
1.0011
4.0232
2.9930
0.9961
1.0000
1.0048
3.0044
(ppm)

(**158b**)

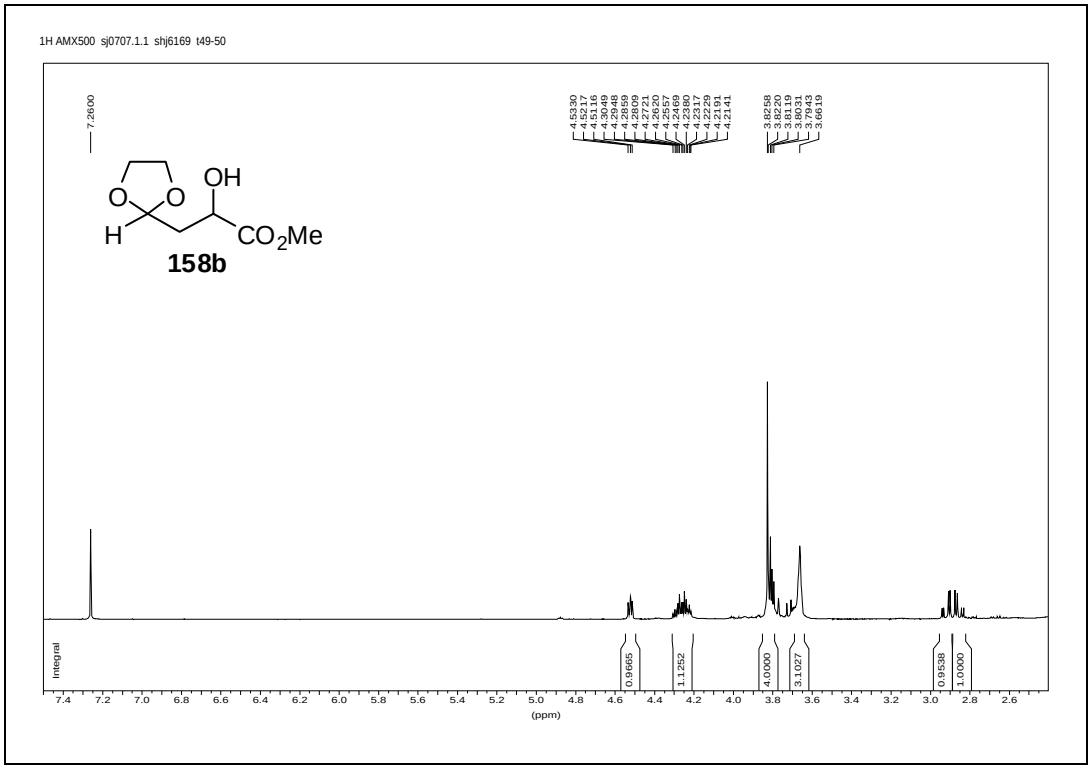
1H AMX500 sj0707.1.1 shj6169 t49-50
7.2600
4.5330
4.5177
4.5116
4.3049
4.2848
4.2659
4.2809
4.2721
4.2520
4.2357
4.2469
4.2380
4.2317
4.2229
4.2191
4.2141
3.8258
3.8220
3.8119
3.8031
3.7943
3.6819
OH
O
O
H
CO2Me
158b
Intégral
0.9665
1.1252
4.0000
3.1027
0.9538
1.0000
(ppm)

(**158c**)

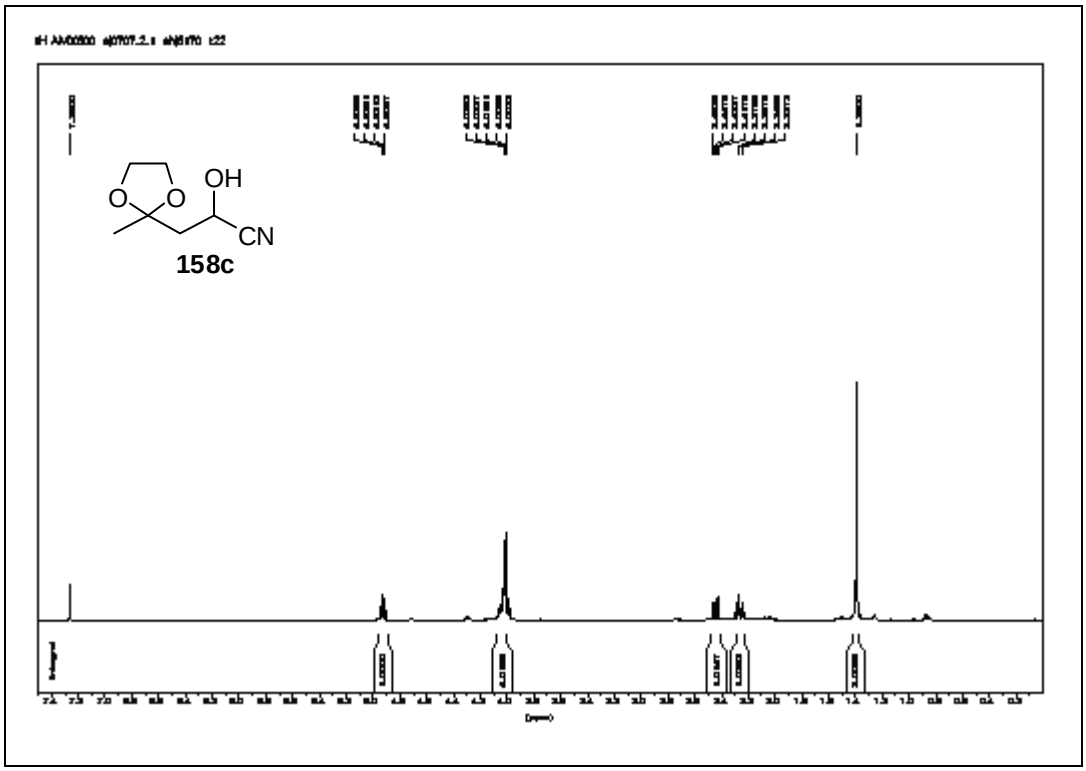
OH
O
O
CN
158c

(158d)

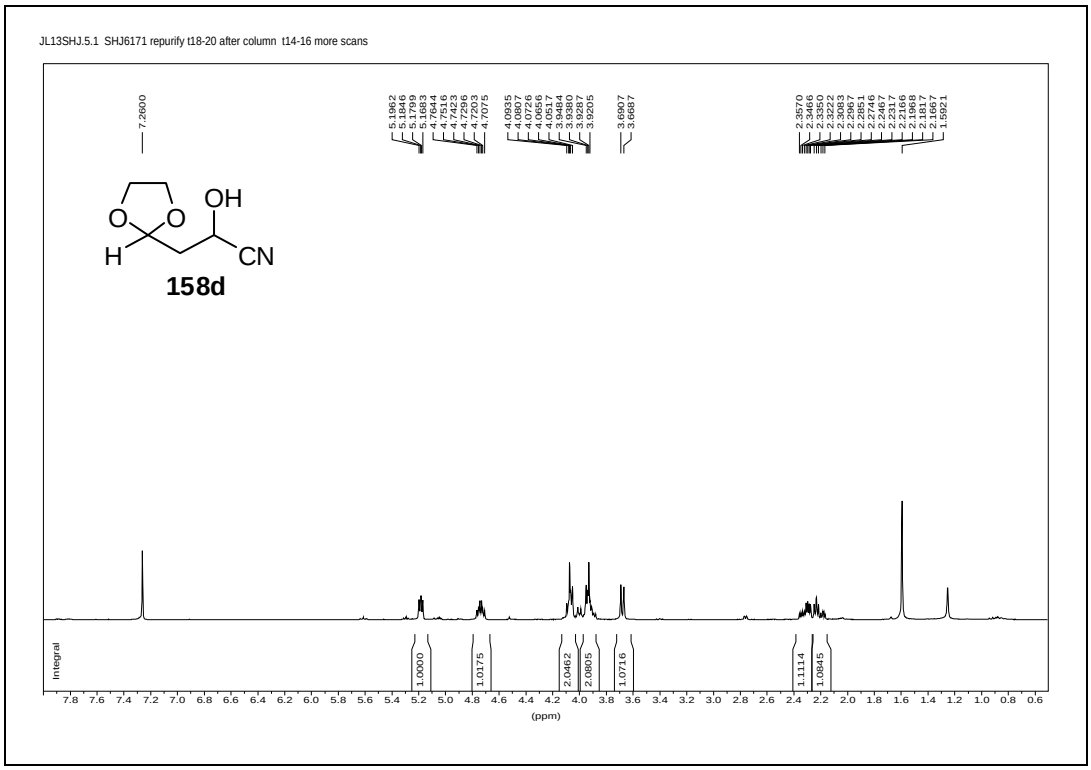
JL13SHJ.5.1 SHJ6171 repurify t18-20 after column t14-16 more scans
7.2600
5.1962
5.1846
5.1799
5.1683
4.7644
4.7516
4.7423
4.7296
4.7203
4.7075
4.0935
4.0807
4.0736
4.0656
4.0517
3.9484
3.9360
3.9287
3.9205
3.6907
3.6687
2.3570
2.3466
2.3350
2.3222
2.3083
2.2957
2.2851
2.2746
2.2467
2.2317
2.2166
2.1968
2.1817
2.1657
1.5921
OH
O
O
H
CN
158d
Integral
1.0000
1.0175
2.0462
2.0805
1.0716
1.1114
1.0845
(ppm)

(160)

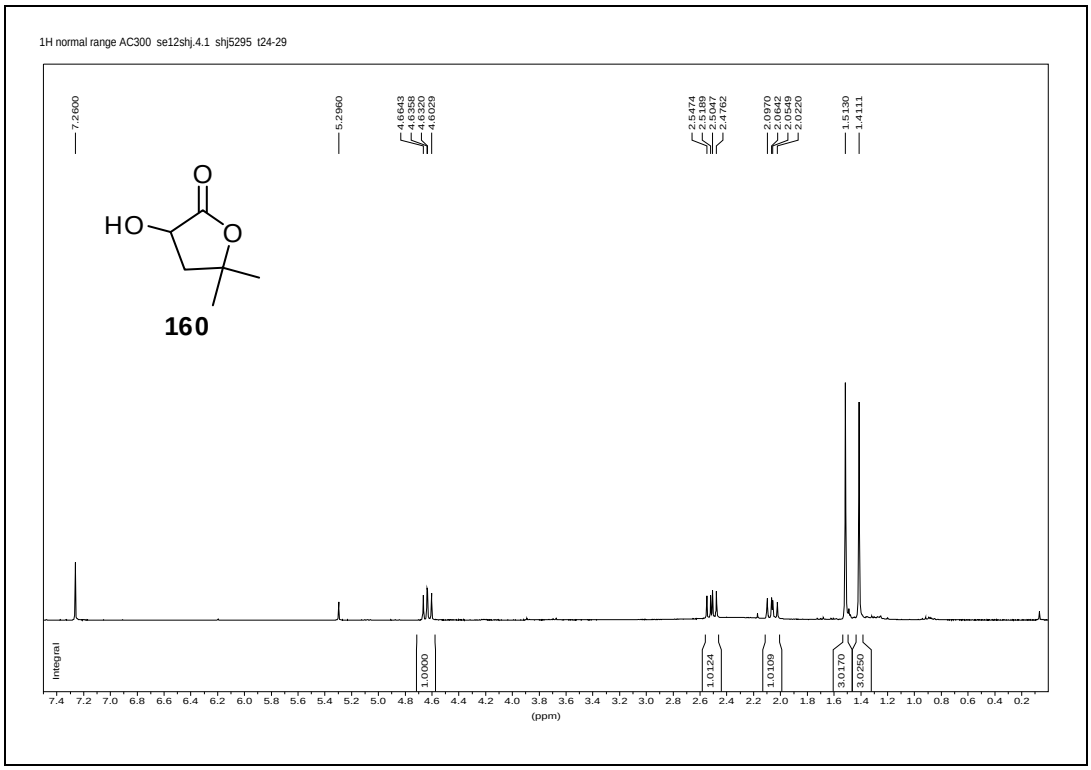
1H normal range AC300 se12shj.4.1 shj5295 t24-29
7.2600
5.2960
4.6643
4.6358
4.6320
4.6029
2.5474
2.5189
2.5047
2.4762
2.0970
2.0642
2.0549
2.0220
1.5130
1.4111
O
HO
O
160
Integral
1.0000
1.0124
1.0109
3.0170
3.0250
(ppm)

Publications

1 Shen, Juan; Nguyen, Thanh Truc; Goh Yong-Peng; Ye, Weiping; Fu Xiao; Xu Junye; Tan Choon-Hong. Chiral Bicyclic Guanidine-Catalyzed Enantioselective Reactions of Anthrones. *J. Am. Chem. Soc.* **2006**, *128*, 13692-13693.

2 Shen, Juan; Tan Choon-Hong. Brønsted-Acid and Brønsted-Base Catalyzed Diels–Alder Reactions, *Org. Biomol. Chem.*, **2008**, *6*, 3229-3236.

3 Shen, Juan; Tan Choon-Hong. Anthrone-Derived NHPI Analogues as Catalysts in Reactions Using Oxygen as an Oxidant, *Org. Biomol. Chem.*, **2008**, 6, 4096-4098.

4 Shen, Juan; Tan, Choon-Hong. 2,3,5,6-Tetrahedro-2,6-bis(phenylmethyl)-1H-imidazo[1,2-a]imidazole. *Electronic Encyclopedia of Reagents for Organic Synthesis*, 2008, *in press*.

5 Shen, Juan; Tan Choon-Hong. Mechanistic and kinetic studies of guanidine catalyzed enantioselective Diels–Alder reactions of anthrones. *Manuscript in preparation*.

6 Shen, Juan. Chiral bicyclic guanidine-catalyzed enantioselective reactions of anthrones. Abstracts of Papers, 233rd ACS National Meeting, Chicago, IL, United States, March 25-29, 2007.